The role of extracellular sulfatase-2 in inflammation.

Maarten Swart



Kennedy Institute of Rheumatology

The Queen's College

University of Oxford

A thesis submitted for the degree Doctor of Philosophy

In Molecular and Cellular Medicine

Word count: 31.671

Abstract

Rheumatoid arthritis (RA) is a chronic inflammatory joint disease whose molecular pathogenesis serves as a useful model for understanding other chronic inflammatory conditions. Activated macrophages are critical for RA pathogenesis, since they promote the inflammation that causes cartilage damage, bone remodelling, pain and irreversible disability. Macrophages are activated by stimuli in their environment, and responses to these stimuli are fine-tuned by their interactions with highly sulfated heparan sulfate (HS) glycosaminoglycans. HS is sulfated in complex patterns, but 6-O-sulfation of HS glucosamine subunits is known to be particularly important for regulating activity of many cytokines, chemokines and growth factors. 6-O-sulfation is hence tightly regulated, and it is the only HS sulfation motif that can be post-synthetically removed by the extracellular sulfatases SULF1 and SULF2. Although extensively studied in cancer and development, the effect of 6-O-sulfation on inflammation and macrophage function is unknown.

In this thesis I showed that *Sulf2* is mainly expressed by macrophages, monocytes and dendritic cells. *Sulf2* is particularly highly expressed by protective resident alveolar macrophages in the lung and resident synovial macrophages in the joint, indicating that *Sulf2* is likely to be important for maintaining homeostasis and suppressing inflammation. Moreover, *Sulf2* is downregulated by many inflammatory stimuli, suggesting that downregulation of *Sulf2* may enable macrophages to convert from a protective phenotype to an activated inflammatory phenotype. Phagocytosis was increased in *Sulf2*-deficient macrophages, while macrophage polarisation was inhibited.

Sulf2-deficient bone marrow chimeras were generated to investigate the role of *Sulf2* in immune function during antigen-induced arthritis (AIA) as an example of a chronic inflammatory disease. These *Sulf2*-deficient mice developed increased knee swelling, which was associated with an increase in pro-arthritic Th17 cells.

In conclusion, SULF2 is important for maintaining homeostasis by suppressing macrophage activation, indicating that therapies reducing 6-O sulfation of HS might be effective for the treatment of RA and other chronic inflammatory diseases.

Table of contents

Chapter 1. Introduction 1

1.1. Rheumatoid arthritis 2

1.1.1. Pathogenesis of RA 3

1.1.2. Murine models for RA 5

1.1.3. Innate immune system in RA 7

1.1.3.1. Neutrophils 7

1.1.3.2. Eosinophils 8

1.1.3.3. Monocytes 8

1.1.3.4. Macrophages 9

1.1.3.5. Dendritic cells 14

1.1.4. Adaptive immune system in RA 15

1.1.4.1. T-cells 15

1.1.4.2. B-cells 18

1.1.5. Fibroblasts 18

1.1.6. Cytokines in RA 19

1.2. Heparan sulfate as a regulator of inflammation 20

1.2.1. Heparan sulfate biosynthesis 20

1.2.1. Ligand binding to heparan sulfate 22

1.2.2. Heparan sulfate biosynthesis enzyme expression by immune cells 23

1.2.2.1. Endothelial HS and leukocyte extravasation 25

1.2.2.2. Function of HS expressed by leukocytes 26

1.3. Sulfatases 27

1.3.1. 6-O-sulfation regulates signalling pathways 27

1.3.2. Sulfatase structure and biochemical characterisation 29

1.3.3. Known pathophysiological roles of SULF1 and SULF2 32

1.3.4. Sulfatase-2 and inflammation 34

1.4. Hypothesis and aims 36

Chapter 2. Materials and methods 37

2.1. Reagents 38
2.1.1. Cell lines and cell culture reagents 38
2.1.2. Antibodies 39
2.2. Human samples 40
2.2.1. Synovium digestion 40
2.3. Mice 41
2.3.1. Maintenance 41
2.3.2. Generation of single cell suspensions 42
2.3.2.1. Generation of blood single cell suspensions 42
2.3.2.2. Generation of bone marrow single cell suspensions 42
2.3.2.3. Generation of spleen and lymph node single cell suspensions 42
2.3.2.4. Generation of lung single cell suspensions 43
2.3.2.5. Generation of joint single cell suspensions 43
2.3.3. Generation of bone marrow chimera 43
2.3.4. Antigen-induced arthritis 44
2.4. Cell culture 45
2.4.1. Cell line culture 45
2.4.2. Primary macrophage and dendritic cell culture 45
2.4.3. siRNA knockdown 45
2.4.4. Assays of immune cell function 46
2.4.4.1. Phagocytosis assays 46
2.4.4.2. Antigen presentation assays and T-cell culture 46
2.4.5. Cytotoxicity assay 47
2.5. Phenotypic characterisation 48
2.5.1. Flow cytometry 48
2.5.2. ELISA 49
2.5.3. Immunoblotting 50
2.5.3.1. Ammediol gels 50
2.5.4. Immunoblotting procedure 50
2.6. Nucleic acid assays 52

2.6.1. RNA isolation and reverse transcription-PCR 52
2.6.2. Quantitative PCR 52
2.6.2.1. TaqMan primers 53
2.7. Histology 56
2.8. RNA-sequencing analysis 57
2.8.1. Single cell RNA-sequencing 57
2.8.2. Bulk-sequencing 57
2.9. Statistical analysis 57

Chapter 3. Sulfatase-2 is highly expressed by macrophages 58

3.1. Introduction 59
3.2. Characterisation of HS biosynthesis and core protein expression in macrophages *in vitro* 61
3.3. Characterisation of *Sulf2* expression *in vivo* 67
3.3.1. *Sulf2* is expressed by dendritic cells, macrophages and monocytes 67
3.4. *Sulf2*-deficiency did not alter immune populations in healthy mice 69
3.5. Discussion 72

Chapter 4. Sulfatase-2 regulates macrophage polarisation and phagocytosis 75

4.1. Introduction 76
4.2. *Sulf2*-null mice show high perinatal lethality 77
4.3. *Sulf2*-deficiency impacted macrophage function 78
4.3.1. *Sulf2* affects macrophage responses to inflammatory stimuli 78
4.3.2. TLR signalling in *Sulf2*-deficient macrophages 79
4.3.3. Inflammasome activation in *Sulf2*-deficient macrophages 80
4.3.4. Autophagy in *Sulf2*-deficient macrophages 81
4.3.5. Phagocytosis in *Sulf2*-deficient macrophages 82
4.4. siRNA knockdown of *Sulf2* altered macrophage phenotype. 84
4.4.1. *Sulf2* knockdown affected responses to inflammatory stimuli 84
4.5. *Sulf2*-deficiency did not affect antigen presentation by dendritic cells *in vitro* 87
4.6. Discussion 92

Chapter 5. Sulfatase-2 protects against experimental arthritis 97

5.1. Introduction 98
5.2. *Sulf2* is expressed at high levels in resident macrophages in the RA joint 99
5.3. Characterisation of *Sulf2* expression in AIA 106
5.4. Antigen-induced arthritis was aggravated in *Sulf2*$^{+/-}$ chimeras 111
5.4.1.1. The effect on disease score and pain 111
5.4.1.2. Effects on immune cell populations 116
5.5. Cytokine expression in *Sulf2*-deficient mice 123
5.6. *Sulf2* expression in human arthritis 125
5.7. Discussion 126

Chapter 6. Discussion 130

6.1. *Sulf2* is expressed by macrophages, monocytes and dendritic cells 132
6.2. *Sulf2* exacerbates experimental arthritis 134
6.3. *Sulf2* affects macrophage polarisation 135
6.4. *Sulf2* suppresses macrophage phagocytosis 136
6.5. Future perspectives 137
6.6. Concluding remarks 139

Chapter 7. Appendices 143

Appendix 1. Supplemental data 142
Appendix 2. Abbreviations 155
Appendix 3. Published materials 159
Appendix 4. Bibliography 160

Acknowledgements 201

List of figures

Figure 1.1. Mucosal origin hypothesis for development of RA. 4

Figure 1.2. Macrophage populations in the joint....12

Figure 1.3. CD4+ T-cells in rheumatoid arthritis. 16

Figure 1.4. Heparan sulfate biosynthesis enzymes. 21

Figure 1.5. Binding of inflammatory mediators to heparan sulfate. 22

Figure 1.6. Expression of heparan sulfate-associated genes in human PBMCs....23

Figure 1.7. 6-O-sulfation can positively or negatively affect signalling. 28

Figure 1.8. The structure of sulfatase-2....30

Figure 1.9. Mechanism of action of sulfatase-2 (SULF2). 32

Figure 2.1. Generation of *Sulf2*-deficient mice. 41

Figure 2.2. Weight loss after bone marrow transplantation. 44

Figure 2.3. Branched DNA amplification in PrimeFlow....49

Figure 3.1 HS-associated gene expression in murine bone marrow-derived macrophages was differently regulated by differentiation with GM-CSF or M-CSF. 62

Figure 3.2. HS elongation and modification enzymes were downregulated by IFNγ+LPS. 64

Figure 3.3. Validation of macrophage polarisation by IFNγ+LPS or IL4+IL13....65

Figure 3.4. *Sulf2* was downregulated by inflammatory stimuli....66

Figure 3.5. SULF2 antibody clone 2B4 recognised additional proteins. 67

Figure 3.6. *Sulf2* was highly expressed by monocytes in murine blood and bone marrow. 68

Figure 3.7. *Sulf2* was mainly expressed by macrophages, monocytes and dendritic cells in spleen and lung. 70

Figure 3.8. Tissue frequencies of immune populations were not affected by *Sulf2*-deficiency. 71

Figure 4.1. *Sulf2*$^{+/-}$ macrophages showed a 50% reduced *Sulf2* expression with no compensation on *Sulf1*. 77

Figure 4.2. Macrophage polarisation was modulated by *Sulf2*. 78

Figure 4.3. Toll-like receptor signalling was not affected by *Sulf2*-deficiency. 79

Figure 4.4. Inflammasome activation was not affected in *Sulf2*-deficient macrophages. 80

Figure 4.5. *Sulf2*-deficiency did not affect autophagy in macrophages. 81

Figure 4.6. Phagocytosis was increased in *Sulf2*-deficient macrophages....82

Figure 4.7. Expression of the efferocytosis receptors *Tyro3* and *Cd36* was increased in in *Sulf2*-deficient macrophages. 83
Figure 4.8. Validation of *Sulf2* knockdown by siRNA in primary murine macrophages. 84
Figure 4.9. siRNA knockdown of *Sulf2* modulated macrophage polarisation. 85
Figure 4.10. siRNA knockdown of *Sulf2* increased phagocytosis. 86
Figure 4.11. Antigen uptake in GM-CSF-derived CD11c+ macrophages was reduced by *Sulf2* deficiency. 88
Figure 4.12. The expression of costimulatory molecules on antigen presenting cells was not affected by *Sulf2*. 89
Figure 4.13. *Sulf2*-deficiency did not affect antigen presentation by dendritic cells *in vitro*. 91
Figure 5.1. *Sulf2* expression in human RA. 99
Figure 5.2. Single cell sequencing analysis of CD45+CD11b+Ly6G- joint cells identified distinct myeloid populations. 101
Figure 5.3. *Sulf2* was predominantly expressed by resident macrophages in the joint. 102
Figure 5.4. Expression of heparan sulfate core proteins and modifying enzymes in the arthritic joint. 104
Figure 5.5. Bone marrow-derived macrophages expressed low *Sulf2* levels. 105
Figure 5.6. Expression of inflammatory markers is increased in antigen-induced arthritis. 106
Figure 5.7. Expression of *Sulf2* was increased at day 7 of antigen-induced arthritis. 107
Figure 5.8. Relative abundance of immune populations in antigen-induced arthritis. 109
Figure 5.9. Expression of *Sulf2* by macrophages, monocytes and dendritic was not altered in the AIA joint. 110
Figure 5.10. Knee swelling was increased and pain decreased in *Sulf2*-deficient BM chimera upon antigen-induced arthritis. 112
Figure 5.11. AIA histology scores were not affected at day 2 in *Sulf2*-deficient BM-chimera mice. 114
Figure 5.12. AIA histology scores were not affected at day 7 in *Sulf2*-deficient BM chimera mice. 115
Figure 5.13. The abundance of immune subsets was not affected in the spleen of AIA mice by *Sulf2*-deficiency. 116
Figure 5.14. Inflamed knees of *Sulf2*-deficient BM chimera mice showed no differences in myeloid and adaptive immune subsets. 117

Figure 5.15. The Th17/Treg ratio was increased in the knee joints of *Sulf2*-deficient mice during AIA. 119

Figure 5.16. The Th17/Treg ratio was not affected in the lymph nodes of *Sulf2*-deficient mice during AIA. 121

Figure 5.17. The number of DCs in the inguinal lymph nodes were not affected by *Sulf2* during AIA. 122

Figure 5.18. Cytokine and macrophage marker gene expression was not altered in knee joints of *Sulf2*-deficient mice. 123

Figure 5.19. *SULF2* was not differentially expressed between synovial membranes of patients with OA and RA. 125

Figure 6.1. The proposed role of Sulf2 in RA. 140

Appendix figure 1. Profiling heparan sulfate-associated gene expression in murine macrophage cell lines. 144

Appendix Figure 2. Gating for myeloid populations in the blood/ bone marrow. 145

Appendix Figure 3. Gating strategy for myeloid populations in the spleen. 146

Appendix Figure 4. Gating for myeloid populations in the lung. 147

Appendix Figure 5. Gating for myeloid populations in the bone marrow. 148

Appendix Figure 6. Fold change in the expression of HS biosynthetic enzymes and core proteins in *in vitro* M1 and M2 polarised macrophages. 149

Appendix Figure 7. Gating strategy for M-CSF/ GM-CSF differentiated bone marrow cells *in vitro*. 150

Appendix Figure 8. Gating strategy for myeloid populations in the knee. 151

Appendix Figure 9. Gating strategy for T-cell subsets in the knee. 152

Appendix Figure 10. T-cell subsets were not affected in the inguinal lymph nodes of *Sulf2*$^{+/-}$ chimera mice at day 2 of AIA. 153

Appendix Figure 11. Gating strategy for T-cell subsets in the inguinal lymph nodes. 154

Appendix Figure 12. Gating strategy for myeloid populations in the inguinal lymph nodes. 154

Appendix Figure 13. HS core protein and biosynthesis enzyme expression in human RA. 155

List of tables

Table 1.1. Monocyte subsets in humans and mice. 8

Table 1.2. Overview of studies examining the role of heparan sulfate genes in immune responses. ..24

Table 2.1. Cell culture reagents....38

Table 2.2. Antibodies. 39

Table 2.3. Reagents required to make 10% Ammediol SDS-PAGE gels. 50

Table 2.4. Buffers for ammediol gels....51

Table 2.5. Mouse TaqMan primers from ThermoFisher Scientific used to measure gene expression in qPCR assays. 53

Table 2.6. TaqMan primers from ThermoFisher Scientific used for microfluidic card analysis of murine heparan sulfate-associated gene expression by qPCR....54

Table 2.7. TaqMan primers from ThermoFisher Scientific for microfluidic card analysis of human heparan sulfate-associated gene expression. 55

Table 4.1. Summary of functional and polarisation effects of *Sulf2* deficiency in macrophages. 93

Chapter 1. Introduction

1.1. Rheumatoid arthritis

Inflammatory responses are critical for the body's defence against infection and tissue injury, and normally ensure that these are quickly resolved (Schett and Neurath, 2018). However, if an infectious agent cannot be removed, or if the immune system is sensitised to attack healthy cells, chronic inflammation can persist for years and contributes to autoimmune diseases, such as rheumatoid arthritis (RA), cancer, cardiovascular diseases, type 2 diabetes and neurodegenerative disorders (Furman et al., 2019). Taken together, chronic inflammatory diseases are the most common cause of death, with 60% of people dying as a consequence of this group of diseases (Fleit, 2014; Roth et al., 2018). As the incidence of chronic inflammatory diseases continues to increase (Roth et al., 2018), it is increasingly important to understand the mechanisms behind these pathologies, and to identify novel targets for intervention. Heparan sulfate (HS) proteoglycans (PG) are known to coordinate signalling, activation and repair pathways in many cell types, but our understanding of their role in orchestrating the behaviour of immune cells is in its infancy. In this thesis, I will focus on RA as an example of a chronic inflammatory disease, to investigate the role of HSPGs in immune cell function and chronic inflammation.

RA is characterised by joint inflammation that may result in cartilage damage, bone remodelling, pain and irreversible disability, with consequent effects on quality of life (Nerurkar et al., 2019). Patients with RA also have an increased risk of cardiovascular disease, which can result in premature mortality. Globally, RA affects approximately 0.25-1% of the world population (Cross et al., 2014) and is twice as common in women as in men. The treatment of RA was revolutionised in the 1990s by development of tumour necrosis factor (TNF)-targeted biologic therapies (Monaco et al., 2015). However, because of their high cost, they are normally only prescribed

in the UK when RA cannot be controlled with anti-inflammatory drugs, such as methotrexate (D. L. Scott et al., 2010), or when these result in toxic side effects. In the UK, the cost of treating RA is >£500 million annually and work-related disability increases the total cost of the disease to £2 billion annually (National Audit Office 2009).

1.1.1. Pathogenesis of RA

The pathogenesis and clinical presentation of RA is variable as both genetic and environmental factors (e.g. smoking and microbiota) contribute to its development (MacGregor et al., 2000). Autoantibodies to citrullinated proteins can be detected in RA patients up to 10 years before clinical signs appear (Brink et al., 2013) suggesting that activation of the immune system precedes disease onset, though it is incompletely understood how environmental and genetic factors contribute to RA pathogenesis. The 'mucosal origins hypothesis' (**Figure 1.1**) proposes that environmental factors generate neo-antigens on various proteins in the lung (via smoking/dust inhalation) or gut (microbiota) by post-translational modifications, such as citrullination of arginine residues (Holers et al., 2018). Individuals with human leukocyte antigen (HLA) DR epitopes that preferentially present these citrullinated peptides to T-cells develop T-cell activation and self-recognizing antibody production by B-cells (Smolen et al., 2018). The presence of these self-recognizing antibodies against citrullinated proteins (anti-citrullinated protein antibody; ACPA) and immunoglobulin G (IgG) (rheumatoid factor; RF) is an important characteristic of RA, although 15-20% of patients are seronegative for these antibodies, indicating that this is not the only mechanism leading to joint inflammation.

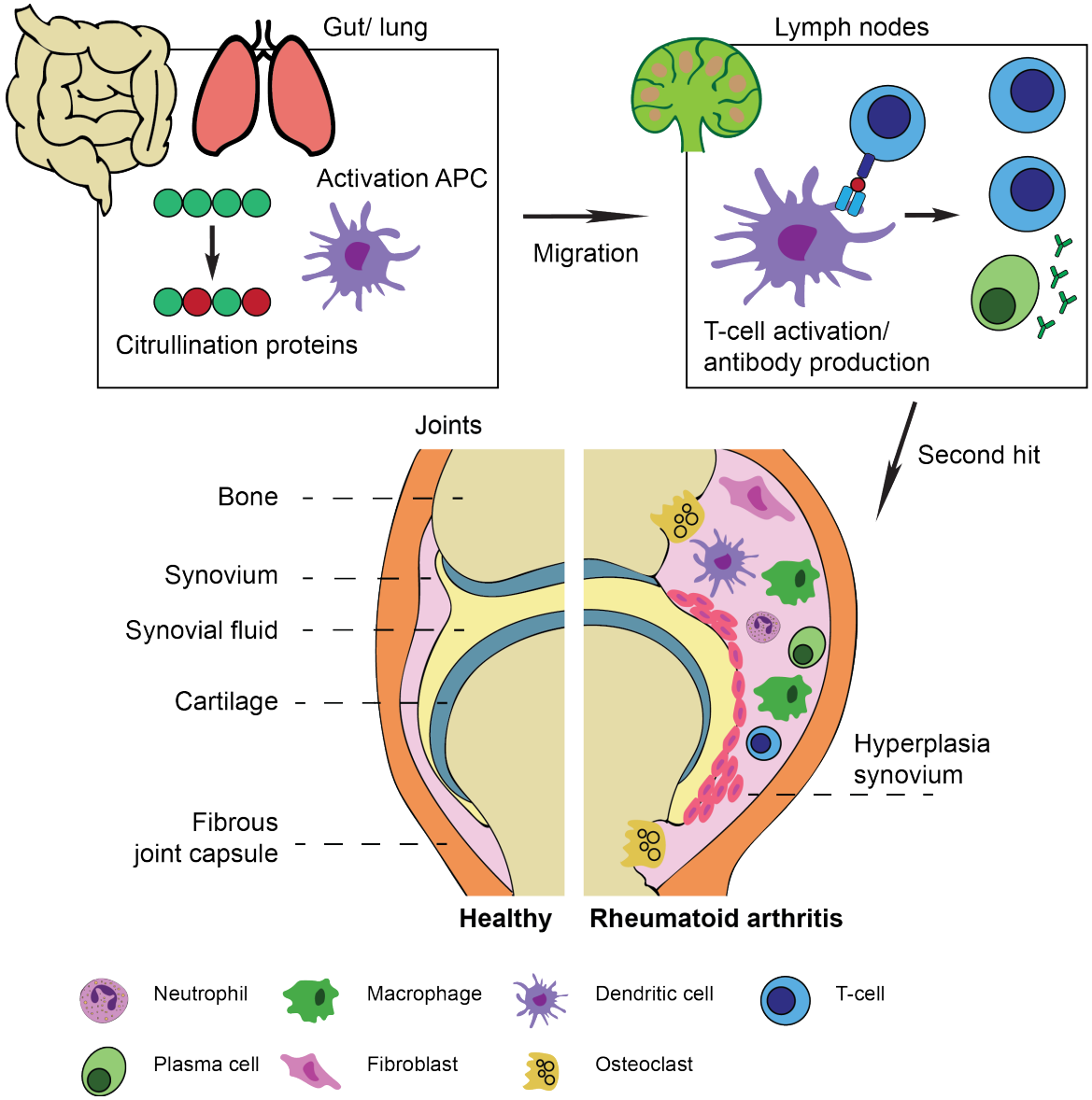


Figure 1.1. Mucosal origin hypothesis for development of RA.
It is hypothesised that environmental factors in, for example, the lung and joint modify proteins by citrullination. These citrullinated peptides can be presented on antigen-presenting cells (APC), which migrate to lymph nodes, where they activate auto-antibody-producing B-cells and T-cells. A second hit might be required to trigger inflammation in the joint, leading to local accumulation of many immune cell types.

It can take over a decade after these processes start for RA to develop and it is incompletely understood why inflammation specifically occurs in the joints. A partial explanation might be that ACPAs cross-react with non-citrullinated type II collagen (Ge et al., 2017), which is predominantly present in articular cartilage. This might activate the complement system to initiate inflammation in the joint (Arend and Firestein, 2012).

It has also been proposed that immune complex formation or microvascular injury are required as a second hit to promote influx of immune cells into the joint. Finally, genetic mouse models indicate that the joints are particularly susceptible to inflammation, possibly due to hypoxia. For example, transgenic TNF-overexpressing (Keffer et al., 1991), IL1RA knockout (Horai et al., 2000) and SKG mice (Sakaguchi et al., 2003) with a mutation in zeta chain of T-cell receptor associated protein kinase 70 (ZAP70) that affects self-tolerance spontaneously develop joint inflammation, despite the fact that the mutation is not targeted to the joint.

Hyperplasia of the synovium (**Figure 1.1**), the connective tissue that lines the synovial cavity containing synovial fluid, is one of the first signs of joint inflammation. Normally the synovium produces synovial fluid that lubricates and provides nutrients for cartilage. The intimal layer containing macrophages and fibroblasts expands first. Activation of these cells by, for example, complement activation promotes the release of inflammatory cytokines and matrix metalloproteinases (MMPs) that degrade collagen and PGs in the joint (Bartok and Firestein, 2010). Dendritic cells take up and present the degradation products to T-cells in the lymph nodes, generating an adaptive immune response to various proteins in the joint. Inflammation in the joint also promotes maturation and activation of osteoclasts that can degrade bone (Schett and Gravallese, 2012). This negative inflammatory feedback loop creates more degradation products, further amplifying inflammation.

1.1.2. Murine models for RA

Animal models have contributed substantially to our understanding of immune processes that drive development of RA. In addition to the genetically engineered TNF-overexpressing (Keffer et al., 1991), IL1RA knockout (Horai et al., 2000) and SKG

mice (Sakaguchi et al., 2003) that spontaneously develop RA (discussed in section **1.1.1**), inducible models that develop RA after immunization are also commonly used. These include collagen-induced arthritis (CIA), antigen-induced arthritis (AIA), collagen antibody-induced arthritis (CAIA) and the K/BxN serum transfer model.

The CIA model is one of the most commonly used (Holmdahl et al., 1986). In this model, mice with the major histocompatibility complex (MHC, the HLA in mice) haplotype q (H-2q) are immunised with collagen type II in complete Freund's adjuvant (CFA), with clinical signs of arthritis appearing 20-30 days after immunisation (Williams, 2007). CIA mimics many characteristics of human RA including joint inflammation, cartilage degradation, bone erosion and joint immobility. However, in contrast to human RA, there is an acute inflammatory phase of relatively short duration (Schurgers et al., 2011).

Mouse strains not carrying the H-2q locus, such as most genetically modified strains, are not generally susceptible to CIA and in this case the AIA model (Brackertz, Mitchell and Mackay, 1977a) is used, in which arthritis is induced by injecting methylated bovine serum albumin (mBSA) into the knee joint of animals previously immunised with mBSA in CFA (van den Berg et al., 2007). The use of cationic antigens, such as mBSA, enhances retention of the antigen in the joint and prolongs the duration of RA symptoms. This model can also be used to study various processes that are relevant to human RA, including immune infiltration, cartilage degradation and bone erosion. However, there is no break in central tolerance, like in CIA and human RA. In addition to the AIA model, the CAIA and the K/BxN serum transfer model can also be used in genetically modified animals. Both methods rely on the transfer of antibodies from mice or patients with arthritis or K/BxN mice that spontaneously develop arthritis. These models depend on immune complex formation and

complement activation, but do not recapitulate the B- and T-cell responses seen in human RA (Caplazi et al., 2015).

1.1.3. Innate immune system in RA

1.1.3.1. Neutrophils

Neutrophils, characterised by lymphocyte antigen 6 complex locus G6D (Ly6G) expression, are the first immune cells to be recruited upon infection and inflammation. Although they have a lifespan of generally less than 24 h, they are important as a first line of defence and can phagocytose pathogens, release anti-bacterial compounds (e.g. myeloperoxidase; MPO), produce reactive oxygen species (ROS) to kill pathogens and produce neutrophil extracellular traps (NET) to trap pathogens (Rosales, 2018).

Although neutrophils have a limited life-span, they are reportedly present at increased levels in the synovial fluid in RA, in particular in early stages of the disease (Kaplan, 2013). It may be of relevance that their life-span can be increased by anti-apoptotic cytokines such as TNF (Parsonage et al., 2008; Raza et al., 2006). Immune complexes in the joint can activate neutrophils to produce high concentrations of ROS, as well as proteases that contribute to cartilage degradation and cytokine activation (Wright et al., 2014). Finally, neutrophil NET activation and release (NETosis) is increased in RA (Khandpur et al., 2013), increasing exposure of intracellular autoantigens. For example, citrullination of histones is required for chromatin decondensation before NETosis. These citrullinated histones are also exposed in the process and can lead to ACPA formation (Pratesi et al., 2014).

1.1.3.2. Eosinophils

Like neutrophils, eosinophils also have secretory granules containing cytokines, chemokines and growth factors (Diny et al., 2017). In contrast to neutrophils, eosinophils have been shown to be protective in RA, as eosinophil-deficient ΔdblGATA mice have aggravated RA (Chen et al., 2016). It is hypothesised that this is caused by differences in the secretory granule content and in the production of anti-inflammatory lipids (Masterson et al., 2015).

1.1.3.3. Monocytes

Monocytes are circulating mononuclear cells that can function both in inflammation and its resolution. There are 3 subsets of monocytes in human and murine blood, based on the expression of respectively cluster of differentiation (CD) 14, CD16 or Ly6 locus C1 (Ly6C) (**Table 1.1**). Classical monocytes make up 80-90%, while the remainder of the monocytes have an intermediate or non-classical phenotype (Guilliams et al., 2018; Ziegler-Heitbrock et al., 2010). Classical monocytes are short-lived in the blood (1 day) after which they can convert into intermediate and subsequently non-classical monocytes (Patel et al., 2017).

Table 1.1. Monocyte subsets in humans and mice.
Three subtypes of monocytes can be detected in human and murine blood, and they can be distinguished primarily by their expression of CD14 and CD16 (human) or Ly6C (mice).

Subset	Human	Mouse
Classical	CD14+CD16-	Ly6C^{high}CCD62L+CD43-CCR2+CX+CR1^{low}
Intermediate	CD14+CD16+	Ly6C^{int}CD62L-CD43+CCR2-
Non-classical	CD14^{low}CD16+	Ly6C-CD62L-CD43++CCR2-CX3CR1^{high}

As Ly6C+ monocytes require the chemokine receptor 2 (CCR2) for trafficking, the function of Ly6C+ monocytes can be studied in murine models by depleting this cell type using anti-CCR2 monoclonal antibodies. This approach demonstrated that

depleting Ly6C+ monocytes decrease CIA development (Brühl et al., 2007). Ly6C+ monocytes predominantly infiltrate the joint in the AIA model, as 80-90% of the monocyte population is positive for Ly6C expression and approximately 50% are Ly6C^{high} (Weiss et al., 2015). *Ccr2*$^{-/-}$ mice showed drastically reduced monocyte infiltration and macrophage accumulation in AIA, indicating that the macrophages are predominantly derived from Ly6C+ monocytes in this model.

However, monocytes also have functions beyond being progenitors for macrophages, and they can contribute directly to inflammation. Monocytes from RA patients have a more activated phenotype (e.g. higher HLA and CD80/CD86 expression) and have been shown to promote enhanced T-cell responses *in vitro* (Yoon et al., 2014; Smiljanovic et al., 2018). Additionally, they can give rise to osteoclasts that are responsible for bone erosions (Komano et al., 2006).

1.1.3.4. Macrophages

Macrophages are important for the maintenance of homeostasis by phagocytosing pathogens, dead cells and debris, immunity and tissue repair (Wynn et al., 2013). Originally, it was thought that macrophages are exclusively derived from circulating monocytes, but more recent studies show that yolk sac and foetal liver cells also contribute to macrophage populations, forming a stable population of long-lived tissue-resident macrophages (Hashimoto et al., 2013; Ginhoux and Guilliams, 2016). After differentiation, they can adopt a range of activation states that affect their function in response to stimuli in their environment. *In vitro*, bone marrow-derived macrophages (BMDM) are commonly classified as either pro-inflammatory M1 or reparative M2 macrophages, which represent two extreme activation signatures. While these phenotypes do not recapitulate the range of phenotypes occurring *in vivo*, this

paradigm has been widely used to study activation *in vitro* (Murray et al., 2014; F. O. Martinez and Gordon, 2014). M1 macrophages produce pro-inflammatory cytokines and are derived by stimulation with interferon (IFN) γ and lipopolysaccharide (LPS), whereas M2 alternatively activated macrophages secrete anti-inflammatory cytokines and are obtained by treatment with interleukin (IL) 4 and IL13. *In vivo*, the variety of factors in the environment promote a range of activation states that differ from these more simplistic *in vitro* M1 and M2 states (F. O. Martinez and Gordon, 2014; Murray et al., 2014).

In healthy joints, macrophages are mainly found in the synovium, and their main functions are thought to be recycling of joint lubricants in the synovial fluid, removal of debris to prevent joint inflammation, and in regulating homeostatic bone and cartilage turnover (Kurowska-Stolarska and Alivernini, 2017). In RA, macrophage numbers and activation are increased, and the cells are thought to be key contributors to the chronic inflammatory state.

Resident synovial macrophages originate from both embryonic cells and bone marrow (BM). Those derived from embryonic cells are termed F4/80+CD11b- embryonic resident synovial macrophages (ESM) and can be detected as early as the mid-embryonic stage E12.5 and increase by proliferation (Tu et al., 2019). BM-derived synovial macrophages (BMSM) are F4/80-CD11b+ and can be detected from the late-embryonic stage (E18.5). ESM were found to be radioresistant, had the highest phagocytic capacity and expressed the anti-inflammatory cytokines IL4 and IL10, while BMSM expressed more of the inflammatory cytokines IL1ß and TNF (Tu et al., 2019).

After birth, these populations converge into one F4/80+CD11b+ population of synovial macrophages (Tu et al., 2019), whose numbers are maintained independently of monocytes. They can be classified into 3 different populations: CX_3CR1+ and 2 CX_3CR1- populations (Culemann et al., 2019). The Trem2+ CX_3CR1+ resident population accounts for 40% of synovial macrophages (**Figure 1.2**), and tight junctions between these cells form a physical barrier that acts as an immunological barrier to protect the joint. They have a half-life of 5 weeks and are replenished from MHC-II+CX_3CR1- interstitial macrophages, independently of monocytes. This interstitial macrophage population also gives rise to anti-inflammatory *Retnla*+ CX_3CR1- alternatively activated macrophages.

In RA, MHC-II+CX_3CR1+ interstitial macrophages expand by proliferation. Although the number and anti-inflammatory function of CX_3CR1+ resident macrophages is not affected in RA, CX_3CR1+ resident macrophages can become activated by, for example, the formation of immune complexes in RA, which disrupt tight junctions and so impair the barrier function of interstitial macrophages and allow increased immune infiltration into the joint (Culemann et al., 2019). Moreover, Ly6C+ pro-inflammatory monocyte-derived macrophages are also recruited to the joint. These macrophages are present in high numbers in RA and their abundance correlates with joint damage (Mulherin et al., 1996). They produce various chemokines (Yeo et al., 2016) that recruit other immune cells and cytokines (Kinne et al., 2007). For example macrophages are the main source of TNF in RA (Feldmann et al., 1996).

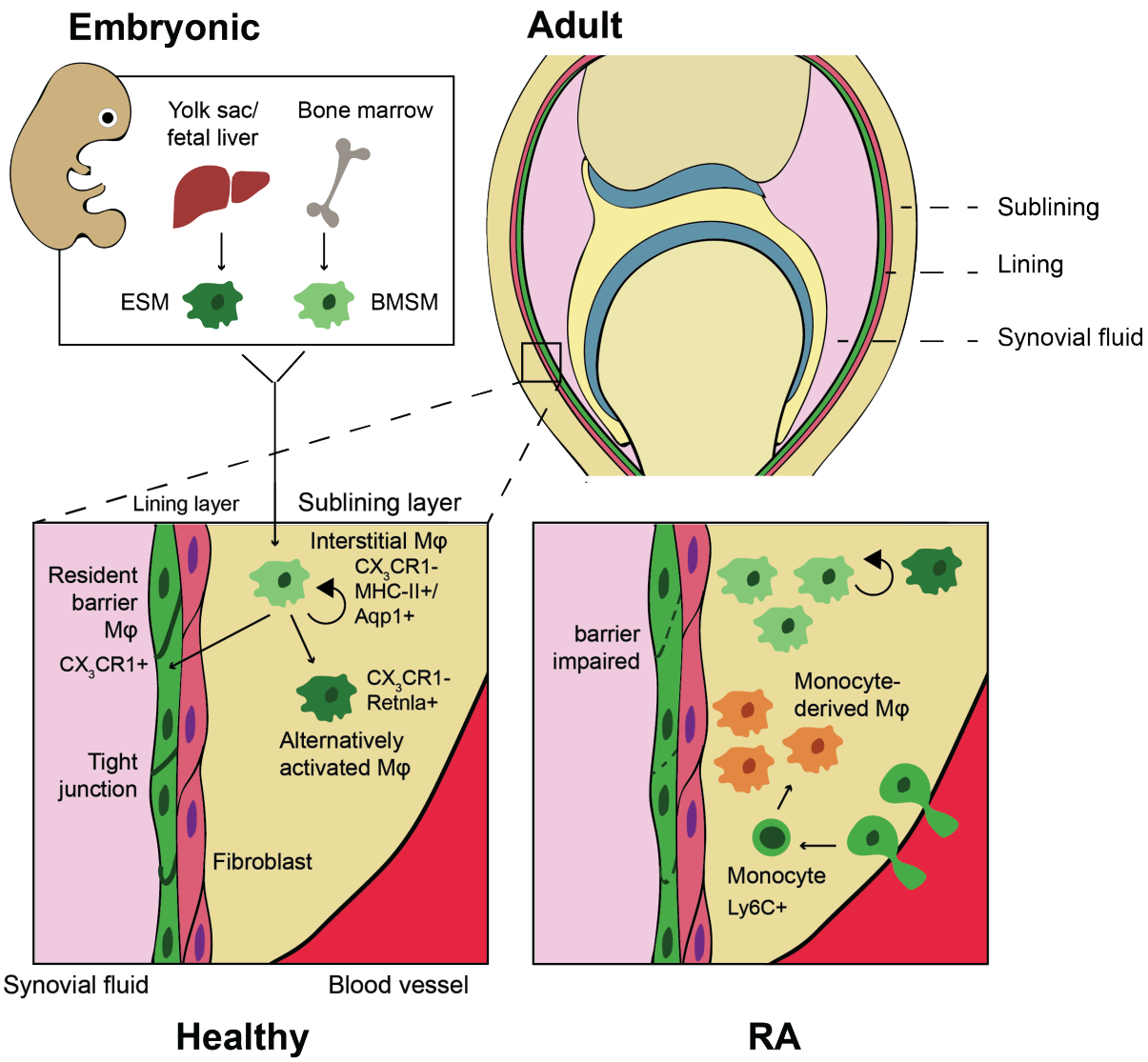


Figure 1.2. Macrophage populations in the joint.

Macrophages in the joint originate from both the embryonic foetal liver/yolk sac (embryonic synovial macrophages, ESM) and bone marrow (bone marrow synovial macrophages, BMSM). Interstitial macrophages in adult joints replenish independently of the bone marrow and give rise to resident barrier macrophages and alternatively activated macrophages. Macrophage numbers are increased in RA due to proliferation of interstitial macrophages and influx of monocytes that differentiate into macrophages (Culemann et al., 2019).

Until recently little was known about the role of function of resident macrophages populations during RA. Human tissue resident macrophages (but not monocyte-derived macrophages) express MerTK, CD206 and CD163 (Kurowska-Stolarska and

Alivernini, 2017; Singh et al., 2004); human homologs of Trem2+ CX_3CR1+ resident barrier macrophages and *Retnla*+ CX_3CR1-alternatively activated macrophages were reported that are respectively MERTK+ $TREM2^{high}$ MERTK+ $FOLR2^{high}$ LYVE1+ (Alivernini et al., 2020). The authors also demonstrated the protective effect of these resident macrophage populations in the joint, as they are increased during disease remission and their abundance negatively correlated with the disease activity score 28 (Alivernini et al., 2020). Moreover, the ratio MerTK+CD206+ to MerTK-CD206- macrophages and the percentage of MerTK+CD206+ were able to predict disease flare. The protective effect might be explained by differences in the secretion of (anti)-inflammatory mediators. For example, MerTK+ resident synovial macrophages produced lower levels of inflammatory cytokines and high levels of the lipid mediator resolvin D1, which is involved in the resolution of inflammation, compared to MerTK- synovial macrophages (Alivernini et al., 2020).

However, it is important to note that cytokines, such as TNF, in the microenvironment can also affect the activation state of macrophages independent of their origin. Recruited inflammatory (M1) macrophages can even acquire a reparative (M2) phenotype in the resolution phase (Misharin et al., 2014).

1.1.3.5. Dendritic cells

Dendritic cells can be divided into classical/myeloid DCs (cDC) and plasmacytoid DCs (pDC) (Satpathy et al., 2012). Immature cDCs efficiently endocytose antigens and their surface expression of MHC-I, -II and costimulatory molecules such as CD80 and CD86 is low. When they encounter danger signals, for example during infection, signalling via pattern-recognition receptors (e.g. the toll-like receptor TLR4) induces DC maturation, which is associated with upregulation of surface expression of MHC-I, -II, costimulatory molecules, and inflammatory cytokines, as well as CCR7-dependent migration to the draining lymph nodes (Dalod et al., 2014). Here, they efficiently present antigens on MHC-I (cDC1) or MHC-II (cDC2) to the T-cell receptor (TCR) on T-cells leading to T-cell activation. In addition to antigen-presentation, T-cells require binding of costimulatory molecules (e.g. binding of CD80 or CD86 to CD28 on T-cells) and inflammatory cytokines that are upregulated upon maturation to become activated (Curtsinger and Mescher, 2010). pDCs are less efficient in antigen presentation, but can secrete high levels of type I IFN and are important for anti-viral immune responses (Chistiakov et al., 2014).

High numbers of both DC subsets are found in arthritic joints and draining lymph nodes (Lebre et al., 2008), and the number of DCs in RA synovium is higher than in osteoarthritic synovium (Yu and Langridge, 2017). In addition, they have a more activated, mature phenotype than OA DCs, and show increased T-cell activation *ex vivo* (Moret et al., 2013). They also secrete higher levels of the chemokines CCL17, CXCL19 and CXCL10, which might contribute to increased immune cell influx into the joint. Monocyte-derived DCs from patients with RA also secrete higher levels of the inflammatory cytokines IL6 and IL23, which can affect T-cell differentiation (Estrada-Capetillo et al., 2013).

1.1.4. Adaptive immune system in RA

1.1.4.1. T-cells

T-cells are characterised by expression of the T-cell co-receptor CD3, which is involved in T-cell receptor (TCR) signalling (Guy and Vignali, 2009). The bulk of T-cells are CD4+ or CD8+, where CD8+ (or cytotoxic) T-cells are primarily equipped to kill pathogen-infected and damaged cells, while CD4+ T-cells can activate various cell types (e.g. innate, non-immune, B-cells and CD8+ T-cells).

The genetic association of certain HLA loci with RA indicates that T-cells are involved in the pathogenesis of RA as the only known function of MHC molecules is to present antigens to T cells. Consistent with this concept, T-cell deficient mice are protected from AIA (Brackertz, Mitchell and Mackay, 1977b; Brackertz, Mitchell, Vadas et al., 1977). Depletion of CD4+ T-cells prevented AIA, while depletion of CD8+ T-cells did not affect AIA (Petrow et al., 1996; Pohlers et al., 2004; Nissler et al., 2004). In contrast, treatment with anti-CD4 diminished induction of arthritis in the CIA model (Chu and Londei, 1996), but had no effect on the severity of established CIA (Yoshino and Cleland, 1992; Alzabin and Williams, 2011), potentially due to shifts in T-cell subsets during the course of CIA. The T helper (Th) 1, Th2, Th17 and regulatory T-cells (Treg) subtypes have been most studied in RA and are discussed in more detail below (**Figure 1.3**).

The presence of IL12 stimulates CD4+ T-cells to differentiate to the Th1 subset, through expression of the T-box transcription factor T-bet, which enables them to produce IFNγ (Zhu and Paul, 2008). This IFNγ+ Th1 subtype was the first subtype shown to be increased in RA (Miltenburg et al., 1992; Dolhain et al., 1996) and these cells are thought to aggravate RA by promoting macrophage activation and TNF production (Mosser and Edwards, 2008). In contrast, *Il12p35*$^{-/-}$ mice have aggravated

CIA (Murphy et al., 2003), while injection of IL12 alleviates CIA (Hess et al., 1996). Mice lacking the *Ifnγr*$^{-/-}$ or treated with anti-IFNγ antibodies also have accelerated CIA (Vermeire et al., 1997; Manoury-Schwartz et al., 1997), and *Ifnγ*$^{-/-}$ mice exhibit increased AIA severity (Irmler et al., 2007). Mechanistically, it was shown that IFNγ inhibits pro-arthritic Th17 development and promotes protective Treg function (Harrington et al., 2005; Kelchtermans et al., 2005).

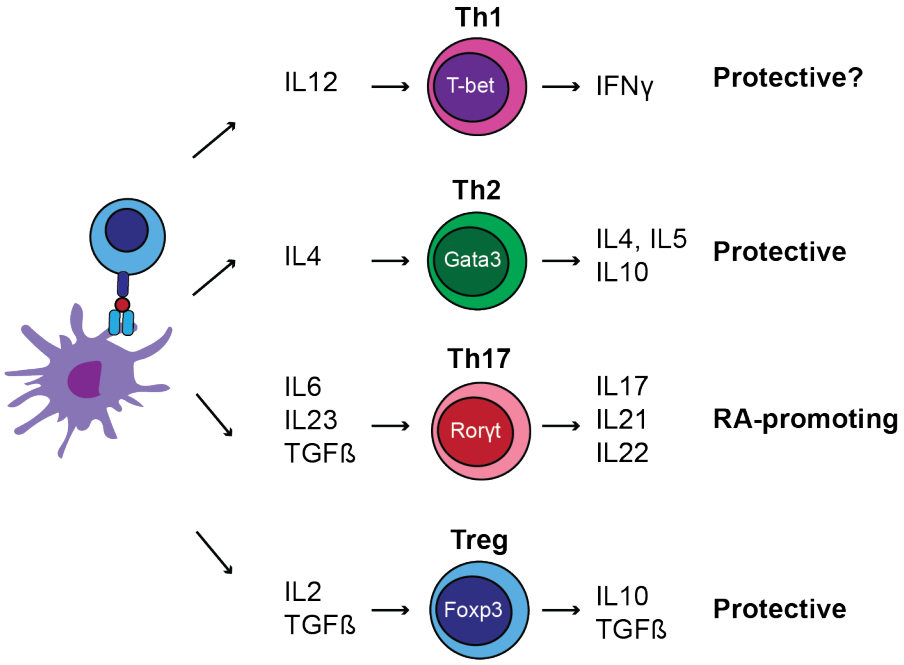


Figure 1.3. CD4+ T-cells in rheumatoid arthritis.
IL12 is responsible for the differentiation of Th1 cells. IL4 promotes Th2 differentiation, IL6, IL23 and TGFß induce the differentiation of RA-promoting Th17 cells. In contrast, IL2 and TGFß skew towards RA-protective Treg differentiation.

IL4 promotes differentiation towards the Th2 subset through the expression of GATA binding protein-3 (GATA3), which augments the expression of IL4, IL5 and IL10 (Zhu and Paul, 2008). Th2 cells are not thought to play an important role in the pathogenesis of RA as evidenced by the fact that they are not increased (Miltenburg et al., 1992; Dolhain et al., 1996). Rather, they play a protective role as expansion of this subset by helminth infection reduces in the K/BxN serum transfer model by

promoting anti-inflammatory macrophage differentiation through IL4 and IL13 (Chen et al., 2016).

Th17 differentiation is driven by IL6, IL23 and transforming growth factor ß (TGFß), which induce activation of the retinoic acid-related orphan receptor (RORγt), and promote production of IL17A/F, IL21 and IL22 (Zhu and Paul, 2008). IL17 promotes inflammation by affecting multiple cell types in the joint. It enhances inflammatory cytokine production by macrophages and fibroblasts (Ogura et al., 2008; Jovanovic et al., 1998), recruits neutrophils (Kolls and Lindén, 2004) and is involved in osteoclast differentiation leading to bone erosion (Sato et al., 2006). The RA-promoting function of Th17 cells was highlighted by a study showing reduced severity and incidence of CIA in *Il17a*$^{-/-}$ mice (Nakae et al., 2003). Blocking IL17 after the onset of arthritis also reduced disease severity in CIA (Lubberts et al., 2004) and AIA (Egan et al., 2008).

In contrast, the presence of IL2 and TGFß stimulates the differentiation of immunosuppressive Tregs, characterised by the expression of CD25 and forkhead box protein 3 (Foxp3) and the secretion of IL10 and TGFß (Zhu and Paul, 2008). Depletion of Tregs using monoclonal antibodies against CD25 aggravated CIA (Morgan et al., 2003), while adoptive transfer of this population ameliorated CIA (Morgan et al., 2005). Inflammatory mediators such as TNF have been shown to impair the immune suppressive function of Tregs (Valencia et al., 2006).

CD8+ T-cells also produce large amounts of IFNγ, but depletion of CD8+ T-cells has no effect on the initiation of CIA (Ehinger et al., 2001). It has been speculated that CD8+ T-cells may play a suppressive role in later stages of disease through production of IFNγ (Suzuki et al., 2008).

1.1.4.2. B-cells

B-cells are characterised by the expression of CD19 and are involved in antibody production, antigen presentation and cytokine production. Depletion of B-cells ameliorates RA (Edwards et al., 2004), but the effect of B-cells in not modelled in all mouse models of arthritis. For example, while AIA was not affected in μMT/μMT mice that lack mature B-cells (Wong et al., 2006), CIA does not develop in B-cell deficient mice (Svensson et al., 1998).

1.1.5. Fibroblasts

Fibroblasts deposit extracellular matrix and contribute to the structural integrity of tissues (Lynch and Watt, 2018). However, their abundance is increased in RA and correlates with disease severity (Izquierdo et al., 2011), as activated fibroblasts adopt a pro-inflammatory and matrix-degrading phenotype (Pap et al., 2000). Unlike immune cells, fibroblasts were not considered to be heterogeneous, but distinct fibroblast subtypes were recently identified (Mizoguchi et al., 2018). Croft et al. (2019) demonstrated that these subtypes have different functions in RA. For example, fibroblast activation protein α (FAPα)+ THY1+ sub-lining fibroblasts promote inflammation, while and FAPα+ THY1- fibroblasts mediate bone and cartilage damage. Different macrophages subsets have been shown to shape the phenotype of fibroblasts. For example, MerTK+CD206+ macrophages promoted expression of genes (e.g. collagen genes and *TGFB1*) involved in tissue repair in fibroblasts, while MerTK-CD206- macrophages induced matrix metalloproteases, chemokines and inflammatory cytokines (Alivernini et al., 2020).

1.1.6. Cytokines in RA

The innate and adaptive immune cell types described in **Chapter 1.1.3 and 1.1.4** produce a plethora of chemokines and cytokines that regulate and orchestrate the immune response. For example, the chemokines recruit more immune cells to the site of inflammation, and the network of cytokines is responsible for communication between immune cells and regulation of their function. The balance between pro- and anti-inflammatory cytokines is critically important for the maintenance of homeostasis, while excess levels of pro-inflammatory cytokines contribute to autoimmune diseases such as RA (Schett et al., 2013). Genetic polymorphisms in cytokines, such as TNF and IL10, have been associated with RA (Van Der Helm-van Mil et al., 2005). Moreover, the efficacy of anti-TNF (Nam et al., 2014) and anti-IL6 (Gabay et al., 2013; Burmester et al., 2017) therapy indicates the importance of cytokines in RA pathogenesis. However, there are limitations to the efficacy of anti-TNF therapy. For example, 30-40% of patients exhibit only partial or temporary responses to anti-TNF therapy (Bek et al., 2017; Lloyd et al., 2010; Buch et al., 2007), and while anti-TNF biologics strongly reduce bone erosion, they are less effective at stopping cartilage degradation (Keystone et al., 2004; Westhovens et al., 2009; Zwerina et al., 2004). Finally, even patients who become asymptomatic can still exhibit progression of joint damage (Lillegraven et al., 2012; Genovese and Kremer, 2004). Novel approaches are thus required to improve treatment of RA.

There is increasing evidence that cytokines, chemokines and other disease-modifying factors are regulated by interaction with HSPGs. Therefore, I will explore the role of HSPGs in RA in this thesis.

1.2. Heparan sulfate as a regulator of inflammation

HSPGs are composed of a core protein that carries one or more linear, covalently-attached HS polysaccharide side chains, consisting of N-acetylglucosamine (GlcNAc) and hexuronic acid disaccharide repeats. These core proteins can either be secreted into the extracellular matrix, like agrin (AGRN), perlecan (HSPG2) and type XVIII collagen (COL18A1), or membrane-bound such as syndecans (SDC), glypicans (GPC) and CD44v3. These core proteins can carry 1-4 HS chains that are composed of 40-300 sugar residues (Sarrazin et al., 2011). The membrane-bound core proteins betaglycan (TGFBR3) and neurophilin-1 (NRP1) are classified as 'part-time' HSPGs as they can also exist without an HS-chain (Sarrazin et al., 2011). It is important to note that these core proteins can also bind ligands and have complex functions that are independent of their HS chains (Sarrazin et al., 2011). However I will focus on the function of the HS chains in this thesis.

1.2.1. Heparan sulfate biosynthesis

These HS side chains are synthesised by a template-independent mechanism, in which up to 25 biosynthetic enzymes (**Figure 1.4**) act together to generate HS chains that are extensively modified by sulfation, enabling interaction with proteins through their positively charged amino acid residues (Arg and Lys) (Billings and Pacifici, 2015). The relative abundance of these 25 HS biosynthesis enzymes is thought to determine HS structure (Sugahara and Kitagawa, 2002; Kreuger and Kjellén, 2012), and changes in their expression have been correlated with changes in HS structure and function during development (Häcker et al., 2005), with age (Minh Bao Huynh et al., 2012; M. B. Huynh et al., 2012; Ghadiali et al., 2017; Yamada et al., 2017) and in many pathological contexts (Lindahl et al., 2013).

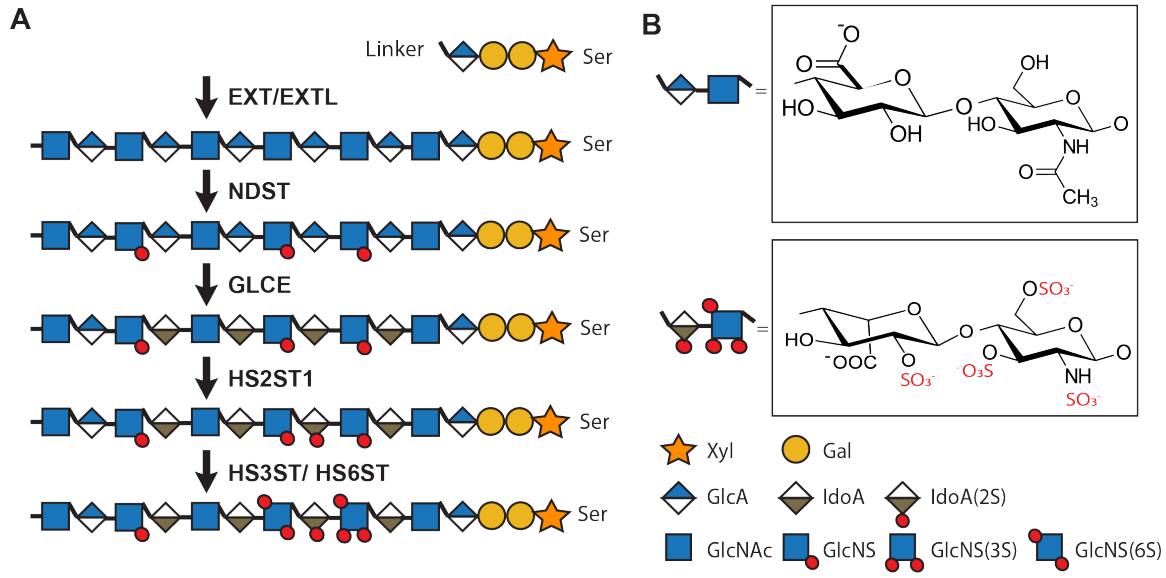


Figure 1.4. Heparan sulfate biosynthesis enzymes.

HS chains are attached to serine residues of the core protein in the Golgi apparatus via a tetrasaccharide linker region, which consists of a xylose, 2 galactose and a glucuronic acid (GlcA) residue. Up to 25 different enzymes are involved in the template-independent synthesis of HS chains. HS chains are elongated by the exostosis (EXT) and exostosin-like (EXTL) glycosyltransferase enzyme family through alternating the addition of N-acetyl glucosamine (GlcNAc) and GlcA. Modification of the HS chain is initiated by the N-deacetylase/ N-sulfotransferase (NDST) family that deacetylates GlcNAc, followed by N-sulfation. Glucuronic acid epimerase (GLCE) can convert GlcA residues into iduronic acid (IdoA) and a 2-O-sulfotransferase (HS2ST1) can then sulfate IdoA. The 6-O-sulfotransferases (HS6ST1-3) and 3-O-sulfotransferases (HS3ST1-6) can sulfate glucosamine. As their isoforms have slightly different substrate specificities and are highly evolutionarily conserved, they are thought to be particularly important for the formation of a complex sulfation pattern that regulates the affinity of protein binding. Post-synthesis, the endosulfatases SULF1 and SULF2 can remove 6-O sulfate groups and heparanase can cleave the HS chains into small oligosaccharides. This figure is adapted from (Swart and Troeberg, 2019).

1.2.1. Ligand binding to heparan sulfate

HSPGs can bind and fine-tune the biological effects of these chemokines, cytokines and growth factors. For example, HS can establish gradients (**Figure 1.5**), protect proteins from proteolysis, fine-tune their bioactivity (e.g. by chemokine oligomerisation) and influence receptor binding (Parish, 2006; Simon Davis and Parish, 2013). This implies that HSPGs are potentially critical regulators of inflammation, but the roles of specific HSPG genes in health and disease has not been defined. To identify genes of interest, it is important to appreciate the complex pathway of HSPG biosynthesis.

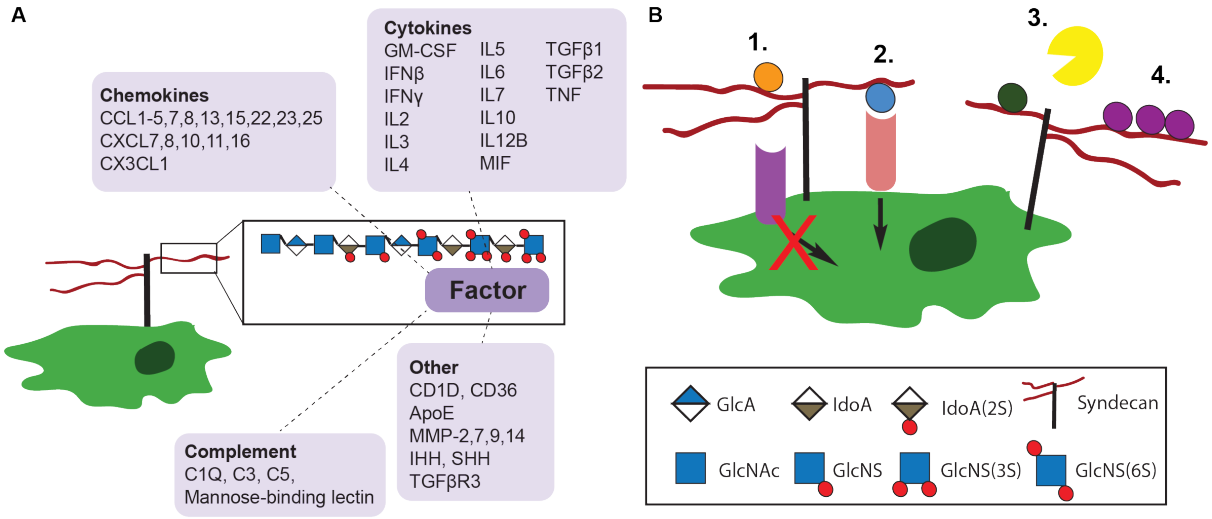


Figure 1.5. Binding of inflammatory mediators to heparan sulfate.
Ori et al. (2011) comprehensively reviewed the >400 different proteins that are known to bind to HS. **A.** Representative examples of HS-binding inflammatory mediators are shown, including examples of HS-binding chemokines, cytokines and complement factors. **B.** Binding to HS can have a variety of effects on ligands. It can prevent binding to cognate receptors (1), function as a co-receptor for signalling (2), inhibit degradation of the ligand (3) or enable formation of ligand gradients (4). For many of HS ligands, the molecular and cellular consequences of binding have yet to be elucidated. Figure adapted from Swart and Troeberg (2019).

1.2.2. Heparan sulfate biosynthesis enzyme expression by immune cells

An RNA-Seq study by Monaco et al. (2019) showed that different types of PBMCs have different patterns of expression of HS core proteins and biosynthesis enzymes, indicating that they might have distinct HS compositions (**Figure 1.6**).

Although HS is widely appreciated to have the potential to regulate inflammation through modulation of chemokine and cytokine abundance, localisation and activity, not much is currently known about the role of HS on immune cells *in vivo*. A few key studies have used *Ndst1*-deficient mice to demonstrate that HS affects immune cell recruitment and function. In this section, I review the studies on *Ndst1*$^{-/-}$ mice, as well as the limited information available on the role of other HS genes in immune cells (**Table 1.2**).

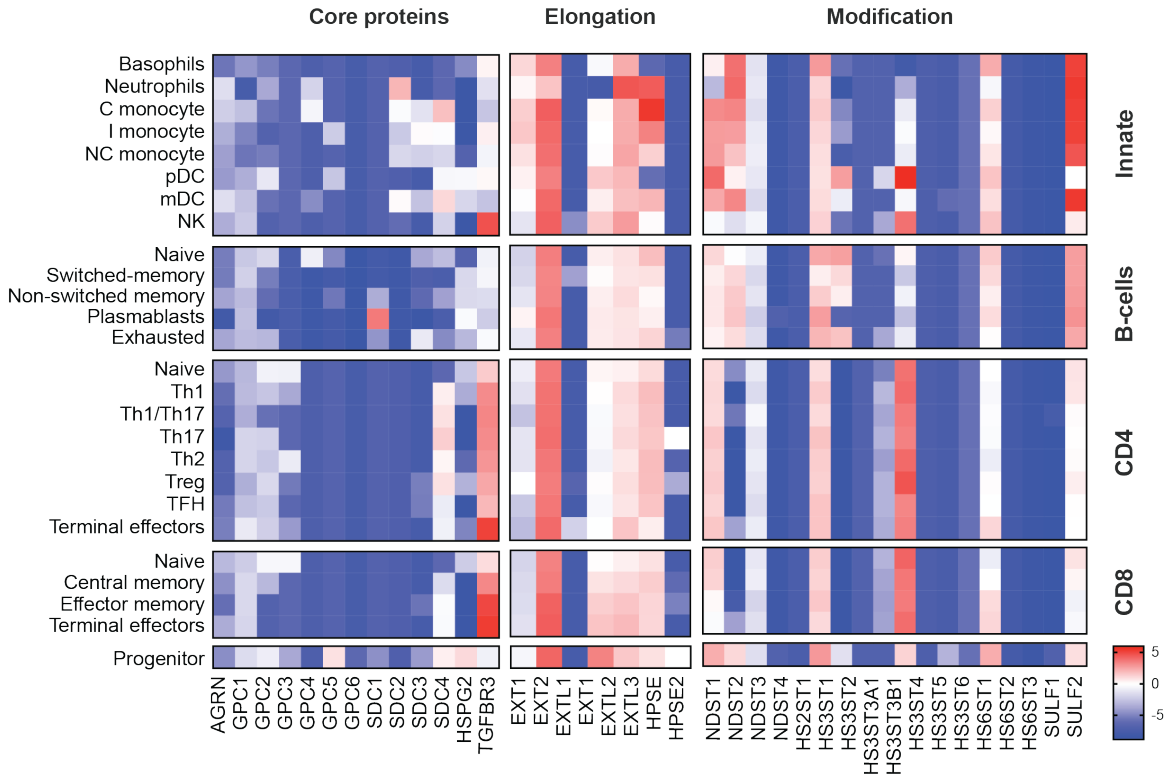


Figure 1.6. Expression of heparan sulfate-associated genes in human PBMCs.
Monaco et al. (2019) performed RNA-Seq on 29 immune cell types isolated from healthy human donors by flow sorting. I analysed this publicly-available dataset to visualise the relative expression the 38 heparan sulfate core proteins, elongation and biosynthetic enzymes. Abbreviations: Tfh, T follicular helper; Tregs, T regulatory; Th, T helper; C, classical; I, intermediate; NC, non-classical; mDCs, myeloid dendritic cells; pDCs, plasmocytoid dendritic cells.

Table 1.2. Overview of studies examining the role of heparan sulfate genes in immune responses.

CD19Cre^{+} (cre recombinase in B-cells), *LysMCre*$^{+}$ (cre recombinase in myeloid cells), *Prox1CreERT2*$^{+}$ (cre recombinase in lymphatic endothelial cells), *SFTPC-rtTA*$^{+/-}$*TetO-cre*$^{+/-}$ (cre recombinase in respiratory endothelium), *TekCre*$^{+}$ (cre recombinase in endothelial cells and early haematopoietic progenitors).

Gene	Model	Phenotype observed	Reference
Ext1	*Ext1*$^{f/f}$*CD19Cre*$^{+}$	• No effect on B-cells	Garner et al. (2008)
Glce	Foetal liver transplantation of *Glce*$^{-/-}$ cells in *Rag-2*$^{-/-}\gamma_c^{-/-}$	• Impaired B-cell survival	Reijmers et al. (2011)
Ndst1	*Ndst1*$^{f/f}$*TekCre*$^{+}$	**Impaired leukocyte infiltration in:** • Peritonitis, contact dermatitis • Asthma • Chronic asthma • Diabetic nephropathy • Glomerulonephritis	Wang et al. (2005) Zuberi et al. (2009) Ge et al. (2014) Talsma et al. (2018)
	Ndst1$^{f/f}$*Prox1CreERT2*	**Impaired immunisation** • Reduced DC migration	Rops et al. (2014) Yin et al. (2014)
	Ndst1$^{f/f}$*LysMCre*$^{+}$	• Increased atherosclerosis/obesity • **Macrophages more inflammatory**	Gordts et al. (2014)
		• Reduced tumour size, **DC migration, but more matured**	El Ghazal et al. (2016)
	Ndst1$^{f/f}$*IckCre*$^{+}$*Ndst2*$^{-/-}$	• Mild T-cell hyper-responsiveness to CD3	Garner et al. (2008)
Hs2st1	*Hs2st1*$^{f/f}$*TekCre*$^{+}$	• Increase leukocyte extravasation in a peritonitis model – **compensatory upregulation of *Ndst1*** • More susceptible to B *Streptococcus* infection **– reduced neutrophil function**	Axelsson et al. (2012) Xu et al. (2015)
Sdc1	*Sdc1*$^{-/-}$	**Increased immune infiltration in:** • Allergic airway model • LPS endotoxemia • Dextran sodium colitis • Delayed type hypersensitivity	J. Xu et al. (2005) Hayashida et al. (2009) Floer et al. (2010) Masouleh et al. (2009)
Sdc4	*Sdc4*$^{-/-}$	• LPS hypersensitivity – **impaired inhibition of IL1 production by TGF** • Reduced tumour size, **less DC migration, but more matured**	Ishiguro et al. (2001) El Ghazal et al. (2016)
Sulf2	*Sulf1*$^{f/f}$*Sulf2*$^{f/f}$ *SFTPC-rtTA*$^{+/-}$*TetO-cre*$^{+/-}$	**Increased neutrophil infiltration** • Lung injury model	Yue (2017)

1.2.2.1. Endothelial HS and leukocyte extravasation

Immune infiltration into tissues during infection and chronic inflammatory diseases such as RA is broadly regulated by three steps. First, cytokines upregulate P- and L-selectin on the luminal side of the endothelium to slow down the rolling of leukocytes. Secondly, chemokines bind to the endothelium and activate G protein-coupled receptors and integrins to establish firm adhesion. Afterwards, leukocytes can migrate through the endothelium to the site of inflammation.

HS on endothelial cells has long been appreciated to affect leukocyte extravasation. For example, studies on mice with *Ndst1* deficiency showed the importance of HS for leukocyte extravasation in models of peritonitis, contact dermatitis, air pouch inflammation (Wang et al., 2005), asthma (Zuberi et al., 2009; Ge et al., 2014), diabetic nephropathy (Talsma et al., 2018) and glomerulonephritis (Rops et al., 2014). Wang *et al.* demonstrated for the first time that neutrophil extravasation was reduced by *Ndst1* deficiency on endothelial cells but not on leukocytes using *Ndst1*$^{f/f}$*TekCre*$^{+}$ mice and bone marrow chimeras. This showed that *Ndst1*-deficiency affected all steps of leukocyte extravasation. Weaker binding of leukocytes to L-selectin increased their rolling speed, and transcytosis of the chemokine IL8 to the luminal endothelial side as well as presentation of IL8 on HS were decreased. In contrast, *Hs2st1* deficiency was found to increase leukocyte extravasation in a peritonitis model, which was attributed to a compensatory upregulation of *Ndst1* (Axelsson et al., 2012).

Endothelial HS has also been shown to be important for trafficking of DCs to lymph nodes. Mice deficient for *Ndst1* in lymphatic endothelial cells (*Ndst1*$^{f/f}$*Prox1CreERT2*$^{+}$) or all endothelial cells (*Ndst1*$^{f/f}$*TekCre*$^{+}$) exhibited reduced migration of DCs, and consequently reduced CD8 (but not CD4) T-cell responses in an ovalbumin (OVA) immunisation model (Yin et al., 2014). Mechanistically, HS was found to be important

for the oligomerisation of CCL21 (which promotes DC maturation and migration) and its presentation to CCR7 on DCs (Yin et al., 2010, 2014).

1.2.2.2. Function of HS expressed by leukocytes

In contrast to its well-known role on endothelial cells, the effects of HS expressed by leukocytes on immune cell function is less well studied and this has been highlighted as an important area for further exploration.

The importance of HS in neutrophil function is exemplified by the fact that *Hs2st1* deletion using TekCre^{+} increased susceptibility of mice to group B *Streptococcus* infection, with reduced anti-bacterial activity and NET formation (D. Xu et al., 2015). Phagocytosis, ROS production and secretion of proteases were unaffected. In contrast to its effect in neutrophils, *Hs2st1* deficiency did not affect macrophage response to bacterial challenge (D. Xu et al., 2015).

In myeloid (*LysMCre*) cells, *Ndst1* deficiency increased atherosclerosis and diet-induced obesity (Gordts et al., 2014). This was associated with an increase in the number of macrophages with a greater inflammatory gene expression profile. 20% of the genes with altered expression in *Ndst1*$^{-/-}$ myeloid cells contained the interferon regulatory factor motif ISGF3, indicating that type-I interferon signalling was particularly affected by *Ndst1* deficiency. The authors proposed that sulfated HS sequesters IFNß, while the reduction in sulfation caused by *Ndst1* deficiency increased the bioavailability of IFNß, allowing it to promote inflammatory gene expression.

Ndst1 has also been shown to be important for DC function. Dendritic cells from Ndst1$^{f/f}$*LysMCre* mice were found to have a more mature phenotype, but trafficking to lymph nodes and tumour growth was reduced (El Ghazal et al., 2016). This might

indicate that HS sulfation is required for the activity of CCR7, which regulates DC maturation and migratory responses to chemokines.

T-cell development appeared to be unaffected in *Ndst1*$^{f/f}$*lckCre*$^{+}$*Ndst2*$^{-/-}$ mice, but these T cells were hyper-responsive to low-dose CD3 activation (Garner et al., 2008). This might be due to impaired sequestration of IL2 in *Ndst1/Ndst2*-deficient T-cells, leading to increased bioavailability of IL2 and amplified T-cell proliferation (Miller et al., 2012).

B-cell maturation and plasma cell generation were shown to be impaired in *Glce*-deficient mice, resulting in attenuated antibody responses (Reijmers et al., 2011). The mechanism was thought to be due to a reduction in B-cells responses to the HS-binding proliferative mediator APRIL.

1.3. Sulfatases

1.3.1. 6-O-sulfation regulates signalling pathways

During HS biosynthesis, sulfate groups can be added to the N-, 2-O-, 3-O- and 6-O-position of the saccharide rings by sulfotransferase enzymes. 6-O sulfation is the only sulfation pattern that can be post-synthetically fine-tuned, and removed in the extracellular environment (El Masri et al., 2017). 6-O-sulfate groups can be added in the Golgi apparatus by HS6ST1, HS6ST2 and HS6ST3, or removed by the extracellular sulfatases SULF1 and SULF2 (Morimoto-Tomita et al., 2002).

This modification is thus under uniquely strict extracellular control, indicating it is likely to have a central role in regulating HS activity. Indeed, 6-O-sulfation has been shown to have substantial effects on the binding of HS to many of its ligands, and so also to HS regulation of ligand bioactivity. For example, removal of 6-O sulfate by SULF1 or SULF2 has been shown to diminish fibroblast growth factor (FGF) 1 and

FGF2 signalling (A. Seffouh et al., 2013; Uchimura et al., 2006; Dai et al., 2005) as well as TGFß binding and signalling (Chen et al., 2017; Yue et al., 2013).

The mechanism through which 6-O de-sulfation prevents FGF signalling is well defined. Here, HS functions as a cofactor during binding of FGF to the FGF receptor (FGFR) and forms a ternary FGF/HS/FGFR ternary complex (**Figure 1.7**) that activates intracellular kinase domain of FGFR by phosphorylation (Ornitz and Itoh, 2015). However, the magnitude of the effect seems to be dependent on the extend of 6-O desulfation, as complete desulfation abrogated both FGF1 and FGF2 signalling, while more physiological partial desulfation only affected FGF1 signalling (A. Seffouh et al., 2013).

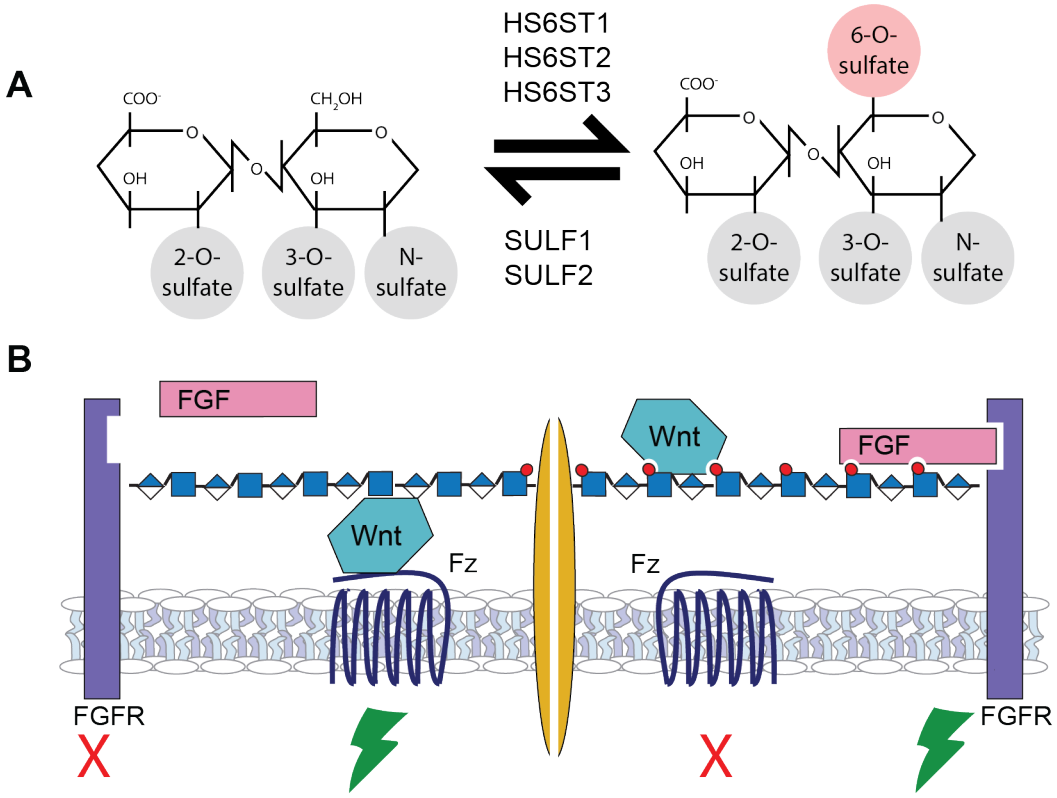


Figure 1.7. 6-O-sulfation can positively or negatively affect signalling.
A. SULF2 catalyses the removal of 6-O sulfate groups from HS. **B**. Wnt signalling is positively regulated by SULF2, as 6-O desulfation allows formation of the Fz/Wnt/HS complex required for active signalling. In contrast, SULF2 negatively regulates FGF signalling, as the FGFR/FGF/HS complex required for signalling can only be formed in the presence of 6-O sulfate groups.

In contrast, the sulfatases can positively regulate signalling by bone morphogenetic protein (BMP) (Otsuki et al., 2010), glial cell line-derived neurotrophic factor (GDNF) (Ai et al., 2007), vascular endothelial growth factor (VEGF) (Korf-Klingebiel et al., 2019) and Wnt (Nawroth et al., 2007). Mechanistically the regulation of Wnt signalling by sulfatases is most defined. 6-O desulfation weakens the Wnt/HS interaction (Ai et al., 2003), which enhances signalling through the HS/Wnt/Frizzled (Fz) complex (**Figure 1.7**). However, the signalling pathways that are affected by the sulfatases SULF1 and SULF2 have not been systematically studied and it is very likely that they are involved in the regulation of many more pathways.

1.3.2. Sulfatase structure and biochemical characterisation

Before reviewing studies on the biological effects of SULF1 and SULF2 (**paragraph 1.3.3**), I will briefly describe their structure and the biochemistry of their activities. *Sulf1* and *Sulf2* are both highly conserved (approximately 95% homology) between mice and humans, but there is only 65% homology between *Sulf1* and *Sulf2* in each species. The sulfatases are synthesised as a pre-pro-protein and contain four domains (**Figure 1.8**): a signal peptide, catalytic domain, hydrophilic highly basic domain (HD) and a C-terminal domain (Morimoto-Tomita et al., 2002; Tang and Rosen, 2009). After removal of the signal peptide from the pre-protein, the 133 kDa (I. Seffouh et al., 2019) pro-protein is cleaved in the HD domain by furin-type proteases to generate a 75 kDa N-terminal and a 50 kDa C-terminal subunit, which are linked by a disulfide bond (Nagamine et al., 2010). The predicted molecular weight based on the amino acid sequence is 98 kDa, indicating that the enzyme is highly glycosylated since glycosylation accounts for 35% of the molecular weight. This might be important for localisation and enzymatic activity (Ambasta et al., 2007).

Little is known about the C-terminal domain, which is thought to be involved in glucosamine recognition due to its sequence homology with lysosomal glucosamine-6-sulfatase (Tang and Rosen, 2009; Ai et al., 2006). The catalytic and hydrophilic domain are more extensively studied (I. Seffouh et al., 2019), with both known to be important for the endosulfatase activity (i.e. removal of 6-O sulfate groups).

The catalytic domain contains a conserved Cys residue, which is post-translationally modified into N-formylglycine (FGly) and is essential for generic sulfatase activity (arylsulfatase). In short, the active site is hydroxylated and removes 6-O sulfate in a transesterification reaction (Hanson et al., 2004). However, in the absence of the HD domain, no endosulfatase activity is observed as this domain is required for high affinity binding to HS (Morimoto-Tomita et al., 2002; Tang and Rosen, 2009).

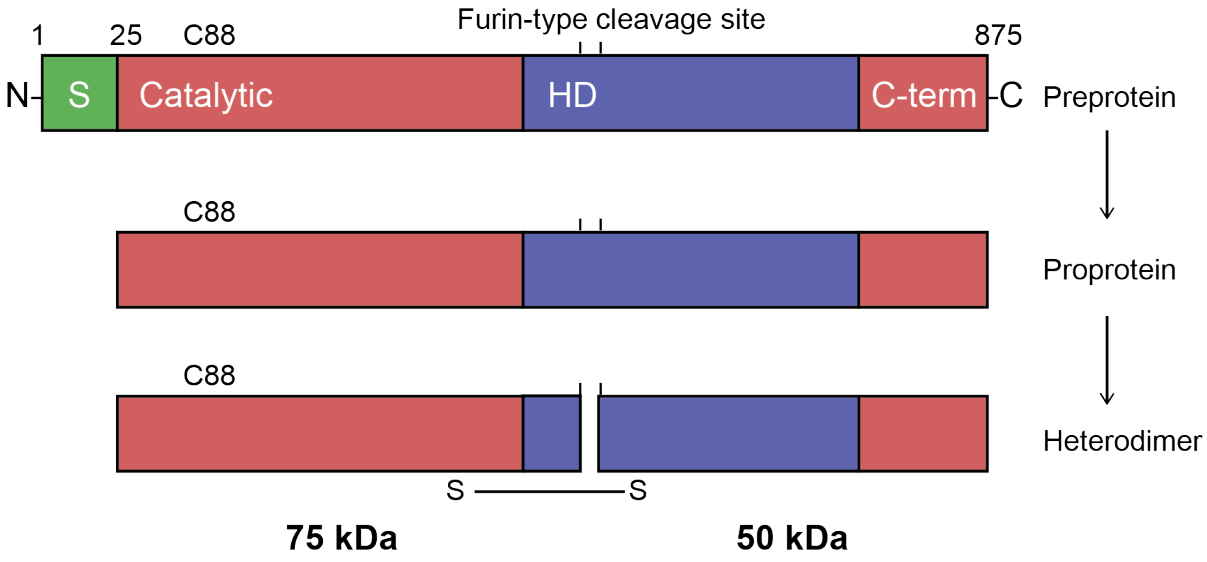


Figure 1.8. The structure of sulfatase-2.

Murine sulfatase-2 (SULF2) consists of 875 amino acids and has four domains: a signal peptide, a catalytic domain with cysteine-88 (C88) that is essential for sulfatase activity, a hydrophilic HD domain involved in heparan sulfate binding and a C-terminal domain that resembles glucosamine-6-sulfatase. Furin-type proteases cleave the proprotein into two subunits that are linked by a disulfide bond.

It is thought that the HD domain has multiple HS binding sites (Milz et al., 2013; A. Seffouh et al., 2019) that are involved in binding and positioning of HS in the catalytic domain. This domain shows poor sequence homology between SULF1 and SULF2, indicating that they have different substrate specificities. Little is currently known about substrate specificity, but the enzyme most strongly targets trisulfated hexa(2S)-GlcNS(6S) disaccharides, with reduced but detectable binding to disulfated hexa-GlcNS(6S) disaccharides (A. Seffouh et al., 2013; Pempe et al., 2012; Staples et al., 2011; A. Seffouh et al., 2019). SULFs have a high affinity (*Kd* = 4 nM) for heparin, which contains a high content of trisulfated hexasaccharides (A. Seffouh et al., 2019). They preferentially target these tri- and disaccharides towards the non-reducing end (NRE) of HS (Huang et al., 2014), which is most accessible for protein binding. Mechanistically, SULFs are thought to recessively remove 6-O-sulfate groups from the non-reducing end towards the reducing end (RE) as it moves in this direction over the HS chain (A. Seffouh et al., 2013). Upon reaching a non-sulfated (Nac) domain, the affinity of the HD domain for HS drops and the SULFs dissociate from the HS chain (**Figure 1.9**).

The abundance of the preferred trisulfated hexa(2S)-GlcNS(6S) disaccharide substrate in HS is relatively low (Staples et al., 2011), the maximum change in sulfation after desulfation by SULF1 or SULF2 is estimated to be 5-7% from *in vitro* studies (Ai et al., 2003). Nevertheless, these small changes have been shown to drastically affect binding of HS ligands and the biological activity of various signalling pathways.

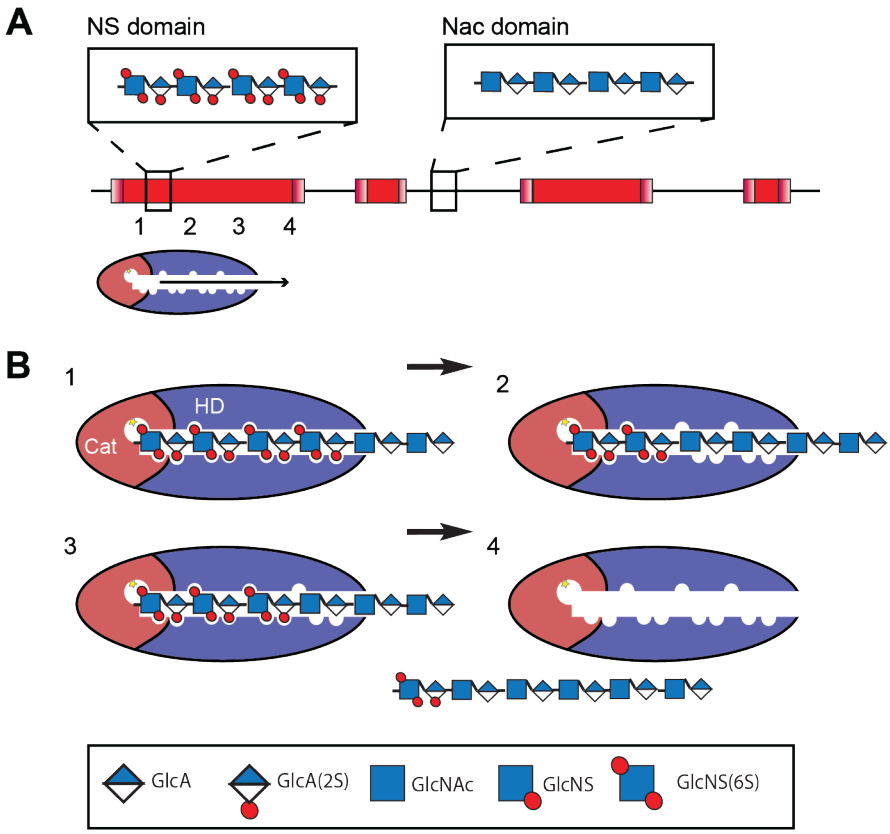


Figure 1.9. Mechanism of action of sulfatase-2 (SULF2).

Sulfatase-2 preferentially binds to GlcA/IdoA(2S)GlcNS(6S) trisulfated disaccharides via its hydrophilic domain (HD) and can processively remove 6-O-sulfate groups from the heparan sulfate (HS) chain via its catalytic domain (Cat), while moving over the HS chain from the non-reducing end (NRE) to the reducing end (RE). The affinity for HS decreases when SULF2 reaches a non-sulfated (Nac) domain, causing it to dissociate.

1.3.3. Known pathophysiological roles of SULF1 and SULF2

Sulf1 and *Sulf2* are both widely expressed, and knockout of both *Sulf1* and *Sulf2* resulted in highly penetrant perinatal lethality with oesophageal contractile dysfunction (Ai et al., 2007), skeletal and renal abnormalities (Holst et al., 2007; Lamanna et al., 2006).

In contrast, no major developmental defects were identified in either *Sulf1*$^{-/-}$ or *Sulf2*$^{-/-}$ mice (Holst et al., 2007; Lum et al., 2007; Lamanna et al., 2006; Ratzka et al., 2008). One explanation for this may be compensation between SULF1 and SULF2. For example, one study reported no apparent change in 6-O sulfation in *Sulf2*$^{-/-}$ mouse

embryonic fibroblasts (Lamanna et al., 2006), but this may be tissue-dependent as a 2-3 fold increase in 6-O-sulfated disaccharides was detected in the cerebellum of *Sulf2*$^{-/-}$ mice in another study (Kalus et al., 2015). Additionally, some effects appear to be strain-dependent, including a 20% reduction in weight and increased perinatal lethality (Lum et al., 2007; Lamanna et al., 2006). Increased lethality was suggested to be due to defects in neuronal and brain development (Kalus et al., 2015; Ai et al., 2007; Kalus et al., 2009). A global developmental delay was also recently described in a patient with a disruptive *SULF2* mutation, which was accompanied by feeding difficulties, vertebral anomalies and defects in brain development (Kirola et al., 2019).

Sulf1$^{-/-}$ and *Sulf2*$^{-/-}$ mice developed more spontaneous and surgically-induced osteoarthritis (OA) (Otsuki et al., 2010), which was associated with a decrease in BMP signalling (involved in cartilage repair) and an increase in FGF signalling (promotes the expression of enzymes contributing to cartilage degradation). In addition, a single nucleotide polymorphism upstream of *SULF2* has been associated with OA (Evangelou et al., 2014; Loughlin, 2015). In contrast with this apparent protective role, expression of both sulfatases is increased in OA and aged cartilage (Otsuki et al., 2008; Chanalaris et al., 2019), possibly indicating their involvement in attempted tissue repair pathways.

Sulfatase expression is also increased after myocardial infarction, with *Sulf1* predominantly expressed by endothelial cells and *Sulf2* by inflammatory cells (Korf-Klingebiel et al., 2019). *Sulf1*$^{-/-}$ and *Sulf2*$^{-/-}$ mice also showed impaired tissue repair in a myocardial infarction model, which resulted in increased scar size and cardiac dysfunction (Korf-Klingebiel et al., 2019). Mechanistically, increased 6-O sulfation in these mice enhanced binding of VEGF to HS and thereby inhibiting its angiogenic effect necessary for infarct repair.

Studies on idiopathic pulmonary fibrosis (IPF) have identified SULF2 as an important negative regulator of TGFß1 signalling in *vivo*. SULF2 is also a target gene of TGFß1 signalling, pointing to a negative feedback loop between SULF2 and TGFß1. TGBß1 signalling increases the expression of *Sulf2* (Yue et al., 2013; Alhasan et al., 2014), which in turn inhibits TGFß1 signalling. *Sulf2*$^{-/-}$ mice (epithelial-specific conditional knockout) exhibited enhanced TGFß1 signalling and bleomycin-induced lung injury as a model for IPF (Yue, 2017). Expression of *Sulf2* increases in IPF and after bleomycin exposure (Yue et al., 2013; Yue, 2017), which the authors speculate reflects a failed and chronic attempt to limit TGFß1 signalling and to regenerate the damaged epithelium. In contrast to the protective role of *Sulf2* in pulmonary fibrosis, *Sulf2* knockout (129P2-*Sulf2*$^{Gt(PST111)Byg}$) reduced diet-induced steahepatitis and fibrosis (Kim et al., 2020), indicating the complexity of the role of *Sulf2* in fibrosis.

Expression of *Sulf1* and *Sulf2* is dysregulated in many cancers (Vivès et al., 2014; Rosen and Lemjabbar-Alaoui, 2010; Hammond et al., 2014), with *Sulf2* being a direct transcriptional target of p53 (Chau et al., 2009; Adamsen et al., 2007). However, total and phosphorylated p53 and p21 levels are increased in *Sulf2*$^{-/-}$ mice (Yue, 2017), which might result in cell cycle arrest. It could be hypothesised that upregulation of *Sulf2* in cancer decreases p53 and p21 levels and allows continuation of the cell cycle after DNA damage.

1.3.4. Sulfatase-2 and inflammation

The function of 6-O sulfation on immune cells is unknown to date, but it is tempting to speculate that 6-O-sulfation may regulate immune responses by modifying the biological activity of HS-binding chemokines, cytokines and growth factors as it has been shown to do in other cell types (El Masri et al., 2017).

It is currently unknown which factors regulate *Sulf2* expression in immune cells, but it has been shown to be increased by TGFß in renal epithelial cells (Alhasan et al., 2014), by TNF in nucleus pulposis cells (Johnson et al., 2017) and by IL-1α in HeLa cells (Macur et al., 2018). In the previously discussed RNA-Seq study of PBMCs from healthy human donors, Monaco et al. (2019) demonstrated that *SULF1* is not expressed by immune cells, whereas *SULF2* is predominantly expressed in myeloid cells, such as basophils, neutrophils, monocytes and mDCs, but to lesser extend in B-cells and the lowest levels in T-cells (**Figure 1.6**). This might indicate that *SULF2* could be important for the function of myeloid cells, which might, in turn, modulate T cell activity. Strikingly, *Sulf2* is most highly expressed in resident alveolar macrophages (AM) in the lung (Immunological Genome Project, www.immgen.org), indicating a potential anti-inflammatory role for SULF2.

1.4. Hypothesis and aims

This potential anti-inflammatory role of SULF2 led me to hypothesise that SULF2 is involved in the inhibition of immune responses and could protect against rheumatoid arthritis.

The aims of my research were to:

1. Profile *Sulf2* expression *in vivo* and characterise the regulation of *Sulf2* expression *in vitro* (**Chapter 3**).
2. Investigate the function of *Sulf2* in macrophage biology (**Chapter 4**).
3. Establish the role of *Sulf2* in inflammatory arthritis (**Chapter 5**).

Chapter 2. Materials and methods

2.1. Reagents

2.1.1. Cell lines and cell culture reagents

RAW264.7 and J774.2 murine macrophage-like cell lines were obtained from laboratory stocks.

Table 2.1 summarises cell culture reagents used. IFNγ (BioLegend), IL1, IL2, IL4, IL6, IL13, IL23, M-CSF, GM-CSF and TGFß were all purchased from Peprotech, Ultra-pure LPS from *Escherichia coli* 0111:B4 was purchased from InvivoGen.

Table 2.1. Cell culture reagents.

Reagents	Manufacturer
2-Mercaptoethanol	Gibco
Dimethyl sulfoxide (DMSO)	Santa Cruz Biotechnology
Dulbecco's Modified Eagle's (DMEM) medium	Lonza
Foetal bovine serum (FBS)	Gibco
Rosewell Park Memorial Institute (RPMI) medium	Lonza
Penicillin/ Streptomycin (P/S)	Lonza

2.1.2. Antibodies

Table 2.2 provides an overview of the antibodies used.

Table 2.2. Antibodies.

Commercial antibodies used in flow cytometry (FC) and western blot (WB) are listed.

Target	Isotype	Species	Clone	Company	Method
CCR7	Rat IgG2a, κ	Mouse	4B12	BioLegend	FC
CD3	Hamster IgG_1, κ	Mouse	145-2C11	BD Biosciences	FC
CD4	Rat / IgG2a, κ	Mouse	RM4-5	eBioscience	FC
CD8	Rat IgG2a, κ	Mouse	53.6-7	BioLegend	FC
CD19	Rat IgG2a, κ	Mouse	ID3/CD19	BioLegend	FC
CD25	Rat IgG1, λ	Mouse	PC61	BioLegend	FC
CD11b	Rat IgG2b, κ	Mouse	M1/70	BioLegend	FC
CD11c	Hamster IgG_1, λ2	Mouse	HL3	BD biosciences	FC
CD36	Arm. Ham IgG	Mouse	MH36	BioLegend	FC
CD40	Rat IgG2a, κ	Mouse	3/23	BioLegend	FC
CD45	Rat IgG2b, κ	Mouse	30-F11	BioLegend	FC
CD80	Hamster IgG	Mouse	16-10A1	BioLegend	
CD86	Rat IgG2a, κ	Mouse	GL1	BD Pharmingen	FC
CD169	Rat IgG2a, κ	Mouse	3D6.112	BioLegend	FC
CD204	Human IgG1	Mouse	REA148	Miltenyi Biotech	FC
F4/80	Rat / IgG2a, κ	Mouse	BM8	BioLegend	FC
CD206	Rat IgG2a, κ	Mosue	C068C2	BioLegend	FC
Foxp3	Rat / IgG2a, κ	Mouse	FJK-16s	eBioscience	FC
IL17	Rat IgG1, κ	Mouse	TC11-18H10.1	BD Pharmingen	FC
IFNγ	Rat IgG1, κ	Mouse	XMG1.2	BioLegend	FC
Ki-67	Rat IgG2a, κ	Mouse	16A8	BioLegend	FC
LC3	Rabbit	Mouse	Polyclonal	Sigma	WB
Ly6C	Rat IgG2c, κ	Mouse	HK1.4	BioLegend	FC
Ly6G	Rat IgG2a, κ	Mouse	1A8	BD Biosciences	FC
Marco	Mouse IgG2a, κ	Human/ mouse	F-3	Santa Cruz	FC
Mertk	Rat IgG2a	Mouse	FAB5912P	R&D systems	FC
MHC-I	Hamster IgG	Mouse	Sf1-1.1	BD Biosciences	FC
MHC-II	Rat IgG2b, κ	Mouse	M5/114.15.2	BD Biosciences	FC
Rorγt	Rat IgG2a, κ	Human/ mouse	AFKJS-9	eBioscience	FC

2.2. Human samples

2.2.1. Synovium digestion

Tissue samples were obtained from the Oxford Musculoskeletal Biobank and were collected with informed donor consent in full compliance with national and institutional ethical requirements, the United Kingdom Human Tissue Act, and the Declaration of Helsinki (HTA Licence 12217 and Oxford REC C 09/H0606/11). No information was available about the sex, age, disease stage or current therapy, so the results were not stratified according to these parameters. Synovium was digested according to Piccinini et al. (2016). In brief, fat was removed and the tissues were chopped into small pieces before digestion with 0.5 mg/ml Liberase (Roche) for 1.5 hour (h) at 37 °C. Subsequently, the cells were sieved through a 100 µm cell strainer (Greiner) and red blood cells were lysed in red blood cell lysis solution (MACS Miltenyi Biotech) for 5 minutes (min). Cells were frozen in FBS with 10 % DMSO at -80 °C (Santa Cruz Biotechnology) until required for analysis.

2.3. Mice

2.3.1. Maintenance

Wild-type C57BL/6 were purchased from Charles-River, *Sulf2*-deficient (*Sulf2*$^{+/-}$) and *Sulf2* null (*Sulf2*$^{-/-}$) mice on a C57BL/6 background (**Figure 2.1**) were kindly provided by Dr A. Redpath and Dr N. Smart (Department of Physiology and Anatomy, University of Oxford) and OT-II TCR transgenic mice were kindly provided by Dr E. Compeer. All experiments were carried out in accordance with the Home Office Animals Scientific Procedures Act 1986 under personal license ICA3D92DA and the project license of Prof. Richard Williams (30/3441).

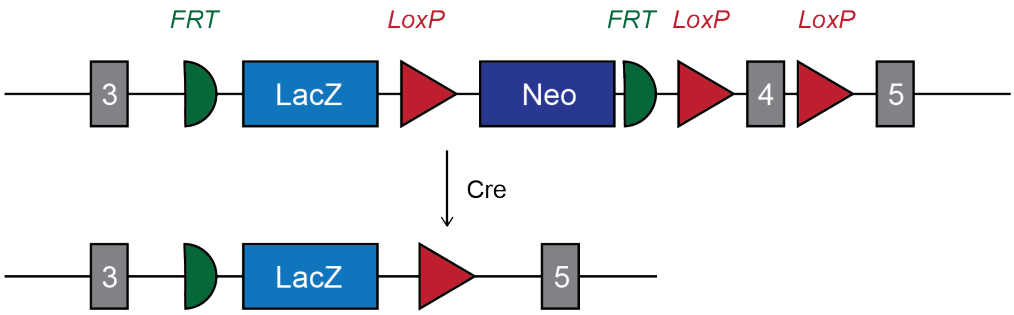


Figure 2.1. Generation of *Sulf2*-deficient mice.
The embryonic stem (ES) cell line *Sulf2*$^{tm1a(KOMP)Wtsi}$ (RRID:MMRRC_063144-UCD) was purchased from the KOMP repository by Dr A. Redpath and Dr N. Smart. These cells contain a null allele through insertion of a LacZ gene trap cassette upstream of exon 4, which is essential for the catalytic domain of *Sulf2*. However, skipping over the *LacZ* cassette can restore gene expression. To prevent this, a floxed *Neo* cassette was also inserted. Exon 4 and the *Neo* cassette can be removed by Cre recombinase to inactivate *Sulf2* gene expression. Instead, the *LacZ* cassette coding for Beta-galactosidase will be expressed. A conditional knockout can be generated by removing the *LacZ* and *Neo* cassette using Flp recombinase, which recognises *FRT* sites. *Sulf2*-deficient mice were generated by injecting these ES stem cells into blastocysts, which resulted in chimeras that were bred to germline transmission of the *Sulf2* null allele. These mice were crossed by Dr A. Redpath with Tg(Pkgk1-cre)Lni mice that constitutively express the Cre recombinase to remove the *Neo* cassette and exon 4 of *Sulf2*.

2.3.2. Generation of single cell suspensions

Mice were sacrificed by CO_2 inhalation for 5 min. Blood was collected by cardiac puncture.

2.3.2.1. Generation of blood single cell suspensions

Blood was collected by cardiac puncture and was collected in 500 µl Alver's solution. Red blood cells were lysed by adding an equal volume of red blood cell lysis buffer (Sigma) for 5 min at room temperature (RT).

2.3.2.2. Generation of bone marrow single cell suspensions

Bone marrow cells were isolated from the femurs and tibias of mice. Briefly, following removal of muscle, bones were submerged in 70 % ethanol for 1 min to sterilise the tissue. Subsequently, bone marrow was flushed out of the bones using a 26G needle after removing the bone ends. Red blood cells were lysed by adding 500 µl red blood cell lysis buffer (Sigma) for 2 min at RT and the resultant material filtered through a 70 µm cell strainer (VWR). Red blood cell lysis was omitted for the generation of bone marrow chimeras.

2.3.2.3. Generation of spleen and lymph node single cell suspensions

Single cell suspensions from spleen and lymph node were obtained by pressing the spleen and lymph nodes through a 70 µm cell strainer. Red blood cells in the spleen were lysed by adding 500 µl red blood cell lysis buffer (Sigma) for 2 min at RT.

2.3.2.4. Generation of lung single cell suspensions

Lungs were cut into small pieces and placed in RPMI with 5 % FBS, collagenase IV (4 mg/10 ml) and DNase I (1.5 mg/10 ml) for 40 min at 37 °C. Subsequently, the samples were passed through a 70 µm cell strainer. Red blood cells in the spleen were lysed using 500 µl red blood cell lysis buffer (Sigma) for 2 min at RT.

2.3.2.5. Generation of joint single cell suspensions

Hindlegs were removed without breaking the bones and muscle was removed while leaving the knee joint capsule intact. Cytokines were extracted by pulling the bones apart and incubating them for 1 h at 37 °C in 500 µl RPMI. Cells were removed by centrifugation and the supernatants were stored at -80 °C. Subsequently, the synovium was digested in 500 µl RPMI with 200 µg/ ml liberase and 50 µg/ml DNase for 30 min at 37 °C. Single cell suspensions were obtained by pressing the synovium through a 70 µm cell strainer. Red blood cells were lysed using 500 µl red blood cell lysis buffer (Sigma) for 2 min at RT.

2.3.3. Generation of bone marrow chimera

Mice were irradiated with two sub-lethal doses of 5.5 Gy at a 4 h interval in a Gulmay X-ray irradiator (table height 400 mm, 1.8 Gy/min, 210 KV, 13 mA for 3 min). 2 h after the last irradiation dose, recipient mice were injected in the tail vein with 5 million bone marrow cells in 150 µl RPMI with 2 % FBS (without P/S) from donor mice. 1 % Baytril antibiotic (Bayer) was given in autoclaved drinking water for 2 weeks following the intravenous injection. Mice were weighed daily to ensure that they lost no more than 15 % of their body weight, in accordance with the project license requirements. The

mice lost up to 10 % weight within 5 d after bone-marrow transplantation, but their weights recovered quickly (**Figure 2.2**). The mice were allowed to recover for 7 weeks.

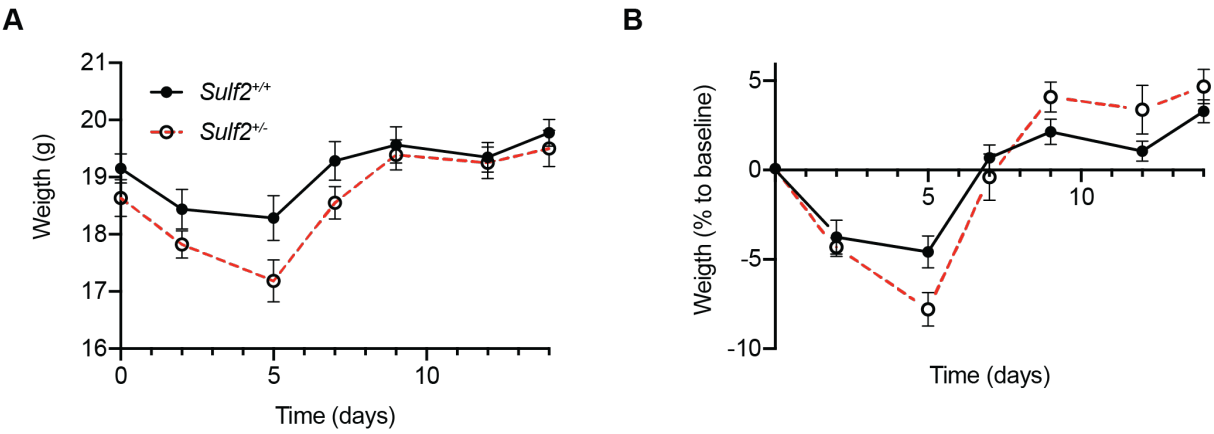


Figure 2.2. Weight loss after bone marrow transplantation.

8-week-old C57BL/6 mice were irradiated and reconstituted with *Sulf2*$^{+/+}$ and *Sulf2*$^{+/-}$ bone marrow cells. **A.** The mice were weighed for 2 weeks to monitor their **B.** percentage weight loss.

2.3.4. Antigen-induced arthritis

mBSA (2 mg/ml) was added 1:1 to CFA (BD Difco) and the mixture emulsified using a Minilysis homogeniser (Bertin Technologies). Mice were subcutaneously immunised with 100 µg methylated BSA (mBSA; Sigma, (2x 50 µl 1 mg/ml) in CFA. Arthritis was induced 3 weeks later by intra-articular (i.a.) tibiofemoral injection of 100 µg mBSA in 10 µl sterile PBS (right knee) or PBS control (left knee).Knee swelling was measured daily for 7 days post i.a. injection using a calliper. Pain was assessed by measuring weight bearing on mBSA-injected compared to PBS-injected paws using a dynamic weight-bearing chamber 2.0 (Bioseb).

2.4. Cell culture

2.4.1. Cell line culture

The mouse macrophage cell line RAW264.7 was cultured in RPMI supplemented with 1 % P/S, 5 % FBS and 50 µM 2-mercaptoethanol. The mouse monocyte/macrophage cell line J774.2 was cultured in DMEM (Lonza) supplemented with 1 % P/S (Lonza) and 5 % FBS (Gibco).

2.4.2. Primary macrophage and dendritic cell culture

Cells were plated (5 million cells per 10 cm dish) and cultured at 37 °C; 5 % CO_2 in RPMI supplemented with 10 % FBS, 1 % P/S and 50 µM 2-mercaptoethanol for 7 days (d) with 100 ng/ml M-CSF or 20 ng/ml GM-CSF (both Peprotech). Subsequently, the cells were cultured for 18 h with 20 ng/ml IL-4 and 20 ng/mL IL-13 (both Peprotech) or with 100 ng/ml LPS (InvivoGen) and 100 ng/ml IFNγ (BioLegend) in order to generate M2- and M1-like macrophages respectively.

2.4.3. siRNA knockdown

After 5 d of culture, M-CSF-derived bone marrow-derived macrophages (BMDMs) were replated overnight (O/N) at 0.8 million cells/ml with 100 ng/ml M-CSF. On the following day, the cells were transfected with 50 nM ON-TARGET plus non-targeting (NT) or *Sulf2* siRNA (Dharmacon) using jetPRIME reagent (Polyplus) in serum-free RPMI without P/S. Briefly, siRNA was diluted in 100 µl JetPRIME buffer per ml of culture medium. Next, 3 µl JetPRIME reagent was added, vortexted for 10 seconds (sec), spun down and incubated for 10 min at RT. Finally, the 100 µl was added to cells in 0.9 ml of serum-free medium and incubated for 4 h. After 4 h, the medium was

changed to RPMI with 10% FBS, 1 % P/S and 50 µM 2-mercaptoethanol. Medium was changed every 24 h.

2.4.4. Assays of immune cell function

2.4.4.1. Phagocytosis assays

Cells were incubated with 1 µm fluorescent microspheres (Fluoresbrite plain yellow-green particles, Polysciences Inc; multiplicity of infection, MOI 50 for 30 min), fluorescein-conjugated *Escherichia coli* K-12 BioParticles (MOI 5 for 15 min), or fluorescein-conjugated *S. cerevisiae* zymosan A Bioparticles (MOI 5 for 20 min) to study phagocytosis.

To study efferocytosis, macrophages were incubated with apoptotic Jurkat T cells (MOI 2 for 45 min). These were generated by incubating 2 million Jurkat cells/ml with 1 µM calcein-acetoxymethyl (calcein-AM, Thermo Fisher) for 2 h at 37 °C. The cells were washed 3x with PBS and apoptosis was induced by exposing the cells to 305 nm UV light at 2 inches from the light source for 2.5 h until 30 % of the cells visibly blebbed.

Antigen uptake was measured by incubating cells with 0.1 mg/ml Alexa-647 labelled ovalbumin (Molecular Probes) for 1 h at 37 °C. Subsequently, the cells were stained and analysed by flow cytometry. To control for binding to the cell without uptake, a control was used in all phagocytosis assays in which the particles were incubated with cells on ice.

2.4.4.2. Antigen presentation assays and T-cell culture

GM-CSF or M-CSF-treated cells were plated in a 96-well U-bottomed-well plate (10.000 cells per well) and loaded with 0.1 mg/ml ovalbumin (OVA; InvivoGen) for 1 h

at 37 °C and activated with 100 ng/ml LPS (InvivoGen) for 4 h. CD4+ T-cells were enriched from the spleen of OT-II mice using the MojoSort mouse CD4+ T-cell isolation kit (BioLegend) according manufacturer's instructions. These CD4+ OT-II T-cells carry the Vβ 5.1/5.2 T-cell receptor (TCR) that is specific for OVA 323-339 presented on MHC-II (Barnden et al., 1998). CD4+ T-cells were labelled with 5 µM CellTrace Violet (Invitrogen) for 20 min at 37 °C in PBS and unbound dye was quenched with RPMI with 10% FBS. CD4+ T-cells (100.000 per condition) with and without 10 µg/ml OVA peptide 323-339 (Peptides International) were added to the GM-CSF and M-CSF derived cells after OVA and LPS were washed off. The cells were incubated for 4 d after which the supernatants were stored at – 80 °C and the cells were analysed by flow cytometry.

2.4.5. Cytotoxicity assay

A CytoTox 96 Cytotoxicity assay (Promega) was performed according to manufacturer's instructions. This assay detects the enzyme lactate dehydrogenase (LDH), which is released from damaged cells . It converts lactate to pyruvate and NAD^+ to NADH. NADH can then subsequently reduce the substrate INT (iodonitrotetrazolium violet) into a red formazan product.

2.5. Phenotypic characterisation

2.5.1. Flow cytometry

Cells were first stained with the fixable live/dead dye Zombie near-infra red (NIR; BioLegend) or aqua dye (ThermoFisher Scientific) for 10 min at RT. The cells were washed in PBS and non-specific antibody binding was blocked with anti-mouse CD16/CD32 (BD Biosciences) for 10 min at 4 °C. For extracellular staining, cells were incubated with fluorochrome-conjugated antibodies at 4 °C for 30 min in PBS with 1 % FBS. Subsequently, the cells were washed twice, and fixed in BD CellFIX (BD Biosciences) for 10 min on ice.

To detect intracellular cytokines, cells were stimulated for 4 h with 20 ng/ml PMA, 1 ug/ml ionomycin in the presence of the protein transport inhibitors GolgiPlug and GolgiStop (both BD Biosceinces; 1/1000) that contain respectively brefeldin A and monensin. For intracellular staining, cells were fixed in Foxp3/Transcription factor staining buffer (Invitrogen) at 4 °C for 30 min, and then incubated with fluorochrome-conjugated antibodies at 4 °C for 30 min in Permeabilisation buffer (Invitrogen).

Sulf2 mRNA was detected using the PrimeFlow RNA assay (Invitrogen) after extracellular staining according to manufacturer's protocol. The cells were permeabilised and RNA was fixed before hybridisation with a target probe set containing 20-40 oligonucleotide pairs at 40 °C for 2 h. Branched DNA amplification was used for signal amplification (**Figure 2.3**), by hybridisation of pre-amplifying primers for 1.5 h at 40 °C, and then with amplifying primers for 1.5 h at 40 °C, followed by incubation with label probes for 1 h at 40 °C.

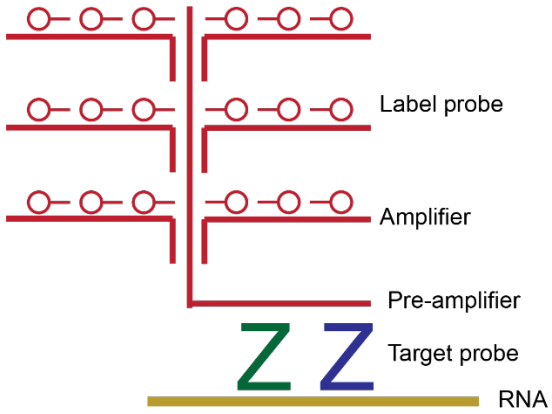


Figure 2.3. Branched DNA amplification in PrimeFlow.
Target probe sets contain 20-40 specific oligonucleotides that hybridise with the target gene. Only 1 target probe pair is shown above. Signal amplification is achieved using branched DNA amplification, which forms 'tree'-like structures by hybridisation of pre-amplifier and amplifier oligonucleotides. These trees can bind 400 label probes and achieve 8000-fold signal amplification.

Data were acquired on an LSR-II or Fortessa X20 flow cytometer (BD Biosciences). Absolute cell numbers were calculated by dividing the number of events of the population of interest by the number of events in the live gate and multiplying this by the manual live cell count.

2.5.2. ELISA

Murine IL1β (Invitrogen) and IL6 (R&D Systems) in culture supernatants were measured by ELISA according to the manufacturer's protocol. Briefly, plates were coated with anti- IL1β or -IL6 antibody O/N at 4 °C. Non-specific binding was blocked with 2 % BSA in PBS for 1 h at RT. A standard curve was generated by making serial dilutions of recombinant IL1β or IL6. Samples and standard were incubated on the plate for 2 h at RT. Subsequently the detection antibody was added for 2 h at RT followed by HRP-conjugate for 20 min at RT. IL1β and IL6 was visualised by adding

100 µl 3,3',5,5'-tetramethylbenzidine (TMB) for a maximum of 20 min at RT. The reaction was stopped by addition of 50 µl of 2 N sulfuric acid.

2.5.3. Immunoblotting

2.5.3.1. Ammediol gels

10% Ammediol SDS-PAGE gels were cast in Hoefer Gel Casters according to **Table 2.3**. First, the lower gel was cast and allowed to polymerise for 2 h after oxygen exclusion using H_2O-saturated butanol. Subsequently, the upper gel was cast and allowed to set for 1 h before storage at 4 °C wrapped in plastic to prevent dehydration.

Table 2.3. Reagents required to make 10% Ammediol SDS-PAGE gels.

Target	Lower gel	Upper gel
30 % (w/v) acrylamide/bisacrylamide	13 ml	1.6 ml
Lower gel buffer	9.8 ml	-
Upper gel buffer	-	3.2 ml
50 % sucrose	8.4 ml	3.2 ml
dH_2O	7.9 ml	4.8 ml
10 % ammonium persulfate (APS)	137 µl	156 µl
TEMED	14 µl	34 µl

2.5.4. Immunoblotting procedure

Up to 2 million cells were lysed in SDS sample buffer (**Table 2.4**) with protease inhibitor cocktail (Sigma) and denatured by heating at 95 °C for 10 min. Proteins were separated by molecular weight on 10 % ammediol gels at 120-180 V for up to 80 min. Proteins were transferred on polyvinylidene difluoride (PVDF) membranes using Trans-Blot Turbo apparatus (BioRad). Non-specific binding was blocked with 5 % dry skimmed milk in TBS-Tween20 for 1 h at RT. The membranes were incubated with primary antibodies in blocking solution O/N at 4 °C. They were washed with TBS-Tween20 and incubated with HRP-conjugated secondary antibodies in blocking

solution for 1 h at RT. Immunoreactive bands were visualised using Clarity Western ECL chemiluminescence substrate (BioRad).

Table 2.4. Buffers for ammediol gels

Buffers	Composition
SDS sample buffer (2x)	2 % SDS 5 ml upper gel buffer 0.1 % bromophenol blue 50 % glycerol 1 % ß-mercaptoethanol
Upper gel buffer	84 mM ammediol 62 mM HCl 0.02 % sodium azide
Lower gel buffer	110 mM ammediol 10 mM glycine 0.01% SDS
Upper running buffer	110 mM ammediol 47 mM HCl 0.02 % sodium azide
Lower running buffer	10 mM ammediol 12.5 mM HCl

2.6. Nucleic acid assays

2.6.1. RNA isolation and reverse transcription-PCR

RNA was extracted from cell cultures using RNeasy mini spin-columns (Qiagen) according to manufacturer's protocol and including the optional DNase digestion step.

For RNA extraction from tissues using the TRIzol method, tissues (approximately 100 mg) were first thawed and lysed in 1 ml TRIzol (Ambion, Life Technologies). To isolate RNA from mouse joints, the tissue was first homogenised in a TissueLyser II for 10 min at 30 s^{-1} using Precellys hard tissue Lysing Kit (MK28-R). 100 µl 1-bromo-3-chloropropane (BCP, Sigma) was added to the homogenate and the organic and aqueous phases were separated by centrifugation at 13000 rpm for 20 min at 4 °C. RNA was extracted from the aqueous phase using RNeasy mini spin-columns (Qiagen).

500 ng RNA was reverse transcribed to cDNA in a reaction volume of 20 µl using a High Capacity Reverse Transcription cDNA kit (Applied Biosystems) according to manufacturer's instructions.

2.6.2. Quantitative PCR

Manual qPCRs were carried out in 384-well plates with 10 µl reactions and 6.25 ng cDNA and TaqMan Universal PCR Mastermix (Applied Biosystems).

Custom-designed TaqMan Array Cards (Applied Biosystems) were used to assess HS biosynthesis and core protein gene expression. Data were acquired on a ViiA 7 Real-Time PCR System (Applied Biosystems) and the fold change was calculated using the ΔΔCt method.

2.6.2.1. TaqMan primers

TaqMan primers (**Table 2.5**) and custom-designed TaqMan microfluidic array cards used to detect murine (**Table 2.6**) or human (**Table 2.7**) HS-associated genes were purchased from ThermoFisher Scientific.

Table 2.5. Mouse TaqMan primers from ThermoFisher Scientific used to measure gene expression in qPCR assays.

Target	Assay ID
18s	Mm04205640_g1
Arg1	Mm00475988_m1
Atg7	Mm00512209_m1
Axl	MM00437221_m1
Cdkn1a	MM04205640_g1
Cdkn2a	Mm00494449_m1
Elane	Mm00469310_m1
Gapdh	Mm03302249_g1
Gas6	Mm00490378_m1
Hs6st1	Mm0122968_s1
Ifnγ	Mm01168134_m1
Il1b	Mm00434228_m1
Il6	Mn00446190_m1
Il10	Mn01288386_m1
Il12b	Mm00434174_m1
Il17a	Mm00439619_m1
Il23a	Mn01160011_g1
Itgb3	Mm004439880_m1
Mertk	Mm00434920_m1
Mfge8	Mm00500549_m1
Mrc1	Mm01329362_m1
Mpo	Mm01298424_m1
Nos2	Mm00440489_m1
Pparg	Mm00440940_m1
Pros1	Mm01343426_m1
Retnla	Mm00445109_m1
Rplp0	Mm00725448_s1
Sdc1	Mm00448918_m1
Sdc2	Mm04207492_m1 Mm00484718_m1
Sdc3	Mm01179833_m1
Sdc4	Mm00488527_m1
Socs3	Mm00545913_s1
Stat1	Mm01257286_m1
Stat6	Mm01160477_m1
Sulf1	Mm00552283_m1
Sulf2	Mm01248029_m1
Tgfb1	Mn01178820_m1
Tnf	Mn00443258_m1
Tyro3	Mm00444547_m1

Table 2.6. TaqMan primers from ThermoFisher Scientific used for microfluidic card analysis of murine heparan sulfate-associated gene expression by qPCR.

Target	Assay ID
18s	Hs99999901_s1
Adam15	Mm01212741_g1
Adamts1	Mm013441609_m1
Adamts4	Mm005560608_m1
Agrn	Mm01545823_g1
Chst11	Mm00517562_m1
Chst15	Mm005132207_m1
Ext1	Mm01194490_m1
Ext2	Mm00468775_m1
Extl1	Mm00517161_m1
Extl2	Mm00469621_m1
Extl3	Mm01317041_m1
Gapdh	Mm99999915_g1
Glce	Mm004736607_m1
Gpc1	Mm01290371_m1
Gpc2	Mm00549653_g1
Gpc3	Mm00516722_m1
Gpc4	Mm00515035_m1
Gpc5	Mm01235111_m1
Gpc6	Mm00516232_m1
Hpse	Mm004617608_m1
Hpse2	Mm011985307_m1
Hs2st1	Mm00478684_m1
Hs3st1	Mm019640308_s1
Hs3st2	Mm00616933_m1
Hs3st3a1	Mm007809007_s1
Hs3st3b1	Mm030529707_s1
Hs3st4	Mm03649146_m1
Hs3st5	Mm01192940_m1
Hs3st6	Mm01299930_m1
Hs6st1	Mm012296908_s1
Hs6st2	Mm00479296_m1
Hs6st3	Mm01225470_s1
Hspg2	Mm01181173_g1
Lrp1	Mm00464608_m1
Ndst1	Mm00447005_m1
Ndst2	Mm004478108_m1
Ndst3	Mm00453184_m1
Ndst4	Mm004807607_m1
Rplp0	Mm007254408_s1
Sdc1	Mm012758609_m1
Sdc2	Mm04207492_m1
Sdc3	Mm01179833_m1
Sdc4	Mm004885207_m1
Sulf1	Mm00552283_m1
Sulf2	Mm012480209_m1
Tgfbr3	Mm008035308_m1
Timp3	Mm00441826_m1

Table 2.7. TaqMan primers from ThermoFisher Scientific for microfluidic card analysis of human heparan sulfate-associated gene expression.

Target	Assay ID
18S	Hs99999901_s1
ADAM15	Hs00187052_m1
ADAMTS1	Hs00192708_m1
ADAMTS4	Hs00199841_m1
AGRN	Hs00394748_m1
CHST11	Hs00905281_s1
CHST15	Hs01031067_m1
EXT1	Hs00609162_m1
EXT2	Hs00181158_m1
EXTL1	Hs00184929_m1
EXTL2	Hs01018237_m1
EXTl3	Hs00918601_m1
GAPDH	Hs99999905_m1
GLCE	Hs00392011_m1
GPC1	Hs00892476_m1
GPC2	Hs00415099_m1
GPC3	Hs01018936_m1
GPC4	Hs00155059_m1
GPC5	Hs00270114_m1
GPC6	Hs00170677_m1
HPSE	Hs00935036_m1
HPSE2	Hs00222435_m1
HS2ST1	Hs00202138_m1
HS3ST1	Hs00245421_s1
HS3ST2	Hs00428644_m1
HS3ST3A1	Hs00925624_s1
HS3ST3B1	Hs00797512_s1
HS3ST4	Hs00901124_s1
HS3ST5	Hs00999394_m1
HS3ST6	Hs03007244_m1
HS6ST1	Hs00757137_m1
HS6ST2	Hs02925656_m1
HS6ST3	Hs00542178_m1
HSPG2	Hs00194179_m1
LRP1	Hs00233856_m1
NDST1	Hs00925442_m1
NDST2	Hs00234335_m1
NDST3	Hs01128584_m1
NDST4	Hs00224024_m1
RPLP0	Hs99999902_m1
SDC1	Hs00896423_m1
SDC2	Hs00299807_m1
SDC3	Hs01568665_m1
SDC4	Hs00161617_m1
SULF1	Hs00290918_m1
SULF2	Hs01016476_m1
TGFBR3	Hs01114253_m1
TIMP3	Hs00165949_m1

2.7. Histology

Knee joints were fixed in 10% (vol/vol) formalin for 24 h and decalcified in 10% (vol/vol) EDTA for 4 weeks. Samples were dehydrated before they were embedded in paraffin wax. Coronal sections were dewaxed in xylene (2x 5 min), rehydrated in 100% ethanol (3x 1 min) and water (1 min) before staining with haematoxylin and eosin (H&E) or fast green/ safranin-O. For H&E staining, sections were staining with Harris haematoxylin for 6½ min, differentiated in acid alcohol (70% EtOH with 0.37% HCl) for 40 sec, incubated in blueing agent (0.25% ammonia in water) and stained with 1% aqueous eosin for 1.45 min in a DRS 2000 stainer (Sakura). For fast green/ safranin-O staining, sections were stained with Harris haematoxylin for 30 sec, acid alcohol for 20 sec, blueing agent for 1 min, fast green for 6 min, 1% acetic acid for 15 sec and safranin-O for 2 min. Samples were dehydrated in 100% EtOH (3x 1 min) and xylene (3x 1min) before mounting the coverslips with di-n-butylphtalate (DPX) mounting media in a G2 coverslipper machine (Sakura).

2.8. RNA-sequencing analysis

2.8.1. Single cell RNA-sequencing

Published single cell RNA sequencing (scRNA seq) expression matrices from Culemann et al. (2019) were analysed using Seurat 3.0 (Stuart et al., 2019) under R 4.0.0 with RStudio 1.3.959. Cells with more than 5% mitochondrial gene expression were excluded from the analysis. The expression matrices were log-normalised, integrated using the standard workflow in Seurat 3.0 and cell cycle scores were regressed out during data scaling. Dimensionality reduction was performed by principal component (PCA) analysis and the cells were clustered by Uniform Manifold Approximation and Projection (UMAP). Differential expression testing was performed using the non-parametric Wilcoxon rank sum test.

2.8.2. Bulk-sequencing

Published bulk RNA sequencing (RNA seq) count matrices from Culemann et al. (2019) were analysed using the negative binominal model using DESeq2 1.28.1 (Love et al., 2014) under R 4.0.0 with RStudio 1.3.959 to identify differentially expressed genes. Gene ontology or biological processes (GO) analysis was performed with TopGO 2.40.0 to identify the affected biological processes.

2.9. Statistical analysis

PCA analysis and the generation of heatmaps was performed in R (version 3.5.2) and R studio (version 1.1.453). Data were analysed in GraphPad Prism (8.4.1). The D'Agostino-Pearson test was used to check if data were normally distributed. Data are presented as mean ± SEM or median ± IQR where appropriate. Further details of specific tests used are included in the following chapters.

Chapter 3. Sulfatase-2 is highly expressed by macrophages

3.1. Introduction

Macrophages are a part of the innate immune system and are important for maintaining homeostasis by phagocytosis of pathogens and dead cells, repair after tissue injury and immune regulation (Hirayama et al., 2018). In response to environmental cues, they adopt an activation status that affects their function. Classically, pro-inflammatory (which were previously termed 'M1') macrophages are derived *in vitro* by treatment with IFNγ+LPS, whereas IL4+IL13 are used to generate reparative (previously termed 'M2') macrophages. However, *in vivo* the presence of bacterial components that provide pathogen-associated molecular patterns (PAMPs), tissue breakdown products functioning as damage-associated molecular patterns (DAMPs), cytokines, chemokines and growth factors results in a more complex range of activation statuses (F. O. Martinez and Gordon, 2014; Murray et al., 2014).

The bioactivity of many of these environmental factors can be strongly regulated by their binding to HS proteoglycans, which consist of a core protein with one or more covalently attached HS glycosaminoglycan polymer side chains. As discussed in **Chapter 1.2.1** at least 25 different enzymes are involved in the elongation and subsequent modification of HS chains by elongation, epimerisation and sulfation, and it is thought that their relative expression determines the structure of HS chains (Sugahara and Kitagawa, 2002; Kreuger and Kjellén, 2012). In this thesis, I set out to characterise how macrophages respond to signals in their environment by changing the relative expression of these HS biosynthesis enzymes and core proteins.

Macrophage polarisation by IFNγ+LPS or IL4+IL13 has been shown to drastically affect the expression of various HS sulfotransferases in primary human monocyte-derived macrophages, which resulted in changes in HS sulfation motifs (Martinez et al., 2015). As changes in HS structure affect its affinity for proteins (Esko

and Selleck, 2002) and hence also their bioactivity (Stanford et al., 2010), these changes in HS structure have the potential to affect macrophage function. For example, macrophages polarised with IL4+IL13 efficiently presented FGF-2, a classical HS-binding protein, to tumour cells while those polarised with IFNγ+LPS did not (Martinez et al., 2015). HS can also affect the inflammatory function of macrophages, as illustrated by Gordts *et al*. (2014), who reduced HS N-sulfation by NDST1 using an *Ndst1*$^{f/f}$*LysMCre* model, and observed increased IFNß bioavailability, leading to increased inflammatory gene expression (Gordts et al., 2014). As a result, atherosclerosis and diet-induced obesity were increased in these mice.

Although macrophage polarisation has been shown to regulate the expression of various individual biosynthesis enzymes, the expression of all HS core proteins and biosynthesis enzymes in macrophages has not been systematically studied to date. Therefore, I sought to comprehensively characterise the expression of HS core proteins and biosynthesis enzymes upon macrophage activation, to gain an understanding of how the pathway as a whole is controlled in primary macrophages. Additionally, I set out to characterise the expression of *Sulf2*, an HS-modifying enzyme that is strongly regulated upon macrophage activation, by immune cells *in vivo*. Finally, I also assessed whether *Sulf2* affects the *in vivo* abundance of immune cell types at steady state.

3.2. Characterisation of HS biosynthesis and core protein expression in macrophages *in vitro*

First, I characterised how the expression of HS core proteins and biosynthetic enzymes is regulated in murine macrophages. Macrophages were generated by treating bone marrow-derived cells with M-CSF or GM-CSF *in vitro* for 7 days, and gene expression was measured by qPCR using custom-designed TaqMan low-density array cards for HS core proteins and biosynthetic enzymes (**Figure 3.1A**). This showed that murine macrophages expressed 8 of the possible 12 HS core proteins and 14 of the possible 25 HS biosynthetic enzymes. Expression of the core proteins *Tgfbr3* and *Gpc1* was 13- and 4-fold higher respectively in macrophages differentiated with GM-CSF (**Figure 3.1B and C**) than those differentiated with M-CSF. In contrast, the core proteins *Agrn*, *Gpc2*, *Sdc1* and *Sdc4* were expressed at higher levels in M-CSF-differentiated macrophages. Overall, the expression of elongation and modification enzymes was higher in macrophages differentiated with M-CSF by 1.5- to 2-fold. The extracellular sulfatase *Sulf2* was not differentially expressed between M-CSF- and GM-CSF-derived macrophages. Notably, *Hs3st3b1* expression was 25-fold higher in GM-CSF-differentiated macrophages, compared to M-CSF-derived macrophages.

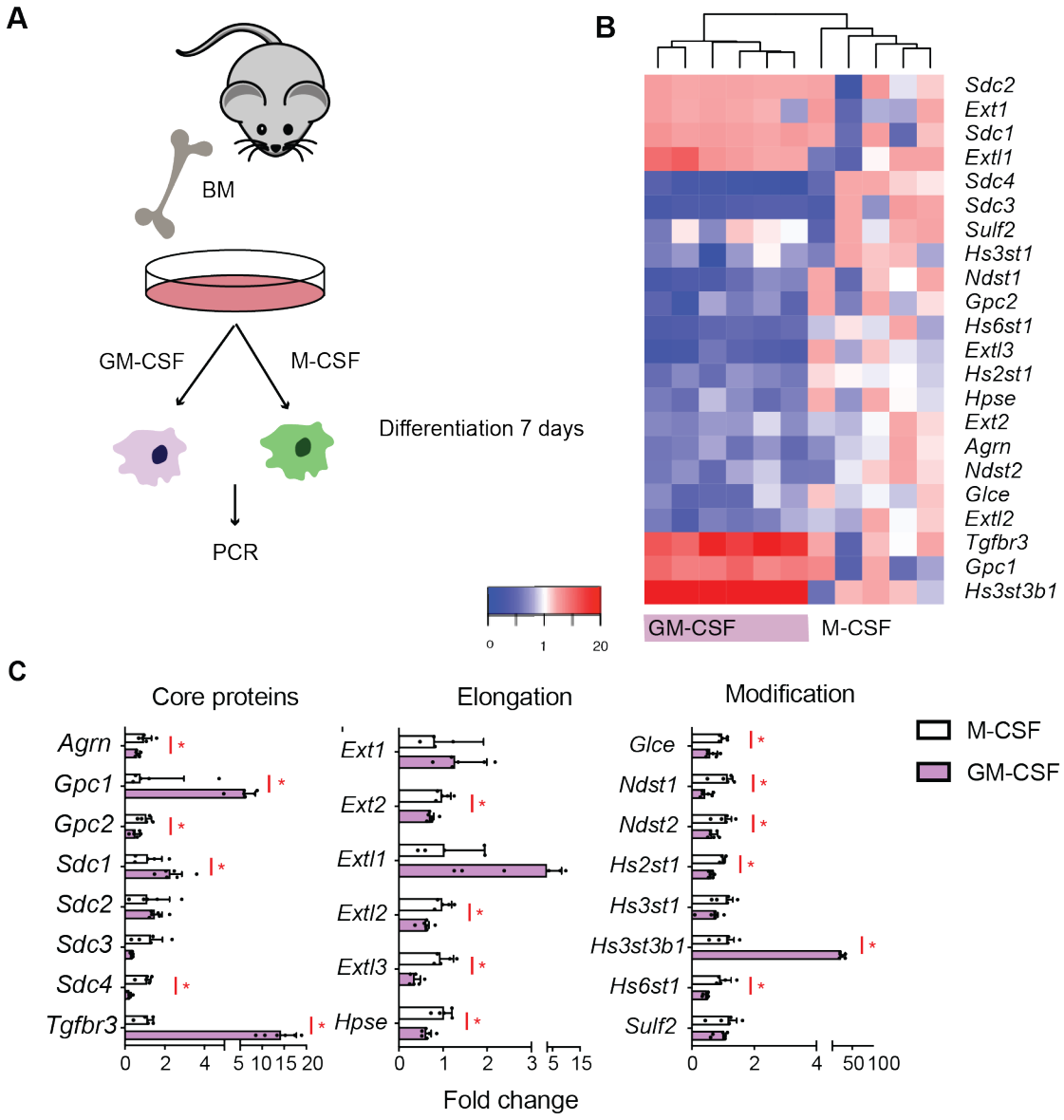


Figure 3.1 HS-associated gene expression in murine bone marrow-derived macrophages was differently regulated by differentiation with GM-CSF or M-CSF.

Macrophages were derived by culturing cells from murine bone marrow for 7 d with 100 ng/ml M-CSF (n=5 mice) or 20 ng/ml GM-CSF (n=6 mice). **B.** RNA was isolated and gene expression levels were measured by qPCR using custom-designed TaqMan low-density array cards, and expressed relative to the geometric mean of the housekeeping genes *18s*, *Gapdh*, and *Rplp0* and to expression in M-CSF-derived cells. Differential expression profiles were visualised using heatmapping. **C.** Fold change in the expression of core proteins and enzymes involved in the elongation and modification of HS relative to M-CSF derived cells is shown. Data are represented as median ± IQR. The p-values and q-values were determined by a Kruskall-Wallis test followed by multiplicity correction using the two-stage step-up method of Benjamini, Krieger and Yekutieli. *, P<0.05.

Next, I also set out to define how macrophage polarisation with IFNγ+LPS or IL4+IL13 affected HS gene expression in these murine macrophages. Gene expression was measured by qPCR using custom-designed TaqMan low-density array cards for HS core proteins and biosynthetic enzymes (**Figure 3.2A**). Activation with IFNγ+LPS generated a distinct gene expression profile (**Figure 3.2B**), as it downregulated the expression of the majority of the HS elongation and modification enzymes (**Figure 3.2C**). Stimulation with IFNγ+LPS also downregulated the core proteins *Tgfbr3* and *Sdc3*, but upregulated *Sdc4*. Stimulation with IL4+IL13 had less of an effect, only significantly increasing expression of the core proteins *Gpc1* (7.5-fold), *Sdc1* (2-fold) and *Sdc4* (3-fold).

Strikingly, *Sulf2*, an enzyme that removes 6-O sulfate groups from HS, was the most strongly downregulated gene, with a 25-40 fold reduction in expression after IFNγ+LPS activation of M-CSF-derived macrophages in comparison with unstimulated macrophages and those stimulated with IL4+IL13 (**Figure 3.2D**). *Hs6st1*, which is responsible for HS 6-O sulfation, was downregulated by 7-fold upon IFNγ+LPS activation. In contrast, *H6st2*, *Hs6st3* and *Sulf1* were not expressed by macrophages *in vitro*, indicating that 6-O sulfation in macrophages is regulated by the relative expression of *Hs6st1* and *Sulf2* (**Figure 1.7**).

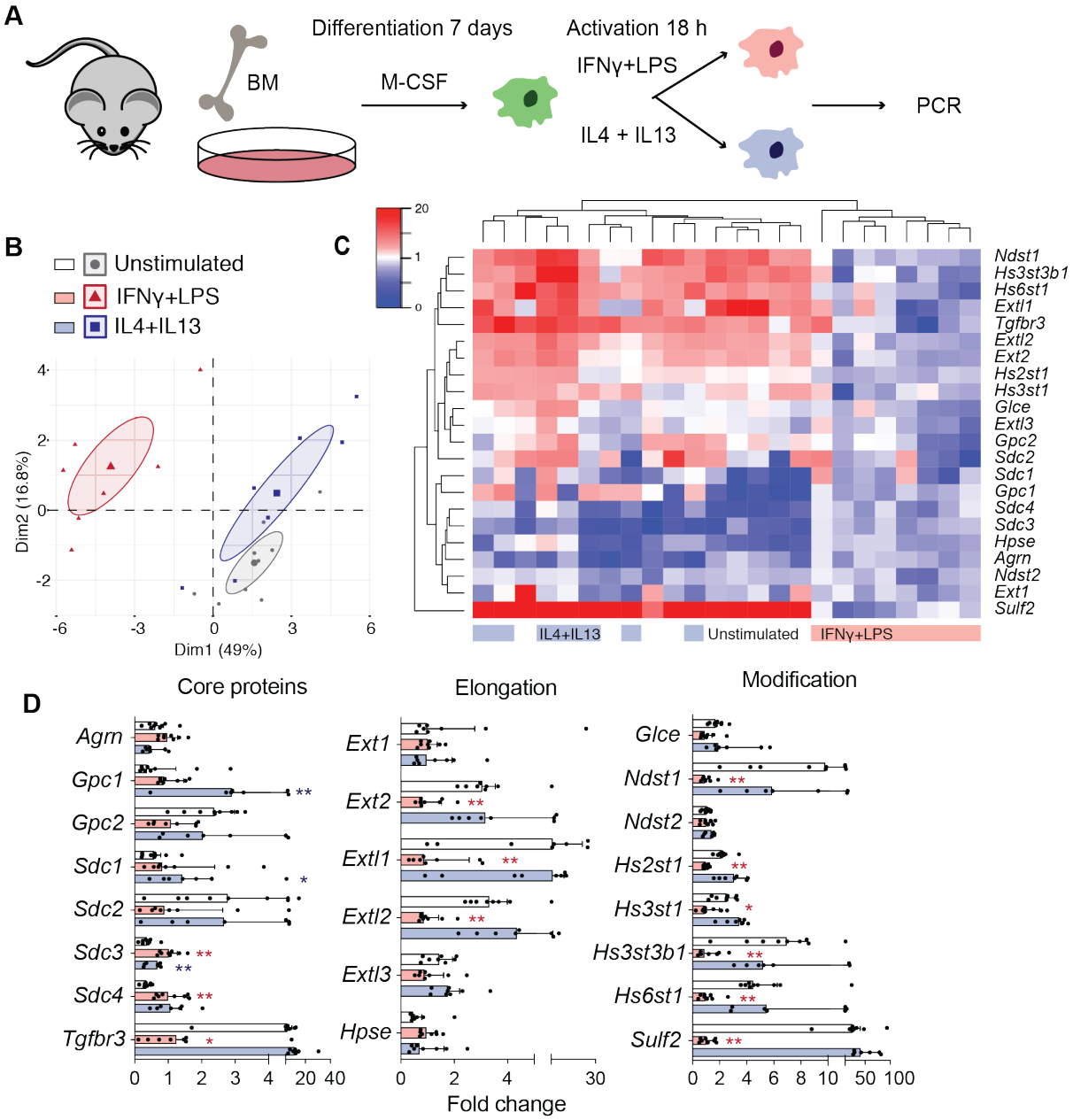


Figure 3.2. HS elongation and modification enzymes were downregulated by IFNγ+LPS. Macrophages were derived by culturing murine bone marrow-derived cells with 100 ng/ml M-CSF for 7 d (unstimulated, n=9 mice). Cells were then stimulated with 100 ng/ml IFNγ+LPS (both 100 ng/ml, n=8 mice) or IL4+IL13 (both 20 ng/ml, n=7 mice) for 18 h. **B.** RNA was isolated and gene expression levels were measured by qPCR using custom-designed TaqMan low-density array cards relative to the geometric mean of the housekeeping genes *18s*, *Gapdh*, and *Rplp0*. PCA analysis of the results is shown, with the ellipses indicating the 95% confidence interval. (Dim, dimension). **C.** Differential expression profiles were also visualised using heatmapping. **D.** Fold change in the expression of core proteins and enzymes involved in the elongation and modification of HS is shown for untreated and IL4+IL13 relative to IFNγ+LPS stimulated M-CSF-derived cells. Data are represented as median ± IQR. The p-values and q-values were determined by a Kruskall-Wallis test followed by multiplicity correction using the two-stage step-up method of Benjamini, Krieger and Yekutieli. *, P<0.05; **, P<0.01 (compared to unstimulated cells).

As stimulation with IL4+IL13 only had minor effects on the expression of HS core proteins, I measured the expression of polarisation markers to exclude the possibility that inefficient polarisation was responsible for the lack of effects seen with IL4+IL13. Stimulation of macrophages with IFNγ+LPS strongly upregulated *Il6* and *Nos2* (**Figure 3.3**), whereas IL4+IL13 upregulated *Arg1* and *Fizz1*, indicating that stimulation with IFNγ+LPS and IL4+IL13 was effective.

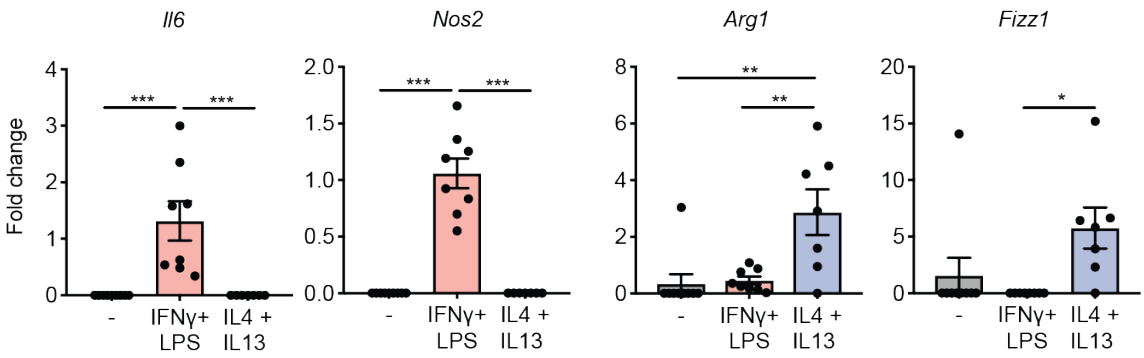


Figure 3.3. Validation of macrophage polarisation by IFNγ+LPS or IL4+IL13.
Macrophages were derived by culturing murine bone marrow-derived cells with 100 ng/ml M-CSF for 7 d (n=9 mice). The cells were then stimulated with IFNγ+LPS (both 100 ng/ml, n=8 mice) or IL4+IL13 (both 20 ng/ml, n=7 mice) for 18 h. RNA was isolated and gene expression levels were measured by qPCR relative to *Rplp0*. Fold change in the expression of *Il6* and *Nos2* relative to IFNγ+LPS-stimulated cells; and of *Arg1* and *Fizz1* relative to IL4+IL13-stimulated cells is shown. Data are represented as mean ± SEM, analysed by one-way ANOVA with Bonferroni's correction for multiple comparisons. *, P<0.05; **, P<0.01; ***, P<0.001.

I also set out to characterise the expression of HS core proteins and biosynthetic enzymes in the murine macrophage cell lines J774.2 and RAW264.7 (**Appendix figure 1**). Strikingly, both cell lines did not express *Gpc2*, *Hpse*, *Sulf2* or *Tgfbr3*. J774.2 cells in particular expressed lower levels of 8 other biosynthetic enzymes and core proteins, but expressed 30-fold higher levels of *Hs3st1* and *Hs3st3b1*.

Sulf2 was strongly downregulated by IFNγ+LPS, which prompted me to investigate whether other inflammatory mediators could also inhibit *Sulf2* expression. Macrophages were differentiated with M-CSF and stimulated for 6 h with various mediators. Apart from IL13, all mediators tested reduced *Sulf2* expression (**Figure 3.4**).

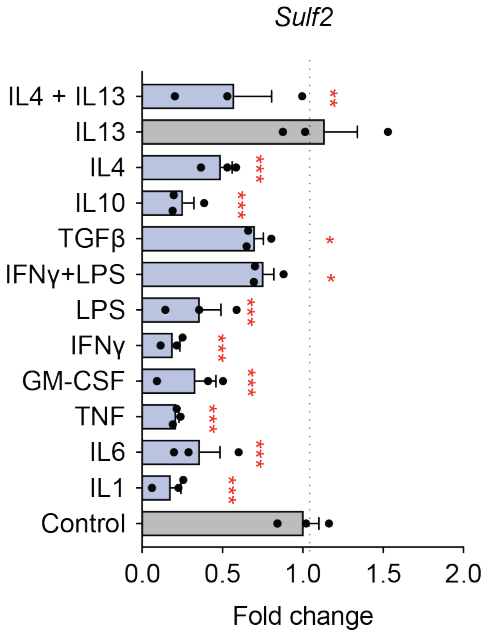


Figure 3.4. *Sulf2* was downregulated by inflammatory stimuli.
Murine macrophages were derived by culturing cells from murine bone marrow with 100 ng/ml M-CSF for 7 d (n=3 mice). Subsequently, the cells were stimulated for 6 h with 100 ng/ml of IL1, IL6, GM-CSF, IFNγ, LPS, IFNγ+LPS or IL10, or with 50 ng/ml of TNF, 20 ng/ml of IL4 and/or IL13, or 10 ng/ml of TGFβ. RNA was isolated and gene expression levels were measured by qPCR relative to *Rplp0* and to untreated controls. Data are represented as mean ± SEM, analysed by one-way ANOVA with Bonferroni's correction for multiple comparisons. *, P<0.05; **, P<0.01; ***, P<0.001.

Since *Sulf2* was the most highly regulated of the HS-associated genes during macrophage polarisation (**Figure 3.2**), I decided to investigate its effect on macrophage function *in vitro* and *in vitro*. As a first step towards this, I aimed to profile *Sulf2* expression in immune cell populations *in vivo.*

3.3. Characterisation of *Sulf2* expression *in vivo*

3.3.1. *Sulf2* is expressed by dendritic cells, macrophages and monocytes

I attempted to validate antibodies for detecting SULF2 by western blotting in BM-derived macrophages from *Sulf2*$^{+/-}$ and *Sulf2*$^{-/-}$ mice, which were generated by Dr A. Redpath and Dr N. Smart (University of Oxford, **Figure 2.1**). I tested several antibodies, and found that only one detected a protein at the expected molecular mass (130 kDa) in macrophage cell lysates. I also attempted to detect SULF2 in the supernatants using TCA-precipitation, but I was not able to detect SULF2 in these samples (data not shown). This 130 kDa band was absent in *Sulf2*$^{-/-}$ macrophages and reduced in *Sulf2*$^{+/-}$ macrophages (**Figure 3.5**), suggesting the antibody does recognise SULF2. However, this was a minor band, and the presence of several other higher intensity bands indicates that the antibody also binds to other proteins, and so cannot be used to detect SULF2 by flow cytometry or histochemistry.

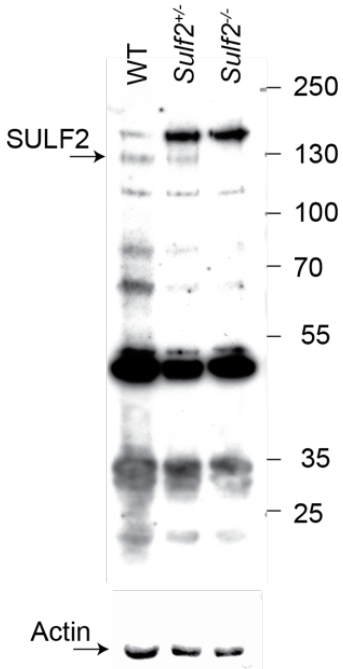


Figure 3.5. SULF2 antibody clone 2B4 recognised additional proteins.
BM cells from WT and *Sulf2*$^{+/-}$ mice were cultured for 7 d with 100 ng/ml M-CSF to differentiate macrophages. Western blotting with anti-human/mouse SULF2 clone 2B4 (R&D Systems) was performed to visualise SULF2, with an expected molecular mass of 130 kDa.

Therefore, I used the PrimeFlow *in situ* hybridisation assay to detect *Sulf2* mRNA after immunophenotyping by flow cytometry as no specific antibodies for SULF2 are available (**Figure 3.5**). This demonstrated that *Sulf2* is predominantly expressed by monocytes in the blood and bone marrow of mice (**Figure 3.6**).

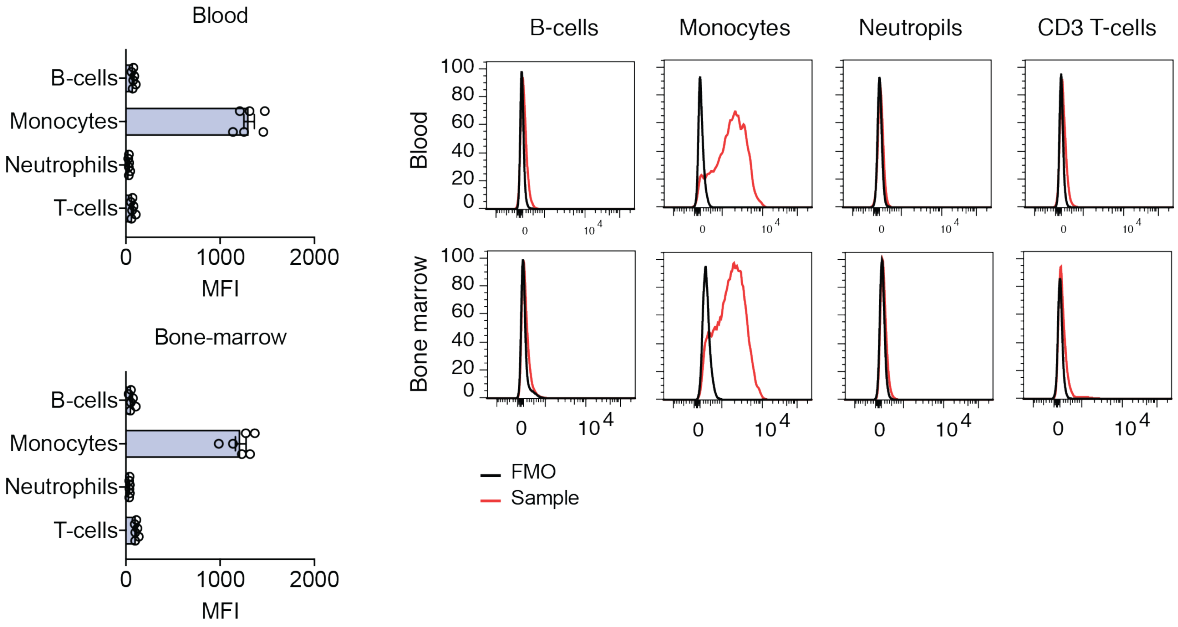


Figure 3.6. *Sulf2* was highly expressed by monocytes in murine blood and bone marrow. *Sulf2* expression was quantified in immune populations in the blood (n=6) and bone marrow (n=6) of C57BL/6 mice using the PrimeFlow *in situ* hybridisation assay. *Sulf2* expression is analysed by flow cytometry and expressed as the mean fluorescence intensity (MFI) minus the *Sulf2* fluorescence minus one (FMO). The gating strategy is shown in **Appendix Figure 2**. Representative histograms are shown and data are represented as mean ± SEM.

Subsequently, I profiled the spleen and lung more extensively to investigate *Sulf2* expression in DCs and macrophages. *Sulf2* was mainly expressed by dendritic cells, macrophages and monocytes in the spleen and lung (**Figure 3.7**), while *Sulf2* levels in B-cells, neutrophils and T-cells were negligible in the spleen and undetectable in the lung. However, the expression levels of *Sulf2* in myeloid cells appears to be subtype specific. For example, CD4+ T-cell activating cDC2s express 6-fold higher

levels of *Sulf2* than CD8+ T-cell-activating cDC1s. In addition, resident alveolar macrophages (AM) that reside in the alveolar air space expressed the highest *Sulf2* levels, while interstitial macrophages (IM) that are located in the bronchovascular bundles expressed 3.5-fold lower *Sulf2* levels. *Sulf2* was not detected in non-immune cells in the lung.

3.4. *Sulf2*-deficiency did not alter immune populations in healthy mice

Despite the relatively restricted expression of *Sulf2* in certain myeloid cell subtypes, it is possible that it might be required for the development of additional immune cell types. I addressed this question by phenotyping immune populations in the spleen, lung and bone-marrow of WT and *Sulf2*$^{+/-}$ mice. This analysis showed no significant differences in the proportion or absolute numbers of B-cells, dendritic cells, eosinophils, macrophages, neutrophils or T-cells in these tissues (**Figure 3.8**).

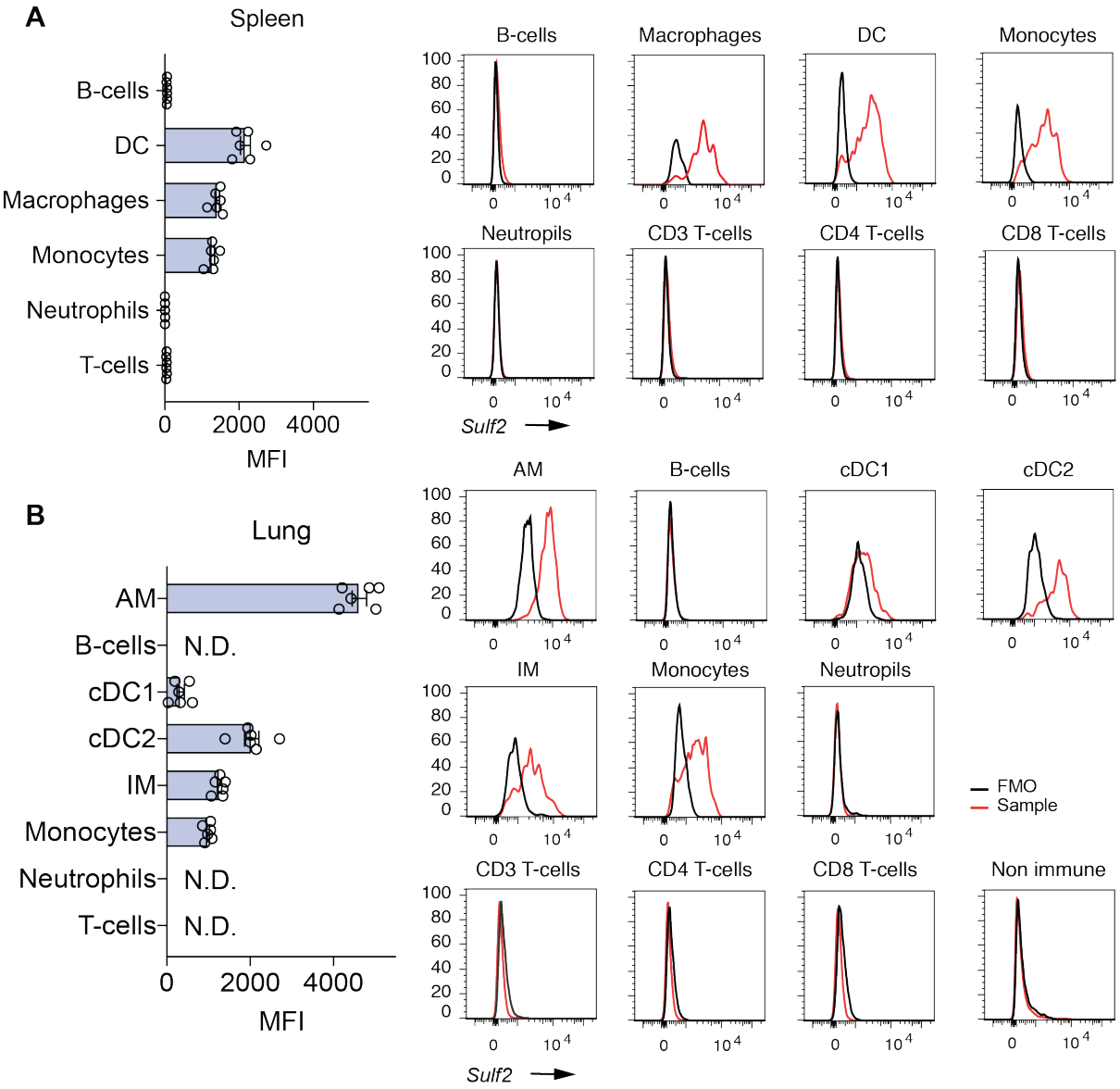


Figure 3.7. *Sulf2* was mainly expressed by macrophages, monocytes and dendritic cells in spleen and lung.

Sulf2 expression was quantified in immune populations in the **A.** spleen (n=6) and **B.** lung (n=6) of C57BL/6 mice using the PrimeFlow *in situ* hybridisation assay. *Sulf2* expression was analysed by flow cytometry and expressed as the mean fluorescence intensity (MFI) minus the *Sulf2* fluorescence minus one (FMO). Representative histograms are shown and data are represented as mean ± SEM. The gating strategy is shown in **Appendix Figure 3** and **Appendix Figure 4**. Abbreviations: AM, alveolar macrophages; IM, interstitial macrophages.

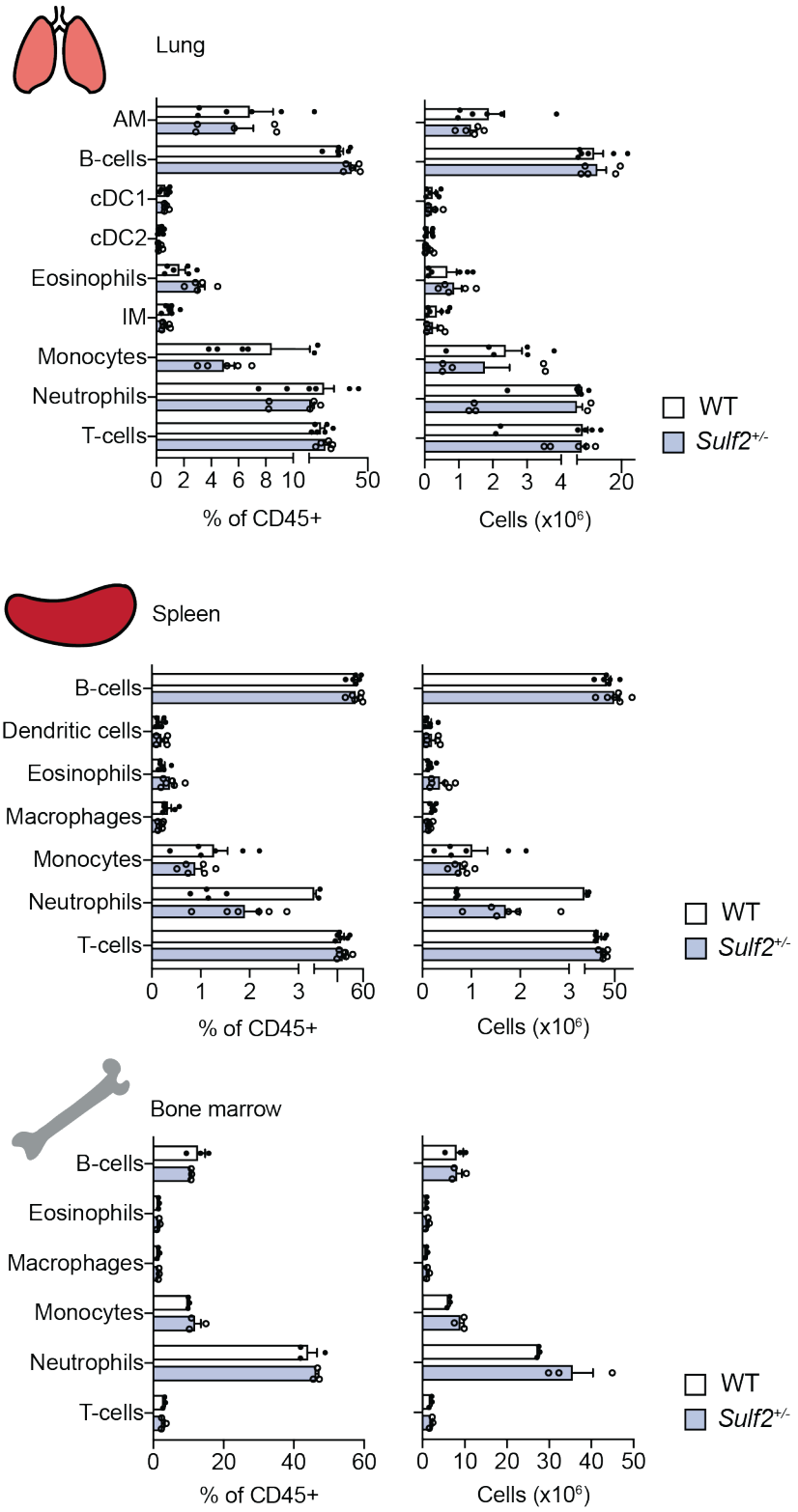


Figure 3.8. Tissue frequencies of immune populations were not affected by *Sulf2*-deficiency. Lungs (n=6), spleens (n=6) and bone marrow (n=3) of C57BL/6 WT and *Sulf2*$^{+/-}$ mice were digested and immune cell populations were analysed by flow cytometry. The gating strategy is shown in **Appendix Figure 3**, **Appendix Figure 4** and **Appendix Figure 5.** Data are represented as mean ± SEM, analysed by multiple T-tests. Abbreviations: AM, alveolar macrophages; IM, interstitial macrophages.

3.5. Discussion

The functions of HS in immune cells are poorly understood, largely because of the technical challenges that still remain in glycosaminoglycan research. In this chapter, I carried out the most comprehensive profiling of HSPG expression in murine macrophages to date, and showed that this pathway is differentially regulated in macrophage subsets, with higher expression in M-CSF-differentiated macrophages than in GM-CSF-differentiated macrophages. This implies that M-CSF-differentiated macrophages might carry more extensively sulfated HS. The molecular consequences of this difference and its effects on macrophage phenotype require further investigation. Additionally, there is considerable scope to investigate the roles of individual HS-associated genes. For example, *Hs3st3b1* was highly expressed in GM-CSF-differentiated macrophages, indicating a potential role for this enzyme in these cells.

Stimulation of M-CSF-differentiated macrophages with IFNγ+LPS drastically reduced expression of HS biosynthesis genes. I performed a meta-analysis of micro-array data from human and murine macrophage polarisation (**Appendix Figure 6**) that validated these findings (Swart and Troeberg, 2019). As a consequence of the reduced HS biosynthesis expression, human M1 macrophages have been shown to bear half the amount of HS compared to M2 macrophages, with a lower overall level of sulfation, particularly 2-O sulfation (Martinez et al., 2015). Therefore, I hypothesise that sulfated surface expression of HS on macrophages is important for the maintenance of homeostasis, and that reducing HS expression enables macrophages to become inflammatory.

Despite the overall similarity between HS regulation in murine and human macrophages, I observed some slight differences when comparing my and other

murine data sets with that for human macrophages (**Appendix Figure 6**). For example, *EXTL2*, *NDST1* and *HS3ST3B1* are upregulated by IFNγ+LPS in human macrophages, while they are downregulated in murine macrophages. The consequences of these differences are unclear, and may be affected by compensatory changes in other related genes. Further study into this area is required.

Among the genes downregulated by IFNγ+LPS in M-CSF-differentiated macrophages, *Sulf2* was the most strongly affected, with its expression reduced by 25-fold. Expression of *Sulf2* was also reduced by 40-fold compared to IL4+IL13-stimulated macrophages. This suggests that the primary role of SULF2 is in M0 and/or M2 cells, not in M1-like cells. *Sulf2* expression may be regulated directly by IFNγ-receptor and/or TLR4 signalling, or inflammatory mediators secreted in response to IFNγ+LPS exposure may be responsible for the pronounced decrease in *Sulf2* expression in these cells. In either case, the reduced expression of *Sulf2* in M1 compared to M0 and M2 macrophages may point to it having a largely anti-inflammatory role. I thus decided to focus my further mechanistic studies on *Sulf2*.

I found that *Sulf2* is predominantly expressed in murine macrophages, monocytes and DCs *in vivo*, while expression in neutrophils, B-cells and T-cells is low in the blood, bone marrow, spleen and lung. This high expression in myeloid cells is in agreement with RNA sequencing data from immune cell types isolated from human blood by Monaco et al. (2019), although they also reported moderate *SULF2* expression in human neutrophils and B-cells and low expression in T cells. These differences might be attributed to differences in the detection limits of PrimeFlow and RNA sequencing, but may also reflect differences in *Sulf2* expression between species. Good antibodies

are still not commercially available for SULF2, and availability of these would help the field progress.

I found particularly high expression of *Sulf2* in AMs. These originate from foetal monocytes (Guilliams et al., 2013; Schneider et al., 2014), reside in the air space of alveoli and are strongly immunosuppressive (Kopf et al., 2015; Allard et al., 2018). This is in line with data reported in the Immunological Genome Project (www.immgen.org) and potentially indicates that *Sulf2* has an immuno-inhibitory role in macrophages. However, I did not observe any difference in abundance of macrophages or other immune subsets in the lung, spleen and bone at steady state in *Sulf2*$^{+/-}$ mice, suggesting that *Sulf2* is not necessary for haematopoiesis and maturation of immune cells at steady state.

Overall, I have shown that stimulation of macrophages with IFNγ+LPS *in vitro* reduces the expression of HS biosynthesis genes and in particular reduces expression of the extracellular sulfatase *Sulf2*. Furthermore, *Sulf2* expression was downregulated by several inflammatory stimuli, indicating that downregulation of *Sulf2* during inflammation may act as a phenotypic switch redirecting macrophages from housekeeping to inflammatory functions. *In vivo*, resident immunosuppressive AMs express high *Sulf2* levels, supporting the housekeeping role of *Sulf2*. In addition to macrophages, monocytes and DCs also express *Sulf2 in vivo*. Therefore, I set out to investigate the functional role of *Sulf2* in macrophages and DCs *in vitro* in **Chapter 4**.

Chapter 4. Sulfatase-2 regulates macrophage polarisation and phagocytosis

4.1. Introduction

6-O sulfation of HS, which is catalysed by the 6-O sulfotransferases HS6ST1-3, is important for the regulation of many signalling pathways as described in **Chapter 1.3.1**. For example, 6-O sulfation is critical for FGF (A. Seffouh et al., 2013) and TGFß signalling (Yue et al., 2013). It is the only modification pattern that can be post-synthetically modified by the sulfatases SULF1 and SULF2 that remove 6-O sulfate groups, regulating signalling pathways downstream of growth factors such as BMP (Otsuki et al., 2010), GDNF (Ai et al., 2007), VEGF (Korf-Klingebiel et al., 2019) and Wnt (Nawroth et al., 2007). Sulfatase-deficient mouse models showed aggravated OA (Otsuki et al., 2010), myocardial infarction (Korf-Klingebiel et al., 2019) and pulmonary fibrosis (Yue, 2017), due to dysregulation of BMP, FGF, VEGF and TGFß signalling. However, the role of *Sulf2* in the regulation of immune cell function remains unexplored.

In **section 3.3** I demonstrated that *Sulf2* in mainly expressed by macrophages (and in particular resident macrophages), monocytes and DCs. I also showed in **section 3.2** that *Hs6st1* and *Sulf2* are the only enzymes regulating 6-O-sulfation of HS that are expressed at detectable levels in murine macrophages. Additionally, I have shown that *Sulf2* expression in macrophages is strongly downregulated by inflammatory stimuli, indicating that suppression of *Sulf2*-expression may enable macrophages to change from a protective to an inflammatory phenotype. However, the function of *Sulf2* in immune cells, such as macrophages and DCs, has not been directly investigated to date. Therefore, in this chapter, I aimed to assess the function of *Sulf2 in vitro*, using *Sulf2*-deficient macrophages and DCs, as well as siRNA knockdown of *Sulf2*. I investigated whether *Sulf2* affects macrophage polarisation, TLR signalling,

inflammasome activation, autophagy, phagocytosis and antigen presentation by macrophages and DCs.

4.2. *Sulf2*-null mice show high perinatal lethality

6-O sulfation is the only sulfation pattern that can be post-synthetically edited by the extracellular sulfatases SULF1 and SULF2 that remove 6-O sulfate groups (El Masri et al., 2017), indicating it is important for regulating the bioactivity of HS-binding proteins. Following my observation that *Sulf2* was the most strongly downregulated HS proteoglycan gene in response to IFNγ+LPS stimulation, I sought to characterise the role of *Sulf2* in macrophage and dendritic cell function.

Sulf2$^{-/-}$ mice showed perinatal lethality and only a few *Sulf2*$^{-/-}$ mice were generated (personal communication, Dr A. Redpath). Therefore, I used *Sulf2*$^{+/-}$ mice to study the role of *Sulf2* on immune function. BM-derived *Sulf2*$^{+/-}$ macrophages had 50% reduced *Sulf2* expression, without compensation in expression of *Sulf1* (**Figure 4.1**).

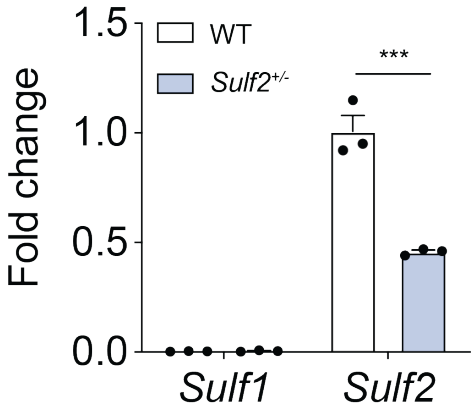


Figure 4.1. *Sulf2*$^{+/-}$ macrophages showed a 50% reduced *Sulf2* expression with no compensation on *Sulf1*.

Macrophages were derived by culturing cells from murine bone marrow of wild-type (WT) and *Sulf2*$^{+/-}$ mice with 100 ng/ml M-CSF for 7 d (n=3 per group). RNA was isolated and gene expression levels were measured by qPCR relative to *Rplp0.* Fold change in expression of *Sulf1* and *Sulf2* relative to *Rplp0* and *Sulf2* expression in WT cells. Data are represented as mean ± SEM, analysed by multiple T-test. ***, P<0.001.

4.3. *Sulf2*-deficiency impacted macrophage function

4.3.1. *Sulf2* affects macrophage responses to inflammatory stimuli

Next, I sought to investigate the function of *Sulf2* in macrophages. To that end, I generated macrophages from bone marrow of *Sulf2*$^{+/-}$ mice using M-CSF *in vitro* and activated these with IFNγ+LPS or IL4+IL13 to assess the effect on macrophage polarisation. I found that *Nos2* and *Socs3* expression was reduced in *Sulf2*$^{+/-}$ macrophages upon activation with IFNγ+LPS, while *Tnf* expression was increased (**Figure 4.2A+B**). Upon stimulation with IL4+IL13, *Arg1*, *Cd206* and *Fizz1* expression was reduced in *Sulf2*$^{+/-}$ macrophages (**Figure 4.2A+C**).

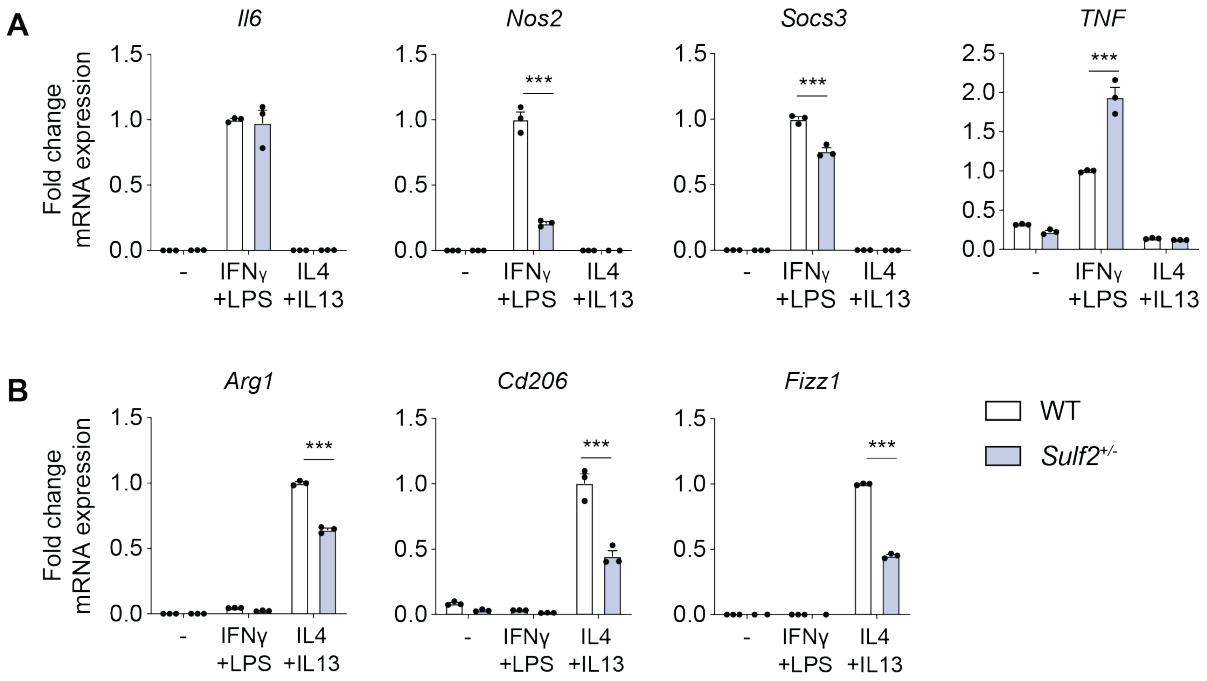


Figure 4.2. Macrophage polarisation was modulated by *Sulf2*.

Macrophages were derived by culturing cells from murine bone marrow of wild-type (WT) and *Sulf2*$^{+/-}$ mice with 100 ng/ml M-CSF for 7 d (n=3 per group). Cells were then stimulated with IFNγ+LPS (both 100 ng/ml) or IL4+IL13 (both 20 ng/ml) for 18 h. Afterwards, RNA was isolated and gene expression levels were measured by qPCR relative to *Rplp0*. **A.** Fold change in expression of pro-inflammatory markers relative to IFNγ+LPS-treated WT cells. **B.** Fold change in reparative markers relative to IL4+IL13-treated WT cells. Data are represented as mean ± SEM, analysed by two-way ANOVA with Bonferroni's correction for multiple comparisons. ***, P<0.001.

4.3.2. TLR signalling in *Sulf2*-deficient macrophages

LPS is a component of the membrane of Gram-negative bacteria and activates macrophages through TLR4 (Park and Lee, 2013). As *Sulf2* affected IFNγ+LPS-driven macrophage polarisation, I set out to determine if *Sulf2* affects cytokine production upon stimulation with TLR ligands. Macrophages were cultured with M-CSF and subsequently activated with Pam3CSK (for TLR1/ TLR2), FSL-1 (for TLR2), Poly I:C HMW (TLR3), LPS (for TLR4), IFNγ or IFNγ+LPS. Only IFNγ+LPS slightly increased IL6 secretion by *Sulf2*$^{+/-}$ macrophages as measured by ELISA (**Figure 4.3**), compared to WT macrophages.

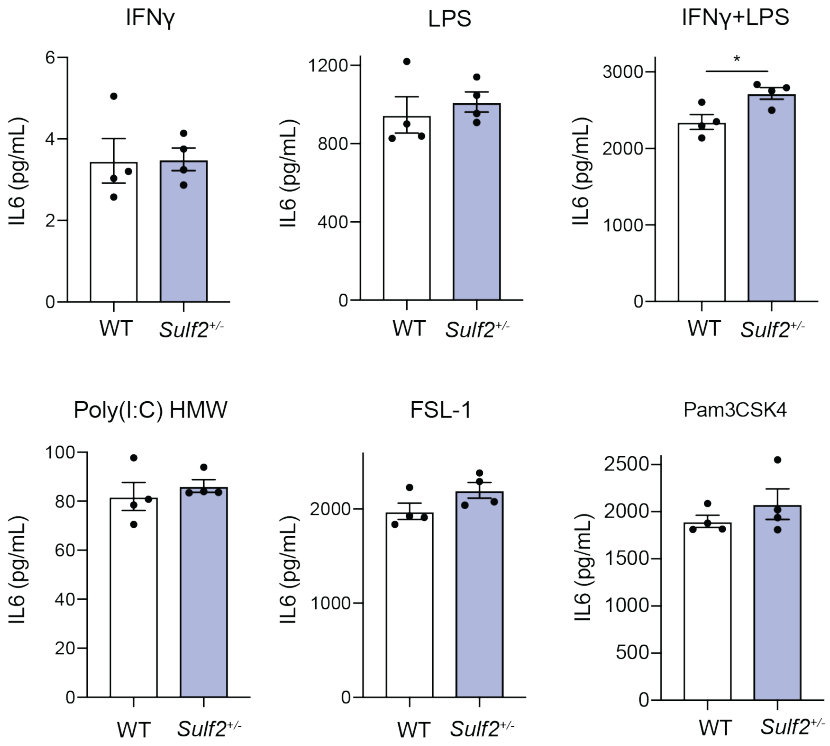


Figure 4.3. Toll-like receptor signalling was not affected by *Sulf2*-deficiency.
Macrophages were derived by culturing cells from WT and *Sulf2*$^{+/-}$ murine bone marrow with 100 ng/ml M-CSF for 7 d (n=4 per group). The cells were stimulated with IFNγ, LPS, IFNγ+LPS (all at 100 ng/ml), FSL-1 (100 ng/ml), 10 ng/ml poly(I:C) or 100 ng/ml Pam3CSK4. IL6 secretion was measured by ELISA. Data are represented as mean ± SEM, analysed by a two-tailed Student's T-test. *, P<0.05.

4.3.3. Inflammasome activation in *Sulf2*-deficient macrophages

Inflammasome activation is important for the release of another inflammatory cytokine, IL1β, and rapid inflammatory pyroptotic cell death (Swanson et al., 2019). Two signals are required for inflammasome activation: LPS and for example nigericin, a microbial toxin that acts as a potassium ionophore (Cullen et al., 2015). As polarisation in response to IFNγ+LPS was affected by *Sulf2*, I aimed to determine if inflammasome activation by LPS and nigericin was differentially regulated in *Sulf2*$^{+/-}$ macrophages. However, no effect on pyroptotic cell death or IL1β production was seen (**Figure 4.4**).

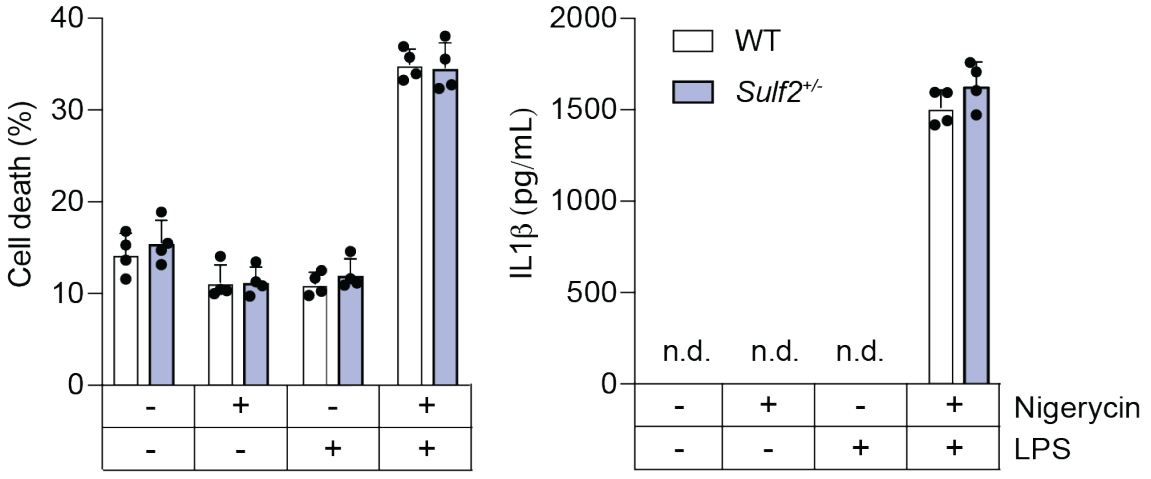


Figure 4.4. Inflammasome activation was not affected in *Sulf2*-deficient macrophages.
Macrophages were derived by culturing cells from WT and *Sulf2*$^{+/-}$ murine bone marrow with 100 ng/ml M-CSF for 7 d (n=4 per group). Cells were stimulated with 100 ng/ml LPS for 6 h, and for the last 2 h of culture 5 μM nigericin was added to stimulate NLRP3 inflammasome activation. Cell death was determined using the LDH assay and IL1β secretion was measured by ELISA. Data are represented as mean ± SEM, analysed by two-way ANOVA with Bonferroni's correction for multiple comparisons.

4.3.4. Autophagy in *Sulf2*-deficient macrophages

Autophagy is also important for macrophage polarisation as it reduces inflammatory macrophage polarisation (Liu et al., 2015). HS has previously been shown to affect autophagy (Reynolds-Peterson et al., 2017), which prompted me to assess if *Sulf2* regulates macrophage autophagy. I found that autophagy was not significantly affected in *Sulf2*$^{+/-}$ cells, as measured by western blotting for LC3-II (**Figure 4.5A+B**), a protein important for autophagosome formation. As LC3-II is subsequently degraded after fusion of the autophagosome with the lysosome, bafilomycin was added to inhibit autolysosome fusion. This showed that autophagic flux was also not affected in *Sulf2*$^{+/-}$ macrophages, as calculated by quantification of LC3-II levels in bafilomycin-treated versus untreated cells (**Figure 4.5A+C**).

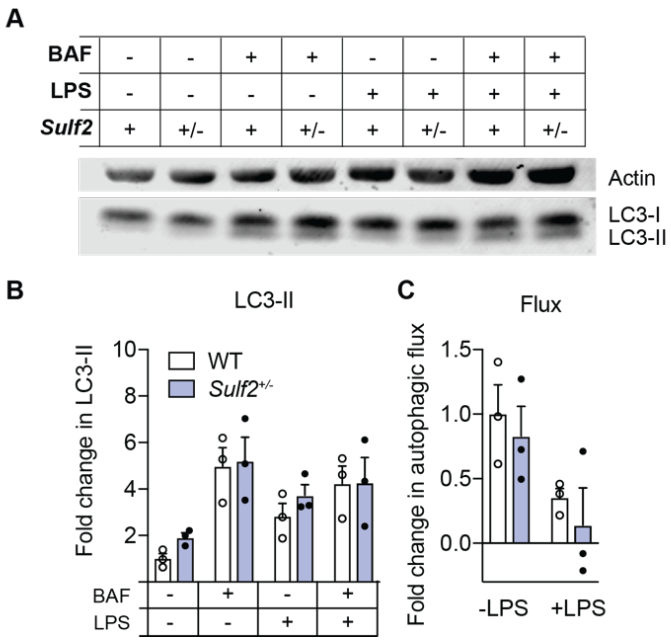


Figure 4.5. *Sulf2*-deficiency did not affect autophagy in macrophages.
Macrophages were derived by culturing cells from WT and *Sulf2*$^{+/-}$ murine bone marrow with 100 ng/ml M-CSF for 7 d (n=3 per group). Macrophages were stimulated with 100 ng/ml LPS for 18 h and incubated with 100 nM bafilomycin (BAF) for 2 h. Cells were lysed and LC3-I and -II expression analysed by western blotting. **A.** A representative western blot is shown. **B.** Fold change in LC3-II normalised to actin and **C**, the fold change in autophagic flux (BAF – untreated) normalised to actin are shown. Data are represented as mean ± SEM, analysed by two-way ANOVA with Bonferroni's correction for multiple comparisons.

4.3.5. Phagocytosis in *Sulf2*-deficient macrophages

Phagocytosis is one of the most important functions of macrophages as it is required for the elimination of pathogens, diseased and damaged cells (Hirayama et al., 2018). Therefore, I measured the phagocytic capacity of M-CSF-derived *Sulf2*-deficient macrophages using fluorescent polystyrene beads and apoptotic cells. I found that phagocytosis of polystyrene beads was increased by 25% and phagocytosis of apoptotic cells (efferocytosis) was increased by 43% in *Sulf2*-deficient cells (**Figure 4.6**), compared to WT cells.

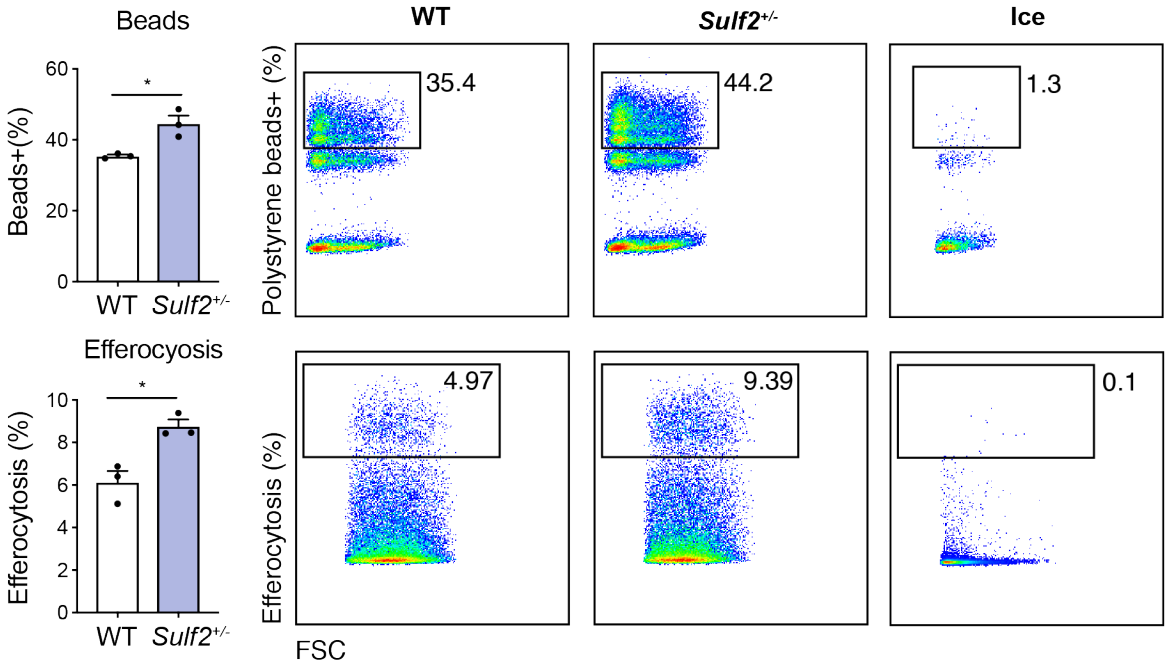


Figure 4.6. Phagocytosis was increased in *Sulf2*-deficient macrophages.
Macrophages were derived by culturing cells from WT and *Sulf2*$^{+/-}$ murine bone marrow with 100 ng/ml M-CSF for 7 d (n=3 per group). To measure phagocytosis, the cells were incubated with fluorescent polystyrene beads (50 MOI) or apoptotic cells (1 MOI). The percentage of cells positive for fluorescent phagocytic signal was determined by flow cytometry. Representative dot plots are shown. Data are represented as mean ± SEM, analysed by two-way Student's T-test. *, P<0.05.

As efferocytosis of dead cells was most strongly increased in *Sulf2*-deficient macrophages, I set out to investigate if efferocytosis receptor expression was regulated by *Sulf2*. The TAM receptors MERTK, AXL and TYRO3 can indirectly recognise phosphatidylserine (PS) on apoptotic cells via the bridging molecules Gas6 and Protein S (Pros1) resulting in the uptake of apoptotic cells (Lew et al., 2014). The integrin αvβ3 (*Itgb3*) is also involved in the uptake of apoptotic cells via the bridging molecule MFGE8. Finally, the scavenger receptor CD36 also contributes to efferocytosis (Ferracini et al., 2013). The expression of the efferocytosis receptor *Tyro3* and the scavenger receptor *Cd36* were 1.7 and 1.3 fold higher in *Sulf2*$^{+/-}$ macrophages (**Figure 4.7**), compared to WT macrophages. However, the expression of the other efferocytosis receptor and bridging molecules that were measured were not affected.

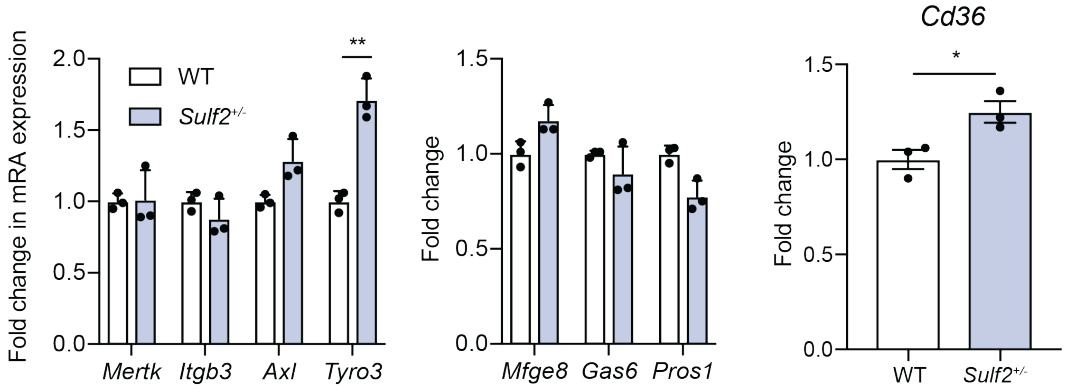


Figure 4.7. Expression of the efferocytosis receptors *Tyro3* and *Cd36* was increased in in *Sulf2*-deficient macrophages.

Macrophages were derived by culturing cells from WT and *Sulf2*$^{+/-}$ murine bone marrow with 100 ng/ml M-CSF for 7 d (n=3 per group). Afterwards, RNA was isolated and gene expression levels were measured by qPCR relative to *Rplp0* and to WT cells. Fold change in mRNA expression of efferocytosis receptors (*Mertk*, *Itgb3*, *Axl*, *Tyro3*), linkers (*Mfge8*, *Gas6*, *Pros1*) and the scavenger receptor *Cd36* were measured. Data are represented as mean ± SEM, analysed by multiple T-test. *, P<0.05; **, P<0.01.

4.4. siRNA knockdown of *Sulf2* altered macrophage phenotype.

4.4.1. *Sulf2* knockdown affected responses to inflammatory stimuli

To investigate whether the effects observed in *Sulf2*$^{+/-}$ macrophages were due to compensation, I aimed to confirm the effect on polarisation marker expression and phagocytosis in *Sulf2*$^{+/-}$ macrophages by short-term knockdown of the 6-O endosulfatase *Sulf2* using siRNA. *Sulf2* was downregulated by 84% at 24 h after knockdown and up to 90% 48 h after knockdown (**Figure 4.8**).

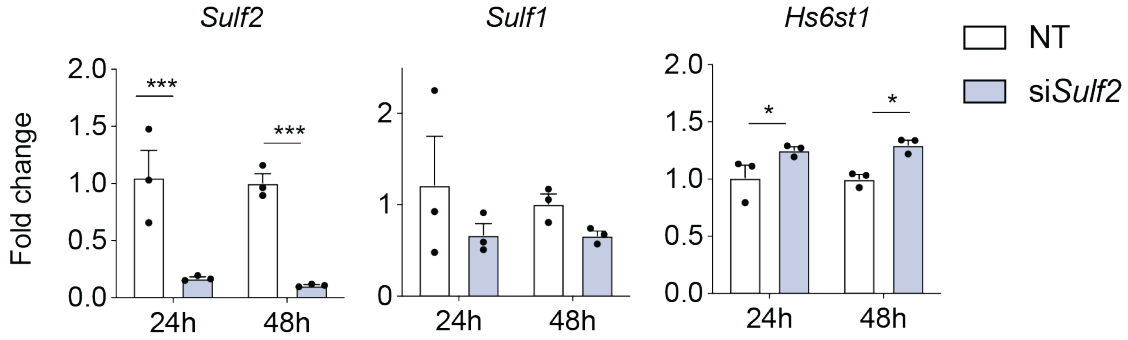


Figure 4.8. Validation of *Sulf2* knockdown by siRNA in primary murine macrophages.
Macrophages were derived by culturing cells from murine bone marrow with 100 ng/ml M-CSF for 5 d (n=3 per group). The cells were transfected with 50 nM non-targeting siRNA (NT) or siRNA against *Sulf2* (si*Sulf2*) using jetPRIME reagent. 24 and 48 h after siRNA treatment, RNA was isolated and gene expression levels were measured by qPCR relative to *Rplp0* and to NT-treated cells. Data are represented as mean ± SEM, analysed by two-way ANOVA with Bonferroni's correction for multiple comparisons. *, P<0.05; ***, P<0.001.

No compensatory effects were observed on the other 6-O endosulfatase *Sulf1*, which is minimally expressed in macrophages. The enzymes HS6ST1, HS6ST2 and HS6ST3 catalyse the opposite reaction to SULF1 and SULF2, as they promote sulfation of HS (**Figure 1.7**). As *Hs6st2* and *Hs6st3* are not expressed in macrophages, I measured the expression of *Hs6st1* to determine if this gene compensates for reduced *Sulf2* expression. In contrast to *Sulf2*$^{+/-}$ macrophages

(where no compensation was observed, **Figure 4.1**), an upregulation of *Hs6st1* by 20% was found 24 h and 48 h after knockdown of *Sulf2* (**Figure 4.8**).

Next, I determined if knockdown of *Sulf2* affected macrophage polarisation by IFNγ+LPS or IL4+IL13 (**Figure 4.9A**). Knockdown of *Sulf2* reduced the expression of *Nos2* and increased the expression of *Stat1* (**Figure 4.9B**) after stimulation with IFNγ+LPS. Moreover, it decreased *Fizz1* by 72% upon stimulation of IL4+IL13 (**Figure 4.9C**).

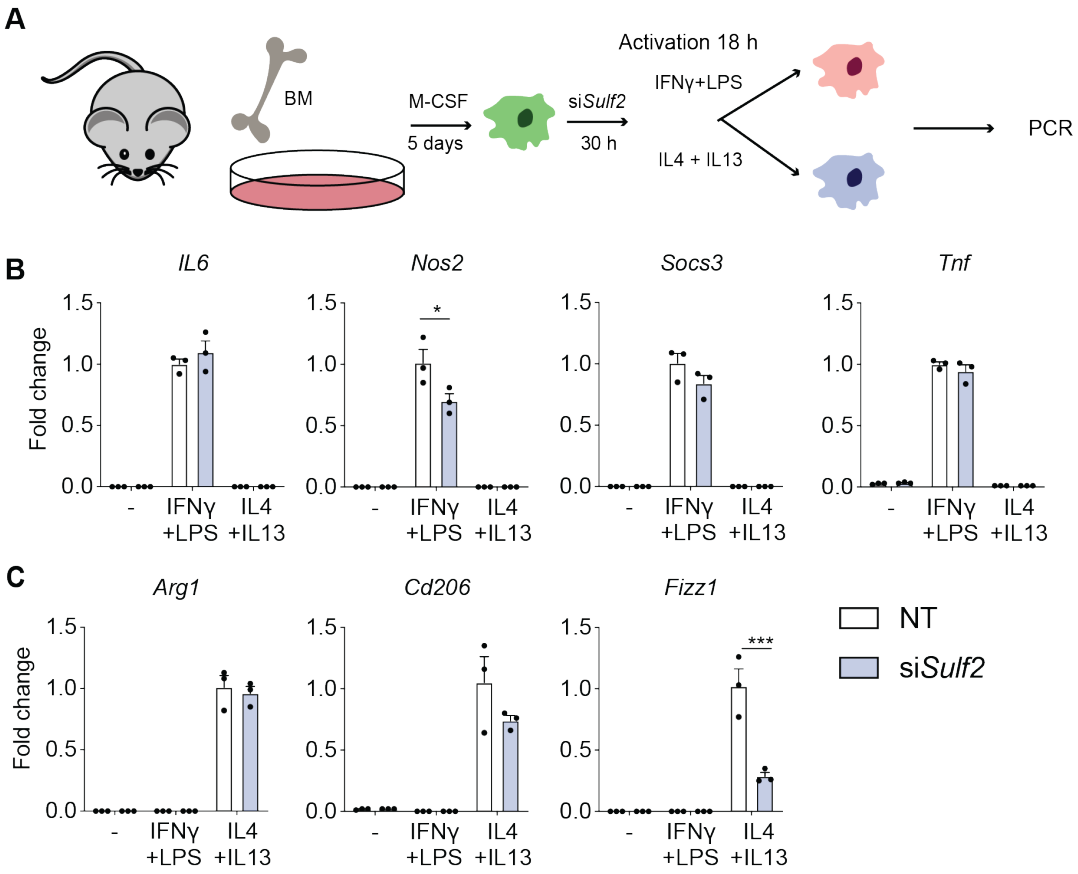


Figure 4.9. siRNA knockdown of *Sulf2* modulated macrophage polarisation.

A. Macrophages were derived by culturing cells from murine bone marrow with 100 ng/ml M-CSF for 5 d. The cells were transfected with 50 nM non-targeting siRNA (NT) or siRNA against *Sulf2* (si*Sulf2*) using jetPRIME reagent (n=3 per group). 30 h after siRNA treatment, the cells were stimulated with IFNγ+LPS (both 100 ng/ml) or IL4+IL13 (both 20 ng/ml) for 18 h. Afterwards, RNA was isolated and gene expression levels were measured by qPCR relative to *Rplp0*. **B.** Inflammatory macrophage markers relative to NT-treated cells stimulated with IFNγ+LPS and **C.** reparative macrophage markers relative to NT-treated cells stimulated with IL-4+IL13 were measured. Data are represented as mean ± SEM, analysed by two-way ANOVA with Bonferroni's correction for multiple comparisons. *, P<0.05; ***, P<0.001.

While this profile differs somewhat from that in *Sulf2*$^{+/-}$ macrophages (**Figure 4.2**), the data indicate that *Sulf2* might inhibit polarisation towards both inflammatory and reparative macrophages.

I also measured the phagocytic capacity of M-CSF-derived macrophages after knockdown of *Sulf2* using fluorescent polystyrene beads and apoptotic cells. As was seen in the *Sulf2*$^{+/-}$ macrophages (**Figure 4.6**), phagocytosis of all the phagocytic substrates tested was increased upon *Sulf2* knockdown (**Figure 4.10**), with stronger effects seen for apoptotic cells (75% increase) than for polystyrene beads (51%).

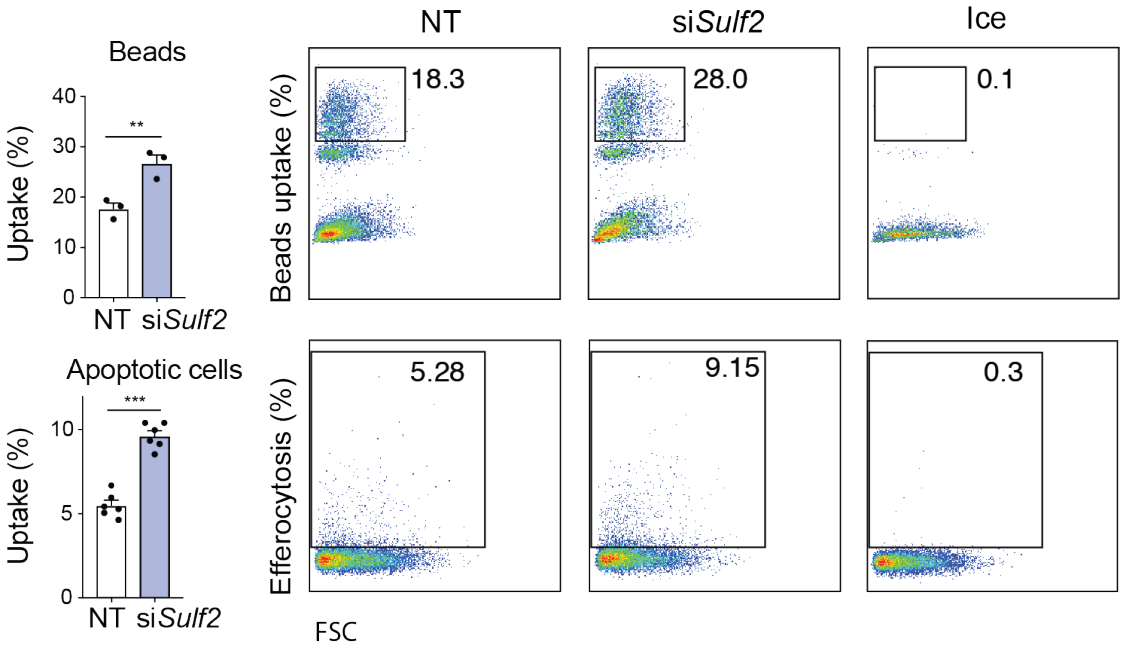


Figure 4.10. siRNA knockdown of *Sulf2* increased phagocytosis.

Macrophages were derived by culturing cells from murine bone marrow with 100 ng/ml M-CSF for 5 d. The cells were transfected with 50 nM non-targeting siRNA (NT) or siRNA targeting *Sulf2* (si*Sulf2*) using jetPRIME reagent. After 48 h, cells were incubated with a 50-fold multiplicity of infection (MOI) of fluorescent polystyrene (n=3) beads or 1 MOI apoptotic cells (n=6). The percentage of cells positive for fluorescent phagocytic signal was determined by flow cytometry. Gates were drawn based on a control with cells incubated on ice to correct for binding of phagocytosis reagents to the cell surface. Representative dot plots are shown. This is a representation of 2 independent experiments. Data are represented as mean ± SEM, analysed by a two-tailed Student's T-test. **, P<0.01; ***, P<0.001.

4.5. *Sulf2*-deficiency did not affect antigen presentation by dendritic cells *in vitro*

Both macrophages and in particular DCs are also essential for the regulation of adaptive immune responses by antigen presentation. In an effort to assess if antigen presentation by macrophages or dendritic cells was affected by *Sulf2*, I generated BM-derived macrophages and dendritic cells from WT and *Sulf2*$^{+/-}$ mice. In short, CD11c+MHC-II+ dendritic cells and CD11c+ and CD11c- macrophages were derived using GM-CSF (**Appendix Figure 7**). Macrophages were also derived using M-CSF, and the cells stimulated with LPS.

As *Sulf2* affects phagocytosis, I hypothesised that *Sulf2* differences in antigen uptake can potentially affect antigen presentation. I measured antigen uptake by incubating macrophages and DCs with Alexa647-labeled ovalbumin (OVA). Antigen uptake was highest in M-CSF-derived macrophages and CD11c+ GM-CSF-derived macrophages. Antigen uptake was decreased by *Sulf2* deficiency in the latter CD11c+ macrophages, but was unaffected by *Sulf2* deficiency in DCs, CD11c- GM-CSF- and M-CSF-derived macrophages (**Figure 4.11**).

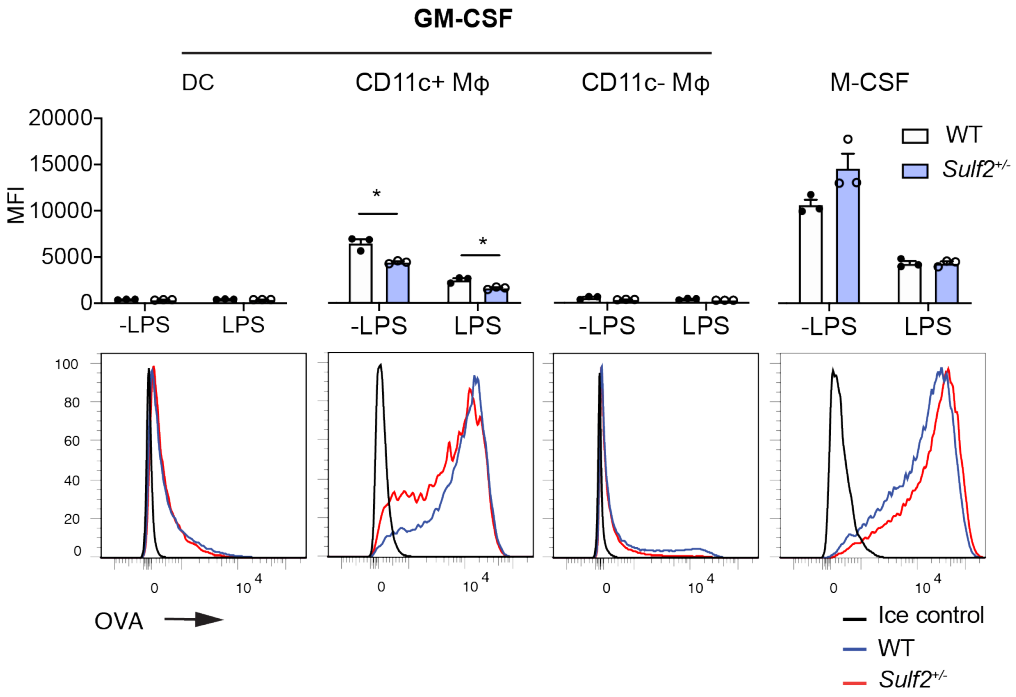


Figure 4.11. Antigen uptake in GM-CSF-derived CD11c+ macrophages was reduced by *Sulf2* deficiency.

BM cells from WT and *Sulf2*$^{+/-}$ mice (n=3) were cultured for 7 d with 100 ng/ml M-CSF to differentiate macrophages or 20 ng/ml GM-CSF to obtain DCs, CD11c+ and CD11c- macrophages. Cells were stimulated with 100 ng/ml of LPS for 6 h. The cells were incubated with 0.1 mg/ml Alexa647-conjugated OVA for 1 h at 37 °C and analysed by flow cytometry. The gating strategy is shown in **Appendix Figure 7**. Uptake of OVA is expressed as the mean fluorescence intensity (MFI). Data are presented as mean ± SEM, analysed by a two-way ANOVA with Bonferroni's correction for multiple comparisons; *, P<0.05.

Next, I measured the expression of MHC-I, MHC-II and co-stimulatory molecules on these cells by flow cytometry. Dendritic cells expressed high levels of MHC-II, which is responsible for antigen presentation to CD4 T-cells, and also high levels of the costimulatory molecules CD80 and CD86. Additionally, expression of these markers was increased by LPS stimulation, which promotes DC maturation. In contrast to the DCs, GM-CSF macrophages expressed low levels of MHC-I, CD80 and CD86. M-CSF-derived macrophages expressed the highest levels of MHC-I and moderate levels of CD86. MHC-II surface expression was modestly, albeit significantly, decreased in LPS-stimulated *Sulf2*$^{+/-}$ DCs, while the expression of co-stimulatory molecules was unaffected (**Figure 4.12**).

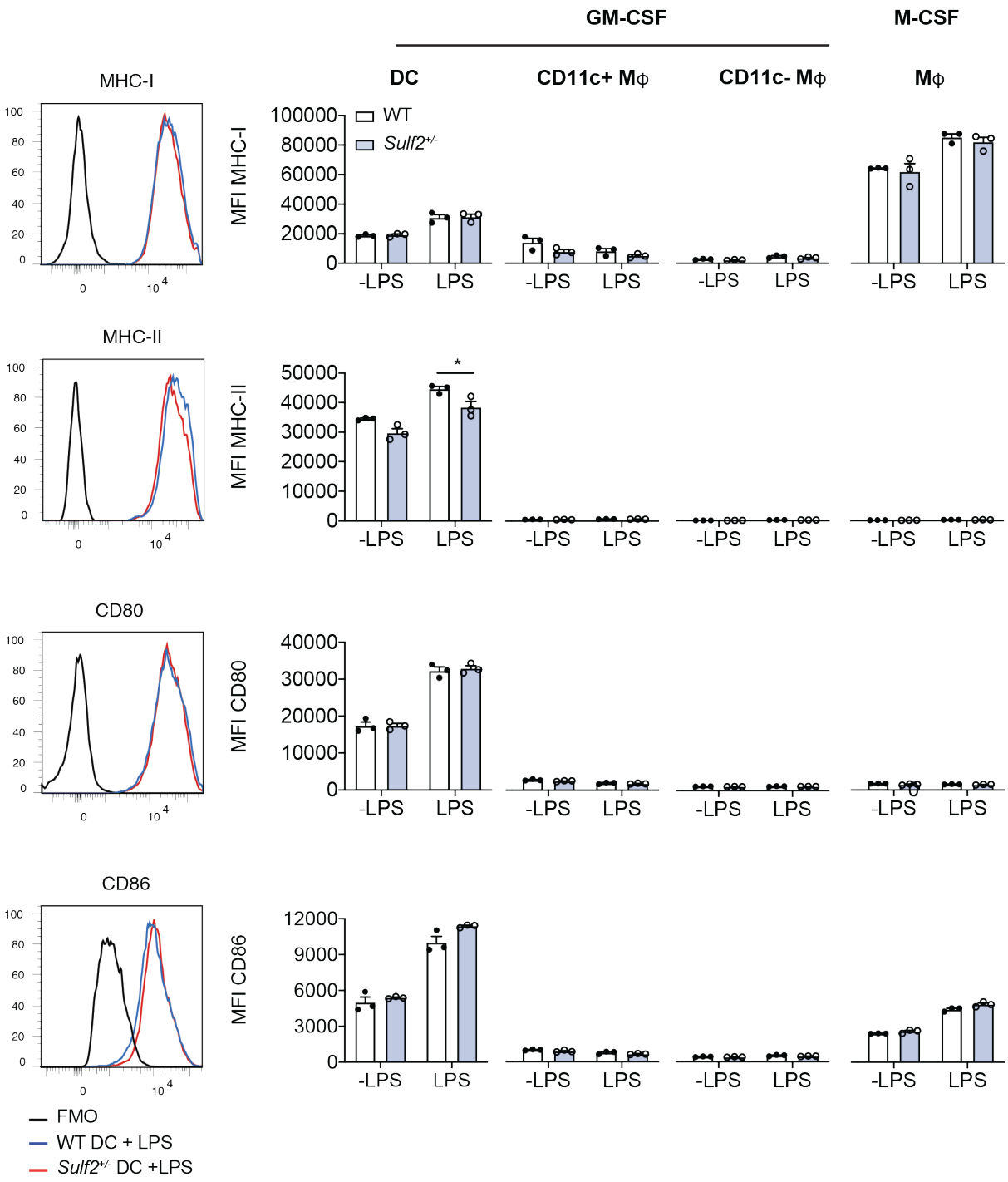


Figure 4.12. The expression of costimulatory molecules on antigen presenting cells was not affected by *Sulf2*.

BM cells from WT and *Sulf2*$^{+/-}$ mice (n=3) were cultured for 7 d with 100 ng/ml M-CSF to differentiate macrophages or 20 ng/ml GM-CSF to obtain DCs, CD11c+ and CD11c- macrophages. The surface expression of MHC-I, MHC-II, CD80 and CD86 was measured by flow cytometry after stimulation with 100 ng/ml LPS for 6 h and expressed as the mean fluorescence intensity (MFI). The gating strategy is shown in **Appendix Figure 7**. Data are presented as mean ± SEM, analysed by a two-way ANOVA with Bonferroni's correction for multiple comparisons; *, P<0.05.

Antigen presentation by LPS-stimulated macrophages and DCs was assessed by co-culturing them with OT-II CD4+ T-cells isolated from mice that carry the Vβ 5.1/5.2 T-cell receptor (TCR) that is specific for OVA 323-339 presented on MHC-II (Barnden et al., 1998). Macrophages and DCs were loaded with OVA, or the OVA 323-339 peptide (OVAp) that does not need processing and can directly bind to MHC-II. OT-II CD4+ T-cells were labelled with CellTrace to measure proliferation of T-cells. Macrophages were not able to promote proliferation of OT-II CD4+ in this context (data not shown), while DCs did. The division index (average number of cell divisions), proliferation index (average number of cell divisions by divided cells), percent of divided cells and the expression of the activation marker CD25 were not affected by reduced expression of *Sulf2* in DCs (**Figure 4.13**).

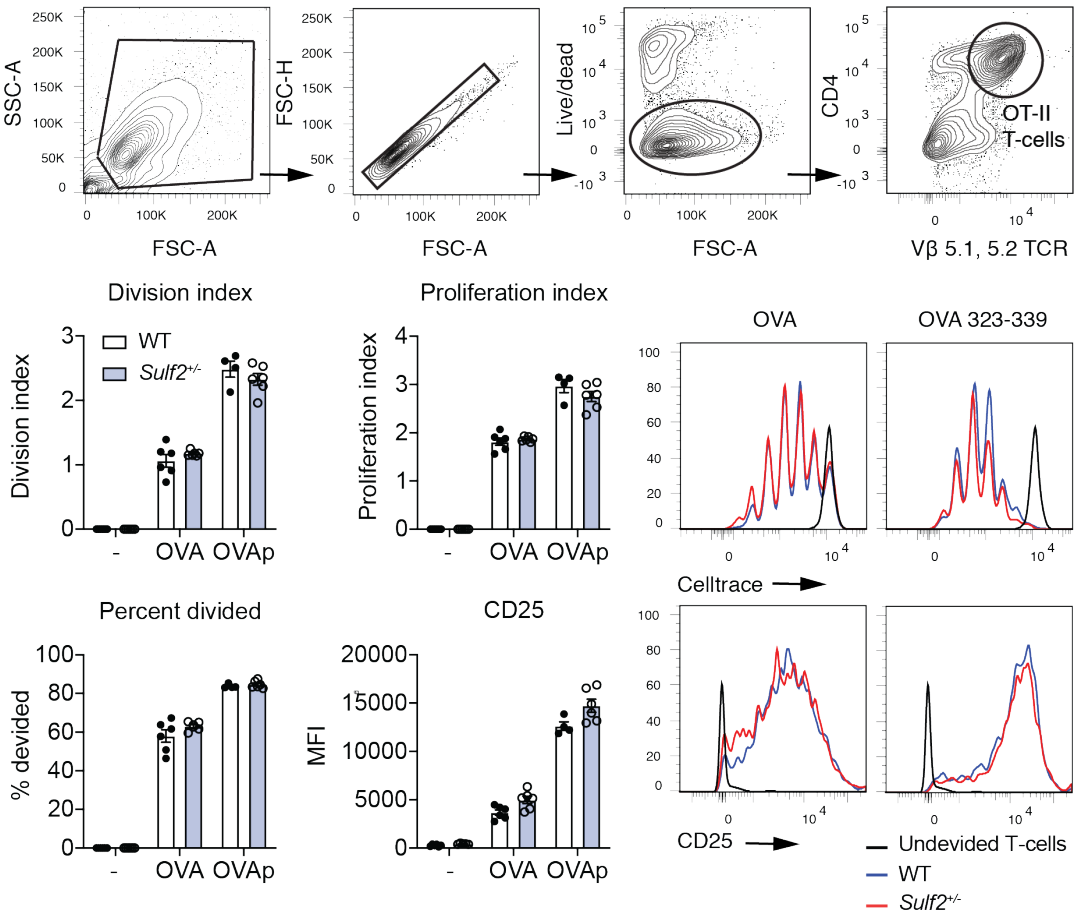


Figure 4.13. *Sulf2*-deficiency did not affect antigen presentation by dendritic cells *in vitro*. BM cells from WT and *Sulf2*$^{+/-}$ mice (n=3) were cultured for 7 d with 20 ng/ml GM-CSF to obtain DCs. DCs were incubated with 0.1 mg/ml OVA for 1 h at 37 °C. Maturation was promoted by stimulation with 100 ng/ml LPS for 4 h. CD4+ T-cells were isolated from spleens of OT-II transgenic mice that carry the Vβ 5.1/5.2 T-cell receptor (TCR) that is specific for OVA 323-339. The isolated cells were labelled with 5 µM CellTrace Violet to track their proliferation. Subsequently, DCs (10^4 cells) were co-cultured with CellTrace Violet-labelled CD4 T-cells (10^5 cells) in the presence of 10 µM OVA 323-339 peptide (OVAp) for 4 d. After 4 days, the expression of CD25 and the proliferation of CD4 OT-II T-cells (gating strategy shown in top panel) was measured by flow cytometry and the division index, proliferation index and percent divided cells were determined using FloJo's proliferation tool. Data are presented as mean ± SEM, analysed by a two-way ANOVA with Bonferroni's correction for multiple comparisons.

4.6. Discussion

In this chapter, I studied the effect of *Sulf2* on macrophage and DC function *in vitro*, by profiling its effects on functions such as in polarisation in response to cytokines and phagocytosis. Initially, I examined the impact of *Sulf2* deficiency in M-CSF-derived macrophages on their subsequent polarisation in response to IFNγ+LPS and IL4+IL13. This showed an apparent reduction in polarisation towards both pro- and anti-inflammatory phenotypes. Overall, stronger effects were seen in *Sulf2*$^{+/-}$ macrophages than in si*Sulf2*-treated cells, possibly reflecting more pronounced effects on 6-O-sulfation by genetic ablation that by siRNA treatment.

Firstly considering polarisation in response to IL4+IL13 stimulation, I saw reduced expression of all M2 markers analysed in *Sulf2*$^{+/-}$ macrophages i.e. *Fizz1, Cd206* and *Arg1* (**Table 4.1**). The same was observed for *Fizz1* in si*Sulf2*-treated cells, with a trend towards reduced expression of *Cd206*. Little is known about the role of FIZZ1 in macrophages, but the C-type mannose receptor CD206 is expressed on various resident macrophage types (Gordon et al., 2014) and it has been shown to dampen proinflammatory cytokine expression (Kambara et al., 2015). It is thought that ARG-1 is important for the resolution of inflammation and tissue repair as it inhibits T-cell proliferation by L-arginine depletion (Munder, 2009). Overall, this indicates that *Sulf2*$^{+/-}$ macrophages stimulated with IL4+IL13 are less anti-inflammatory.

A somewhat more complex picture was seen in response to IFNγ+LPS stimulation, with reduced expression of *Nos2* and *Socs3*, but increased expression of *Tnf* in *Sulf2*$^{+/-}$ macrophages (**Table 4.1**). The increase in *Tnf* expression indicates that *Sulf2*$^{+/-}$ macrophages may have a more inflammatory phenotype. *Nos2* is generally considered to promote inflammation, since NOS2 shifts arginine metabolism in macrophages toward the production of NO, which is important for the generation of

antimicrobial agents and consequently pathogen killing (Schairer et al., 2012). However, studies using *Nos2*$^{-/-}$ mice demonstrate NO also inhibits M1 polarisation and inflammatory gene expression (Lu et al., 2015; Xiong et al., 2004) by inhibiting the transcription factor IRF5 through nitration (Xue et al., 2018). Decreased *Nos2* expression may thus also indicate that *Sulf2*-deficient macrophages are more inflammatory. Similarly, *Socs3* limits inflammation, so its increased expression in *Sulf2*-deficient macrophages points to them having a more inflammatory phenotype.

Table 4.1. Summary of functional and polarisation effects of *Sulf2* deficiency in macrophages.

	Gene/ function	***Sulf2*$^{+/-}$**	**si*Sulf2***
M0	Phagocytosis	▲	▲
M1	*Il6*	-	-
	Nos2	▼	▼
	Socs3	▼	-
	Tnf	▲	-
M2	*Arg1*	▼	-
	Cd206	▼	-
	Fizz1	▼	▼

The mechanism(s) leading to these effects on macrophage polarisation are not known, but it is tempting to speculate that the increase in 6-O sulfation caused by SULF2 deficiency affects binding and signalling of IFNγ+LPS or IL4+IL13. For example, both IL4 (Lortat-Jacob et al., 1997) and IFNγ (Sadir et al., 1998) have been shown to bind to HS. Moreover, binding of IFNγ to HS has been shown to prevent binding to the IFNγ receptor (Sadir et al., 1998). While the effects of 6-O-sulfation on IL4 and IFNγ binding to HS have not been investigated, the results in this chapter suggest that 6-O-sulfation may inhibit IL4 receptor signalling, since *Sulf2* deficiency (leading to increased 6-O-sulfation) reduces responses to IL4. However, the role of 6-O sulfation in the regulation of IFNγ signalling is less clear as it negatively regulates *Nos2* and *Socs3* expression

while positively regulating *TNF* epression. However, it cannot be excluded that inflammatory mediators upregulated by IFNγ+LPS are also subject to regulation by binding to HS and therefore complicate the results. Such hypotheses could be tested *in vitro*, by examining the effect of 6-O-sulfation on IL4 and IFNγ binding to HS, and on subsequent interaction with cognate receptors. This would define whether 6-O-sulfation helps present these ligands to their receptors, or whether it sequesters them away and blocks signalling.

In vivo, the picture is likely to be even more complex, as HS can affect cytokine activity not only at the level of receptor engagement, but also via effects on localisation and stability. For example, HS has been shown to enhance IFNγ activity *in vivo* (Lortat-Jacob and Grimaud, 1991; Lortat-Jacob et al., 1996), through the formation of a gradient and protection from degradation (Lortat-Jacob, 2006). The relative importance of effects on receptor binding and localisation/protection from degradation may differ in different contexts, and *in vitro* experiments may not recapitulate the *in vivo* effects. This prompted me to analyse the effects of *Sulf2 in vivo* in a murine RA model (**Chapter 5**). In addition to its effects on IFNγ, it is likely that *Sulf2* affects the bioactivity of many other inflammatory mediators (Ori et al., 2011), thereby affecting multiple aspects of macrophage function (**Figure 1.5**). This complexity further supports the need for *in vivo* analysis of *Sulf2*'s effects.

Furthermore, I examined the effect of *Sulf2*-deficiency on behaviour of unstimulated M-CSF-differentiated macrophages using several phenotypic assays. Among these, I found an effect only on phagocytosis, with increased phagocytosis (**Table 4.1**) of polystyrene beads and particularly apoptotic cells in macrophages with reduced *Sulf2*

expression (both *Sulf2*$^{+/-}$ and si*Sulf2*). Phagocytosis can have pro-or anti-inflammatory effects depending on the substrate, which highlights the importance of an *in vivo* model to investigate the role of *Sulf2* in RA. For example, Fc- or MR-mediated phagocytosis induces pro-inflammatory cytokine production (Aderem and Underhill, 1999), while the uptake of apoptotic cells suppress inflammation (Rothlin et al., 2007; Elliott et al., 2017).

It is tempting to speculate that the increase in expression of efferocytosis and phagocytosis receptors contributes to the enhanced phagocytosis. For example, I found an increase in expression of the receptors *Tyro3* and *Cd36.* However, *Tyro3* is minimally expressed in macrophages (Zagórska et al., 2014) and resting macrophages predominantly phagocytose apoptotic cells through MERTK (Seitz et al., 2007). It is also possible that *Sulf2* regulates the bioavailability of Gas6, since Gas6 contains a HS-binding domain (Manfioletti et al., 1993) and has been hypothesised to bind to HS (Wu et al., 2017). As phagocytosis of multiple substrates was increased in macrophages with reduced *Sulf2* expression, it is more likely that a common pathway is affected. For example, expression of the scavenger receptor *Cd36* was increased, and this receptor can perform both phagocytosis and efferocytosis (Ferracini et al., 2013). However, I cannot exclude the possibility that other pathways might be involved in the increase in phagocytosis in *Sulf2*$^{+/-}$ and si*Sulf2* macrophages. HS itself might also function as a phagocytosis receptor (Chmiela et al., 1995; Fukasawa et al., 1997; Dehio et al., 1998) and it could be hypothesised that the increase in 6-O sulfation in macrophages with a reduced *Sulf2* expression directly enhances binding and internalisation of beads and apoptotic cells.

In summary, *Sulf2* did not directly regulate short-term inflammatory signalling of macrophages, but rather modulated macrophage programming responses, and in turn their functions. My results show that *Sulf2* is important for the polarization of macrophages (either M1- or M2-directed), and that it inhibits phagocytosis of particulates and apoptotic cells. In **Chapter 5**, I tested the hypothesis that *Sulf2* modulates macrophage behaviour and hence inflammation *in vivo* using an inflammatory model of arthritis.

Chapter 5. Sulfatase-2 protects against experimental arthritis

5.1. Introduction

Macrophages are pivotal for promoting the development of RA as they produce various chemokines (Yeo et al., 2016) that recruit other immune cells and cytokines (Kinne et al., 2007). However, specific resident macrophage subtypes in the joint have been shown to be protective in RA by secreting anti-inflammatory mediators (Alivernini et al., 2020).These resident macrophages have an embryonic origin (Tu et al., 2019). The resident CX_3CR1+ barrier macrophages (**Figure 1.2**) at the synovial lining form tight junctions that constitute an immunological barrier protecting the joint (Culemann et al., 2019). Interstitial CX_3CR1- macrophages found in deeper layers of the synovial tissue replenish the barrier macrophages and give rise to protective alternatively-activated macrophages (Culemann et al., 2019). Inflammation during RA development activates the CX_3CR1+ macrophages, disrupting the tight junctions and impairing barrier function, paving the way for immune infiltration into the joint (Culemann et al., 2019). This facilitates infiltration of Ly6C+ monocytes into the joint and their differentiation into macrophages (Weiss et al., 2015; Udalova et al., 2016).

In this Chapter, I re-analysed scRNA seq data published by Culemann et al. (2019) to investigate which macrophages subtypes predominantly express *Sulf2* in the joint. I also characterised *Sulf2* expression in immune cells in AIA, which models various processes in mice that are important during human RA, such as immune infiltration, cartilage degradation and bone erosion (van den Berg et al., 2007). Inflammation is promoted in this model by injecting mBSA into the joint of a mouse previously immunised with mBSA in CFA. Finally, I sought to investigate if *Sulf2* expression in immune cells impacts the development of AIA using *Sulf2*-deficient bone marrow chimera mice.

5.2. *Sulf2* is expressed at high levels in resident macrophages in the RA joint

First I set out to determine which immune populations express SULF2 in RA joints by mining published scRNA seq datasets. Data from Zhang et al. (2019) indicate that human fibroblasts and monocytes/ macrophages express the highest levels of *SULF2* in RA joints (**Figure 5.1**).

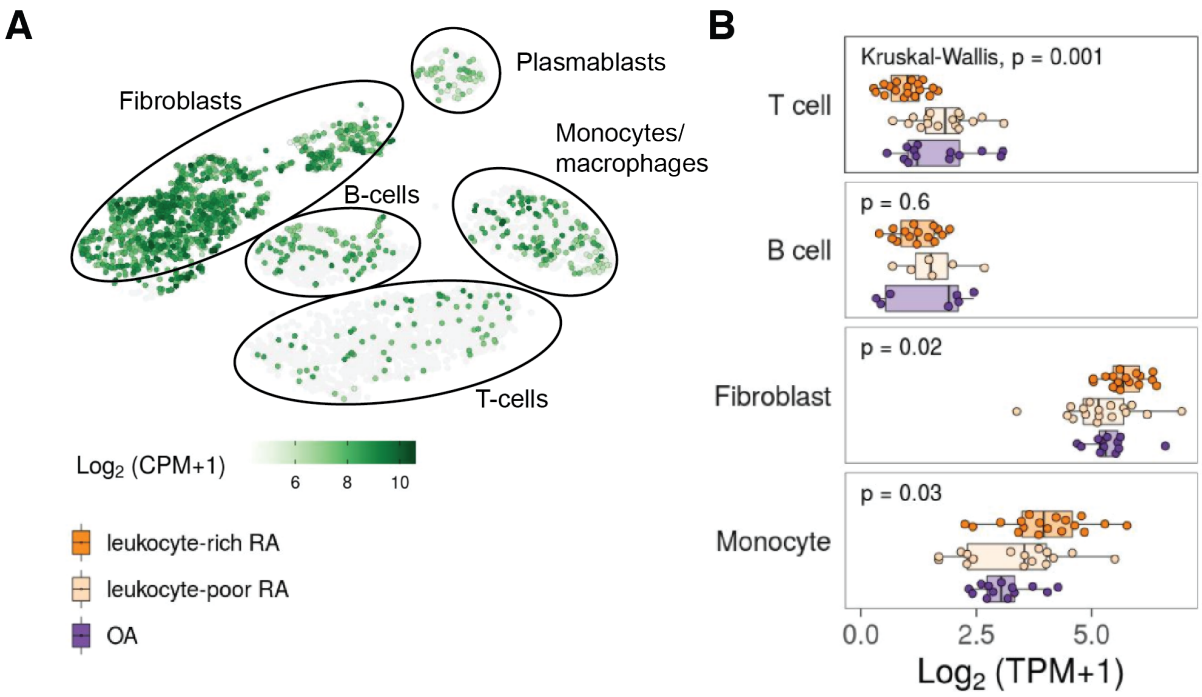


Figure 5.1. *Sulf2* expression in human RA.

A. High-dimensional transcriptomic clustering of single cell RNAseq data from Zhang et al., 2019 show *SULF2* expression in 5 immune populations. **B.** Bulk RNAseq data from Zhang et al., show *SULF2* expression in leukocyte-rich, -poor RA and OA.

Next I aimed to investigate which macrophage subtypes in the joint predominantly express *Sulf2*. To that end, I re-analysed published scRNA-seq data comparing CD45+CD11b+Ly6G- cells isolated from knee joints of control, healthy mice with those isolated 5 days after K/BxN serum transfer as a model for RA (Culemann et al., 2019). In order to be able to compare the expression between individual subsets in health and disease, I integrated the health and disease datasets. In line with the previously reported findings (Culemann et al., 2019), my analysis revealed an osteoclast population and 4 resident macrophage subsets: *Aqp1*+, *MHC-II*+, *Retnla*+ and *Cx3cr1*+ macrophages (**Figure 5.2**).

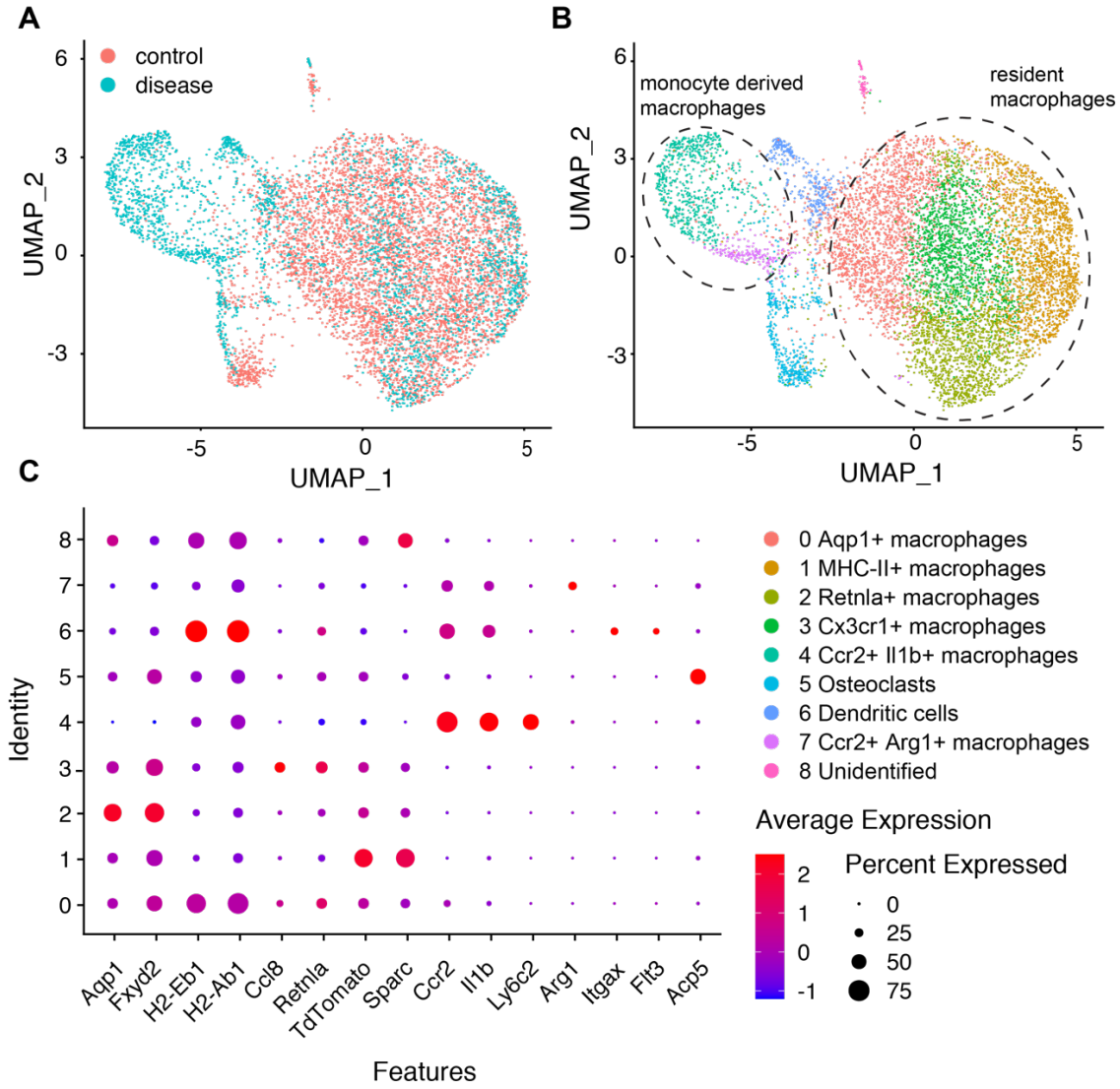


Figure 5.2. Single cell sequencing analysis of CD45+CD11b+Ly6G- joint cells identified distinct myeloid populations.

scRNA-seq data of CD45+CD11b+Ly6G- cells from knee joints of healthy mice (5830 cells, control) and mice 5 days post K/BxN serum transfer (2959 cells, disease) (Culemann et al., 2019) were **A.** integrated and re-analysed and **B.** clustered by UMAP to reveal 4 resident macrophages populations and 2 monocyte-derived populations. **C.** A dot plot shows the average expression of selected marker genes in each cluster, where the dot size represents the percentage of cells that express each gene.

In addition, the diseased dataset also revealed 2 monocyte-derived macrophage populations (*Ccr2+ IL1b+* and *Ccr2+ Arg1+* macrophages) and DCs. Differential expression testing identified that *Sulf2* was expressed 2-fold higher (log2 fold change, 0.94, adjusted p-value 1.7×10^{-110}) in resident macrophages compared to monocyte-

derived macrophages (**Figure 5.3A, B, D**). However, its expression was similar in resident macrophages from healthy and diseased joints (**Figure 5.3C**).

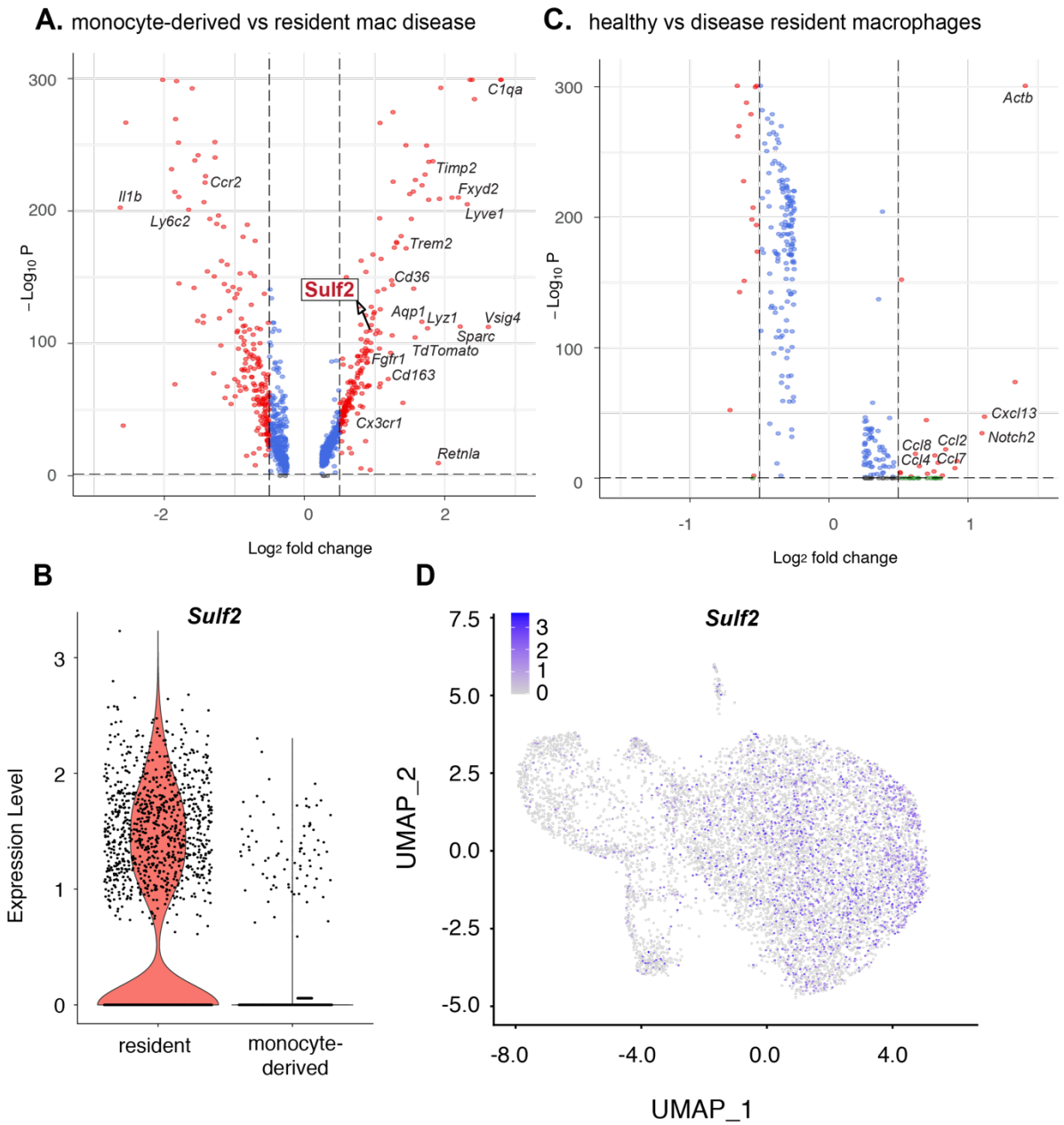


Figure 5.3. *Sulf2* was predominantly expressed by resident macrophages in the joint.
scRNA-seq data of CD45+CD11b+Ly6G- knee joint cells from healthy mice (5830 cells) and mice 5 days post K/BxN serum transfer (2959 cells, disease) (Culemann et al., 2019) were integrated and re-analysed and clustered by UMAP. Differential expression testing was performed using the non-parametric Wilcoxon rank sum test. **A.** A volcano plot shows differentially expressed genes between monocyte-derived and resident macrophages in diseased joints. **B.** *Sulf2* expression is shown in a violin plot. **C.** A volcano plot shows differentially expressed genes between resident macrophages in healthy and diseased joints. **D.** A feature plot illustrates *Sulf2* expression by individual cells in the integrated dataset.

I also analysed the dataset to ascertain which core proteins and other modifying enzymes are expressed in the joint. This showed that macrophages predominantly expressed the core proteins *Cd44*, *Nrp1* (neuropilin 1), *Sdc3* and *Sdc4* (**Figure 5.4A**). *Nrp1* was expressed at higher levels by resident macrophages, while *Cd44* and *Sdc4* expression was higher in monocyte-derived macrophages (**Figure 5.4B**). Interestingly, apart from *Sulf2*, HS modifying enzymes were expressed at low levels in all clusters.

I also reanalysed bulk RNA-seq data from Culemann et al. (2019), to compare *Sulf2* expression in *Cx3cr1*+ lining, *Cx3cr1*- interstitial macrophages and BMDMs. These data indicate that *Sulf2* expression was 1.6-fold higher (log2 fold change 0.74, adjusted p-value 4.05×10^{-5}) in *Cx3cr1*+ lining macrophages than in *Cx3cr1*- interstitial macrophages (**Figure 5.5A**). However, it is important to note that these lining macrophages have a distinctly different gene expression profile from BMDMs. For example, *Sulf2* expression was 24.5-fold higher (log2 fold change 4.61, adjusted p-value 4.8×10^{-201}) in *Cx3cr1*+ lining macrophages than in BMDMs (**Figure 5.5B**). GO analysis revealed that cell death, metabolism and pathways involving macromolecules are most strongly upregulated in lining macrophages in the joint, compared to BMDMs (**Figure 5.5C**). This emphasises the importance of studying *Sulf2* function in immune cells *in vivo*.

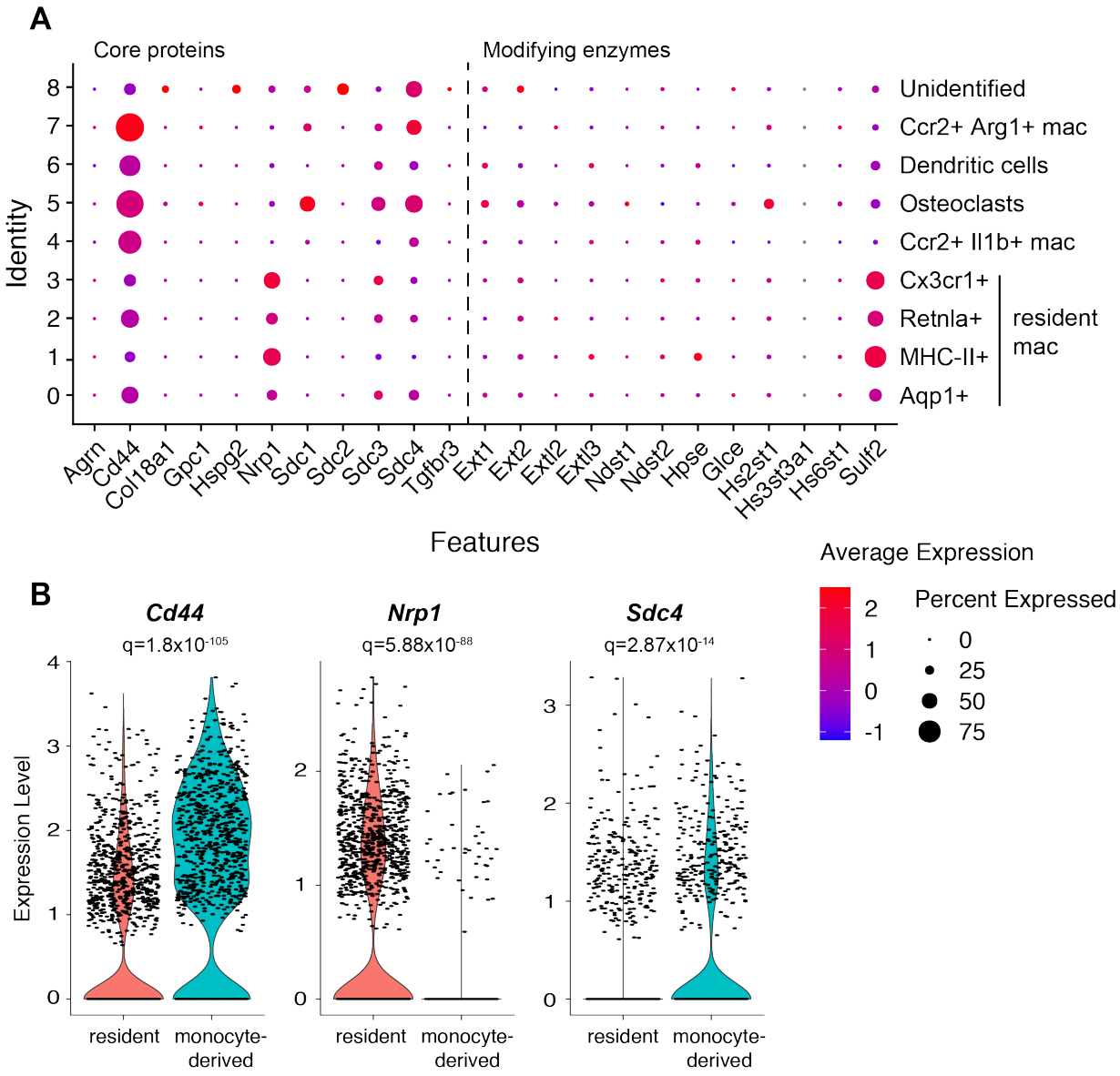


Figure 5.4. Expression of heparan sulfate core proteins and modifying enzymes in the arthritic joint.

scRNA-seq data of CD45+CD11b+Ly6G- knee joint cells from healthy mice (5830 cells) and mice 5 days post K/BxN serum transfer (2959 cells, disease) (Culemann et al., 2019) were integrated and re-analysed and clustered by UMAP. **A.** A dot plot shows the average expression of heparan sulfate core proteins and modifying enzymes in each cluster in diseased joints, where the dot size represents the percentage of cells that express each gene. **B.** Violin plots of significantly differentially expressed genes between resident and monocyte-derived macrophages. Differential expression testing was performed using the non-parametric Wilcoxon rank sum test. Adjusted p-values (q) are shown.

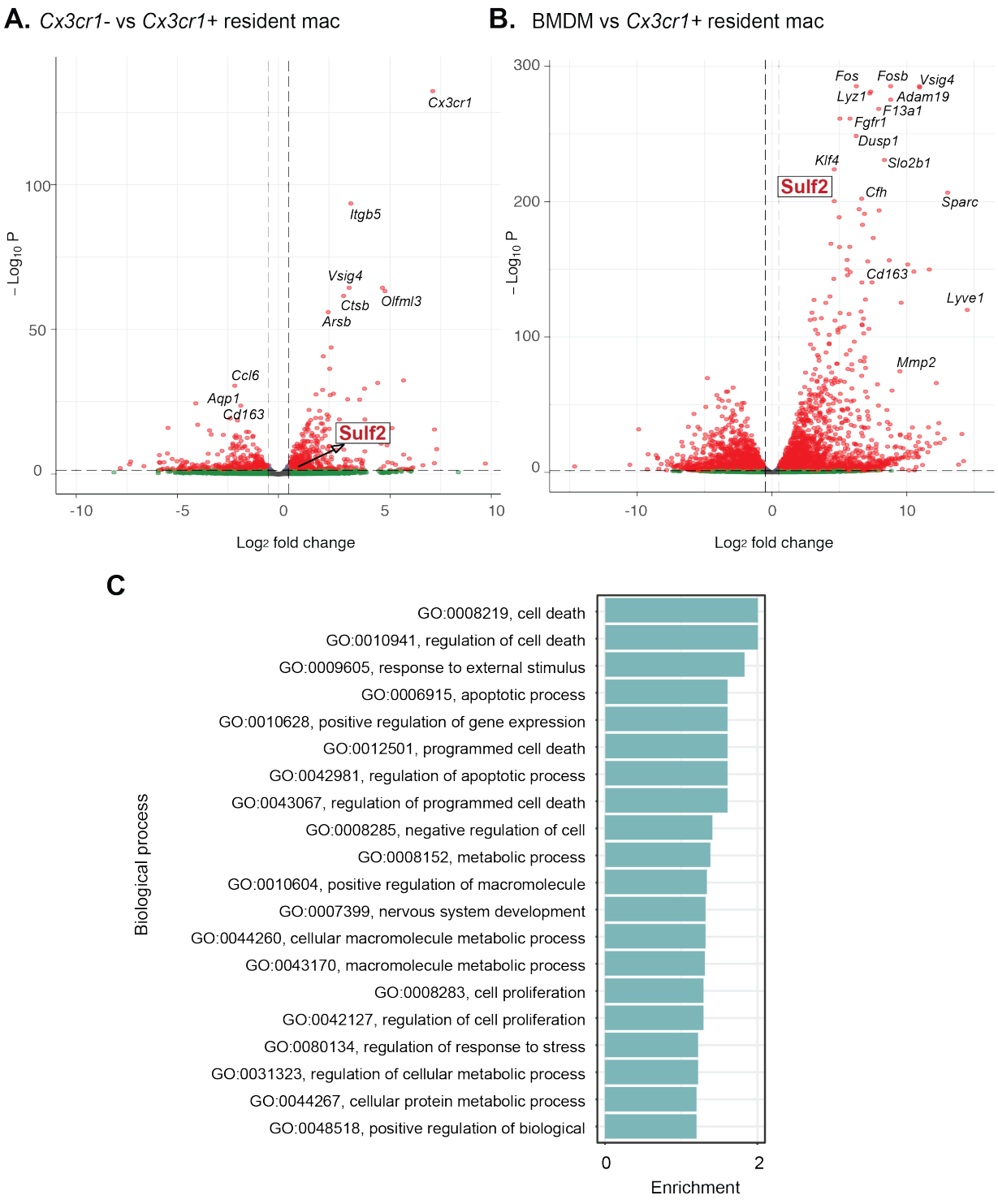


Figure 5.5. Bone marrow-derived macrophages expressed low *Sulf2* levels.

Bulk sequencing data from sorted synovial *Cx3cr1*+ lining macrophages and *Cx3cr1*- interstitial macrophages and *in vitro*-cultured bone marrow-derived macrophages (BMDMs) (Culemann et al., 2019). **A.** Differential gene expression between *Cx3cr1*- *versus* *Cx3cr1*+ resident macrophages and **B.** BMDMs versus *Cx3cr1*+ resident macrophages was performed using DESeq2. **C.** Gene ontology (GO) analysis was performed with TopGO to identify biological process that are differentially regulated in BMDMs compared to *Cx3cr1*+ resident macrophages.

5.3. Characterisation of *Sulf2* expression in AIA

Antigen-induced arthritis (AIA) is a widely used model for studying immune responses that are relevant for human RA. Joint inflammation is initiated by injecting mBSA in the knee joints of mice previously immunised with mBSA in CFA. I isolated RNA from knee joints 1, 3 and 7 days after intra-articular injection of mBSA to determine the peak of inflammation in this model. Inflammatory markers were already upregulated 24 h after injection of mBSA, but peaked at day 3 and then decreased (**Figure 5.6**). In contrast, *Cd206* expression continued to increase after day 3.

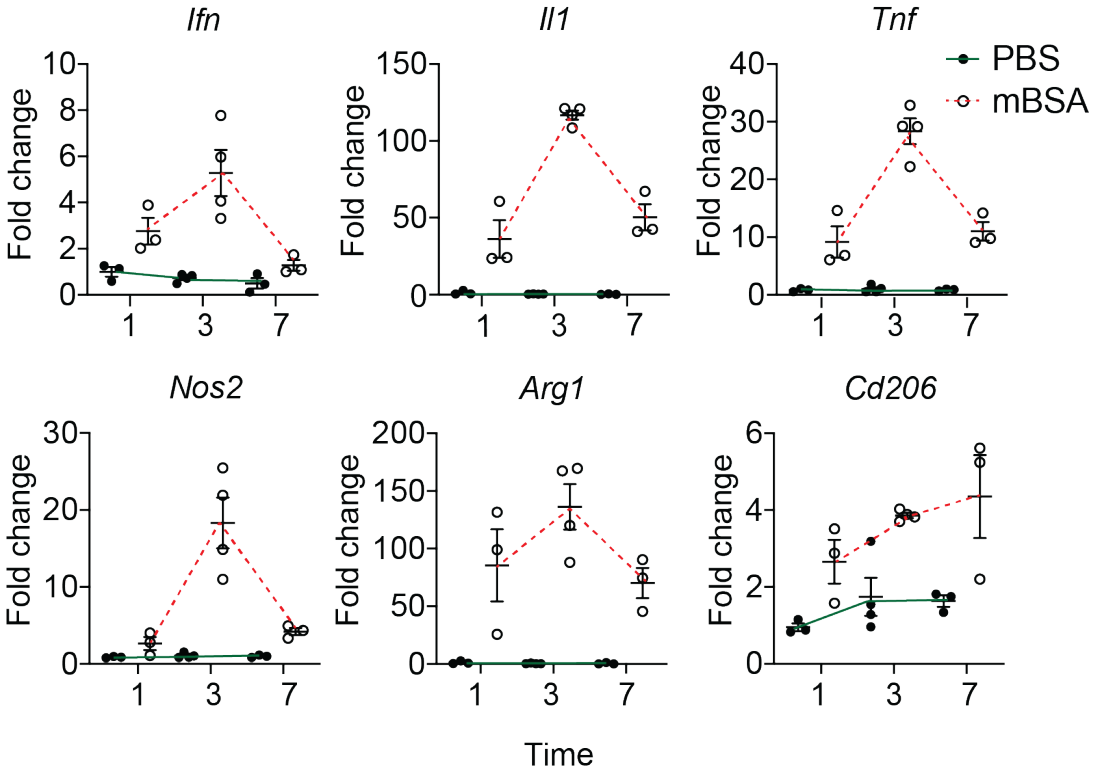


Figure 5.6. Expression of inflammatory markers is increased in antigen-induced arthritis. C57BL/6 mice were subcutaneously (s.c.) immunised with 100 µg mBSA in CFA. 3 weeks later AIA was induced by intra-articular (i.a.) tibiofemoral injection of 100 µg mBSA (right knee) or PBS (left knee). 1 (n=3 mice per group), 3 (n=4 mice per group) or 7 (n=3 mice per group) days after i.a. injection, RNA was isolated from knee joints and gene expression levels were measured by qPCR relative to *Rplp0* and to PBS-injected knees 1 day after i.a. injection. Data are represented as mean ± SEM.

Sulf2 expression was not increased at the peak of inflammation (day 3), but increased by 3.1-fold at day 7 in mBSA injected joints compared to PBS-injected joints (**Figure 5.7A**).

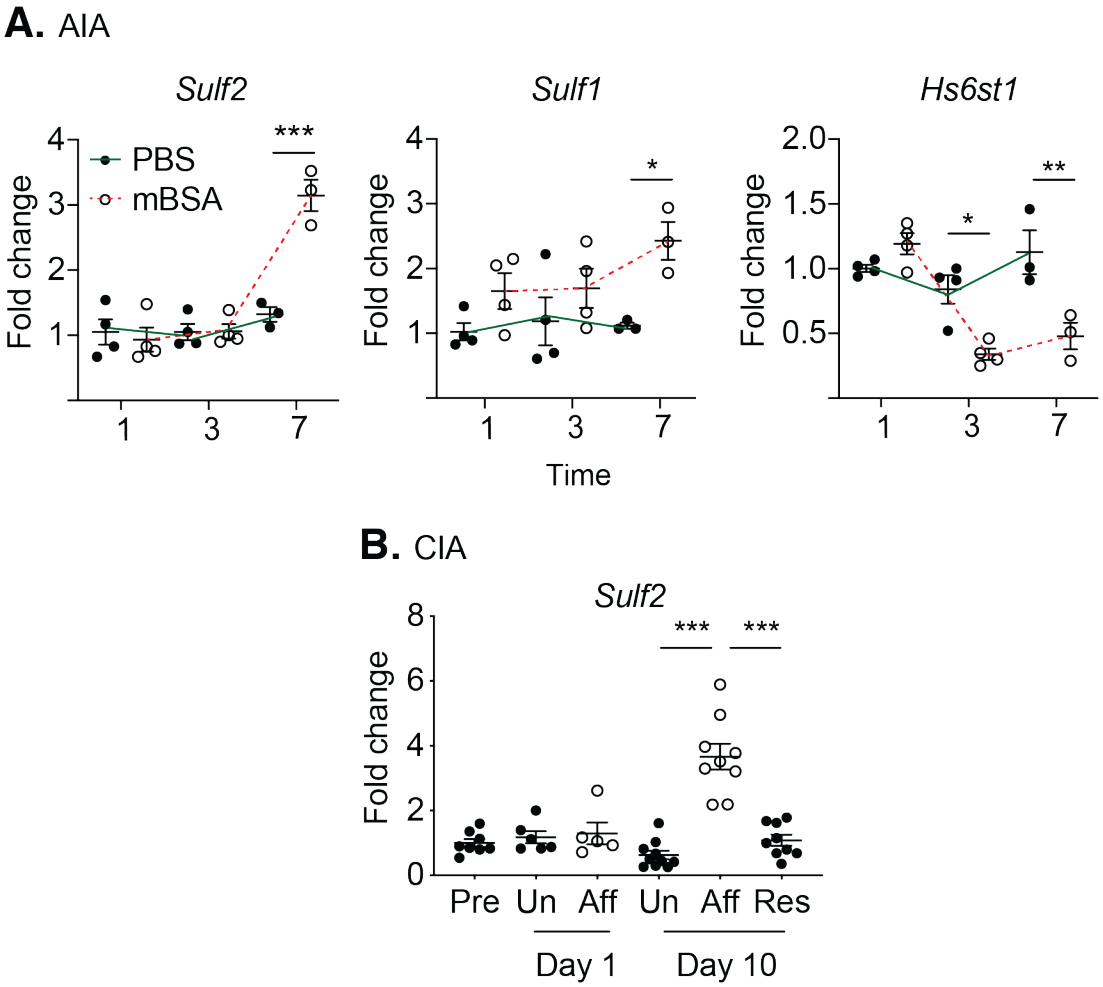


Figure 5.7. Expression of *Sulf2* was increased at day 7 of antigen-induced arthritis.
A. In the AIA murine arthritis model, C57BL/6 mice were subcutaneously (s.c.) immunised with 100 µg mBSA in CFA and AIA was induced 3 weeks later by intra-articular (i.a.) tibiofemoral injection of 100 µg mBSA (right knee) or PBS (left knee). 1 (n=3 mice per group), 3 (n=4 mice per group) or 7 (n=3 mice per group) days after i.a. injection, RNA was from knee joints isolated and gene expression levels of *Sulf2*, *Sulf1* and *Hs6st1* were measured by qPCR relative to *Rplp0* and to PBS-injected knees 1 day after i.a. injection. **B.** RNA was isolated by Dr F. Clanchy from paws of healthy mice (pre), non-arthritic paws (Un) or arthritic paws (Aff) of arthritic mice, or paws from mice that did not develop disease (Res). *Sulf2* expression levels were measured by qPCR relative to *Rplp0* and to paws of healthy mice. Data are represented as mean ± SEM, analysed by a two-way ANOVA and a one-way ANOVA with Bonferroni's correction for multiple comparisons. *, P<0.05; **, P<0.01; ***, P<0.001.

Sulf1 expression also increased by 2.4-fold at day 7, while *Hs6st1* that adds 6-O sulfate groups was decreased by 2.9-fold at day 3 and maintained low expression on day 7 (**Figure 5.7A**). Overall, this increase in *Sulf1* and *Sulf2* and decrease in *Hs6st1* indicates 6-O sulfation is likely to decrease in the arthritis joint. The increase in *Sulf2* in AIA was validated by Dr F. Clanchy (Kennedy Institute of Rheumatology, University of Oxford) in RNA samples from knee joints of mice with collagen-induced arthritis (CIA). In this model, mice are immunised with type II collagen in CFA and subsequently develop RA. *Sulf2* was upregulated by 4-fold in affected joints 10 days after the onset of CIA (**Figure 5.7B**).

To investigate which immune cell types regulate their expression of *Sulf2* in AIA, I used PrimeFlow to measure *Sulf2* expression 2 and 7 days after induction of AIA. Cells were extracted from knee joints, and stained with antibodies identifying immune cell types and a probe for *Sulf2* mRNA. Numbers of macrophages and, to a lesser extent, dendritic cells, were most strongly increased in the joint at day 2, and remained higher in mBSA- compared to PBS-injected joints at day 7. CD4 T-cells but not CD8 T-cells were increased at day 7 (**Figure 5.8**).

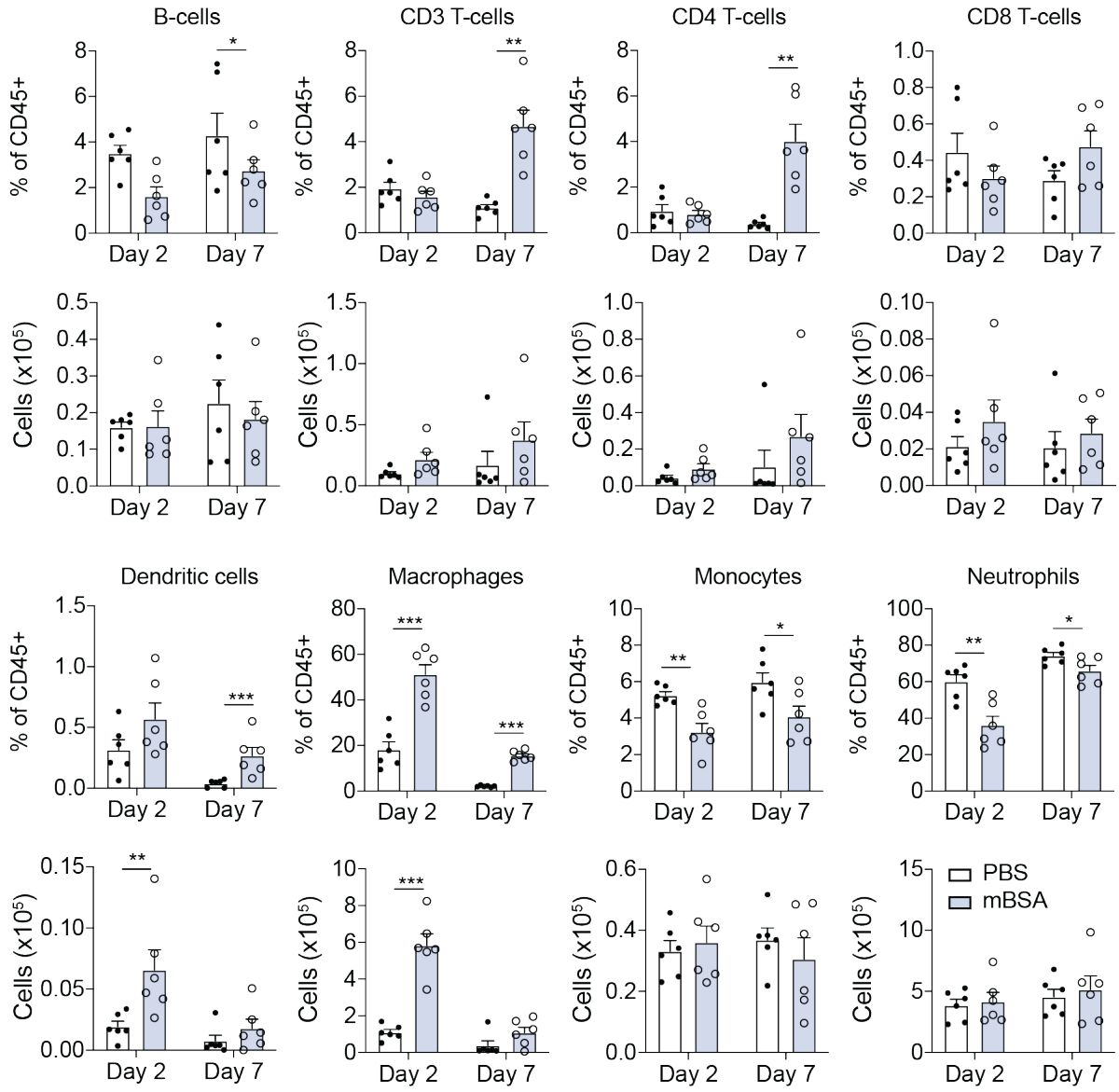


Figure 5.8. Relative abundance of immune populations in antigen-induced arthritis.
C57BL/6 mice were subcutaneously (s.c.) immunised with 100 µg mBSA in CFA. 3 weeks later, arthritis (n=6 per group) was induced by intra-articular (i.a.) tibiofemoral injection of 100 µg mBSA (right knee) or PBS (left knee). 2 or 7 days after i.a. injection, the knees were digested and cells were analysed by flow cytometry. The gating strategy is shown in **Appendix Figure 8**. Data are represented as mean ± SEM, analysed by a mixed two-way ANOVA with Bonferroni's correction for multiple comparisons. *, P<0.05; **, P<0.01; ***, P<0.001.

Macrophages, monocytes and dendritic cells expressed *Sulf2* in the joint, and *Sulf2* expression was not different in mBSA- compared to PBS-injected knee joints (**Figure**

5.9). I also did not observe any differences in *Sulf2* expression in macrophage subsets based on MHC-II, Ly6C and CD11c expression (data not shown).

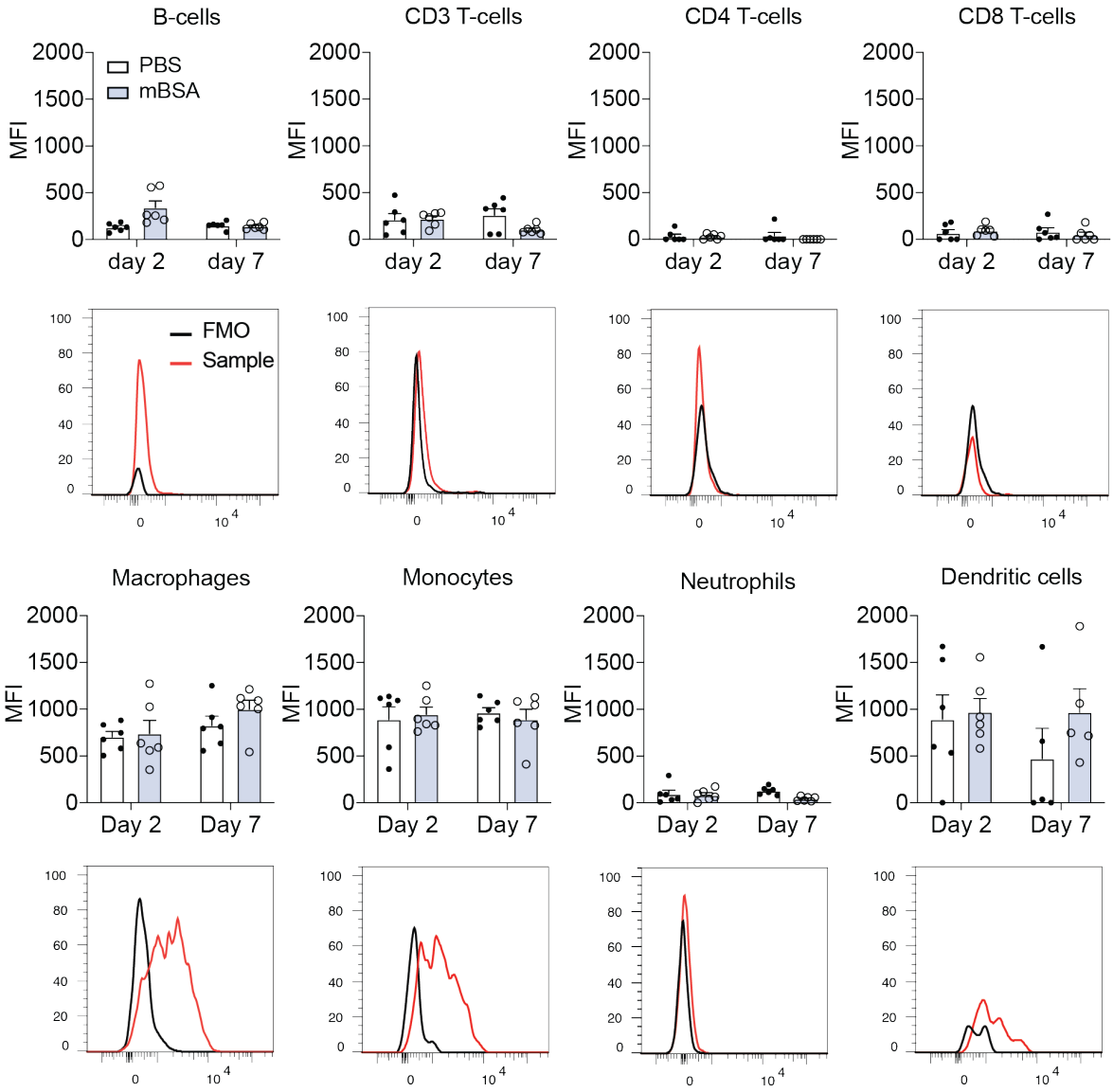


Figure 5.9. Expression of *Sulf2* by macrophages, monocytes and dendritic was not altered in the AIA joint.

C57BL/6 mice were subcutaneously (s.c.) immunised with 100 µg mBSA in CFA (n=6 per group). 3 weeks later arthritis was induced by intra-articular (i.a.) tibiofemoral injection of 100 µg mBSA (right knee) or PBS (left knee). 2 or 7 days after i.a. injection, the knees were digested and *Sulf2* expression was quantified using the PrimeFlow *in situ* hybridisation assay. Cells were analysed by flow cytometry and *Sulf2* expression expressed as the mean fluorescence intensity (MFI) minus the *Sulf2* fluorescence minus one (FMO). Representative histograms for *Sulf2* expression are shown, with data represented as mean ± SEM., analysed by a mixed two-way ANOVA with Bonferroni's correction for multiple comparisons. The gating strategy is shown in **Appendix Figure 8**.

5.4. Antigen-induced arthritis was aggravated in *Sulf2*$^{+/-}$ chimeras

5.4.1.1. The effect on disease score and pain

To understand the role of *Sulf2* expressed by immune cells in arthritis, BM chimeras were made by using 8-week old WT mice as recipients, and 8-week old WT or *Sulf2*$^{+/-}$ mice as donors. WT-recipient mice were sub-lethally irradiated and reconstituted with WT or *Sulf2*$^{+/-}$ BM cells. After 7 weeks of recovery, they were immunised with mBSA in CFA. 3 weeks later, arthritis was induced by injecting mBSA (right) or PBS (left) in the knee joints (**Figure 5.10A**).

Knee swelling peaked 1 day after intra-articular mBSA injection, plateaued, and then decreased from day 3 . The swelling during the peak and plateau phase were similar in WT and *Sulf2*$^{+/-}$ chimera mice. However, swelling resolved less quickly in the *Sulf2*$^{+/-}$ chimeras and knee swelling was significantly higher in *Sulf2*$^{+/-}$ chimeras from day 5-7 (**Figure 5.10B**). To investigate if pain behaviour was affected in *Sulf2*$^{+/-}$ chimeras, weight bearing on the mBSA-injected knee was compared to the PBS-injected knee. Pain was expressed as the ratio of weight mice put on the PBS-injected knee divided by the mBSA-injected knee. This ratio was decreased by 25% in *Sulf2*$^{+/-}$ chimeras compared to WT chimeras, indicating that these mice put more weight on the mBSA-injected (arthritic) knee and thus have less pain (**Figure 5.10C)**.

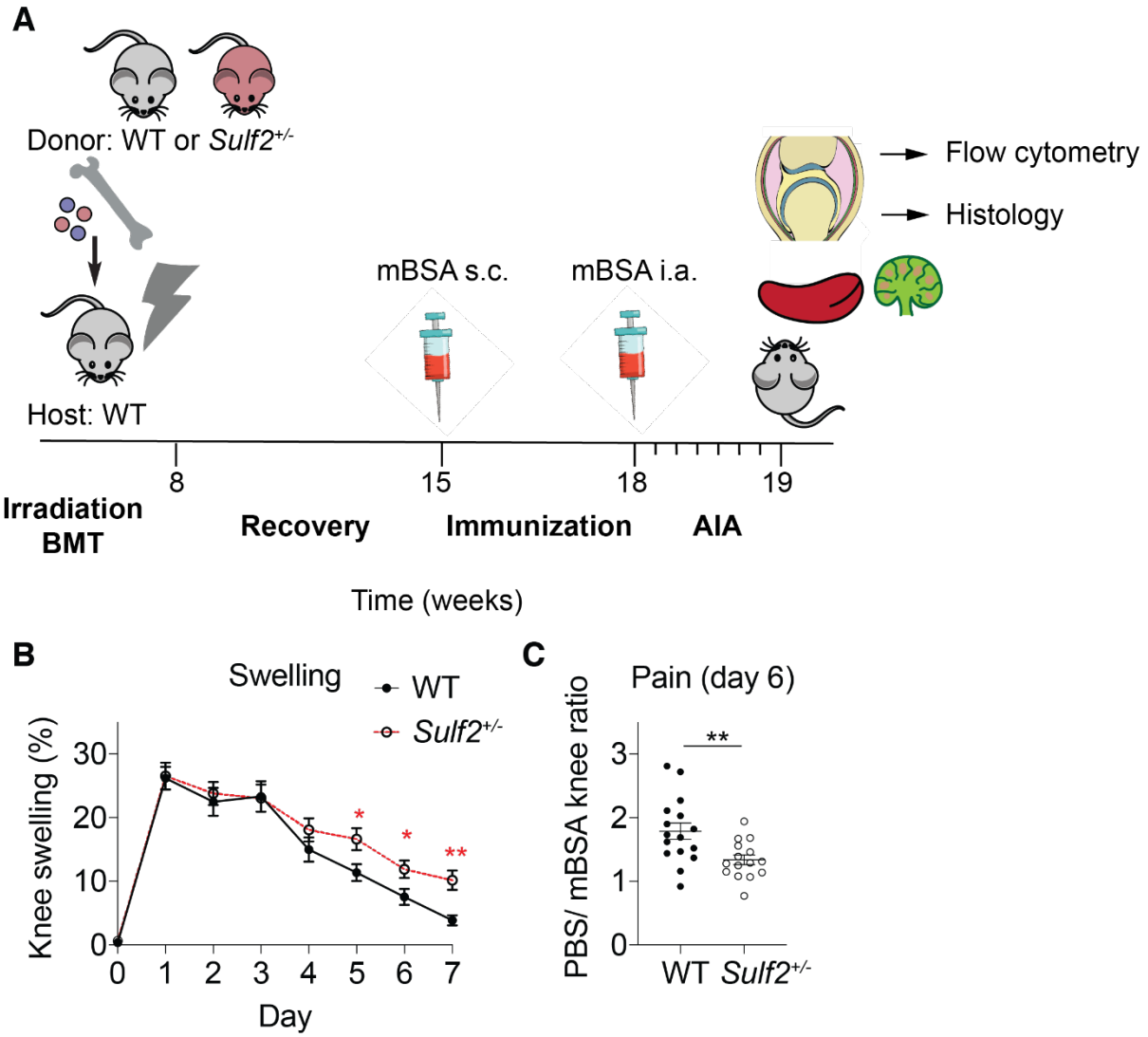


Figure 5.10. Knee swelling was increased and pain decreased in *Sulf2*-deficient BM chimera upon antigen-induced arthritis.

A. Recipient C57BL/6 mice were sub-lethally irradiated and the BM of WT or *Sulf2*$^{+/-}$ C57BL/6 mice were transplanted into recipient mice (n=16 per group). After 7 weeks of recovery, the mice were subcutaneously (s.c.) immunised with 100 µg mBSA in CFA. 3 weeks later arthritis was induced by intra-articular (i.a.) tibiofemoral injection of 100 µg mBSA (right knee) or PBS (left knee). **B.** Knee swelling was measured daily for 7 days post i.a. injection using a calliper. **C.** Pain was assessed by measuring weight bearing on mBSA-injected compared to PBS-injected paws using a Bioseb weight-bearing chamber. Data are represented as mean ± SEM (n=15), analysed by a multiple T-test and a two-tailed Student's T-test. *, P<0.05; **, P<0.01.

Knee pathology was further examined by histology at day 2 and day 7 to assess the degree of immune infiltrate, synovial thickening, bone erosion, cartilage damage and chondrocyte death. Immune infiltrate was scored on a scale of 1-3 after H&E staining, which stains nuclei blue and both cytoplasm and extracellular matrix pink. The basic dye Safranin-O binds strongly to proteoglycans, therefore stains cartilage red and was used to quantify cartilage damage and chondrocyte death. Minimal bone erosion and no cartilage degradation or chondrocyte death was detected at day 2, while these were clearly visible at day 7. No differences in these markers of knee pathology were found 2 days (**Figure 5.11**) after induction of AIA. However, the total histological score was higher 7 days after induction of AIA, with an increase in synovial thickening, subsynovial infiltrate and BM-density (**Figure 5.12**).

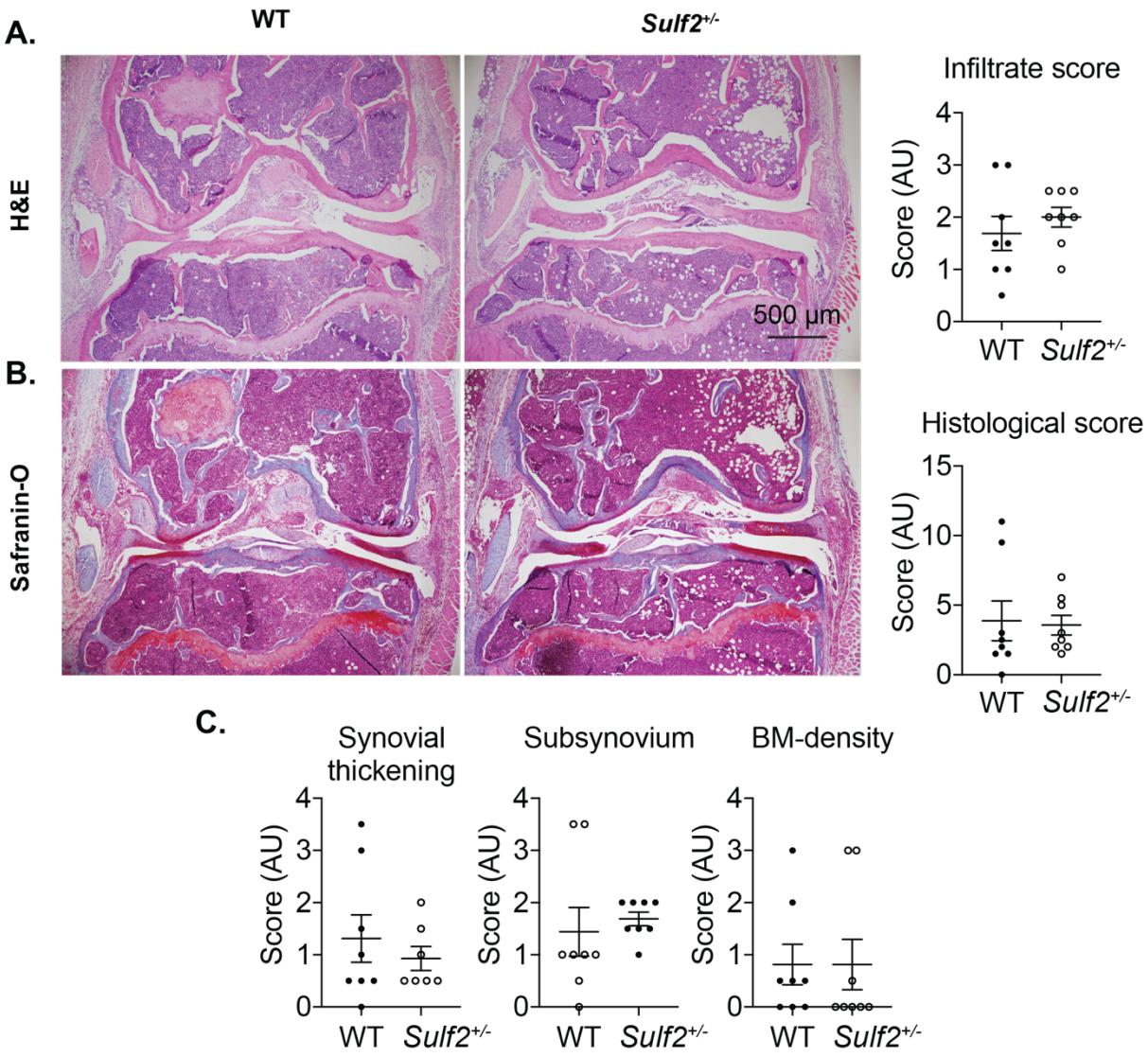


Figure 5.11. AIA histology scores were not affected at day 2 in *Sulf2*-deficient BM-chimera mice. WT and *Sulf2*$^{+/-}$ bone marrow chimeric mice (n=8) were immunised with 100 µg mBSA in CFA and arthritis was induced 3 weeks later by intra-articular tibiofemoral injection of 100 µg mBSA (right knee). 2 days later, the mice were sacrificed and disease severity in the knees was visualised using safranin-O and H&E staining. The extend of immune infiltrate and the total histological score, which was composed of the subsynovium, synovium, BM density score, were quantified. Data are represented as mean ± SEM, analysed by a two-tailed Mann-Whitney u test. Images were taken at 4x magnification.

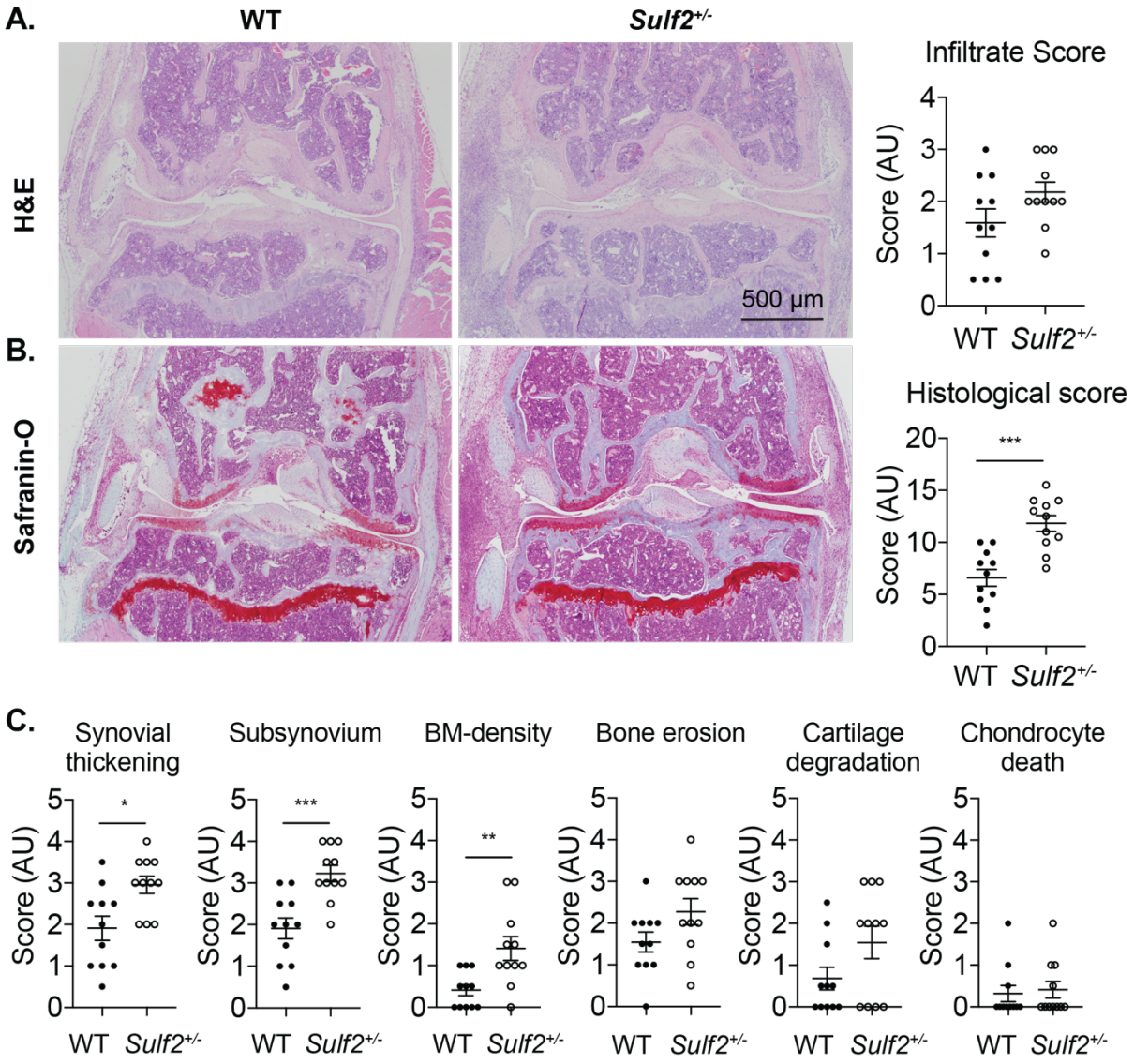


Figure 5.12. AIA histology scores were not affected at day 7 in *Sulf2*-deficient BM chimera mice. WT (n=11) and *Sulf2*$^{+/-}$ bone marrow chimeric mice (n=11) were immunised with 100 µg mBSA in CFA and arthritis was induced 3 weeks later by intra-articular tibiofemoral injection of 100 µg mBSA (right knee). 7 days later, the mice were sacrificed and disease severity in the knees was visualised using a safranin-O and H&E staining. The extend of **A.** immune infiltrate and **B.** the total histological score, which was composed of **C.** the subsynovium, synovium, bone marrow (BM) density, bone erosion, cartilage degradation and chondrocyte death score, were quantified. Data are represented as mean ± SEM, analysed by a two-tailed Mann-Whitney u test. Images were taken at 4x magnification.

5.4.1.2. Effects on immune cell populations

In an effort to assess if differences in the abundance of immune populations underlie the elevated knee pathology in *Sulf2*-deficient chimeras, I digested knee joints 2 and 7 days post AIA induction and analysed the immune populations by flow cytometry. The abundance of other myeloid populations was unaffected at day 2 and day 7 (**Figure 5.14**). Myeloid populations were also unaffected in the spleens of *Sulf2*$^{+/-}$ chimeras at day 2 (**Figure 5.13**). Adaptive immune cells infiltrate into the joint after day 2, but the percentage and number of B-cells, CD3, CD4 and CD8 T-cells were unaffected in joints from *Sulf2*$^{+/-}$ mice compared with WT **(Figure 5.14**).

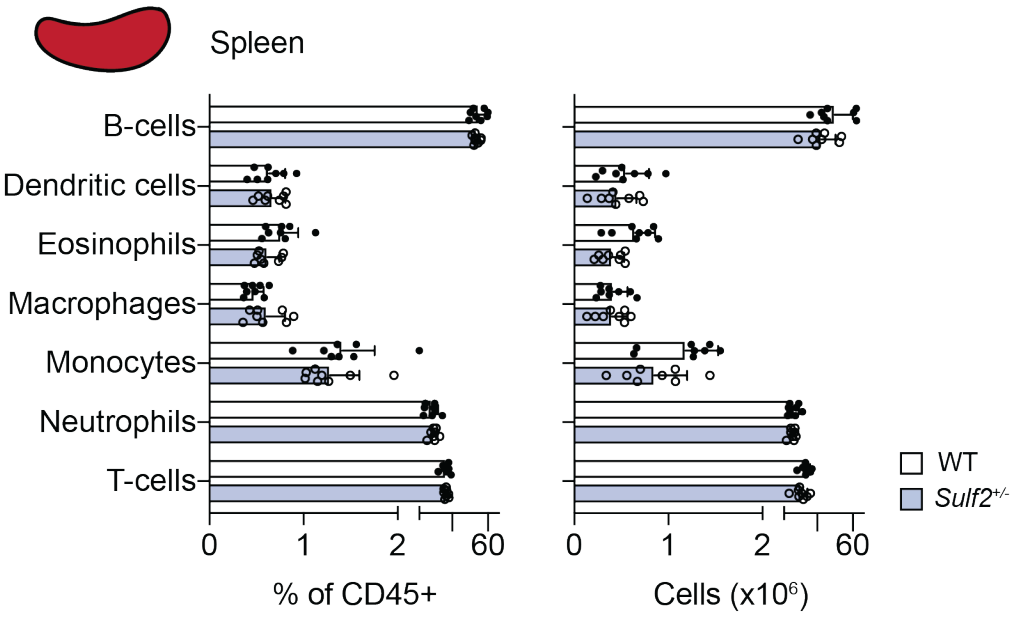


Figure 5.13. The abundance of immune subsets was not affected in the spleen of AIA mice by *Sulf2*-deficiency.

Sulf2$^{+/-}$ bone marrow chimeric mice were immunised with 100 µg mBSA in CFA (n=8 per group) and arthritis was induced 3 weeks later by intra-articular tibiofemoral injection of 100 µg mBSA (right knee). 2 days later, the spleens were analysed by flow cytometry. The gating strategy is shown in **Appendix Figure 3**. Data are represented as mean ± SEM, analysed by a multiple T-test.

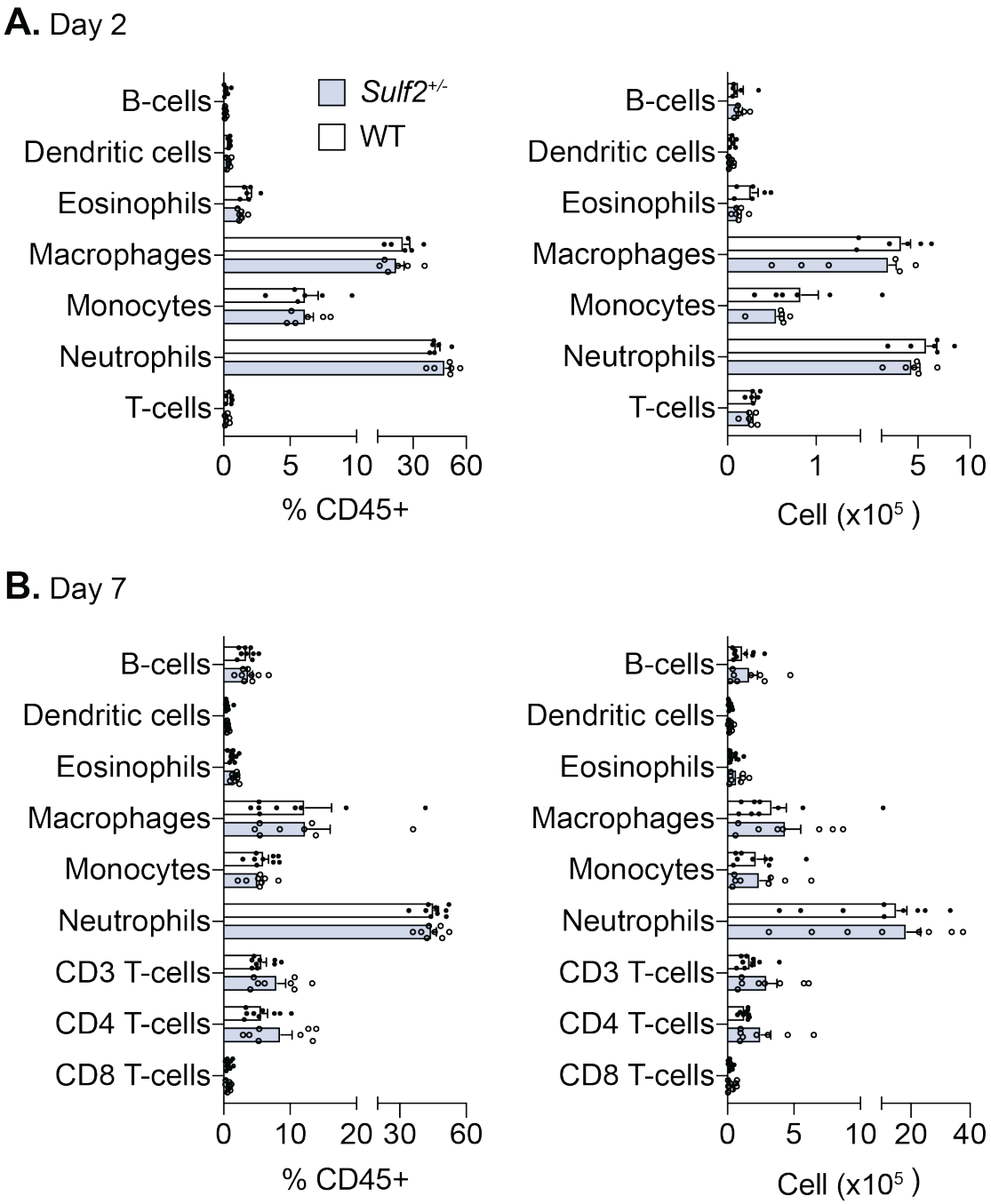


Figure 5.14. Inflamed knees of *Sulf2*-deficient BM chimera mice showed no differences in myeloid and adaptive immune subsets.

Sulf2$^{+/-}$ bone marrow chimeric mice were immunised with 100 µg mBSA in CFA and arthritis was induced 3 weeks later by intra-articular tibiofemoral injection of 100 µg mBSA (right knee). **A.** 2 days (n=6) and **B.** 7 days (n=9) later, the knees were digested and the prevalence of myeloid and adaptive immune populations was determined by flow cytometry. The gating strategy is shown in **Appendix Figure 8** and **Appendix Figure 9**. Data are represented as mean ± SEM, analysed by a multiple T-test.

IL17 produced by Th17 cells is thought to be crucial for the development of RA and contributes to the pathogenesis of AIA (Egan et al., 2008). Thus, I stimulated isolated joint cells with PMA/ionomycin and blocked cytokine release with the protein transport inhibitors brefeldin and monensin to analyse CD4 T-cell subsets. IFNγ+ Th1, IFNγ+IL17+ double positive T-cells and Tregs were not significantly affected in joints from *Sulf2*$^{+/-}$ chimeras. However, IL17+ Th17 cells were 30% higher in mBSA-injected knee joints of *Sulf2*$^{+/-}$ chimeras (expressed as a percentage of all CD4 T-cells), and the total number of Th17 cells was increased by 3-fold (**Figure 5.15A+B**). In contrast to Th17 cells, Tregs are considered to be protective in AIA (Narendra et al., 2018) and an imbalance in the Th17/Treg ratio is thought to underly the pathogenesis of RA (Lee, 2018). In line with the increase in Th17 cells, I also observed a 2-fold increase in the Th17/Treg ratio in *Sulf2*$^{+/-}$ chimeras (**Figure 5.15C**).

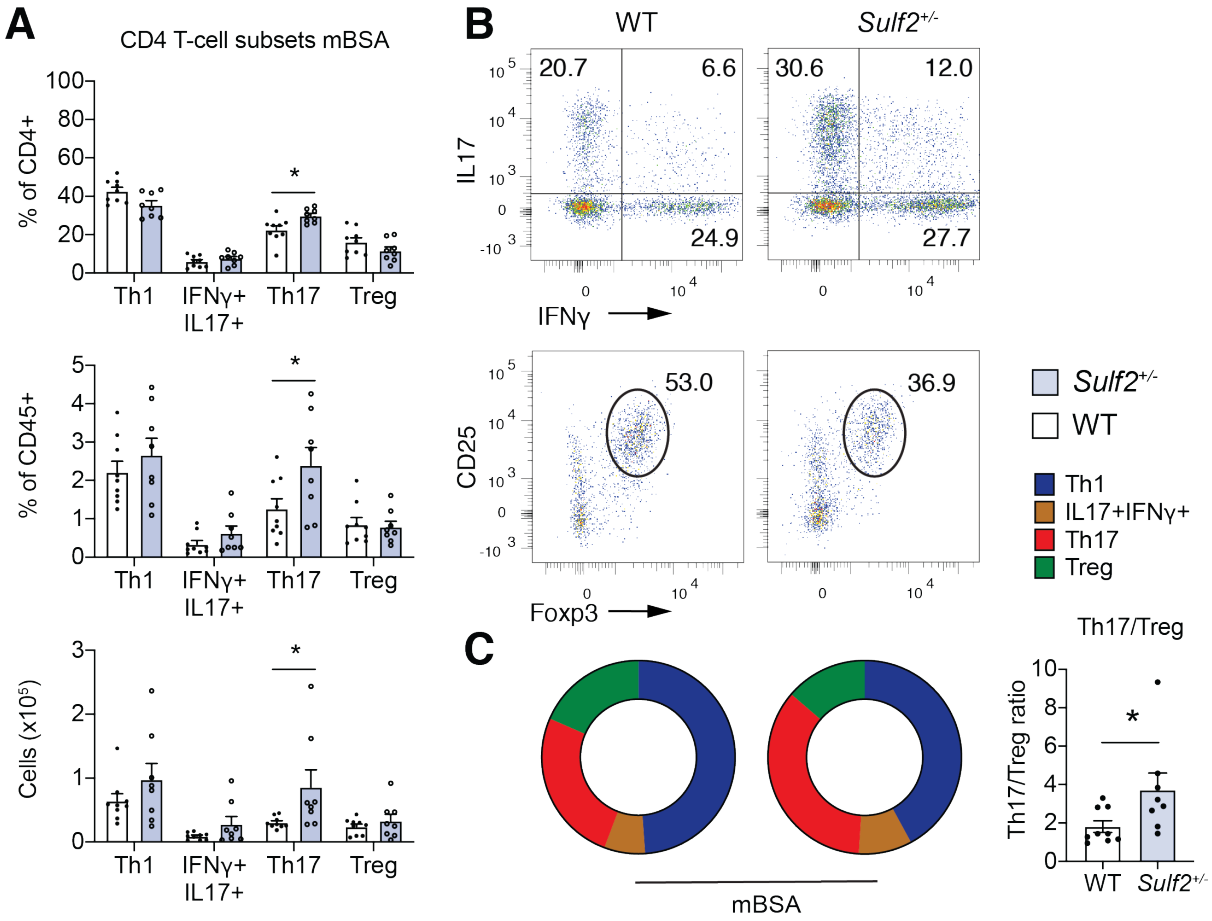


Figure 5.15. The Th17/Treg ratio was increased in the knee joints of *Sulf2*-deficient mice during AIA.

A. *Sulf2*$^{+/-}$ bone marrow chimeric mice were immunised with 100 µg mBSA in CFA and arthritis was induced 3 weeks later by intra-articular tibiofemoral injection of 100 µg mBSA (right knee) or PBS (left knee) (n=9). 7 days later, the knees were digested and cells were stimulated for 4 h with 20 ng/ml PMA, 1 ug/ml ionomycin in the presence of protein transport inhibitors. T-cell subsets were analysed by flow cytometry. The gating strategy is shown in **Appendix Figure 9**. The percentage of CD4+, CD45+ and total number of IFNγ+ Th1, IFNγ+IL17+, IL17+ Th17 and CD25+Foxp3+ regulatory T-cells (Tregs) is shown. Data are represented as mean ± SEM, analysed by a multiple T-test. *, P<0.05. **B.** Representative dot plots for CD4+ T-cell subsets in mBSA-injected knee joints. **C.** The Th17/Treg ratio was altered in *Sulf2*$^{+/-}$ chimeras, showing an altered balance between Th17 and Tregs. Data are represented as mean ± SEM, analysed by a two-tailed Student's T-test. *, P<0.05.

In order to assess if the enrichment of the Th17 T-cell subset was a local or a systemic effect, I also analysed T-cell subsets in the inguinal lymph nodes 7 days after induction of AIA. The total number of CD3+, CD4+ and CD8+ T-cells was 30% lower in *Sulf2*$^{+/-}$ chimeras (**Figure 5.16**). Although no differences in the percentage of CD4 T-cell subsets was found, the total numbers of Th1 and particularly Tregs were reduced with no effect on the Th17/Treg ratio, indicating that this is likely to be a local effect in the knee joint. I also analysed T-cell subsets 2 days after the onset of AIA in the inguinal lymph nodes (**Appendix Figure 10**) to confirm that there are no systemic effects on CD4+ T-cell subsets at earlier time points. No differences in the percentage of T-cell subsets or their absolute number was found.

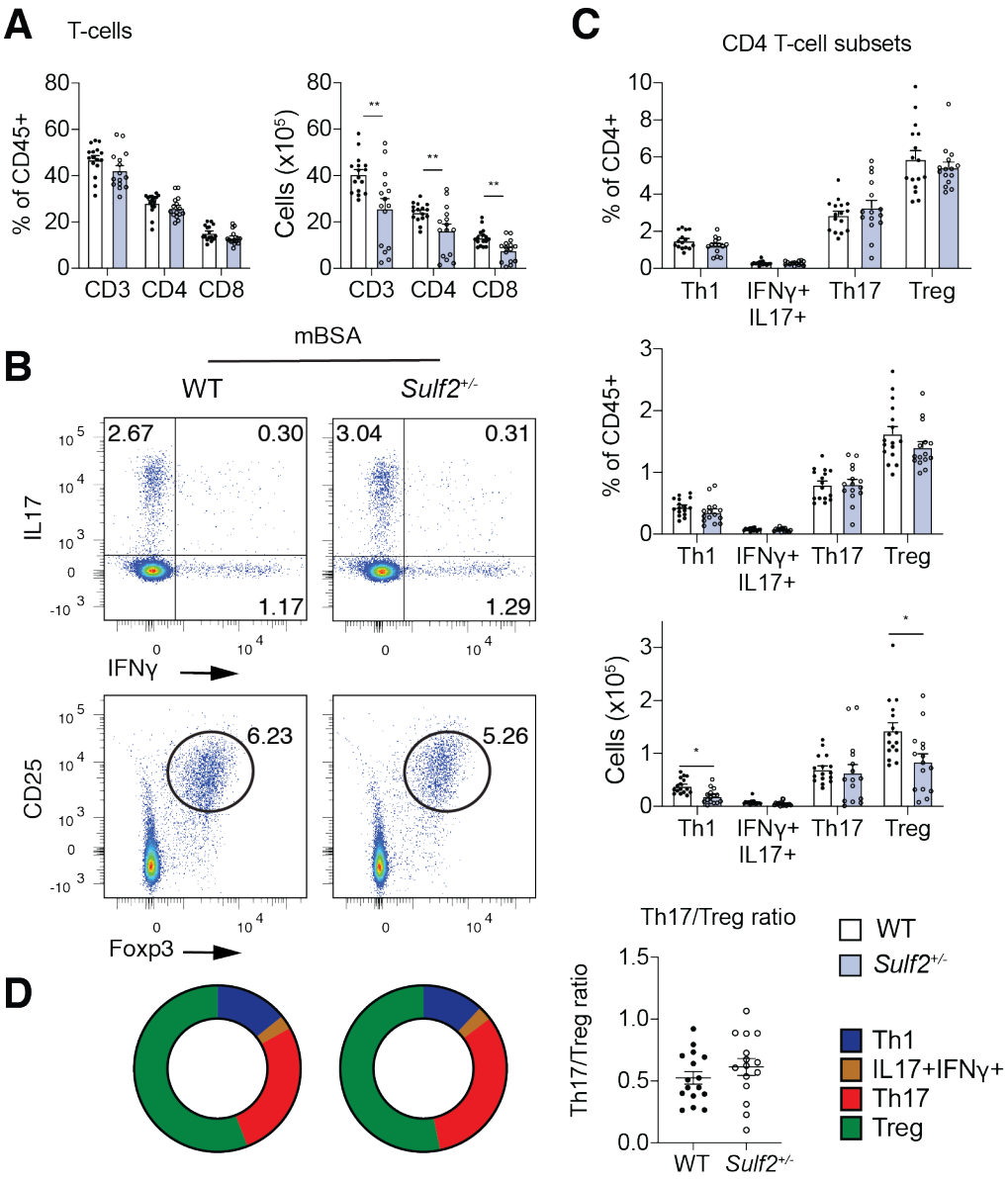


Figure 5.16. The Th17/Treg ratio was not affected in the lymph nodes of *Sulf2*-deficient mice during AIA.

Sulf2$^{+/-}$ bone marrow chimeric mice were immunised with 100 µg mBSA in CFA and arthritis was induced 3 weeks later by intra-articular tibiofemoral injection of 100 µg mBSA (right knee) (n=16). 7 days later, cells were isolated from the inguinal lymph nodes that drain the knees and the cells were stimulated for 4 h with 20 ng/ml PMA, 1 ug/ml ionomycin in the presence of protein transport inhibitors. **A.** CD3+, CD4+ and CD8+ T-cell subsets were analysed by flow cytometry. The gating strategy is shown in **Appendix Figure 11**. **B.** Representative dot plots for CD4+ T-cell subsets in inguinal lymph nodes are shown. **C.** The percentage of CD4+, CD45+ and total number of IFNγ+ Th1, IFNγ+IL17+, IL17+ Th17 and CD25+Foxp3+ regulatory T-cells (Tregs) is shown. **D.** The Th17/Treg ratio shows the balance between Th17 and Tregs. Data are represented as mean ± SEM, analysed by multiple T-tests. *, P<0.05.

I also aimed to investigate if DC migration to the lymph nodes was affected during AIA. Therefore, I measured the number of dendritic cells in the inguinal lymph nodes of *Sulf2*$^{+/-}$ chimeras 2 after the onset of AIA. No difference in the number of DCs in the inguinal lymph nodes was found (**Figure 5.17**), indicating that migration of DCs to the lymph nodes was not affected.

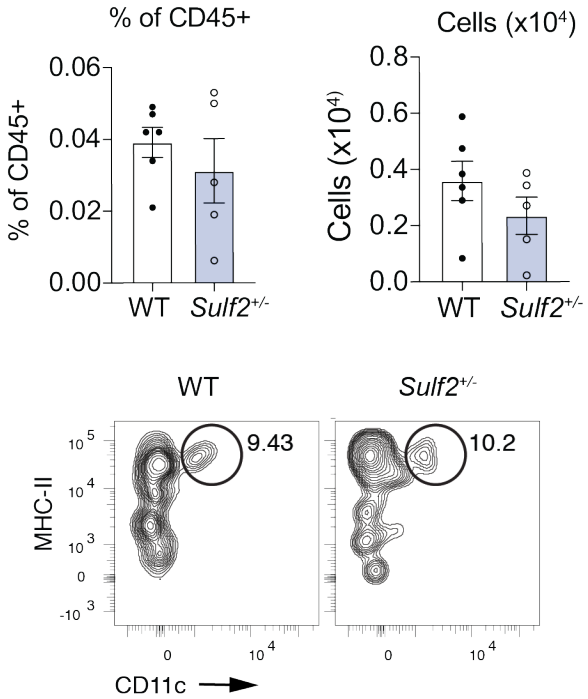


Figure 5.17. The number of DCs in the inguinal lymph nodes were not affected by *Sulf2* during AIA.

Sulf2$^{+/-}$ bone marrow chimeric mice were immunised with 100 µg mBSA in CFA and arthritis was induced 3 weeks later by intra-articular tibiofemoral injection of 100 µg mBSA (right knee) or PBS (left knee) (n=6). 2 days later, cells were isolated from the inguinal lymph nodes that drain the knees. The number of DCs was measured by flow cytometry. The gating strategy is shown in **Appendix Figure 12**. Representative dot plots for DCs in the inguinal lymph nodes are shown. Data are represented as mean ± SEM, analysed by a two-tailed Student's T-test.

5.5. Cytokine expression in *Sulf2*-deficient mice

As antigen presentation was not affected by *Sulf2 in vitro* (**section 4.5**), I aimed to investigate if cytokine abundance in the knee joints was altered and whether cytokine levels correlated with the increase in Th17 cells. Therefore, I digested the knee joints of wild type and *Sulf2*-deficient chimeras 7 days after AIA induction and measured cytokine expression by qPCR. However, I observed no differences in the expression of the Th17-polarizing cytokines *Il6, Il12b* (a subunit of IL12 and IL23), *Il23* or *Tgfβ*. Additionally *Sulf2* deficiency did not affect the expression of *Il1β*, *Il10* or *Tnf* (**Figure 5.2A**).

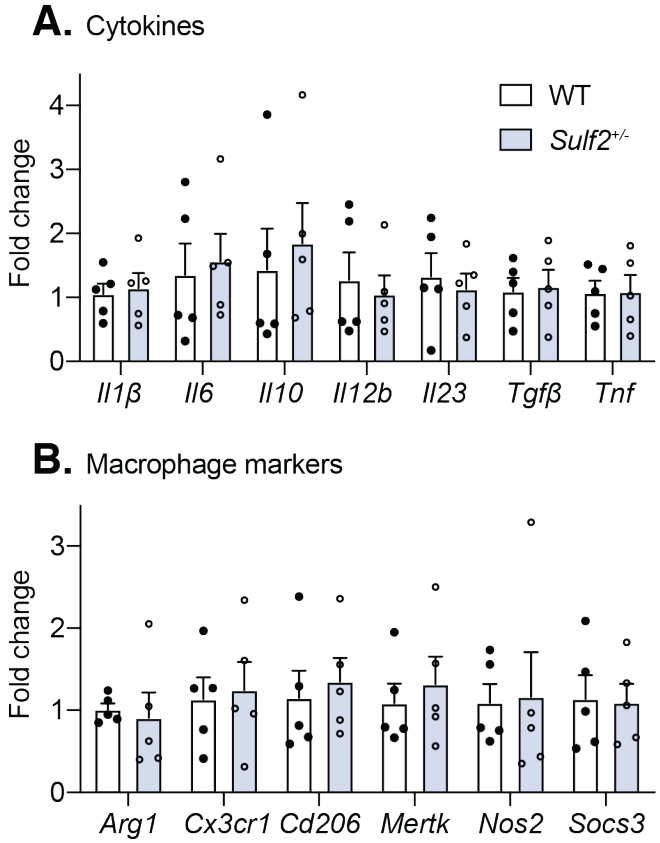


Figure 5.18. Cytokine and macrophage marker gene expression was not altered in knee joints of *Sulf2*-deficient mice.

Wild type (WT) and *Sulf2*$^{+/-}$ bone marrow chimeric mice were immunised with 100 µg mBSA in CFA and arthritis was induced 3 weeks later by intra-articular tibiofemoral injection of 100 µg mBSA. 7 days later the knees were digested, RNA was isolated and gene expression levels were measured by qPCR relative to *Rplp0* and to WT knees. Data are represented as mean ± SEM, analysed by multiple T-tests.

To further investigate if *Sulf2* affects macrophage phenotype *in vivo* as observed *in vitro* (**section 4.3.1**), I also quantified the expression of various macrophage markers. However, no differences were found in expression of *Arg1*, *Cx3cr1*, *Cd206*, *Mertk, Nos2* or *Socs3* (**Figure 5.2B**).

5.6. *Sulf2* expression in human arthritis

Finally, I aimed to determine if *SULF2* expression is also increased in human RA. First, *SULF2* expression was measured in blood (analysis performed by Dr L. Topping) where no differences in *SULF2* expression were observed in patients with RA, compared to healthy blood donors (**Figure 5.19A**). However, the local inflammatory environment in the joint might be required for local upregulation of *SULF2*. Nevertheless, no differences in *SULF2* expression were found between synovial membranes of RA patients, compared to synovial membranes from patients with osteoarthritis as a non-inflammatory control (**Figure 5.19B**). **Appendix Figure 13** shows the expression of other HS core proteins and biosynthetic enzymes in human synovial membranes.

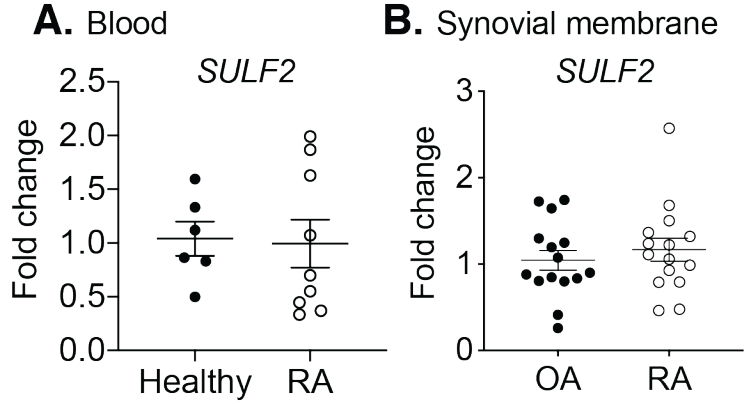


Figure 5.19. *SULF2* was not differentially expressed between synovial membranes of patients with OA and RA.

A. *SULF2* expression levels were measured by Dr L. Topping, using RNA isolated from human peripheral blood mononuclear cells of patients with RA and healthy controls by qPCR relative to *RPLP0* and healthy donors. **B.** I isolated RNA from synovial membranes of patients with RA or OA as non-inflammatory controls. Gene expression levels were measured by qPCR using custom-designed TaqMan low-density array cards relative to the geometric mean of *18S, GAPDH* and RPLP0 and OA samples. Data are represented as mean ± SEM, analysed by a two-tailed Student's T-test.

5.7. Discussion

In this chapter, I show that *Sulf2* is primarily expressed by macrophages, monocytes and DCs in the knee joint during the AIA arthritis model. Reanalysis of a published scRNA-seq dataset comparing CD45+CD11b+Ly6G- cells isolated from joints of healthy mice with those isolated 5 days after K/BxN serum transfer as a model for RA (Culemann et al., 2019) revealed that resident macrophages in the joint express 2-fold higher levels of *Sulf2* than monocyte-derived macrophages. *Sulf2* was particularly highly expressed by *Cx3cr1*+ lining macrophages, which have been shown to inhibit inflammation through formation of tight junctions that shield the joints (Culemann et al., 2019).

Reanalysis of this published scRNA-seq dataset also showed that *Sulf2* expression by the resident macrophage population in the joint was not affected by inflammation in the K/BxN serum transfer model (Culemann et al., 2019). Similarly, I found that *Sulf2* expression in monocytes, macrophages and DCs did not change during the AIA time course, as the average expression per cell in these populations was the same in PBS-injected knees and mBSA-injected knees 2 and 7 days after the onset of AIA. I was not able to measure the expression of *Sulf2* in non-immune cells in the joint due to the small number of these cells that were detected after digestion. However, analysis of single cell and bulk RNA sequencing data from Zhang et al. (2019) indicates that fibroblasts express high levels of *Sulf2* in RA joints (**Figure 5.1**).

Although the average *Sulf2* gene expression per myeloid cell was not affected at day 2 and day 7 of AIA, I found that total *Sulf2* gene expression in the whole knee joints was upregulated at day 7. This may be due to influx of *Sulf2*-expressing myeloid cells during AIA, or may be due to increased expression in the fibroblast population. This increased expression occurs during the resolution phase of AIA, when expression

of *Sulf2*-suppressing inflammatory mediators is reduced after the peak of inflammation at day 3. In line with these kinetics of *Sulf2* expression in AIA, *Sulf2* was also upregulated at day 10 (but not day 1) of CIA, further supporting a role of *Sulf2* in the resolution of inflammation. Expression of *Sulf1* was also increased at day 7 and *Hs6st1* downregulated at day 3-7 in AIA. Together, this indicates that 6-O sulfation is likely to decrease during AIA and in particular during the resolution phase. This implies that 6-O sulfation has pro-inflammatory effects and may contribute to the development of RA or hamper its resolution.

However, I did not observe an increase in *SULF2* in synovial membranes of patients with RA, compared to patients with OA as a non-inflammatory control. *IL6* and *TNF* levels were similar in the RA and OA samples (**Appendix Figure 13**), possibly reflecting the late disease stage at which both samples groups were collected. As it was not easy to obtain surgical healthy synovial membranes, I have not been able to ascertain whether *SULF2* is upregulated in human synovial membranes during the course of RA.

In order to investigate the role of *Sulf2* expressed by immune cells during inflammation in AIA, I generated *Sulf2*-deficient bone marrow chimeric mice. In line with the potential immunoinhibitory role of *Sulf2* suggested by my findings in **Chapter 4,** I observed an increase in AIA joint swelling and exacerbated histological AIA score in *Sulf2*-deficient bone marrow chimeric mice, indicating a protective role of SULF2 in arthritis. This was accompanied by an increase in abundance of pro-inflammatory Th17 cells and a shift in the Th17/Treg ratio in mBSA-injected knee joints of *Sulf2*-deficient mice. Previous studies have shown that Th17 cells (Egan et al., 2008) contribute to disease while Tregs are protective (Frey et al., 2005), so this shift demonstrates that *Sulf2*

expression by myeloid cells is critical for the modulation of arthritogenic T-cell responses and the promotion of tolerogenic ones.

As T-cells express minimal to undetectable levels of *Sulf2* (**Chapter 3**), I hypothesised that *Sulf2* expression in macrophages and dendritic cells was driving differences in the Th17/Treg subset. Importantly, the increase in Th17 was specific to the joint, and not observed in the lymph nodes, indicating that the local environment in the joint is responsible for the enrichment of Th17 over Treg cells. Considerable plasticity exists between the CD4+ T-cell subsets (Dupage and Bluestone, 2016). For example, Tregs can be converted into Th17-like cells by IL6, IL1β and IL23 (Koenen et al., 2008; Yang et al., 2008). This has also been demonstrated in CIA, where $CD25^{lo}$Foxp3+CD4+ are converted into Th17-like cells by fibroblast-derived IL6 (Komatsu et al., 2014). Therefore, I hypothesise that changes in cytokine levels or their signalling in the local microenvironment of the joint cause the increase in the Th17/Treg ratio in *Sulf2*$^{+/-}$-BM chimeras. Gene expression of Th17-polarizing cytokines in the synovium was not affected by *Sulf2*-deficiency at the time points studied, suggesting that *Sulf2* is not acting by regulating gene expression of these proteins. Th17 polarizing cytokines such as IL6, IL12b (subunit of IL23) and TGFβ are known to bind to HS (Ori et al., 2011). It is plausible that 6-O desulfation by SULF2 affects their binding to HS and hence their sequestration and signalling. It may be informative to compare the secretomes of WT and *Sulf2*$^{+/-}$ macrophages using quantitative proteomics to explore this possibility.

While knee swelling and Th17 numbers were higher in *Sulf2*-deficient bone marrow chimeric mice, analysis of weight-bearing in monoarthritic mice indicated that pain was decreased in these chimeras 6 days after the onset of AIA. This was surprising, since

inflammation in the joint is generally considered to contribute to pain in RA (Walsh and McWilliams, 2014), and inflammatory mediators like TNF and IL17 (Woolf et al., 1997; Richter et al., 2012; Ebbinghaus et al., 2017) have also been shown to contribute to pain in arthritis. These cytokines promote the production of the chemokine CXCL1 that recruits neutrophils to the joint, which in turn are responsible for hyperalgesia (McNamee et al., 2011). Neutrophils release hyperalgesic mediators like prostaglandin E2 (PGE_2) that can activate nociceptive neurons responsible for pain sensation (Loynes et al., 2018; Cunha et al., 2008). The paradoxical increase in IL17 and reduction in pain may reflect the involvement of pain pathways other than those driven by IL17 in the chimeras. Some pain mediators (e.g. kininogen-1, angiotensinogen) are known to bind to HS (Ori et al., 2011) or be affected by HS (Lindahl et al., 2013), so changes in 6-O-sulfation may affect pain pathways.

Overall, this chapter demonstrates that *Sulf2* protects from experimental arthritis by modulating pro-arthritogenic T cell responses. Potential mechanisms for these effects are discussed in **Chapter 6**.

Chapter 6. Discussion

Macrophages are critical for tissue homeostasis as they are involved in phagocytosis of pathogens and debris, activation and regulation of adaptive immunity, and tissue repair (Wynn et al., 2013). *In vitro*, macrophages are classically polarised by IFNγ and LPS into pro-inflammatory (M1) macrophages, or by IL4 and IL13 to become reparative M2 macrophages (Martinez and Gordon, 2014; Murray et al., 2014). Mosser and Edwards (2008) proposed a more informative functional classification of macrophages, consisting of three functional classes: classical macrophages (microbial activity), wound-healing macrophages (tissue repair) and regulatory macrophages (anti-inflammatory activity). IFNγ and TNF give rise to classically activated macrophages, IL4 skews towards wound-healing macrophages, and immune complexes, prostaglandins, G-protein coupled receptor ligands, glucocorticosteroids, apoptotic cells and IL10 promote the differentiation of regulatory macrophages. The combination of these mediators can give rise to a range of activation states between these three functional classes (Mosser and Edwards, 2008; Fleming and Mosser, 2011).

The response of macrophages to stimuli such as cytokines, chemokines and growth factors can be regulated by interaction of these proteins with negatively-charged HS chains (**Figure 1.5**). For example, HS has been shown to promote or inhibit receptor binding of its protein ligands, to reduce their susceptibility to proteolysis, and to establish concentration gradients *in vivo* (Parish, 2006; Simon Davis and Parish, 2013). HS chains acquire their negative charge by extensive sulfation during their template-independent synthesis by a group of up to 25 biosynthetic enzymes (Billings and Pacifici, 2015). 6-O sulfation in particular is strictly controlled as it is added by the HS6ST1-3 sulfotransferases during HS biosynthesis and can be removed post-synthetically in the extracellular environment by the

sulfatases SULF1 and SULF2 (Morimoto-Tomita et al., 2002), while 2-O, 3-O and N-sulfation cannot be post-synthetically modified.

Many studies have shown that regulation of 6-O-sulfation is critical for various signalling pathways (**Figure 1.7)** that can affect the behaviour of non-immune cells. My data reveal for the first time that *Sulf2* modulates immune cell functions. In this thesis, I investigated how the 6-O sulfotransferase *Sulf2* affects macrophage function and inflammation in the AIA experimental arthritis model.

6.1. *Sulf2* is expressed by macrophages, monocytes and dendritic cells

I used *Sulf2*$^{+/-}$ mice to study the role of *Sulf2* in immune function due to the severe perinatal lethality in *Sulf2*$^{-/-}$ mice observed by our collaborators (A. Redpath and N. Smart, University of Oxford, **Figure 2.1**) in the *Sulf2*-null line they generated and which I used for this study. This effect appears to be strain-dependent, since others have generated *Sulf2*$^{-/-}$ animals without any evident major development defects (Otsuki et al., 2010; Korf-Klingebiel et al., 2019), while other studies have reported strain-dependent weight loss and increased perinatal lethality (Lum et al., 2007; Lamanna et al., 2006). Such strain-dependent effects have also been reported for mice lacking other HS biosynthetic enzymes, such as *Hs3st1* (HajMohammadi et al., 2003) and *Hs6st1* (Habuchi et al., 2007; Izvolsky et al., 2008). For example, Habuchi et al. (2007) observed high embryonic and perinatal lethality in *H6st1*-null mice that have reduced 6-O sulfation, while Izvolsky et al. (2008) did not observe any major developmental defects at birth in an independently-derived *Hs6st1*-null line. However, they reported growth retardation, weight loss and perinatal lethality in young adult mice.

Most *Sulf2*-null mice used in other studies have been generated by targeting the first exons, and potential skipping of the gene trap (*Lacz)* cassette could partially restore *Sulf2* expression in such mice. In support of this possibility, one study reported that up to 9.1% of *Sulf2* expression still remained in the spleen of *Sulf2*-null compared with WT animals (Holst et al., 2007). In contrast, the mice used in the present study were generated by deleting the critical exon 4, which encodes the enzyme's active site (manuscript in preparation, Dr A. Redpath and Dr N. Smart). This strategy makes exon skipping less likely, and is more likely to result in full deletion of SULF2 activity.

Additionally, the effects of *Sulf2* deletion on levels of 6-O-sulfation are unclear, since this has not been analysed in most published studies, most likely due to the fact that disaccharide analysis is normally restricted to specialist laboratories. In two of the few studies where HS structure was examined, MEFs from *Sulf2*-null mice showed no differences in levels of 6-O sulfation (Lamanna et al., 2006; Ratzka et al., 2008). This is likely to reflect compensation by *Sulf1* or the *Hs6st* enzymes. However, it should be noted that there could be localised changes in 6-O sulfation on the HS chains in these studies that impact ligand binding.

Despite these caveats, *Sulf2*-null mice have contributed to our understanding of the role of 6-O sulfation and *Sulf2* has been shown to be protective in various disease models. For example, *Sulf2* null mice have elevated surgically-induced OA (Otsuki et al., 2010), impaired tissue repair after myocardial infarction (Korf-Klingebiel et al., 2019) and aggravated bleomycin-induced lung injury (Yue, 2017). However, the function and expression of *Sulf2* in immune cells remained unexplored.

In **Chapter 3** I showed that *Sulf2* is predominantly expressed by macrophages, monocytes and dendritic cells. Resident AMs in the lung expressed the highest *Sulf2* levels among the tested cell types, and resident macrophages in the joint also

expressed high *Sulf2* levels. I found no differences in the abundance of immune populations in the lung, spleen and bone of *Sulf2*$^{+/-}$ mice at steady state, suggesting that *Sulf2* does not affect haematopoiesis and maturation of immune cells at steady state *in vivo*. However, its expression profile indicates that *Sulf2* potentially has an immunosuppressive or regulatory role in macrophages. A similarly anti-inflammatory role has been demonstrated in non-immune cells in other studies, for example, epithelial-specific *Sulf2* deletion increased neutrophil influx and inflammatory cytokine (GM-CSF, IL6, IL8 and CXCL10) levels after bleomycin-induced lung damage (Yue, 2017), and silencing of *SULF2* in cancer cells increased inflammatory gene (type I IFN-induced genes and *CXCL1*) expression (Tessema et al., 2012). My data indicate for the first time that this protective function is also apparent in immune cells.

6.2. *Sulf2* exacerbates experimental arthritis

As non-immune cells such as fibroblasts also express high levels of *Sulf2* (Zhang et al., 2019), I generated *Sulf2*$^{+/-}$ bone marrow chimera mice to investigate the role of *Sulf2* expressed by macrophages and other immune cells. In line with the potential regulatory role of *Sulf2*, I showed that these mice developed more severe AIA with exacerbated knee swelling and more pro-arthritic T-cell profiles with an increase in the Th17/Treg ratio (**Chapter 5**). While T-cells lack *Sulf2* expression (**Chapter 3**), macrophages, monocyte and DCs express *Sulf2* at a high level, indicating that *Sulf2* might modulate T-cell polarisation by regulating myeloid cell function. In **Chapter 4** I showed that antigen presentation by DCs and macrophages was not affected by *Sulf2*. In addition, I observed in **Chapter 5** that the increase in the Th17/Treg ratio was only detectable in the knee joint, pointing out the potential role of *Sulf2* in synovial macrophages, monocytes and dendritic cells in the regulation of T-cell responses. It

is possible that *Sulf2* expression by these cells impacts local cytokine bioavailability or signalling in the joint of the Th17 polarising cytokines IL6, IL23 or TGFβ and thereby shifting the Th17/Treg ratio.

Surprisingly, the mice appeared to have less pain despite the increase in inflammation (discussed in **Chapter 5**). Although *Sulf2* has been shown to be important for nervous system development and maintenance (Ai et al., 2007; Kalus et al., 2009), a defect in the nervous system in these mice is unlikely as *Sulf2*-deficiency was limited to immune cells in the chimeras. However, HS on immune cells might affect the bioavailability of pain mediators, such as kininogen-1, angiotensinogen, that bind to HS (Ori et al., 2011).

6.3. *Sulf2* affects macrophage polarisation

In **Chapter 4** I also showed that *Sulf2* affects macrophage programming and I postulate that this is due to effects on bioactivity, signalling and availability of polarising cytokines. Differences in macrophage programming may contribute to the establishment of a pro-arthritogenic T cell response, rather than a regulatory one. For example, IL4+IL13-stimulated *Sulf2*-deficient macrophages had a less protective phenotype, as they expressed lower levels of the M2 markers *Arg1*, *Cd206* and *Fizz1*. This might contribute to the reduction in Tregs in the joint as M2 regulatory macrophages have been shown to induce Tregs (Cao et al., 2010; Schmidt et al., 2016; Sun et al., 2017).

Moreover, *Sulf2*-deficient macrophages stimulated with IFNγ+LPS may have a more inflammatory phenotype, as they expressed less *Nos2*, *Socs3* and more *Tnf*. Furthermore, *Sulf2* expression is inhibited by inflammatory cytokines such as IFNγ+LPS. Therefore, *Sulf2* appears to regulate inflammation through a negative

feedback loop, where inflammation reduces *Sulf2* expression and this lower *Sulf2* expression in turn enables macrophages to adopt a more inflammatory phenotype.

6.4. *Sulf2* suppresses macrophage phagocytosis

I also observed in **Chapter 4** that macrophages with a reduced *Sulf2* expression performed phagocytosis and efferocytosis more efficiently. Efferocytosis of infected (Torchinsky et al., 2009) or activated (Notley et al., 2015) apoptotic cells can promote inflammation in some cases. For example, intravenous injection of apoptotic LPS-activated DCs induced secretion of the Th17-promoting cytokine IL6 in AIA (Notley et al., 2015). However, efferocytosis is generally considered to be protective in RA (van den Brand et al., 2013; Waterborg et al., 2018) as it limits accumulation of apoptotic and secondary necrotic cells that release pro-inflammatory mediators in the joint (Roth et al., 2015). Additionally, efferocytosis dampens inflammatory and Th17-inducing cytokine production by macrophages through SOCS3 (Rothlin et al., 2007). Roberts et al. (2017) demonstrated that signals from the tissue microenvironment are crucial for this immunologically silent clearance of apoptotic cells. Therefore, it cannot be excluded that *Sulf2* affects the responsiveness of macrophages to these signals and therefore that *Sulf2*-deficiency shifts macrophages from performing immunologically silent efferocytosis to developing inflammatory responses. However, it is also possible that other phagocytic substrates, such as Fc- or MR-mediated phagocytosis might contribute the increase in Th17 through induction of pro-inflammatory cytokines (Aderem and Underhill, 1999).

6.5. Future perspectives

I have identified *Sulf2* as a negative regulator of inflammation and macrophage function with a protective role in inflammatory disease. However, the precise link between macrophage and T-cell biology that is regulated by *Sulf2* is yet to be determined. It is likely that a combination of macrophage programming with an enhanced phagocytosis and antigen uptake contribute to an increase in pathogenic T-cell responses in the joints of *Sulf2*-deficient chimeric mice, driving tissue inflammation. I am planning to conduct bulk RNAseq analysis of *Sulf2*-deficient synovial macrophages from AIA joints to give further insight into *Sulf2* effects on macrophage phenotype, and the molecular drivers of antigen uptake and phagocytosis. Additionally, this RNAseq analysis can potentially be used to identify which signalling pathways are affected by *Sulf2* in macrophages by investigating if the regulated genes have a common promotor sequence.

In order to gather precise information on the subsets of macrophages that are driving these immune changes, a more selective deletion of *Sulf2* might be required. Currently, I have been unable to specifically assess the function of *Sulf2* in resident macrophages in the joint using *Sulf2*$^{+/-}$ BM-chimeras as this subset is thought to be radioresistant (Culemann et al., 2019). However, available methods of conditional deletion might not be able to precisely delete *Sulf2* in specific cell subsets (McCubbrey et al., 2017; Shi et al., 2018). For example, the Csfr1^{Cre} (also known as M-CSF receptor^{Cre}) targets macrophages and monocytes, but its specificity is low as deletion is also observed in DCs, neutrophils and T-cells (Deng et al., 2010). The Cx_3CR1^{Cre} also targets monocytes and macrophages, but deletion has also been reported in mast cells and DCs (Abram et al., 2014). The LysM^{Cre} also targets neutrophils and DCs in addition to macrophages (Clausen et al., 1999), and the CD64^{Cre} also targets B-cells

and DCs (C. L. Scott et al., 2018), while the CD11c^{Cre} also targets DCs (C. L. Scott et al., 2018). The F4/80^{Cre} (Schaller et al., 2002) might be a good candidate, but it is not often used as it not expressed by many resident macrophages (Abram et al., 2014).

Moreover, it will be important to determine if SULF2 affects signalling in an autocrine or paracrine fashion. Korf-Klingebiel et al. (2019) hypothesised that SULF2 is secreted and can therefore also modify 6-O sulfation on other cells in their environment. However, SULF2 has also been detected on the cell surface (Sandoval et al., 2020). This could be due to strong binding of SULF2 to HS directly after it has been secreted. However, it is not known what fraction of SULF2 is surface-bound and how much is secreted, or whether this distribution is altered in inflammation. Nawroth et al. (2007) concluded that SULF2 can affect signalling in an autocrine fashion, because WT (SULF2-expressing) human pancreatic cancer cells grew faster than *SULF2*-silenced cells in response to Wnt in co-culture. My data indicate that SULF2 mainly regulates the HS structure and immune function in an autocrine fashion, as WT *Sulf2*-secreting fibroblasts in the joint would otherwise overwhelm the effect of *Sulf2*$^{+/-}$ immune cells in the BM chimera experiments shown here. To investigate whether *Sulf2* can also affect HS on other cells after it has been secreted, CD45.1 WT and CD45.2 *Sulf2*$^{+/-}$ M-CSF-derived macrophages could be co-cultured, so that they can be flow-sorted after culture before analysis, and compared with separately cultured WT and *Sulf2*$^{+/-}$ macrophages.

Finally, it may be important to study the structure of SULF2 during inflammation in more detail, as it has been demonstrated that SULF2 can be alternatively spliced and that this can alter its function (Gill et al., 2014, 2016; Gill et al., 2011; Graham et al., 2016). For example, high expression of a spliced, catalytically-inactive variant of *SULF2* in various tumors has been shown to titrate out catalytically active SULF2,

increasing 6-O sulfation and altering signaling pathways in cancer. These variants might also be important for inflammation as they have been reported in pancreatitis (Gill et al., 2014). Moreover, the HD domain is sensitive to (partial) proteolytic degradation that changes the substrate specificity of SULF2, while not affecting its catalytic activity (A. Seffouh et al., 2019; Frese et al., 2009). However, the relevance of alternative splicing and HD domain processing during inflammation is unknown. Overall, this indicates that the substrate specificity of SULF2 is tightly regulated and is likely to influence how it fine-tunes signaling pathways.

6.6. Concluding remarks

In this thesis, I showed that *Sulf2* is predominantly expressed by resident macrophages and that inflammatory stimuli reduce *Sulf2* expression, allowing macrophages to acquire a more inflammatory phenotype. In line with this, *Sulf2* limits Th17-mediated inflammation in experimental arthritis (**Figure 6.1**).

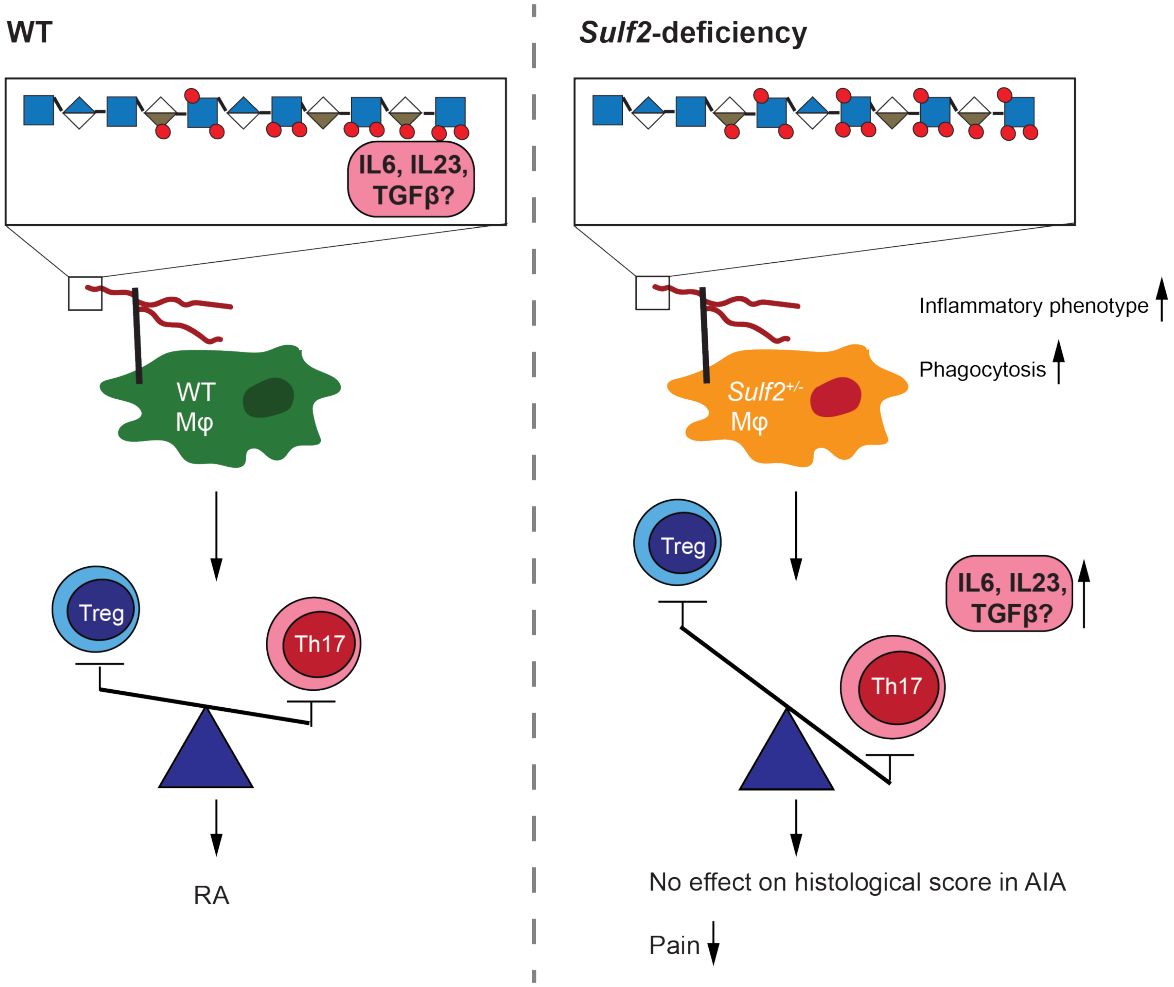


Figure 6.1. The proposed role of Sulf2 in RA.

Sulf2-deficiency increases macrophage 6-O sulfation, which affects the interaction of HS with HS-binding proteins and their signalling. As a result, the macrophages adopt a more inflammatory phenotype. I hypothesise that SULF2 affects the bio-availability and/or signalling of IL6, IL23 or TGFβ that skew the T-cells in the joint towards a pro-arthritic Th17 phenotype. Despite the increase in Th17 cells, no significant differences in the histological antigen-induced arthritis (AIA) score were observed. Additionally, the mice appeared to have less pain.

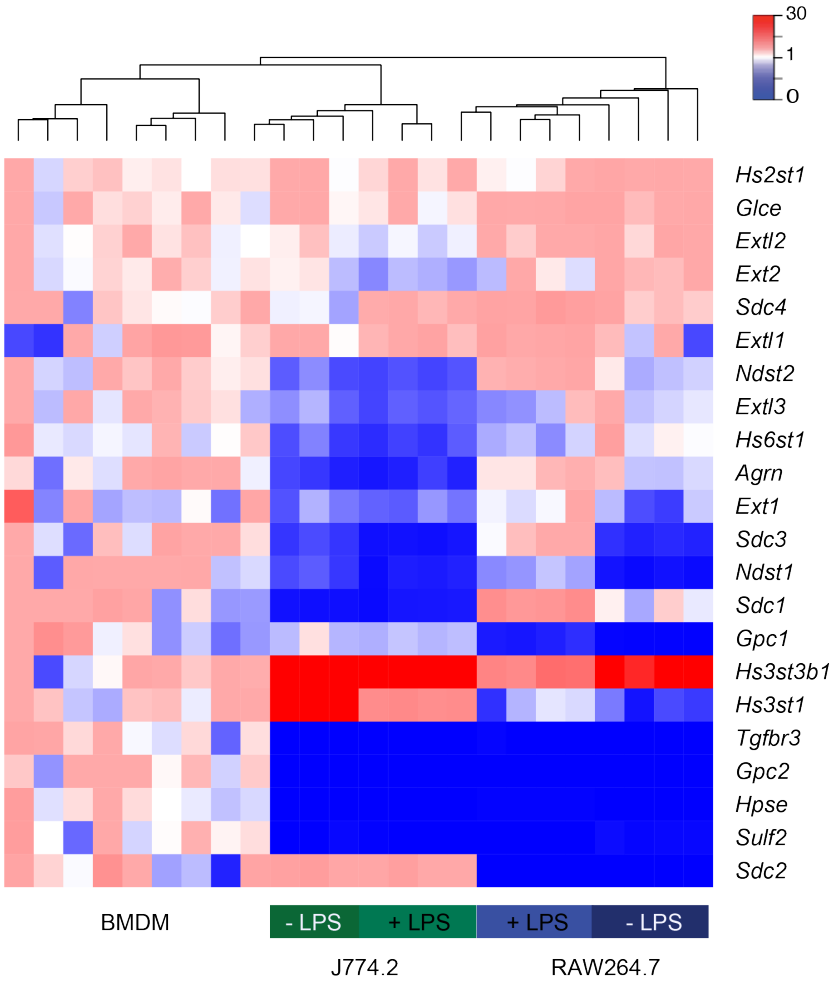
In conclusion, reducing 6-O sulfation of HS by *Sulf2* is important for controlling inflammation and recombinant SULF2 might be a powerful tool to reduce inflammation. For example, intra-articular injection of SULF1 has been shown to be protective in OA (Otsuki et al., 2017) and intravenous injection of SULF1 reduced post-septic immunosuppression response syndrome (Oshima et al., 2019). To test the therapeutic potential of SULFs further, it would be interesting to explore if intra-articular

injection of SULF2 reduces AIA or CIA in mice. However, clinical use of recombinant SULF2 is unlikely due the complexity of using enzymes as therapeutics. Heparin can also be used to displace HS-binding proteins from HS by competing for their binding. This approach has been shown to reduce inflammation by disrupting chemokine gradients and inhibiting leukocyte infiltration (Wan et al., 2001). However, heparin is not suitable for clinical use due to its anti-coagulant activity. Synthetic heparin mimetics haven been developed to have lower or no anti-coagulant activity (Farrugia et al., 2018; Lindahl et al., 2013), and these may have broader clinical applicability. For example, the of use 2-O and 3-O desulfated heparin (CX-01, Cantex Pharmaceuticals) is being investigated in various cancer types where it is hoped it will disrupt chemokine-mediated cancer metastasis (Kovacsovics et al., 2018). Moreover, small molecule HS-antagonists, such as surfen (bis-2-methyl-4-amino-quinolyl-6-carbamide), can be used to displace HS-binding proteins from HS by binding strongly to the negatively charged sulfate groups on HS (Schuksz et al., 2008). For example, this approach was effective in releasing VEGF from HS and ameliorating tissue damage after myocardial infarction in mice (Korf-Klingebiel et al., 2019). A more elegant approach would be to design small molecules or peptides that mimic the binding site of a specific HS-binding protein (e.g chemokine/ cytokine) and thereby inhibit its binding to HS, as this would minimise potential side effects by other HS-regulated signalling pathways. In support of this approach, a peptide that resemble the cationic HS-binding site of IFNγ delayed allograft rejection (Fernandez-Botran et al., 2002). Overall, therapies based on disrupting of binding of inflammatory mediators to HS have the potential to effectively reduce inflammation in RA and other inflammatory diseases. However, it is important to develop more targeted therapies as HS can affect the binding and function of over 400 proteins (Ori et al., 2011), which

could potentially lead to severe side effects. These might be further mitigated by local delivery, for example to the knee joint in RA.

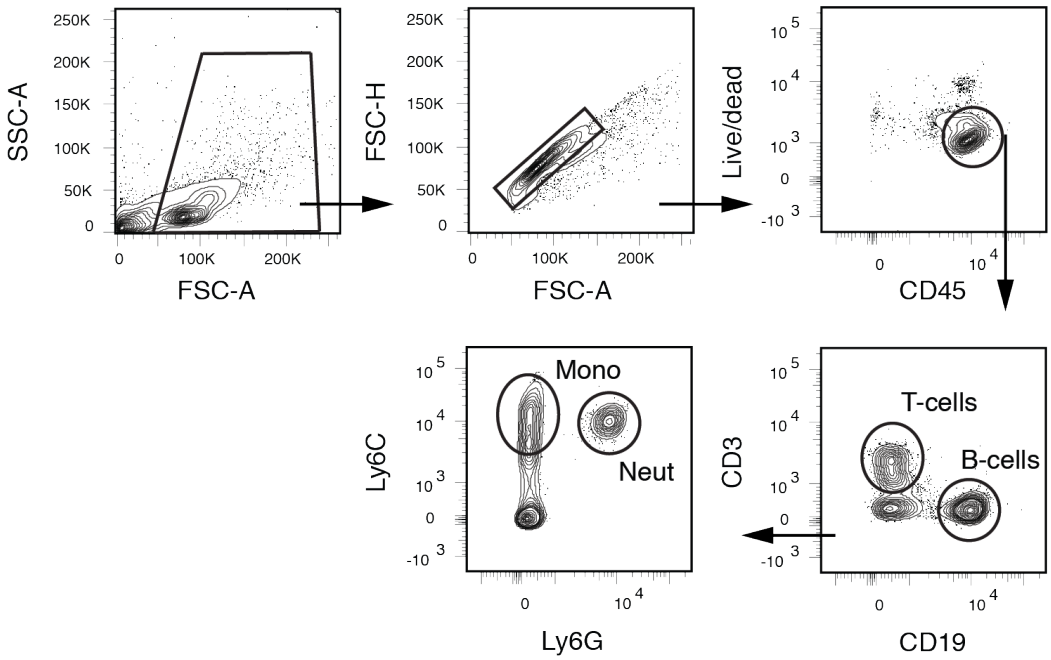
Chapter 7. Appendices

Appendix 1. Supplemental data



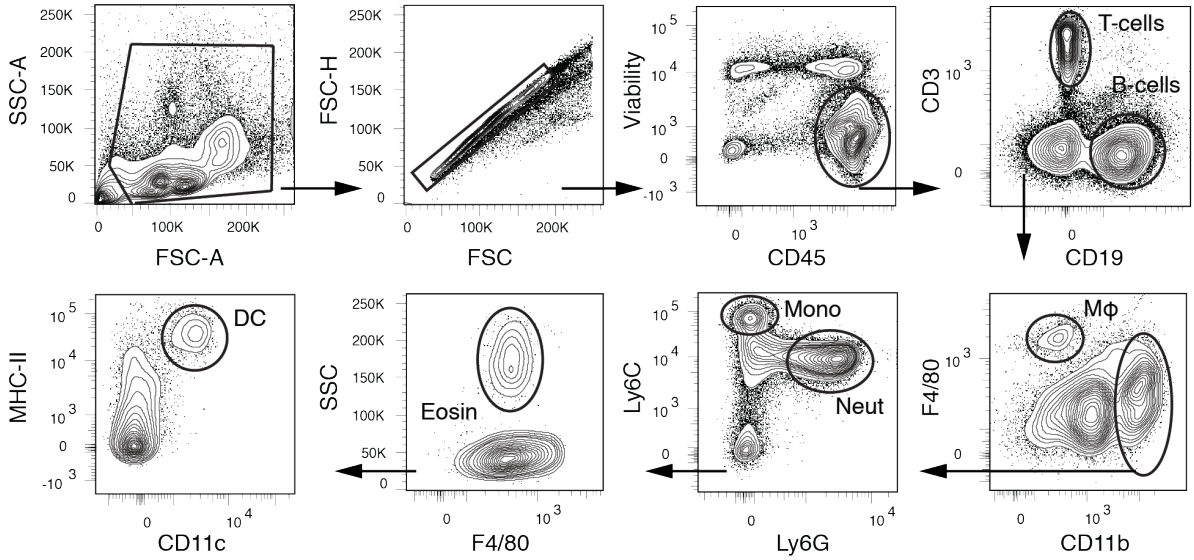
Appendix figure 1. Profiling heparan sulfate-associated gene expression in murine macrophage cell lines.

Bone marrow-derived macrophages (BMDM) were derived by culturing murine bone marrow-derived cells with 100 ng/ml M-CSF for 7 d (n=9 mice). BMDMs, the murine monocyte/macrophage cell line J774.2 (n=3) and the murine macrophage cell line RAW264.7 (n=4) were treated with 100 ng/ml LPS for 18 h (both n=4). RNA was isolated and gene expression levels were measured by qPCR using custom-designed TaqMan low-density array cards relative to the geometric mean of the housekeeping genes *18s*, *Gapdh*, and *Rplp0* and to expression in BMDMs. Differential expression profiles were visualised using heatmapping.



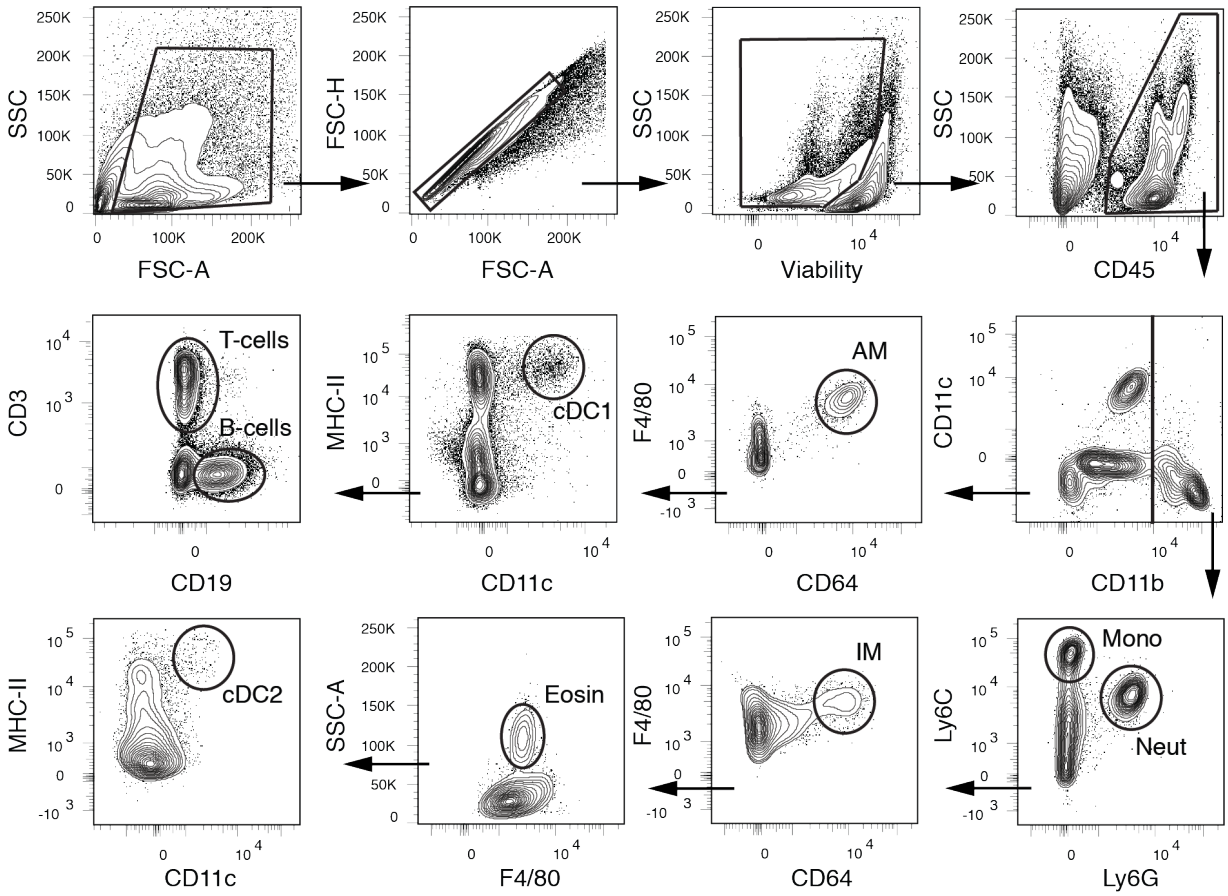
Appendix Figure 2. Gating for myeloid populations in the blood/ bone marrow.

Blood and bone marrow were harvested and the cells were stained with a live/dead stain and markers to identify immune populations. Representative dot plots show that doublets were excluded and live CD45+ cells were gated. Next, CD3+ T-cells, CD19+ B-cells and CD3-CD19- cells were gated. The CD3-CD19- cells were gated on Ly6C+Ly6G- to identify monocytes and Ly6C^{int}Ly6G+ for neutrophils.



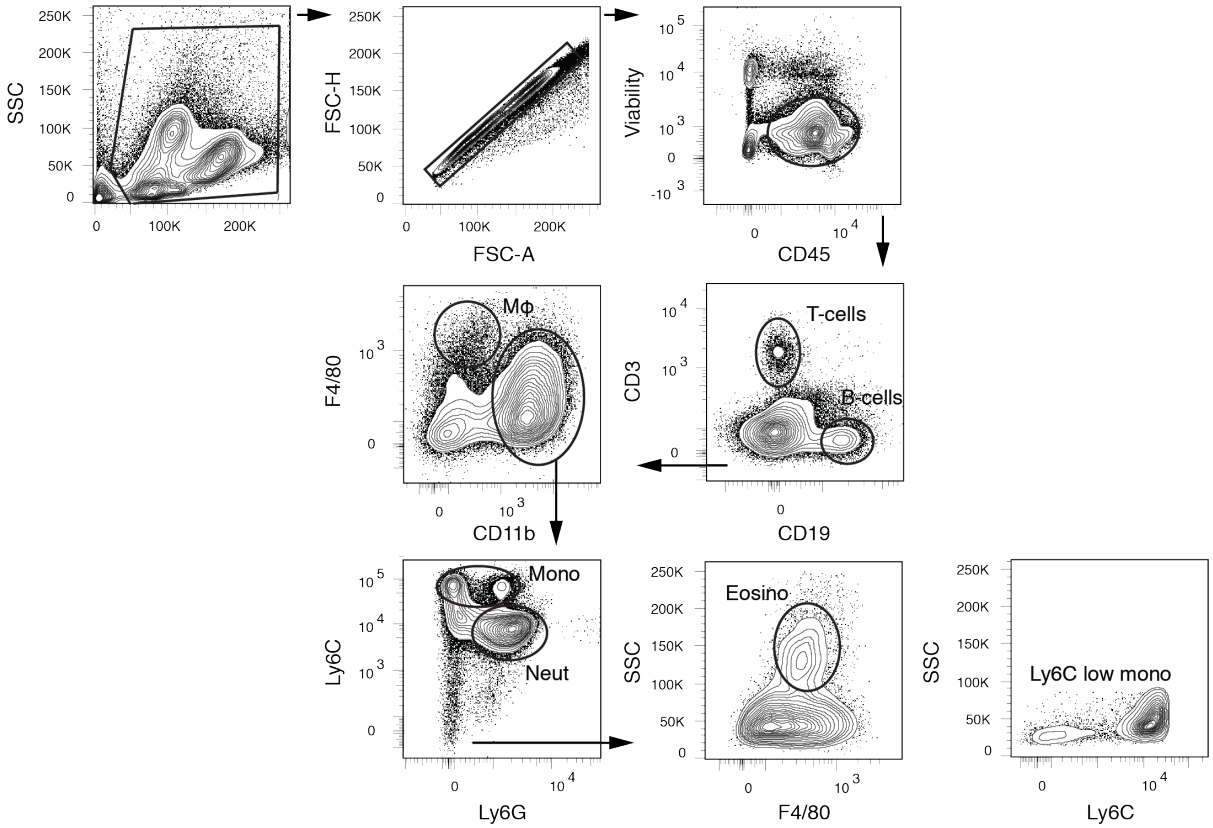
Appendix Figure 3. Gating strategy for myeloid populations in the spleen.

Spleens were harvested and the cells were stained with a live/dead stain and markers to identify immune populations. Representative dot plots show that doublets were excluded and live CD45+ cells were gated. Next, CD3+ T-cells, CD19+ B-cells and CD3-CD19- cells were gated. The CD3-CD19- cells were further gated to identify myeloid populations. Macrophages were identified as F4/80+CD11b^{int} cells. CD11b+ cells were gated on Ly6C+Ly6G- to identify monocytes and Ly6C^{int}Ly6G+ for neutrophils. Eosinophils were gated on lineage negative cells based on their side scatter (SSC). Finally CD11c+MHC-II+ dendritic cells (DCs) were gated after exclusion of eosinophils.



Appendix Figure 4. Gating for myeloid populations in the lung.

Lungs were harvested and the cells were enzymatically digested and then stained with a live/dead stain and markers to identify immune populations. Representative dot plots show that doublets were excluded, live CD45+ and CD11b- or CD11b+ cells were gated before gating individual immune populations. CD11b- cells were further gated on F4/80+CD64+ cells to identify alveolar macrophages (AM). cDC1 cells were gated as F4/80-CD64- CD11c+MHC-II+ and CD3+ T-cells and CD19+ B-cells were gated on the lineage negative cells. The CD11b+ cells were gated on Ly6C+Ly6G- to identify monocytes and Ly6C^{int}Ly6G+ for neutrophils. Interstitial macrophages (IM) were gated as F4/80+CD64+ on the lineage negative cells. Eosinophils were gated on lineage negative cells based on their side scatter (SSC). Finally CD11c+MHC-II+ cDC2s were gated after exclusion of eosinophils.



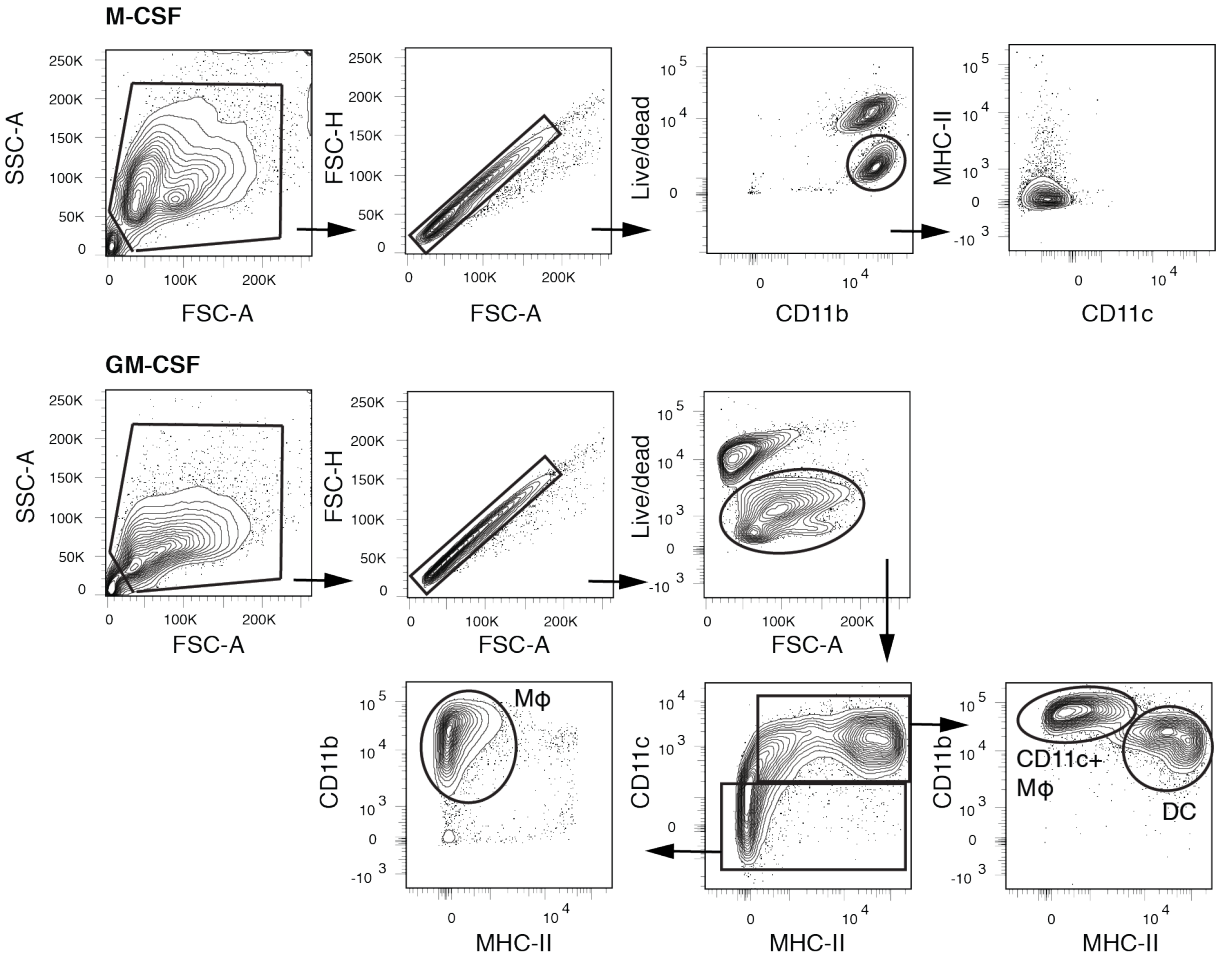
Appendix Figure 5. Gating for myeloid populations in the bone marrow.

Bone marrow was harvested and the cells were stained with a live/dead stain and markers to identify immune populations. Representative dot plots show that doublets were excluded and live CD45+ cells were gated. Next, CD3+ T-cells, CD19+ B-cells and CD3-CD19- cells were gated. The CD3-CD19- cells were further gated to identify myeloid populations. Macrophages were identified as F4/80+CD11b^{int} cells. CD11b+ cells were gated on Ly6C+Ly6G- to identify monocytes and Ly6C^{int}Ly6G+ for neutrophils. Eosinophils were gated on lineage negative cells based on their side scatter (SSC).

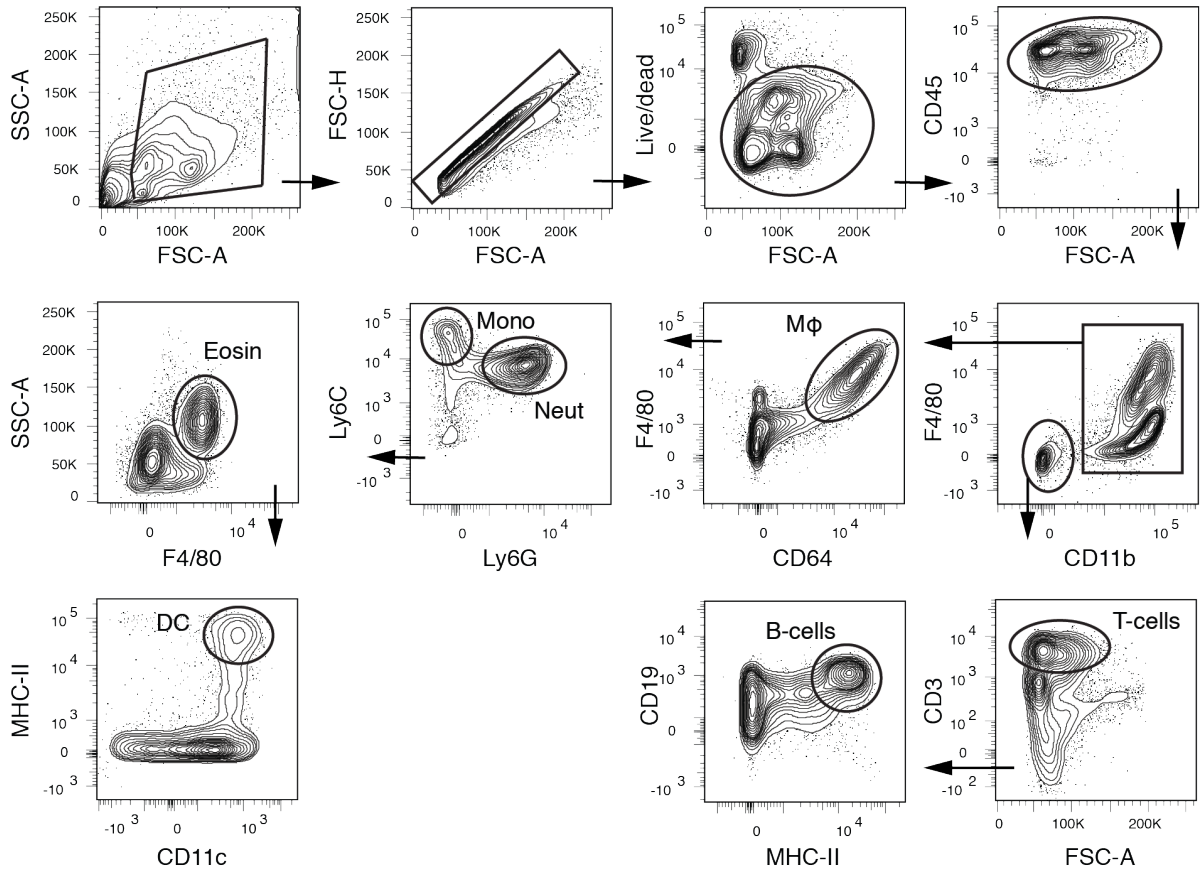
	Human						Mouse		
	Meharaj	Yıldırım-Buharalioğlu	Martinez, F	Derlindanti	Martinez, P	Collins	Swart	Jablonski	Jiang
	IFNγ		IFNγ/LPS				IFNγ/LPS		
	IL-4		IL-4		IL-4/IL-13		IL-4		
Core proteins									
AGRN			2		-	2.1	2	2.5	1.6
GPC1					-	0.1	0.3	0.1	0.2
GPC2	1.2				-	0.2	0.4		
GPC3					-				
GPC4	0.5				-	0.4			
GPC5					-	8			
GPC6					-				
SDC1	0.2				-			5	2.8
SDC2	0.3	0.8	0.08		-	0.04			
SDC3	5		0.3		-	1.8	2		
SDC4	0.5	0.7			-			0.4	0.6
HSPG2	0.8				-	0.01			
TGFBR3					-			0.6	
Polymerases									
EXT1	1.2		2.5		-				1.4
EXT2					-		0.2		
EXTL1	-				-		0.2		
EXTL2	0.7	0.8	3.1		-	2.8	0.2		
EXTL3					-		0.6		1.4
GLCE	0.7	0.8	0.3	0.3	-	0.3	0.4	0.6	
NDST1	1.7				2.1		0.1	0.6	
NDST2	1.5	1.3			2				
NDST3	-								
NDST4	-		1.4						
Sulfotransferases									
HS2ST1	0.4		0.07	0.2	0.2	0.2	0.3	0.7	0.4
HS3ST1	0.7		0.08		0.1		0.4	0.7	
HS3ST2	0.5		0.2	0.3	0.03	0.06			
HS3ST3A1	-								
HS3ST3B1	-		15	5.4	65	35	0.1		
HS3ST4	-	-							
HS3ST5	-								
HS3ST6	-								
HS6ST1	0.5		0.7		0.5	0.5	0.2		
HS6ST2	-								
HS6ST3	-								
Modifyers									
SULF1	-				-				
SULF2	0.6		0.5	0.1	-		0.02	0.3	0.3
HPSE	1.3				-			0.7	0.6
HPSE2	-				-				

Appendix Figure 6. Fold change in the expression of HS biosynthetic enzymes and core proteins in *in vitro* M1 and M2 polarised macrophages.

Using microarray data, I analysed the expression of HS core protein and biosynthetic enzymes upon macrophage polarisation *in vitro* with either IFNγ/LPS (M1) or IL4/IL13 (M2). Genes marked in dark gray show minimal expression in macrophages in my experience. Genes upregulated in M1 compared to M2 macrophages are marked in red (P<0.05) or pink (P>0.05), genes downregulated in M1 macrophages are marked in dark blue (P<0.05) or light blue (P>0.05) and genes that were not measured are marked with a dash (-). Mehraj et al. (2013), Martinez et al. (2006), Derlindati et al. (2015), Yıldırım-Buharalıoğlu et al. (2017) compared human M1 and M2 macrophages by microarray. Jablonski et al. (2015) and Jiang et al. (2017) compared M1 and M2 macrophages by microarray from C57BL/6 or BALB/c mice respectively. Martinez et al. (2015) performed individual qPCRs for NDST's and sulfotransferases in human M1 and M2 macrophages. Collins and Swart compared respectively human and murine M1 and M2 macrophages using custom-design microfluids cards (unpublished data). Figure adapted from Swart and Troeberg (2019).

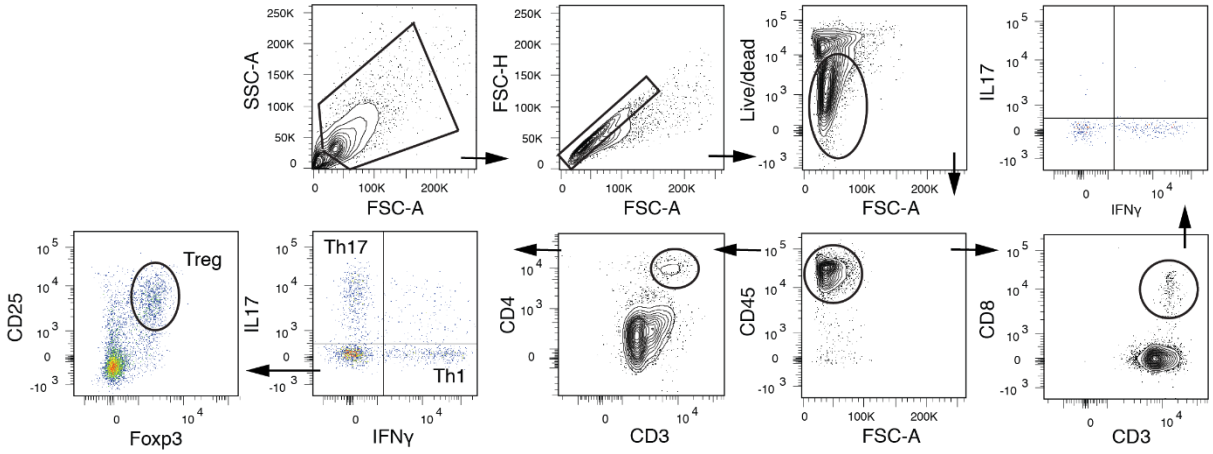


Appendix Figure 7. Gating strategy for M-CSF/ GM-CSF differentiated bone marrow cells *in vitro*. Macrophages were derived by culturing cells from murine bone marrow for 7 d with 100 ng/ml M-CSF or 20 ng/ml GM-CSF and then cells were stained with a live/dead stain and markers against macrophage and dendritic cell (DC) markers. Representative dot plots show the gating strategy. Doublets were excluded before live cells were gated. M-CSF-derived macrophages were identified by CD11b+ expression. GM-CSF-derived cells were gated as CD11c+MHC-II$^{int\text{-}high}$ or CD11c-MHC-II^{low}. CD11c+MHC-II$^{int\text{-}high}$ were further gated as CD11b^{high}MHC-II^{int} or CD11b^{int}MHC-II^{high} to identify CD11c+ macrophages and dendritic cells. CD11c-MHC-II^{low} cells were gated as CD11b+MHC-II$^{low\text{-}int}$ to identify CD11c- macrophages.



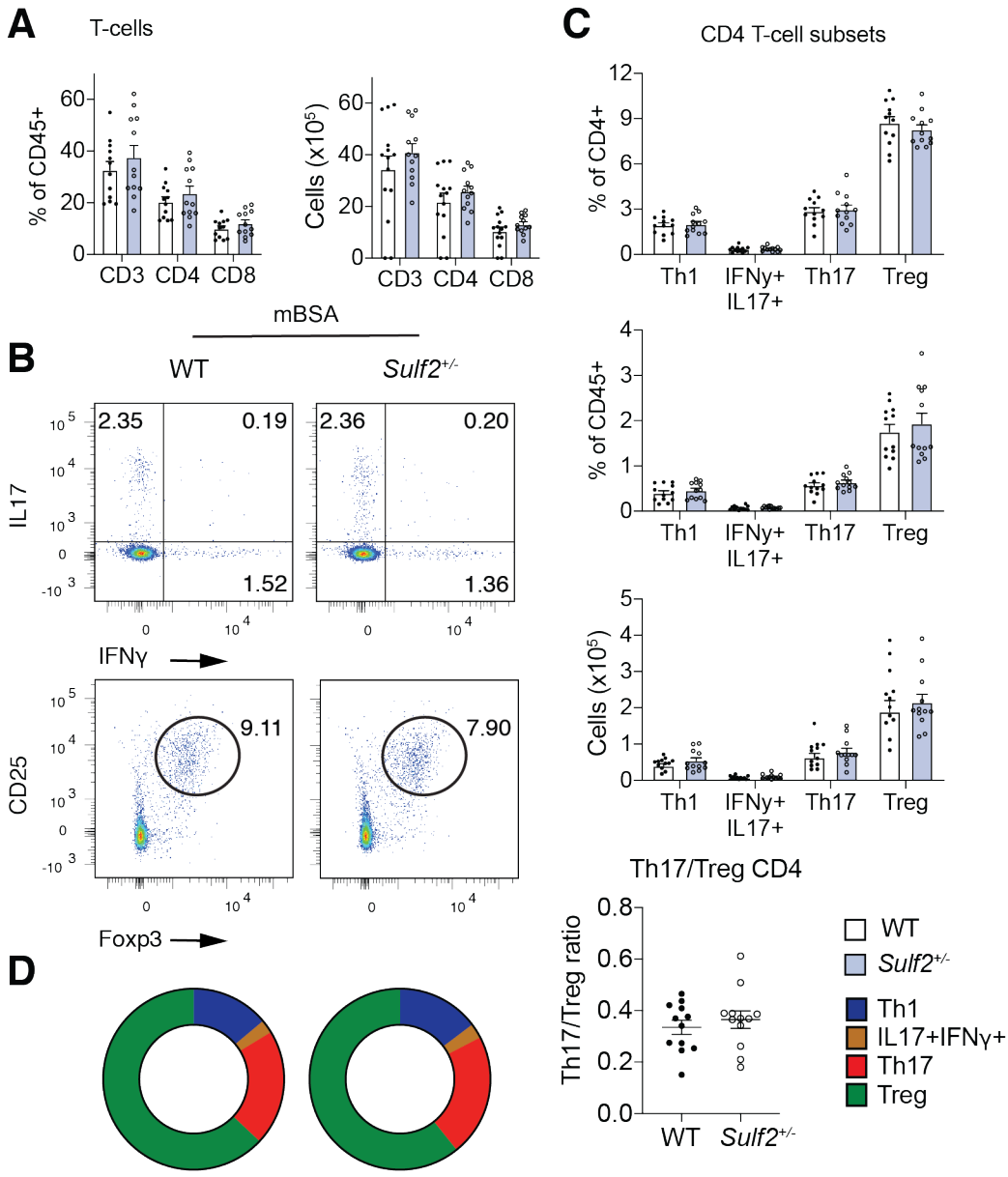
Appendix Figure 8. Gating strategy for myeloid populations in the knee.

Knees were harvested and synovial cells were enzymatically digested and then stained with a live/dead stain and markers to identify immune populations in the joint. Representative dot plots show that doublets were excluded and live CD45+ were gated before gating individual immune populations. CD11b+ cells were first gated to identify myeloid cells in the joint and F4/80+CD64+ cells were gated to identify macrophages. F4/80-CD64- cells were further gated on Ly6C+Ly6G- to identify monocytes and Ly6C^{int}Ly6G+ for neutrophils. Eosinophils were gated on lineage negative cells based on their side scatter (SSC). Finally CD11c+MHC-II+ dendritic cells (DCs) were gated after exclusion of eosinophils. CD3+ T-cells and CD19+MHC-II+ B-cells were gated on CD11b- cells.



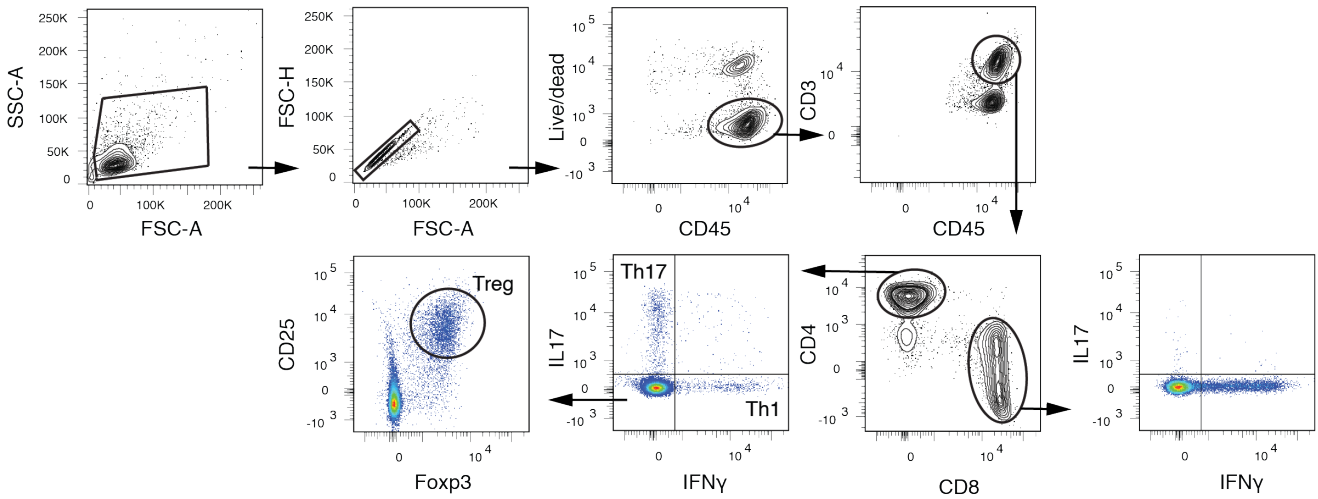
Appendix Figure 9. Gating strategy for T-cell subsets in the knee.

Knees were harvested and synovial cells were enzymatically digested and cells were stimulated for 4 h with 20 ng/ml PMA, 1 ug/ml ionomycin in the presence of protein transport inhibitors. The cells were then stained with a live/dead stain and markers to identify T-cell subtypes in the joint. Representative dot plots show that doublets were excluded and live CD45+ were gated before gating individual immune populations. Subsequently, cells were gated as CD3+CD4+ or CD3+CD8+ T-cells. CD3+CD4+ T-cells were further gated as IL7+, IFNγ+ or IL17+IFNγ+ cells. IL17-IFNγ- cells were further gated for CD25+Foxp3+ cells to identify regulatory T-cells (Tregs). CD3+CD8+ T-cells were further gated on IFNγ+ cells.

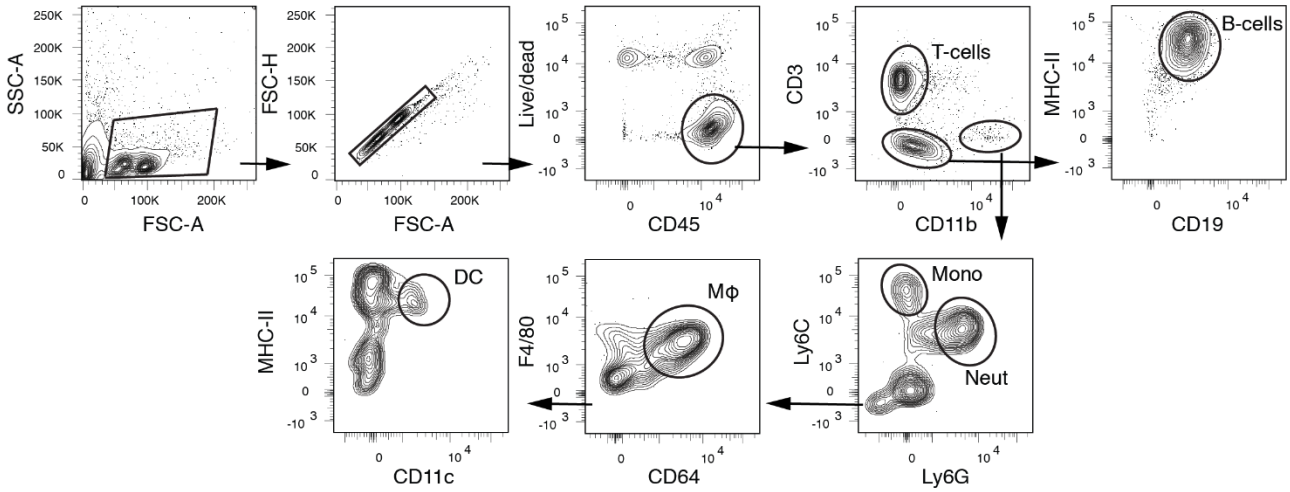


Appendix Figure 10. T-cell subsets were not affected in the inguinal lymph nodes of *Sulf2*$^{+/-}$ chimera mice at day 2 of AIA.

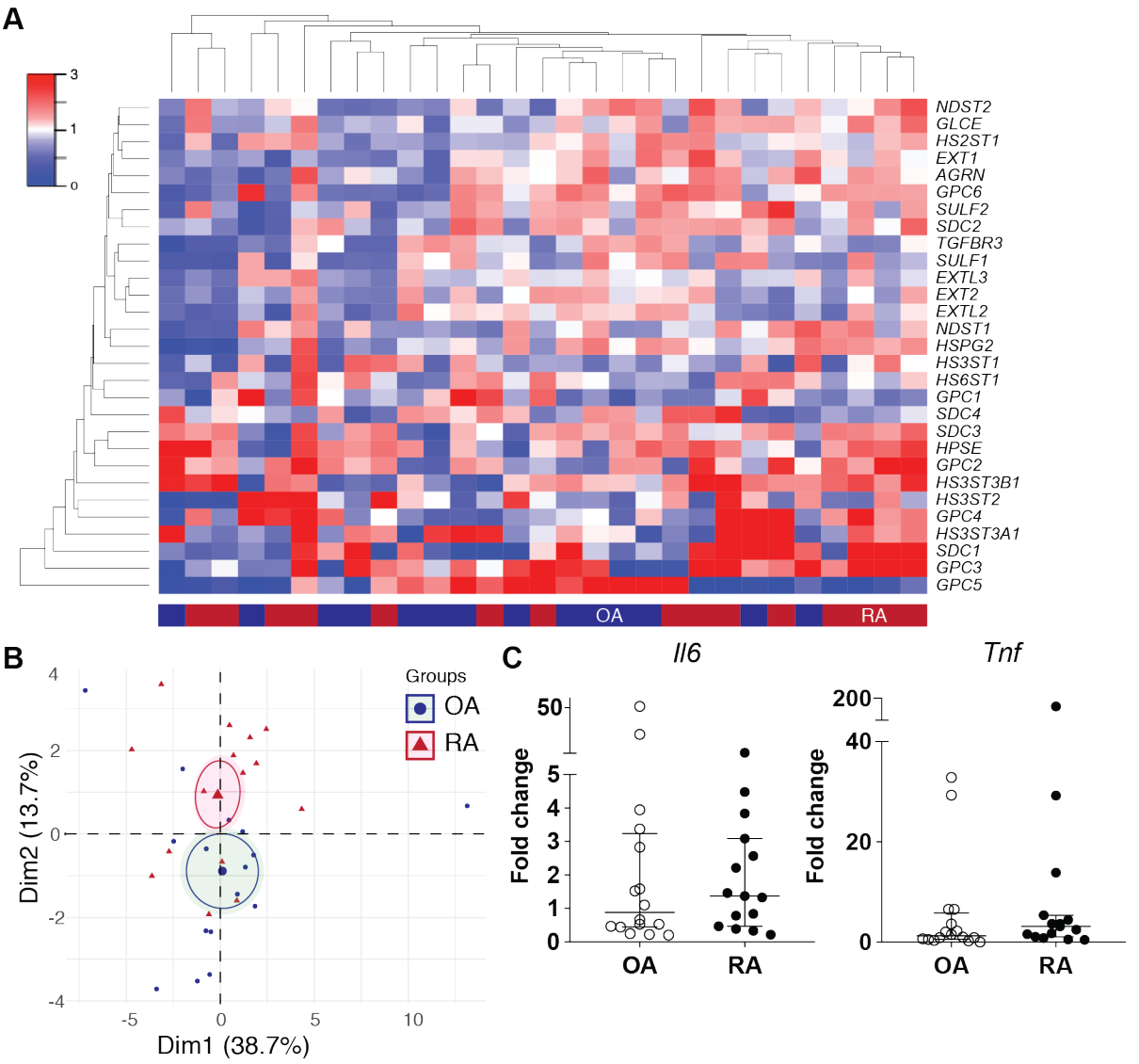
Sulf2$^{+/-}$ bone marrow chimera were immunised with 100 µg mBSA in CFA and arthritis was induced 3 weeks later by intra-articular tibiofemoral injection of 100 µg mBSA (right knee) or PBS (left knee) (n=16). 2 days later, cells were isolated from the inguinal lymph nodes that drain the knees and the cells were stimulated for 4 h with 20 ng/ml PMA, 1 ug/ml ionomycin in the presence of protein transport inhibitors. **A.** CD3+, CD4+ and CD8+ T-cell subsets were analysed by flow cytometry. The gating strategy is shown in **Appendix Figure 11**. **B.** Representative dot plots for CD4+ T-cell subsets in inguinal lymph nodes are shown. **C.** The percentage of CD4+, CD45+ and total number of IFNγ+ Th1, IFNγ+IL17+, IL17+ Th17 and CD25+Foxp3+ regulatory T-cells (Tregs) is shown. **D.** The Th17/Treg ratio shows the balance between Th17 and Tregs. Data are represented as mean ± SEM, analysed by multiple T-tests.



Appendix Figure 11. Gating strategy for T-cell subsets in the inguinal lymph nodes.
Lymph nodes were harvested and cells were stimulated for 4 h with 20 ng/ml PMA, 1 ug/ml ionomycin in the presence of protein transport inhibitors. The cells were then stained with a live/dead stain and markers to identify T-cell subtypes. Representative dot plots show that doublets were excluded and live CD45+ were gated before gating individual immune populations. Subsequently, cells were gated as CD3+CD4+ or CD3+CD8+ T-cells. CD3+CD4+ T-cells were further gated as IL7+, IFNγ+ or IL17+IFNγ+ cells. IL17-IFNγ- cells were further gated for CD25+Foxp3+ cells to identify regulatory T-cells (Tregs). CD3+CD8+ T-cells were further gated on IFNγ+ cells.



Appendix Figure 12. Gating strategy for myeloid populations in the inguinal lymph nodes.
Lymph nodes were harvested and cells then stained with a live/dead stain and markers to identify immune populations. Representative dot plots show that doublets were excluded and live CD45+ were gated before gating individual immune populations. Subsequently, cells were gated as CD11b-CD3+, CD11b-CD3- and CD11b+ cells. CD19+MHC-II+ B-cells were gated on CD11b-CD3- cells. CD11b+ cells were further gated to identify myeloid immune populations. Ly6C+Ly6G- cells were gated to identify monocytes and Ly6C^{int}Ly6G+ cells for neutrophils. Macrophages were gated as F4/80+CD64+ cells on the lineage negative cells. Finally, dendritic cells (DCs) were identified by gating on lineage negative CD11c+MHC-II+ cells.



Appendix Figure 13. HS core protein and biosynthesis enzyme expression in human RA. RNA was isolated from synovial membranes of patients with RA and OA and gene expression levels were measured by qPCR using custom-designed TaqMan low-density array cards, and expressed relative to the geometric mean of the housekeeping genes *18S*, *GAPDH* and *RPLP0* and to expression in OA samples. **A.** Differential expression profiles were visualised using heatmapping. **B.** PCA analysis of the results is shown, with the ellipses indicating the 95% confidence interval. (Dim, dimension). **C.** Fold change in the expression of *IL6* and *TNF* relative to OA samples is shown. Data are represented as median ± IQR, analysed by a Mann-Whitney u test.

Appendix 2. Abbreviations

AIA	Antigen-induced arthritis
APC	Antigen-presenting cell
ACPA	Anti-citrullinated protein antibody
AM	Alveolar macrophage
APS	ammonium persulfate
BM	Bone marrow
BMDM	Bone marrow-derived macrophage
BMSM	Bone marrow-derived synovial macrophage
BMP	Bone morphogenetic protein
CAIA	Collagen antibody-induced arthritis
CCL	C-C motif chemokine ligand
CCR	C-C chemokine receptor
CD	Cluster of differentiation
CXCL	C-X-C motif chemokine ligand
CXCR	C-X-C motif chemokine receptor
cDC	Classical dendritic cell
CFA	Complete Freund’s Adjuvant
CIA	Collagen-induced arthritis
d	Days
DAMP	Damage-associated molecular pattern
DC	Dendritic cell
DMARD	Disease-modifying antirheumatic drugs
DMEM	Dulbecco’s Modified Eagle’s medium
DMSO	Dimethyl sulfoxide
DNA	Deoxyribonucleic acid
DPX	di-n-butylphtalate
ESM	Embryonic resident synovial macrophages
EXT	Exostosis glycosyltransferase enzyme
EXTL	Exostosis-like glycosyltransferase enzyme
FBS	Foetal bovine serum
FC	Flow cytometry
FGF	Fibroblast growth factor

FGly	N-formylglycine
FMO	Fluorescence minus one
Foxp3	Forkhead box protein 3
Gata-3	GATA binding protein-3
GDNF	Glial cell line-derived neurotrophic factor
GlcA	Glucuronic acid
GLCE	Glucuronic acid epimerase
GlcNAc	N-acetylglucosamine
GM-CSF	Granulocyte-macrophage colony-stimulating factor
h	Hour
HD	Hydrophilic highly basic domain
H&E	Haematoxylin and eosin
HLA	Human leukocyte antigen
HS	Heparan sulfate
HS2ST	2-O-sulfotransferase
HS3ST	3-O-sulfotransferase
HS6ST	6-O-sulfotransferase
i.a.	Intra-artiular
IdoA	Iduronic acid
IFN	Interferon
Ig	Immunoglobulin
IL	Interleukin
IM	Interstitial macrophage
IPF	Idiopathic pulmonary fibrosis
IQR	Interquartile range
LPS	Lipopolysaccharide
Ly6G	Lymphocyte antigen 6 complex locus G6D
mBSA	Methylated bovine serum albumin
M-CSF	Macrophage colony-stimulating factor
MerTK	Tyrosine-protein kinase Mer
MHC	Major histocompatibility complex
min	Minute
MMP	Matrix metalloproteinase
MOI	Multiplicity of infection

MPO	Myeloperoxidase
NET	Neutrophil extracellular trap
NETosis	NET activation and release
NIR	Near-infra red
NRE	Nonreducing end
NDST	N-deacetylase/ N-sulfotransferase
NT	Non-targeting
OA	Osteoarthritis
OVA	Ovalbumin
PAMP	Pattern-associated molecular pattern
PBMC	Peripheral blood mononuclear cell
PBS	Phosphate buffered saline
PCA	Principal component analysis
PCR	Polymerase chain reaction
PG	Proteoglycan
PGE_2	Prostaglandin E2
pDC	Plasmacytoid DC
P/S	Penicillin/ Streptomycin
PVDF	Polyvinylidene difluoride
RA	Rheumatoid arthritis
RE	Reducing end
RF	Rheumatoid factor
RNA	Ribonucleic acid
RNA seq	RNA sequencing
RORγt	Retinoic acid-related orphan receptor
ROS	Reactive oxygen species
RPMI	Roswell Park Memorial Institute medium
RT	Room temperature
s.c.	Subcutaneous
scRNA seq	Single cell RNA sequencing
SDS	Sodium dodecyl sulfate
sec	Seconds
SEM	Standard error of the mean
SULF	Sulfatase

T-bet	T-box transcription factor
TBS	Tris-buffered saline
TEMED	Tetramethylethylenediamine
TCR	T-cell receptor
TGF	Transforming growth factor
Th	T helper cell
TLR	Toll-like receptor
TNF	Tumour necrosis factor
Treg	Regulatory T-cells
UMAP	Uniform Manifold Approximation and Projection
VEGF	Vascular endothelial growth factor
WB	Western blot
Wnt	Wingless-related integration site
ZAP70	Zeta chain of T cell receptor associated protein kinase 70

Appendix 3. Published materials

Abstracts presented at scientific conferences

- Versus Arthritis Annual Fellows' Meeting 2019 (Loughborough, UK), Awarded best oral presentation by a PhD student.
- Attended Gordon Research Conference on Proteoglycans 2018 (Andover, USA) – poster presentation at GRC and oral presentation at preceding Gordon Research Seminar.
- Attended AtheroFlux meeting (Eretria, Greece) – poster presentation.
- Versus Arthritis Annual Fellows' Meeting 2018 (Loughborough, UK), Awarded poster by a PhD student.
- British Society for Matrix Biology 2017 (Oxford, UK) – poster presentation.

Published material

Swart, M., & Troeberg, L. 2019. Effect of polarisation and chronic inflammation on macrophage expression of heparan sulfate proteoglycans and biosynthesis enzymes. *Journal of Histochemistry & Cytochemistry* 67 (1): 9–27.

Appendix 4. Bibliography

Abram, C. L., Roberge, G. L., Hu, Y. & Lowell, C. A. 2014. Comparative analysis of the efficiency and specificity of myeloid-Cre deleting strains using ROSA-EYFP reporter mice. *Journal of Immunological Methods*, 408: 89–100.

Adamsen, B. L., Kravik, K. L., Clausen, O. P. F. & Angelis, P. M. De. 2007. Apoptosis, cell cycle progression and gene expression in TP53-depleted HCT116 colon cancer cells in response to short-term 5-fluorouracil treatment. *International Journal of Oncology*, 31 (6): 1491–1500.

Aderem, A. & Underhill, D. M. 1999. Mechanisms of phagocytosis in macrophages. *Annual Review of Immunology*, 17 (1): 593–623.

Ai, X., Do, A.-T., Kusche-Gullberg, M., Lindahl, U., Lu, K. & Emerson, C. P. 2006. Substrate specificity and domain functions of extracellular heparan sulfate 6-O - endosulfatases, QSulf1 and QSulf2. *Journal of Biological Chemistry*, 281 (8): 4969–76.

Ai, X., Do, A.-T., Lozynska, O., Kusche-Gullberg, M., Lindahl, U. & Emerson, C. P. 2003. QSulf1 remodels the 6-O sulfation states of cell surface heparan sulfate proteoglycans to promote Wnt signaling. *The Journal of Cell Biology*, 162 (2): 341–51.

Ai, X., Kitazawa, T., Do, A.-T., Kusche-Gullberg, M., Labosky, P. A. & Emerson, C. P. 2007. SULF1 and SULF2 regulate heparan sulfate-mediated GDNF signaling for esophageal innervation. *Development*, 134 (18): 3327–38.

Alhasan, A. A., Spielhofer, J., Kusche-Gullberg, M., Kirby, J. A. & Ali, S. 2014. Role of 6-O-sulfated heparan sulfate in chronic renal fibrosis. *Journal of Biological Chemistry*, 289 (29): 20296–306.

Alivernini, S., MacDonald, L., Elmesmari, A., Finlay, S., Tolusso, B., Gigante, M. R., Petricca, L., Mario, C. Di, Bui, L., Perniola, S., Attar, M., Gessi, M., Fedele, A. L., Chilaka, S., Somma, D., Sansom, S. N., Filer, A., McSharry, C., Millar, N. L., et al. 2020. Distinct synovial tissue macrophage subsets regulate inflammation and remission in rheumatoid arthritis. *Nature Medicine*,.

Allard, B., Panariti, A. & Martin, J. G. 2018. Alveolar macrophages in the resolution of inflammation, tissue repair, and tolerance to infection. *Frontiers in Immunology*, 9: 1777.

Alzabin, S. & Williams, R. O. 2011. Effector T cells in rheumatoid arthritis: Lessons from animal models. *FEBS Letters*, 585 (23): 3649–59.

Ambasta, R. K., Ai, X. & Emerson, C. P. 2007. Quail Sulf1 function requires asparagine-linked glycosylation. *Journal of Biological Chemistry*, 282 (47): 34492–99.

Arend, W. P. & Firestein, G. S. 2012. Pre-rheumatoid arthritis: predisposition and transition to clinical synovitis. *Nature Reviews Rheumatology*, 8 (10): 573–86.

Axelsson, J., Xu, D., Kang, B. N., Nussbacher, J. K., Handel, T. M., Ley, K., Sriramarao, P., Esko, J. D., Na Kang, B., Nussbacher, J. K., Handel, T. M., Ley, K., Sriramarao, P., Esko, J. D., Kang, B. N., Nussbacher, J. K., Handel, T. M., Ley, K., Sriramarao, P., et al. 2012. Inactivation of heparan sulfate 2-O-sulfotransferase accentuates neutrophil infiltration during acute inflammation in mice. *Blood*, 120 (8): 1742–51.

Barnden, M. J., Allison, J., Heath, W. R. & Carbone, F. R. 1998. Defective TCR expression in transgenic mice constructed using cDNA- based α- and β-chain genes under the control of heterologous regulatory elements. *Immunology and Cell Biology*, 76 (1): 34–40.

Bartok, B. & Firestein, G. S. 2010. Fibroblast-like synoviocytes: key effector cells in rheumatoid arthritis. *Immunological Reviews*, 233 (1): 233–55.

Bek, S., Bojesen, A. B., Nielsen, J. V, Sode, J., Bank, S., Vogel, U. & Andersen, V. 2017. Systematic review and meta-analysis: pharmacogenetics of anti-TNF treatment response in rheumatoid arthritis. *The Pharmacogenomics Journal*, 17 (5): 403–11.

Berg, W. B. van den, Joosten, L. A. B. & Lent, P. L. E. M. van. 2007. Murine antigen-induced arthritis. *Methods in Molecular Medicine*, 136: 243–53.

Billings, P. C. & Pacifici, M. 2015. Interactions of signaling proteins, growth factors and other proteins with heparan sulfate: mechanisms and mysteries. *Connective Tissue Research*, 56 (4): 272–80.

Brackertz, D., Mitchell, G. F. & Mackay, I. R. 1977a. Antigen-induced arthritis in mice. I. Induction of arthritis in various strains of mice. *Arthritis and Rheumatism*, 20 (3): 841–50.

Brackertz, D., Mitchell, G. F. & Mackay, I. R. 1977b. Antigen-induced arthritis in mice. II. Immunologic correlates of arthritis suceptibility in mice. *The Journal of Immunology*, 118 (5): 1639–44.

Brackertz, D., Mitchell, G. F., Vadas, M. A. & Mackay, I. R. 1977. Studies on antigen-induced arthritis in mice. III. Cell and serum transfer experiments. *The Journal of Immunology*, 118 (5): 1645–48.

Brand, B. T. van den, Abdollahi-Roodsaz, S., Vermeij, E. A., Bennink, M. B., Arntz, O. J., Rothlin, C. V., Berg, W. B. van den & Loo, F. A. J. van de. 2013. Therapeutic efficacy of Tyro3, Axl, and Mer tyrosine kinase agonists in collagen-induced arthritis. *Arthritis & Rheumatism*, 65 (3): 671–80.

Brink, M., Hansson, M., Mathsson, L., Jakobsson, P. J., Holmdahl, R., Stenlund, H.,

Rönnelid, J., Klareskog, L. & Rantapää-Dahlqvist, S. 2013. Multiplex analyses of antibodies against citrullinated peptides in individuals prior to development of rheumatoid arthritis. *Arthritis and Rheumatism*, 65 (4): 899–910.

Brühl, H., Cihak, J., Plachý, J., Kunz-Schughart, L., Niedermeier, M., Denzel, A., Rodriguez Gomez, M., Talke, Y., Luckow, B., Stangassinger, M. & Mack, M. 2007. Targeting of Gr-1+,CCR2+ monocytes in collagen-induced arthritis. *Arthritis & Rheumatism*, 56 (9): 2975–85.

Buch, M. H., Bingham, S. J., Bryer, D. & Emery, P. 2007. Long-term infliximab treatment in rheumatoid arthritis: subsequent outcome of initial responders. *Rheumatology*, 46 (7): 1153–56.

Burmester, G. R., Lin, Y., Patel, R., Adelsberg, J. Van, Mangan, E. K., Graham, N. M. H., Hoogstraten, H. Van, Bauer, D., Ignacio Vargas, J. & Lee, E. B. 2017. Efficacy and safety of sarilumab monotherapy versus adalimumab monotherapy for the treatment of patients with active rheumatoid arthritis (MONARCH): A randomised, double-blind, parallel-group phase III trial. *Annals of the Rheumatic Diseases*, 76 (5): 840–47.

Cao, Q., Wang, Y., Zheng, D., Sun, Y., Wang, Y., Lee, V. W. S., Zheng, G., Tan, T. K., Ince, J., Alexander, S. I. & Harris, D. C. H. 2010. IL-10/TGF-β-modified macrophages induce regulatory T cells and protect against adriamycin nephrosis. *Journal of the American Society of Nephrology*, 21 (6): 933–42.

Caplazi, P., Baca, M., Barck, K., Carano, R. A. D., DeVoss, J., Lee, W. P., Bolon, B. & Diehl, L. 2015. Mouse models of rheumatoid arthritis. *Veterinary Pathology*, 52 (5): 819–26.

Chanalaris, A., Clarke, H., Guimond, S. E., Vincent, T. L., Turnbull, J. E. & Troeberg, L. 2019. Heparan sulfate proteoglycan synthesis is dysregulated in human

osteoarthritic cartilage. *The American Journal of Pathology*, 189 (3): 632–47.

Chau, B. N., Diaz, R. L., Saunders, M. A., Cheng, C., Chang, A. N., Warrener, P., Bradshaw, J., Linsley, P. S. & Cleary, M. A. 2009. Identification of SULF2 as an novel transcriptional target of p53 by use of integrated genomic analyses. *Cancer Research*, 69 (4): 1368–74.

Chen, G., Nakamura, I., Dhanasekaran, R., Iguchi, E., Tolosa, E. J., Romecin, P. A., Vera, R. E., Almada, L. L., Miamen, A. G., Chaiteerakij, R., Zhou, M., Asiedu, M. K., Moser, C. D., Han, S., Hu, C., Banini, B. A., Oseini, A. M., Chen, Y., Fang, Y., et al. 2017. Transcriptional induction of periostin by a Sulfatase 2-TGFβ1-SMAD signaling axis mediates tumor angiogenesis in hepatocellular carcinoma. *Cancer Research*, 77 (3): 632–45.

Chen, Z., Andreev, D., Oeser, K., Krljanac, B., Hueber, A., Kleyer, A., Voehringer, D., Schett, G. & Bozec, A. 2016. Th2 and eosinophil responses suppress inflammatory arthritis. *Nature Communications*, 7 (1): 1–12.

Chistiakov, D. A., Orekhov, A. N., Sobenin, I. A. & Bobryshev, Y. V. 2014. Plasmacytoid dendritic cells: development, functions, and role in atherosclerotic inflammation. *Frontiers in Physiology*, 5: 279.

Chmiela, M., Paziak-Domanska, B. & Wadström, T. 1995. Attachment, ingestion and intracellular killing of Helicobacter pylori by human peripheral blood mononuclear leukocytes and mouse peritoneal inflammatory macrophages. *FEMS Immunology & Medical Microbiology*, 10 (3–4): 307–16.

Chu, C. Q. & Londei, M. 1996. Induction of Th2 cytokines and control of collagen-induced arthritis by nondepleting anti-CD4 Abs. *The Journal of Immunology*, 157 (6): 2685–89.

Clausen, B. E., Burkhardt, C., Reith, W., Renkawitz, R. & Förster, I. 1999. Conditional

gene targeting in macrophages and granulocytes using LysMcre mice. *Transgenic Research*, 8 (4): 265–77.

Croft, A. P., Campos, J., Jansen, K., Turner, J. D., Marshall, J., Attar, M., Savary, L., Wehmeyer, C., Naylor, A. J., Kemble, S., Begum, J., Dürholz, K., Perlman, H., Barone, F., McGettrick, H. M., Fearon, D. T., Wei, K., Raychaudhuri, S., Korsunsky, I., et al. 2019. Distinct fibroblast subsets drive inflammation and damage in arthritis. *Nature*, 570 (7760): 246–51.

Cross, M., Smith, E., Hoy, D., Carmona, L., Wolfe, F., Vos, T., Williams, B., Gabriel, S., Lassere, M., Johns, N., Buchbinder, R., Woolf, A. & March, L. 2014. The global burden of rheumatoid arthritis: estimates from the Global Burden of Disease 2010 study. *Annals of the Rheumatic Diseases*, 73 (7): 1316–22.

Culemann, S., Grüneboom, A., Nicolás-Ávila, J. Á., Weidner, D., Lämmle, K. F., Rothe, T., Quintana, J. A., Kirchner, P., Krljanac, B., Eberhardt, M., Ferrazzi, F., Kretzschmar, E., Schicht, M., Fischer, K., Gelse, K., Faas, M., Pfeifle, R., Ackermann, J. A., Pachowsky, M., et al. 2019. Locally renewing resident synovial macrophages provide a protective barrier for the joint. *Nature*, 572: 670–75.

Cullen, S. P., Kearney, C. J., Clancy, D. M. & Martin, S. J. 2015. Diverse activators of the NLRP3 inflammasome promote IL-1β secretion by triggering necrosis. *Cell Reports*, 11 (10): 1535–48.

Cunha, T. M., Verri, W. A., Schivo, I. R., Napimoga, M. H., Parada, C. A., Poole, S., Teixeira, M. M., Ferreira, S. H. & Cunha, F. Q. 2008. Crucial role of neutrophils in the development of mechanical inflammatory hypernociception. *Journal of Leukocyte Biology*, 83 (4): 824–32.

Curtsinger, J. M. & Mescher, M. F. 2010. Inflammatory cytokines as a third signal for T cell activation. *Current Opinion in Immunology*, 22 (3): 333–40.

Dai, Y., Yang, Y., MacLeod, V., Yue, X., Rapraeger, A. C., Shriver, Z., Venkataraman, G., Sasisekharan, R. & Sanderson, R. D. 2005. HSulf-1 and HSulf-2 are potent inhibitors of myeloma tumor growth in vivo. *Journal of Biological Chemistry*, 280 (48): 40066–73.

Dalod, M., Chelbi, R., Malissen, B. & Lawrence, T. 2014. Dendritic cell maturation: functional specialization through signaling specificity and transcriptional programming. *The EMBO Journal*, 33 (10): 1104–16.

Dehio, C., Freissler, E., Lanz, C., Gómez-Duarte, O. G., David, G. & Meyer, T. F. 1998. Ligation of cell surface heparan sulfate proteoglycans by antibodycoated beads stimulates phagocytic uptake into epithelial cells: A model for cellular invasion by Neisseria gonorrhoeae. *Experimental Cell Research*, 242 (2): 528–39.

Deng, L., Zhou, J. F., Sellers, R. S., Li, J. F., Nguyen, A. V., Wang, Y., Orlofsky, A., Liu, Q., Hume, D. A., Pollard, J. W., Augenlicht, L. & Lin, E. Y. 2010. A novel mouse model of inflammatory bowel disease links mammalian target of rapamycin-dependent hyperproliferation of colonic epithelium to inflammation-associated tumorigenesis. *American Journal of Pathology*, 176 (2): 952–67.

Derlindati, E., Dei Cas, A., Montanini, B., Spigoni, V., Curella, V., Aldigeri, R., Ardigò, D., Zavaroni, I. & Bonadonna, R. C. 2015. Transcriptomic analysis of human polarized macrophages: more than one role of alternative activation? *PLOS ONE*, 10 (3): e0119751.

Diny, N. L., Rose, N. R. & Čiháková, D. 2017. Eosinophils in autoimmune diseases. *Frontiers in Immunology*, 8: 484.

Dolhain, R. J. E. M., Heiden, A. N. Van Der, Haar, N. T. Ter, Breedveld, F. C. & Miltenburg, A. M. M. 1996. Shift toward T lymphocytes with a T helper 1 cytokine-secretion profile in the joints of patients with rheumatoid arthritis. *Arthritis and*

Rheumatism, 39 (12): 1961–69.

Dupage, M. & Bluestone, J. A. 2016. Harnessing the plasticity of CD4+ T cells to treat immune-mediated disease. *Nature Reviews Immunology*, 16 (3): 149–63.

Ebbinghaus, M., Natura, G., Segond Von Banchet, G., Hensellek, S., Böttcher, M., Hoffmann, B., Salah, F. S., Gajda, M., Kamradt, T. & Schaible, H. G. 2017. Interleukin-17A is involved in mechanical hyperalgesia but not in the severity of murine antigen-induced arthritis. *Scientific Reports*, 7 (1): 10334.

Edwards, J. C. W., Szczepański, L., Szechiński, J., Filipowicz-Sosnowska, A., Emery, P., Close, D. R., Stevens, R. M. & Shaw, T. 2004. Efficacy of B-cell-targeted therapy with rituximab in patients with rheumatoid arthritis. *New England Journal of Medicine*, 350 (25): 2572–81.

Egan, P. J., Nieuwenhuijze, A. van, Campbell, I. K. & Wicks, I. P. 2008. Promotion of the local differentiation of murine Th17 cells by synovial macrophages during acute inflammatory arthritis. *Arhritis Rheum*, 58 (12): 3720–29.

Ehinger, M., Vestberg, M., Johansson, A. C., Johannesson, M., Svensson, A. & Holmdahl, R. 2001. Influence of CD4 or CD8 deficiency on collagen-induced arthritis. *Immunology*, 103 (3): 291–300.

Elliott, M. R., Koster, K. M. & Murphy, P. S. 2017. Efferocytosis signaling in the regulation of macrophage inflammatory responses. *The Journal of Immunology*, 198 (4): 1387–94.

Esko, J. D. & Selleck, S. B. 2002. Order out of chaos: assembly of ligand binding sites in heparan sulfate. *Annual Review of Biochemistry*, 71 (1): 435–71.

Estrada-Capetillo, L., Hernández-Castro, B., Monsiváis-Urenda, A., Alvarez-Quiroga, C., Layseca-Espinosa, E., Abud-Mendoza, C., Baranda, L., Urzainqui, A., Sánchez-Madrid, F. & González-Amaro, R. 2013. Induction of Th17 lymphocytes

and Treg cells by monocyte-derived dendritic cells in patients with rheumatoid arthritis and systemic lupus erythematosus. *Clinical and Developmental Immunology*, 2013: 1–9.

Evangelou, E., Kerkhof, H. J., Styrkarsdottir, U., Ntzani, E. E., Bos, S. D., Esko, T., Evans, D. S., Metrustry, S., Panoutsopoulou, K., Ramos, Y. F. M., Thorleifsson, G., Tsilidis, K. K., Arden, N., Aslam, N., Bellamy, N., Birrell, F., Blanco, F. J., Carr, A., Chapman, K., et al. 2014. A meta-analysis of genome-wide association studies identifies novel variants associated with osteoarthritis of the hip. *Annals of the Rheumatic Diseases*, 73 (12): 2130–36.

Farrugia, B. L., Lord, M. S., Melrose, J. & Whitelock, J. M. 2018. The role of heparan sulfate in inflammation, and the development of biomimetics as anti-inflammatory strategies. *Journal of Histochemistry & Cytochemistry*, 66 (4): 321–36.

Feldmann, M., Brennan, F. M. & Maini, R. N. 1996. Role of cytokines in rheumatoid arthritis. *Annual Review of Immunology*, 14 (1): 397–440.

Fernandez-Botran, R., Gorantla, V., Sun, X., Ren, X., Perez-Abadia, G., Crespo, F. A., Oliver, R., Orhun, H. I., Quan, E. E., Maldonado, C., Ray, M. & Barker, J. H. 2002. Targeting of glycosaminoglycan-cytokine interactions as a novel therapeutic approach in allotransplantation. *Transplantation*, 74 (5): 623–29.

Ferracini, M., Rios, F. J. O., Pecenin, M. & Jancar, S. 2013. Clearance of apoptotic cells by macrophages induces regulatory phenotype and involves stimulation of CD36 and platelet-activating factor receptor. *Mediators of Inflammation*, 2013: 950273.

Fleit, H. B. 2014. Chronic inflammation. In *Pathobiology of Human Disease: A Dynamic Encyclopedia of Disease Mechanisms*, 300–314. Elsevier Inc.

Fleming, B. D. & Mosser, D. M. 2011. Regulatory macrophages: Setting the threshold

for therapy. *European Journal of Immunology*,. Eur J Immunol.

Floer, M., Götte, M., Wild, M. K., Heidemann, J., Gassar, E. S., Domschke, W., Kiesel, L., Luegering, A. & Kucharzik, T. 2010. Enoxaparin improves the course of dextran sodium sulfate-induced colitis in syndecan-1-deficient mice. *The American Journal of Pathology*, 176 (1): 146–57.

Frese, M. A., Milz, F., Dick, M., Lamanna, W. C. & Dierks, T. 2009. Characterization of the human sulfatase Sulf1 and its high affinity heparin/heparan sulfate interaction domain. *Journal of Biological Chemistry*, 284 (41): 28033–44.

Frey, O., Petrow, P. K., Gajda, M., Siegmund, K., Huehn, J., Scheffold, A., Hamann, A., Radbruch, A. & Bräuer, R. 2005. The role of regulatory T cells in antigen-induced arthritis: aggravation of arthritis after depletion and amelioration after transfer of CD4+CD25+ T cells. *Arthritis Research & Therapy*, 7 (2): R291.

Fukasawa, M., Sekine, F., Miura, M., Nishijima, M. & Hanada, K. 1997. Involvement of heparan sulfate proteoglycans in the binding step for phagocytosis of latex beads by Chinese hamster ovary cells. *Experimental Cell Research*, 230 (1): 154–62.

Furman, D., Campisi, J., Verdin, E., Carrera-Bastos, P., Targ, S., Franceschi, C., Ferrucci, L., Gilroy, D. W., Fasano, A., Miller, G. W., Miller, A. H., Mantovani, A., Weyand, C. M., Barzilai, N., Goronzy, J. J., Rando, T. A., Effros, R. B., Lucia, A., Kleinstreuer, N., et al. 2019. Chronic inflammation in the etiology of disease across the life span. *Nature Medicine*, 25 (12): 1822–32.

Gabay, C., Emery, P., Vollenhoven, R. Van, Dikranian, A., Alten, R., Pavelka, K., Klearman, M., Musselman, D., Agarwal, S., Green, J. & Kavanaugh, A. 2013. Tocilizumab monotherapy versus adalimumab monotherapy for treatment of rheumatoid arthritis (ADACTA): A randomised, double-blind, controlled phase 4

trial. *The Lancet*, 381 (9877): 1541–50.

Garner, O. B., Yamaguchi, Y., Esko, J. D. & Videm, V. 2008. Small changes in lymphocyte development and activation in mice through tissue-specific alteration of heparan sulphate. *Immunology*, 125 (3): 420–29.

Ge, C., Tong, D., Liang, B., Lönnblom, E., Schneider, N., Hagert, C., Viljanen, J., Ayoglu, B., Stawikowska, R., Nilsson, P., Fields, G. B., Skogh, T., Kastbom, A., Kihlberg, J., Burkhardt, H., Dobritzsch, D. & Holmdahl, R. 2017. Anti-citrullinated protein antibodies cause arthritis by cross-reactivity to joint cartilage. *JCI Insight*, 2 (13): e93688.

Ge, X. N., Ha, S. G., Rao, A., Greenberg, Y. G., Rushdi, M. N., Esko, J. D., Rao, S. P. & Sriramarao, P. 2014. Endothelial and leukocyte heparan sulfates regulate the development of allergen-induced airway remodeling in a mouse model. *Glycobiology*, 24 (8): 715–27.

Genovese, M. C. & Kremer, J. M. 2004. Treatment of rheumatoid arthritis with etanercept. *Rheumatic Disease Clinics of North America*, 30 (2): 311–28.

Ghadiali, R. S., Guimond, S. E., Turnbull, J. E. & Pisconti, A. 2017. Dynamic changes in heparan sulfate during muscle differentiation and ageing regulate myoblast cell fate and FGF2 signalling. *Matrix Biology*, 59 (May): 54–68.

Ghazal, R. El, Yin, X., Johns, S. C., Swanson, L., Macal, M., Ghosh, P., Zuniga, E. I. & Fuster, M. M. 2016. Glycan sulfation modulates dendritic cell biology and tumor growth. *Neoplasia*, 18 (5): 294–306.

Gill, R. B., Day, A., Barstow, A., Liu, H., Zaman, G. & Dhoot, G. K. 2011. Sulf2 gene is alternatively spliced in mammalian developing and tumour tissues with functional implications. *Biochemical and Biophysical Research Communications*, 414 (3): 468–73.

Gill, R., Mehra, V., Milford, E. & Dhoot, G. K. 2016. Short SULF1/SULF2 splice variants predominate in mammary tumours with a potential to facilitate receptor tyrosine kinase-mediated cell signalling. *Histochemistry and Cell Biology*, 146 (4): 431–44.

Gill, R., Michael, A., Westley, L., Kocher, H. M., Murphy, J. I. & Dhoot, G. K. 2014. SULF1/SULF2 splice variants differentially regulate pancreatic tumour growth progression. *Experimental Cell Research*, 324 (2): 157–71.

Ginhoux, F. & Guilliams, M. 2016. Tissue-resident macrophage ontogeny and homeostasis. *Immunity*, 44 (3): 439–49.

Gordon, S., Plüddemann, A. & Martinez Estrada, F. 2014. Macrophage heterogeneity in tissues: Phenotypic diversity and functions. *Immunological Reviews*, 262 (1): 36–55.

Gordts, P., Foley, E. M., Lawrence, R., Sinha, R., Lameda-Diaz, C., Deng, L., Nock, R., Glass, C. K., Erbilgin, A., Lusis, A. J., Witztum, J. L. & Esko, J. D. 2014. Reducing macrophage proteoglycan sulfation increases atherosclerosis and obesity through enhanced type I interferon signaling. *Cell Metabolism*, 20 (5): 813–26.

Graham, K., Murphy, J. I. & Dhoot, G. K. 2016. SULF1/SULF2 reactivation during liver damage and tumour growth. *Histochemistry and Cell Biology*, 146 (1): 85–97.

Guilliams, M., Kleer, I. De, Henri, S., Post, S., Vanhoutte, L., Prijck, S. De, Deswarte, K., Malissen, B., Hammad, H. & Lambrecht, B. N. 2013. Alveolar macrophages develop from fetal monocytes that differentiate into long-lived cells in the first week of life via GM-CSF. *Journal of Experimental Medicine*, 210 (10): 1977–92.

Guilliams, M., Mildner, A. & Yona, S. 2018. Developmental and functional heterogeneity of monocytes. *Immunity*, 49 (4): 595–613.

Guy, C. S. & Vignali, D. A. A. 2009. Organization of proximal signal initiation at the TCR:CD3 complex. *Immunological Reviews*, 232 (1): 7–21.

Habuchi, H., Nagai, N., Sugaya, N., Atsumi, F., Stevens, R. L. & Kimata, K. 2007. Mice deficient in heparan sulfate 6-O-sulfotransferase-1 exhibit defective heparan sulfate biosynthesis, abnormal placentation, and late embryonic lethality. *Journal of Biological Chemistry*, 282 (21): 15578–88.

Häcker, U., Nybakken, K. & Perrimon, N. 2005. Developmental cell biology: heparan sulphate proteoglycans: the sweet side of development. *Nature Reviews Molecular Cell Biology*, 6 (7): 530–41.

HajMohammadi, S., Enjyoji, K., Princivalle, M., Christi, P., Lech, M., Beeler, D., Rayburn, H., Schwartz, J. J., Barzegar, S., Agostini, A. I. de, Post, M. J., Rosenberg, R. D. & Shworak, N. W. 2003. Normal levels of anticoagulant heparan sulfate are not essential for normal hemostasis. *Journal of Clinical Investigation*, 111 (7): 989–99.

Hammond, E., Khurana, A., Shridhar, V. & Dredge, K. 2014. The role of heparanase and sulfatases in the modification of heparan sulfate proteoglycans within the tumor microenvironment and opportunities for novel cancer therapeutics. *Frontiers in Oncology*, 4 (July): 195.

Hanson, S. R., Best, M. D. & Wong, C.-H. 2004. Sulfatases: structure, mechanism, biological activity, inhibition, and synthetic utility. *Angewandte Chemie International Edition*, 43 (43): 5736–63.

Harrington, L. E., Hatton, R. D., Mangan, P. R., Turner, H., Murphy, T. L., Murphy, K. M. & Weaver, C. T. 2005. Interleukin 17–producing CD4+ effector T cells develop via a lineage distinct from the T helper type 1 and 2 lineages. *Nature Immunology*, 6 (11): 1123–32.

Hashimoto, D., Chow, A., Noizat, C., Teo, P., Beasley, M. B., Leboeuf, M., Becker, C. D., See, P., Price, J., Lucas, D., Greter, M., Mortha, A., Boyer, S. W., Forsberg, E. C., Tanaka, M., Rooijen, N. van, García-Sastre, A., Stanley, E. R., Ginhoux, F., et al. 2013. Tissue-resident macrophages self-maintain locally throughout adult life with minimal contribution from circulating monocytes. *Immunity*, 38 (4): 792–804.

Hayashida, K., Parks, W. C. & Park, P. W. 2009. Syndecan-1 shedding facilitates the resolution of neutrophilic inflammation by removing sequestered CXC chemokines. *Blood*, 114 (14): 3033–43.

Helm-van Mil, A. H. M. Van Der, Wesoly, J. Z. & Huizinga, T. W. J. 2005. Understanding the genetic contribution to rheumatoid arthritis. *Current Opinion in Rheumatology*, 17 (3): 299–304.

Hess, H., Gately, M. K., Rüde, E., Schmitt, E., Szeliga, J. & Germann, T. 1996. High doses of interleukin-12 inhibit the development of joint disease in DBA/1 mice immunized with type II collagen in complete Freund's adjuvant. *European Journal of Immunology*, 26 (1): 187–91.

Hirayama, D., Iida, T. & Nakase, H. 2018. The phagocytic function of macrophage-enforcing innate immunity and tissue homeostasis. *International Journal of Molecular Sciences*, 19 (1): 92.

Holers, V. M., Demoruelle, M. K., Kuhn, K. A., Buckner, J. H., Robinson, W. H., Okamoto, Y., Norris, J. M. & Deane, K. D. 2018. Rheumatoid arthritis and the mucosal origins hypothesis: protection turns to destruction. *Nature Reviews Rheumatology*, 14 (9): 542–57.

Holmdahl, R., Jansson, L., Larsson, E., Rubin, K. & Klareskog, L. 1986. Homologous type II collagen induces chronic and progressive arthritis in mice. *Arthritis and*

Rheumatism, 29 (1): 106–13.

Holst, C. R., Bou-Reslan, H., Gore, B. B., Wong, K., Grant, D., Chalasani, S., Carano, R. A., Frantz, G. D., Tessier-Lavigne, M., Bolon, B., French, D. M. & Ashkenazi, A. 2007. Secreted sulfatases Sulf1 and Sulf2 have overlapping yet essential roles in mouse neonatal survival. *PLoS ONE*, 2 (6): e575.

Horai, R., Saijo, S., Tanioka, H., Nakae, S., Sudo, K., Okahara, A., Ikuse, T., Asano, M. & Iwakura, Y. 2000. Development of chronic inflammatory arthropathy resembling rheumatoid arthritis in interleukin I receptor antagonist-deficient mice. *Journal of Experimental Medicine*, 191 (2): 313–20.

Huang, Y., Mao, Y., Buczek-Thomas, J. A., Nugent, M. A. & Zaia, J. 2014. Oligosaccharide substrate preferences of human extracellular sulfatase Sulf2 using liquid chromatography-mass spectrometry based glycomics approaches. *PLOS ONE*, 9 (8): e105143.

Huynh, M. B., Morin, C., Carpentier, G., Garcia-Filipe, S., Talhas-Perret, S., Barbier-Chassefiere, V., Kuppevelt, T. H. van, Martelly, I., Albanese, P. & Papy-Garcia, D. 2012. Age-related changes in rat myocardium involve altered capacities of glycosaminoglycans to potentiate growth factor functions and heparan sulfate-altered sulfation. *Journal of Biological Chemistry*, 287 (14): 11363–73.

Huynh, Minh Bao, Villares, J., Sepúlveda Díaz, J. E., Christiaans, S., Carpentier, G., Ouidja, M. O., Sissoeff, L., Raisman-Vozari, R. & Papy-Garcia, D. 2012. Glycosaminoglycans from aged human hippocampus have altered capacities to regulate trophic factors activities but not Aβ42 peptide toxicity. *Neurobiology of Aging*, 33 (5): 1005.e11-1005.e22.

Irmler, I. M., Gajda, M., Bräuer, R., Uchijima, M., Arai, T., Miyamoto, S., Ozeki, T., Hiyoshi, M., Kushida, K. & Inoue, T. 2007. Exacerbation of antigen-induced

arthritis in IFN-gamma-deficient mice as a result of unrestricted IL-17 response. *The Journal of Immunology*, 179 (9): 6228–36.

Ishiguro, K., Kadomatsu, K., Kojima, T., Muramatsu, H., Iwase, M., Yoshikai, Y., Yanada, M., Yamamoto, K., Matsushita, T., Nishimura, M., Kusugami, K., Saito, H. & Muramatsu, T. 2001. Syndecan-4 deficiency leads to high mortality of lipopolysaccharide-injected mice. *Journal of Ciological Chemistry*, 276 (50): 47483–88.

Izquierdo, E., Cañete, J. D., Celis, R., Rey, M. J. Del, Usategui, A., Marsal, S., Sanmartí, R., Criado, G. & Pablos, J. L. 2011. Synovial fibroblast hyperplasia in rheumatoid arthritis: Clinicopathologic correlations and partial reversal by anti-tumor necrosis factor therapy. *Arthritis and Rheumatism*, 63 (9): 2575–83.

Izvolsky, K. I., Lu, J., Martin, G., Albrecht, K. H. & Cardoso, W. V. 2008. Systemic inactivation of Hs6st1 in mice is associated with late postnatal mortality without major defects in organogenesis. *Genesis*, 46 (1): 8–18.

Jablonski, K. A., Amici, S. A., Webb, L. M., Ruiz-Rosado, J. de D., Popovich, P. G., Partida-Sanchez, S. & Guerau-de-Arellano, M. 2015. Novel markers to delineate murine M1 and M2 macrophages. *PLOS ONE*, 10 (12): e0145342.

Jiang, L., Li, X., Zhang, Y., Zhang, M., Tang, Z. & Lv, K. 2017. Microarray and bioinformatics analyses of gene expression profiles in BALB/c murine macrophage polarization. *Molecular Medicine Reports*, 16 (5): 7382–90.

Johnson, Z. I., Doolittle, A. C., Snuggs, J. W., Shapiro, I. M., Maitre, C. L. Le & Risbud, M. V. 2017. TNF-α promotes nuclear enrichment of the transcription factor TonEBP/NFAT5 to selectively control inflammatory but not osmoregulatory responses in nucleus pulposus cells. *Journal of Biological Chemistry*, 292 (42): 17561–75.

Jovanovic, D. V., Battista, J. A. Di, Martel-Pelletier, J., Jolicoeur, F. C., He, Y., Zhang, M., Mineau, F. & Pelletier, J. P. 1998. IL-17 stimulates the production and expression of proinflammatory cytokines, IL-beta and TNF-alpha, by human macrophages. *The Journal of Immunology*, 160 (7): 3513–21.

Kalus, I., Rohn, S., Puvirajesinghe, T. M., Guimond, S. E., Eyckerman-Kölln, P. J., Dam, G. ten, Kuppevelt, T. H. van, Turnbull, J. E. & Dierks, T. 2015. Sulf1 and Sulf2 differentially modulate heparan sulfate proteoglycan sulfation during postnatal cerebellum development: Evidence for neuroprotective and neurite outgrowth prtomoting functions. *PLOS ONE*, 10 (10): e0139853.

Kalus, I., Salmen, B., Viebahn, C., Figura, K. von, Schmitz, D., D'Hooge, R. & Dierks, T. 2009. Differential involvement of the extracellular 6-O-endosulfatases Sulf1 and Sulf2 in brain development and neuronal and behavioural plasticity. *Journal of Cellular and Molecular Medicine*, 13 (11–12): 4505–21.

Kambara, K., Ohashi, W., Tomita, K., Takashina, M., Fujisaka, S., Hayashi, R., Mori, H., Tobe, K. & Hattori, Y. 2015. In vivo depletion of CD206+ M2 macrophages exaggerates lung injury in endotoxemic mice. *American Journal of Pathology*, 185 (1): 162–71.

Kaplan, M. J. 2013. Role of neutrophils in systemic autoimmune diseases. *Arthritis Research & Therapy*, 15 (5): 219.

Keffer, J., Probert, L., Cazlaris, H., Georgopoulos, S., Kaslaris, E., Kioussis, D. & Kollias, G. 1991. Transgenic mice expressing human tumour necrosis factor: a predictive genetic model of arthritis. *The EMBO Journal*, 10 (13): 4025–31.

Kelchtermans, H., Klerck, B. De, Mitera, T., Balen, M. Van, Bullens, D., Billiau, A., Leclercq, G. & Matthys, P. 2005. Defective CD4+CD25+ regulatory T cell functioning in collagen-induced arthritis: an important factor in pathogenesis,

counter-regulated by endogenous IFN-gamma. *Arthritis Research & Therapy*, 7 (2): R402.

Keystone, E. C., Kavanaugh, A. F., Sharp, J. T., Tannenbaum, H., Hua, Y., Teoh, L. S., Fischkoff, S. A. & Chartash, E. K. 2004. Radiographic, clinical, and functional outcomes of treatment with adalimumab (a human anti-tumor necrosis factor monoclonal antibody) in patients with active rheumatoid arthritis receiving concomitant methotrexate therapy: A randomized, placebo-controlled, 52-week trial. *Arthritis & Rheumatism*, 50 (5): 1400–1411.

Khandpur, R., Carmona-Rivera, C., Vivekanandan-Giri, A., Gizinski, A., Yalavarthi, S., Knight, J. S., Friday, S., Li, S., Patel, R. M., Subramanian, V., Thompson, P., Chen, P., Fox, D. A., Pennathur, S. & Kaplan, M. J. 2013. NETs are a source of citrullinated autoantigens and stimulate inflammatory responses in rheumatoid arthritis. *Science Translational Medicine*, 5 (178): 178ra40-178ra40.

Kim, T. H., Banini, B. A., Asumda, F. Z., Campbell, N. A., Hu, C., Moser, C. D., Shire, A. M., Han, S., Ma, C., Krishnan, A., Mounajjed, T., White, T. A., Gores, G. J., LeBrasseur, N. K., Charlton, M. P. & Roberts, L. R. 2020. Knockout of Sulfatase 2 is associated with decreased steatohepatitis and fibrosis in a mouse model of nonalcoholic fatty liver disease. *American Journal of Physiology-Gastrointestinal and Liver Physiology*, July, ajpgi.00150.2019.

Kinne, R. W., Stuhlmüller, B. & Burmester, G.-R. 2007. Cells of the synovium in rheumatoid arthritis. Macrophages. *Arthritis Research & Therapy*, 9 (6): 224.

Kirola, L., Edgar-Zarate, C. L., Rook, B., Rowell, A. C., Wood, T., Uchimura, K., Schwartz, C. E. & Zarate, Y. A. 2019. Phenotypic and molecular description of an individual with a disruptive variant in the SULF2 gene. *Clinical Dysmorphology*, 1.

Koenen, H. J. P. M., Smeets, R. L., Vink, P. M., Rijssen, E. Van, Boots, A. M. H. &

Joosten, I. 2008. Human CD25highFoxp3pos regulatory T cells differentiate into IL-17 producing cells. *Blood*, 112 (6): 2340–52.

Kolls, J. K. & Lindén, A. 2004. Interleukin-17 family members and inflammation. *Immunity*, 21 (4): 467–76.

Komano, Y., Nanki, T., Hayashida, K., Taniguchi, K. & Miyasaka, N. 2006. Identification of a human peripheral blood monocyte subset that differentiates into osteoclasts. *Arthritis Research & Therapy*, 8 (5): R152.

Komatsu, N., Okamoto, K., Sawa, S., Nakashima, T., Oh-Hora, M., Kodama, T., Tanaka, S., Bluestone, J. A. & Takayanagi, H. 2014. Pathogenic conversion of Foxp3+ T cells into TH17 cells in autoimmune arthritis. *Nature Medicine*, 20 (1): 62–68.

Kopf, M., Schneider, C. & Nobs, S. P. 2015. The development and function of lung-resident macrophages and dendritic cells. *Nature Immunology*, 16 (1): 36–44.

Korf-Klingebiel, M., Reboll, M. R., Grote, K., Schleiner, H., Wang, Y., Wu, X., Klede, S., Mikhed, Y., Bauersachs, J., Klintschar, M., Rudat, C., Kispert, A., Niessen, H. W., Lübke, T., Dierks, T. & Wollert, K. C. 2019. Heparan sulfate–editing extracellular sulfatases enhance VEGF bioavailability for ischemic heart repair. *Circulation Research*, 125 (9): 787–801.

Kovacsovics, T. J., Mims, A., Salama, M. E., Pantin, J., Rao, N., Kosak, K. M., Ahorukomeye, P., Glenn, M. J., Deininger, M. W. N., Boucher, K. M., Bavisotto, L. M., Gutierrez-Sanchez, G., Kennedy, T. P., Marcus, S. G. & Shami, P. J. 2018. Combination of the low anticoagulant heparin CX-01 with chemotherapy for the treatment of acute myeloid leukemia. *Blood Advances*, 2 (4): 381–89.

Kreuger, J. & Kjellén, L. 2012. Heparan sulfate biosynthesis. *Journal of Histochemistry & Cytochemistry*, 60 (12): 898–907.

Kurowska-Stolarska, M. & Alivernini, S. 2017. Synovial tissue macrophages: friend or foe? *RMD Open*, 3 (2): e000527.

Lamanna, W. C., Baldwin, R. J., Padva, M., Kalus, I., Dam, G. ten, Kuppevelt, T. H. van, Gallagher, J. T., Figura, K. von, Dierks, T. & Merry, C. L. R. 2006. Heparan sulfate 6-O-endosulfatases: discrete in vivo activities and functional co-operativity. *Biochemical Journal*, 400 (1): 63–73.

Lebre, M. C., Jongbloed, S. L., Tas, S. W., Smeets, T. J. M., McInnes, I. B. & Tak, P. P. 2008. Rheumatoid arthritis synovium contains two subsets of CD83-DC-LAMP- dendritic cells with distinct cytokine profiles. *The American Journal of Pathology*, 172 (4): 940–50.

Lee, G. R. 2018. The balance of Th17 versus Treg cells in autoimmunity. *International Journal of Molecular Sciences*, 19 (3): 730.

Lew, E. D., Oh, J., Burrola, P. G., Lax, I., Zagórska, A., Través, P. G., Schlessinger, J. & Lemke, G. 2014. Differential TAM receptor–ligand–phospholipid interactions delimit differential TAM bioactivities. *ELife*, 3 (September): e03385.

Lillegraven, S., Prince, F. H., Shadick, N. A., Bykerk, V. P., Lu, B., Frits, M. L., Iannaccone, C. K., Kvien, T. K., Haavardsholm, E. A., Weinblatt, M. E. & Solomon, D. H. 2012. Remission and radiographic outcome in rheumatoid arthritis: application of the 2011 ACR/EULAR remission criteria in an observational cohort. *Annals of the Rheumatic Diseases*, 71 (5): 681–86.

Lindahl, U., Kjellen, L. & Kjellén, L. 2013. Pathophysiology of heparan sulphate: Many diseases, few drugs. *Journal of Internal Medicine*, 273 (6): 555–71.

Liu, K., Zhao, E., Ilyas, G., Lalazar, G., Lin, Y., Haseeb, M., Tanaka, K. E. & Czaja, M. J. 2015. Impaired macrophage autophagy increases the immune response in obese mice by promoting proinflammatory macrophage polarization. *Autophagy*,

11 (2): 271–84.

Lloyd, S., Bujkiewicz, S., Wailoo, A. J., Sutton, A. J. & Scott, D. 2010. The effectiveness of anti-TNF-therapies when used sequentially in rheumatoid arthritis patients: a systematic review and meta-analysis. *Rheumatology*, 49 (12): 2313–21.

Lortat-Jacob, H. 2006. Interferon and heparan sulphate. *Biochemical Society Transactions*, 34 (3): 461–64.

Lortat-Jacob, H., Brisson, C., Guerret, S. & Morel, G. 1996. Non-receptor-mediated tissue localization of human interferon-γ: Role of heparan sulfate/heparin-like molecules. *Cytokine*, 8 (7): 557–66.

Lortat-Jacob, H., Garrone, P., Banchereau, J. & Grimaud, J. A. 1997. Human interleukin 4 is a glycosaminoglycan-binding protein. *Cytokine*, 9 (2): 101–5.

Lortat-Jacob, H. & Grimaud, J. A. 1991. Interferon-gamma binds to heparan sulfate by a cluster of amino acids located in the C-terminal part of the molecule. *FEBS Letters*, 280 (1): 152–54.

Loughlin, J. 2015. Genetic contribution to osteoarthritis development: Current state of evidence. *Current Opinion in Rheumatology*, 27 (3): 284–88.

Love, M. I., Huber, W. & Anders, S. 2014. Moderated estimation of fold change and dispersion for RNA-seq data with DESeq2. *Genome Biology*, 15 (12).

Loynes, C. A., Lee, J. A., Robertson, A. L., Steel, M. J. G., Ellett, F., Feng, Y., Levy, B. D., Whyte, M. K. B. & Renshaw, S. A. 2018. PGE2 production at sites of tissue injury promotes an anti-inflammatory neutrophil phenotype and determines the outcome of inflammation resolution in vivo. *Science Advances*, 4 (9): eaar8320.

Lu, G., Zhang, R., Geng, S., Peng, L., Jayaraman, P., Chen, C., Xu, F., Yang, J., Li, Q., Zheng, H., Shen, K., Wang, J., Liu, X., Wang, W., Zheng, Z., Qi, C. F., Si, C.,

He, J. C., Liu, K., et al. 2015. Myeloid cell-derived inducible nitric oxide synthase suppresses M1 macrophage polarization. *Nature Communications*, 6 (March): 6676.

Lubberts, E., Koenders, M. I., Oppers-Walgreen, B., Bersselaar, L. van den, Coenen-de Roo, C. J. J., Joosten, L. A. B. & Berg, W. B. van den. 2004. Treatment with a neutralizing anti-murine interleukin-17 antibody after the onset of collagen-induced arthritis reduces joint inflammation, cartilage destruction, and bone erosion. *Arthritis & Rheumatism*, 50 (2): 650–59.

Lum, D. H., Tan, J., Rosen, S. D. & Werb, Z. 2007. Gene trap disruption of the mouse heparan sulfate 6-O-endosulfatase gene, Sulf2. *Molecular and Cellular Biology*, 27 (2): 678–88.

Lynch, M. D. & Watt, F. M. 2018. Fibroblast heterogeneity: implications for human disease. *Journal of Clinical Investigation*,. American Society for Clinical Investigation.

MacGregor, A. J., Snieder, H., Rigby, A. S., Koskenvuo, M., Kaprio, J., Aho, K. & Silman, A. J. 2000. Characterizing the quantitative genetic contribution to rheumatoid arthritis using data from twins. *Arthritis & Rheumatism*, 43 (1): 30–37.

Macur, K., Grzenkowicz-Wydra, J., Konieczna, L., Bigda, J., Temporini, C., Tengattini, S. & Bączek, T. 2018. A proteomic-based approach to study the mechanism of cytotoxicity induced by interleukin-1α and cycloheximide. *Chromatographia*, 88 (1): 47–56.

Manfioletti, G., Brancolini, C., Avanzi, G. & Schneider, C. 1993. The protein encoded by a growth arrest-specific gene (gas6) is a new member of the vitamin K-dependent proteins related to protein S, a negative coregulator in the blood coagulation cascade. *Molecular and Cellular Biology*, 13 (8): 4976–85.

Manoury-Schwartz, B., Chiocchia, G., Bessis, N., Abehsira-Amar, O., Batteux, F., Muller, S., Huang, S., Boissier, M. C. & Fournier, C. 1997. High susceptibility to collagen-induced arthritis in mice lacking IFN-gamma receptors. *The Journal of Immunology*, 158 (11): 5501–6.

Martinez, F. O. & Gordon, S. 2014. The M1 and M2 paradigm of macrophage activation: time for reassessment. *F1000prime Reports*, 6: 13.

Martinez, F. O., Gordon, S., Locati, M. & Mantovani, A. 2006. Transcriptional profiling of the human monocyte-to-macrophage differentiation and polarization: new molecules and patterns of gene expression. *The Journal of Immunology*, 177 (10): 7303–11.

Martinez, P., Denys, A., Delos, M., Sikora, A. S., Carpentier, M., Julien, S., Pestel, J. & Allain, F. 2015. Macrophage polarization alters the expression and sulfation pattern of glycosaminoglycans. *Glycobiology*, 25 (5): 502–13.

Masouleh, B. K., Dam, G. B. Ten, Wild, M. K., Seelige, R., Vlag, J. van der, Rops, A. L., Echtermeyer, F. G., Vestweber, D., Kuppevelt, T. H. van, Kiesel, L. & Götte, M. 2009. Role of the heparan sulfate proteoglycan syndecan-1 (CD138) in delayed-type hypersensitivity. *The Journal of Immunology*, 182 (8): 4985–93.

Masri, R. El, Seffouh, A., Lortat-Jacob, H. & Vivès, R. R. 2017. The “in and out” of glucosamine 6-O-sulfation: the 6th sense of heparan sulfate. *Glycoconjugate Journal*, 34 (3): 285–98.

Masterson, J. C., McNamee, E. N., Fillon, S. A., Hosford, L., Harris, R., Fernando, S. D., Jedlicka, P., Iwamoto, R., Jacobsen, E., Protheroe, C., Eltzschig, H. K., Colgan, S. P., Arita, M., Lee, J. J. & Furuta, G. T. 2015. Eosinophil-mediated signalling attenuates inflammatory responses in experimental colitis. *Gut*, 64 (8): 1236–47.

McCubbrey, A. L., Allison, K. C., Lee-Sherick, A. B., Jakubzick, C. V. & Janssen, W. J. 2017. Promoter specificity and efficacy in conditional and inducible transgenic targeting of lung macrophages. *Frontiers in Immunology*, 8 (NOV).

McNamee, K. E., Alzabin, S., Hughes, J. P., Anand, P., Feldmann, M., Williams, R. O. & Inglis, J. J. 2011. IL-17 induces hyperalgesia via TNF-dependent neutrophil infiltration. *Pain*, 152 (8): 1838–45.

Mehraj, V., Textoris, J., Amara, A. Ben, Ghigo, E., Raoult, D., Capo, C. & Mege, J.-L. 2013. Monocyte responses in the context of Q fever: From a static polarized model to a kinetic model of activation. *The Journal of Infectious Diseases*, 208 (6): 942–51.

Miller, J. D., Clabaugh, S. E., Smith, D. R., Stevens, R. B. & Wrenshall, L. E. 2012. Interleukin-2 is present in human blood vessels and released in biologically active form by heparanase. *Immunology and Cell Biology*, 90 (2): 159–67.

Miltenburg, A. M. M., Laar, J. M. van, Kuiper, R. de, Daha, M. R. & Breeveld, F. C. 1992. T cells cloned from human rheumatoid synovial membrane functionally represent the Th 1 subset. *Scandinavian Journal of Immunology*, 35 (5): 603–10.

Milz, F., Harder, A., Neuhaus, P., Breitkreuz-Korff, O., Walhorn, V., Lübke, T., Anselmetti, D. & Dierks, T. 2013. Cooperation of binding sites at the hydrophilic domain of cell-surface sulfatase Sulf1 allows for dynamic interaction of the enzyme with its substrate heparan sulfate. *Biochimica et Biophysica Acta (BBA) - General Subjects*, 1830 (11): 5287–98.

Misharin, A. V., Cuda, C. M., Saber, R., Turner, J. D., Gierut, A. K., Haines, G. K., Berdnikovs, S., Filer, A., Clark, A. R., Buckley, C. D., Mutlu, G. M., Budinger, G. R. S. & Perlman, H. 2014. Nonclassical Ly6C− monocytes drive the development of inflammatory arthritis in mice. *Cell Reports*, 9 (2): 591–604.

Mizoguchi, F., Slowikowski, K., Wei, K., Marshall, J. L., Rao, D. A., Chang, S. K., Nguyen, H. N., Noss, E. H., Turner, J. D., Earp, B. E., Blazar, P. E., Wright, J., Simmons, B. P., Donlin, L. T., Kalliolias, G. D., Goodman, S. M., Bykerk, V. P., Ivashkiv, L. B., Lederer, J. A., et al. 2018. Functionally distinct disease-associated fibroblast subsets in rheumatoid arthritis. *Nature Communications*, 9 (1): 1–11.

Monaco, C., Nanchahal, J., Taylor, P. & Feldmann, M. 2015. Anti-TNF therapy: past, present and future. *International Immunology*, 27 (1): 55.

Monaco, G., Lee, B., Xu, W., Mustafah, S., Hwang, Y. Y., Carré, C., Burdin, N., Visan, L., Ceccarelli, M., Poidinger, M., Zippelius, A., Pedro de Magalhães, J. & Larbi, A. 2019. RNA-Seq signatures normalized by mRNA abundance allow absolute deconvolution of human immune cell types. *Cell Reports*, 26 (6): 1627-1640.e7.

Moret, F. M., Hack, C. E., Wurff-Jacobs, K. M. van der, Jager, W. de, Radstake, T. R., Lafeber, F. P. & Roon, J. A. van. 2013. Intra-articular CD1c-expressing myeloid dendritic cells from rheumatoid arthritis patients express a unique set of T cell-attracting chemokines and spontaneously induce Th1, Th17 and Th2 cell activity. *Arthritis Research & Therapy*, 15 (5): R155.

Morgan, M. E., Flierman, R., Duivenvoorde, L. M. van, Witteveen, H. J., Ewijk, W. van, Laar, J. M. van, vries, R. R. P. de & Toes, R. E. M. 2005. Effective treatment of collagen-induced arthritis by adoptive transfer of CD25+ regulatory T cells. *Arthritis & Rheumatism*, 52 (7): 2212–21.

Morgan, M. E., Sutmuller, R. P. M., Witteveen, H. J., Duivenvoorde, L. M. van, Zanelli, E., Melief, C. J. M., Snijders, A., Offringa, R., Vries, R. R. P. de & Toes, R. E. M. 2003. CD25+ cell depletion hastens the onset of severe disease in collagen-induced arthritis. *Arthritis & Rheumatism*, 48 (5): 1452–60.

Morimoto-Tomita, M., Uchimura, K., Werb, Z., Hemmerich, S. & Rosen, S. D. 2002.

Cloning and characterization of two extracellular heparin-degrading endosulfatases in mice and humans. *Journal of Biological Chemistry*, 277 (51): 49175–85.

Mosser, D. M. & Edwards, J. P. 2008. Exploring the full spectrum of macrophage activation. *Nature Reviews Immunology*, 8 (12): 958–69.

Mulherin, D., Fitzgerald, O. & Bresnihan, B. 1996. Synovial tissue macrophage populations and articular damage in rheumatoid arthritis. *Arthritis & Rheumatism*, 39 (1): 115–24.

Munder, M. 2009. Arginase: An emerging key player in the mammalian immune system. *British Journal of Pharmacology*, 158 (3): 638–51.

Murphy, C. A., Langrish, C. L., Chen, Y., Blumenschein, W., McClanahan, T., Kastelein, R. A., Sedgwick, J. D. & Cua, D. J. 2003. Divergent pro- and antiinflammatory roles for IL-23 and IL-12 in joint autoimmune inflammation. *The Journal of Experimental Medicine*, 198 (12): 1951–57.

Murray, P. J., Allen, J. E., Biswas, S. K., Fisher, E. A., Gilroy, D. W., Goerdt, S., Gordon, S., Hamilton, J. A., Ivashkiv, L. B., Lawrence, T., Locati, M., Mantovani, A., Martinez, F. O., Mege, J.-L., Mosser, D. M., Natoli, G., Saeij, J. P., Schultze, J. L., Shirey, K. A., et al. 2014. Macrophage activation and polarization: nomenclature and experimental guidelines. *Immunity*, 41 (1): 14–20.

Nagamine, S., Keino-Masu, K., Shiomi, K. & Masu, M. 2010. Proteolytic cleavage of the rat heparan sulfate 6-O-endosulfatase SulfFP2 by furin-type proprotein convertases. *Biochemical and Biophysical Research Communications*, 391 (1): 107–12.

Nakae, S., Nambu, A., Sudo, K. & Iwakura, Y. 2003. Suppression of Immune Induction of Collagen-Induced Arthritis in IL-17-Deficient Mice. *The Journal of Immunology*,

171 (11): 6173–77.

Nam, J. L., Villeneuve, E., Hensor, E. M. A., Conaghan, P. G., Keen, H. I., Buch, M. H., Gough, A. K., Green, M. J., Helliwell, P. S., Keenan, A. M., Morgan, A. W., Quinn, M., Reece, R., Heijde, D. M. Van Der, Wakefield, R. J. & Emery, P. 2014. Remission induction comparing infliximab and high-dose intravenous steroid, followed by treat-to-target: A double-blind, randomised, controlled trial in new-onset, treatment-naive, rheumatoid arthritis (the IDEA study). *Annals of the Rheumatic Diseases*,.

Narendra, S. C., Chalise, J. P., Biggs, S., Kalinke, U. & Magnusson, M. 2018. Regulatory T-cells mediate IFN-α-induced resistance against antigen-induced arthritis. *Frontiers in Immunology*, 9 (February): 285.

National Adit Office. 2009. Services for people with rheumatoid arthritis. Report by the comptroller and auditor general, HC 823 session 2008–2009.

Nawroth, R., Zante, A. van, Cervantes, S., McManus, M., Hebrok, M. & Rosen, S. D. 2007. Extracellular sulfatases, elements of the Wnt signaling pathway, positively regulate growth and tumorigenicity of human pancreatic cancer cell. *PLoS ONE*, 2 (4): e392.

Nerurkar, L., Siebert, S., McInnes, I. B. & Cavanagh, J. 2019. Rheumatoid arthritis and depression: an inflammatory perspective. *The Lancet. Psychiatry*, 6 (2): 164–73.

Nissler, K., Pohlers, D., Hückel, M., Simon, J., Bräuer, R. & Kinne, R. W. 2004. Anti-CD4 monoclonal antibody treatment in acute and early chronic antigen induced arthritis: Influence on macrophage activation. *Annals of the Rheumatic Diseases*, 63 (11): 1470–77.

Notley, C. A., Brown, M. A., McGovern, J. L., Jordan, C. K. & Ehrenstein, M. R. 2015. Engulfment of Activated Apoptotic Cells Abolishes TGF-β–Mediated

Immunoregulation via the Induction of IL-6. *The Journal of Immunology*, 194 (4): 1621–27.

Ogura, H., Murakami, M., Okuyama, Y., Tsuruoka, M., Kitabayashi, C., Kanamoto, M., Nishihara, M., Iwakura, Y. & Hirano, T. 2008. Interleukin-17 promotes autoimmunity by triggering a positive-feedback loop via interleukin-6 induction. *Immunity*, 29 (4): 628–36.

Ori, A., Wilkinson, M. C. & Fernig, D. G. 2011. A systems biology approach for the investigation of the heparin/heparan sulfate interactome. *Journal of Biological Chemistry*, 286 (22): 19892–904.

Ornitz, D. M. & Itoh, N. 2015. The fibroblast growth factor signaling pathway. *Wiley Interdisciplinary Reviews: Developmental Biology*, 4 (3): 215–66.

Oshima, K., Han, X., Ouyang, Y., Masri, R. El, Yang, Y., Haeger, S. M., McMurtry, S. A., Lane, T. C., Davizon-Castillo, P., Zhang, F., Yue, X., Vivès, R. R., Linhardt, R. J. & Schmidt, E. P. 2019. Loss of endothelial sulfatase-1 after experimental sepsis attenuates subsequent pulmonary inflammatory responses. *American Journal of Physiology. Lung Cellular and Molecular Physiology*, 317 (5): L667–77.

Otsuki, S., Hanson, S. R., Miyaki, S., Grogan, S. P., Kinoshita, M., Asahara, H., Wong, C.-H. & Lotz, M. K. 2010. Extracellular sulfatases support cartilage homeostasis by regulating BMP and FGF signaling pathways. *Proceedings of the National Academy of Sciences of the United States of America*, 107 (22): 10202–7.

Otsuki, S., Murakami, T., Okamoto, Y., Hoshiyama, Y., Oda, S. & Neo, M. 2017. Suppression of cartilage degeneration by intra-articular injection of heparan sulfate 6-O endosulfatase in a mouse osteoarthritis model. *Histology and Histopathology*, 32 (7): 725–33.

Otsuki, S., Taniguchi, N., Grogan, S. P., D'Lima, D., Kinoshita, M. & Lotz, M. 2008.

Expression of novel extracellular sulfatases Sulf-1 and Sulf-2 in normal and osteoarthritic articular cartilage. *Arthritis Research & Therapy*, 10 (3): R61.

Pap, T., Müller-Ladner, U., Gay, R. E. & Gay, S. 2000. Fibroblast biology. Role of synovial fibroblasts in the pathogenesis of rheumatoid arthritis. *Arthritis Research*,. BioMed Central.

Parish, C. R. 2006. The role of heparan sulphate in inflammation. *Nature Reviews Immunology*, 6 (9): 633–43.

Park, B. S. & Lee, J.-O. 2013. Recognition of lipopolysaccharide pattern by TLR4 complexes. *Experimental & Molecular Medicine*, 45 (12): e66–e66.

Parsonage, G., Filer, A., Bik, M., Hardie, D., Lax, S., Howlett, K., Church, L. D., Raza, K., Wong, S.-H., Trebilcock, E., Scheel-Toellner, D., Salmon, M., Lord, J. M. & Buckley, C. D. 2008. Prolonged, granulocyte-macrophage colony-stimulating factor-dependent, neutrophil survival following rheumatoid synovial fibroblast activation by IL-17 and TNFalpha. *Arthritis Research & Therapy*, 10 (2): R47.

Patel, A. A., Zhang, Y., Fullerton, J. N., Boelen, L., Rongvaux, A., Maini, A. A., Bigley, V., Flavell, R. A., Gilroy, D. W., Asquith, B., Macallan, D. & Yona, S. 2017. The fate and lifespan of human monocyte subsets in steady state and systemic inflammation. *The Journal of Experimental Medicine*, 214 (7): 1913–23.

Pempe, E. H., Burch, T. C., Law, C. J. & Liu, J. 2012. Substrate specificity of 6-O-endosulfatase (Sulf-2) and its implications in synthesizing anticoagulant heparan sulfate. *Glycobiology*, 22 (10): 1353–62.

Petrow, P. K., Thoss, K., Katenkamp, D. & Bräuer, R. 1996. Adoptive transfer of susceptibility to antigen-induced arthritis into severe combined immunodeficient (SCID) mice: Role of CD4+ and CD8+ T cells. *Immunological Investigations*, 25 (4): 341–53.

Piccinini, A. M., Williams, L., McCann, F. E. & Midwood, K. S. 2016. Investigating the role of toll-like receptors in models of arthritis. In *Toll-like Receptors. Methods in Molecular Biology*, McCoy C., 1390:351–81. New York, NY: Humana Press.

Pohlers, D., Nissler, K., Frey, O., Simon, J., Petrow, P. K., Kinne, R. W. & Bräuer, R. 2004. Anti-CD4 monoclonal antibody treatment in acute and early chronic antigen-induced arthritis: Influence on T helper cell activation. *Clinical and Experimental Immunology*, 135 (3): 409–15.

Pratesi, F., Dioni, I., Tommasi, C., Alcaro, M. C., Paolini, I., Barbetti, F., Boscaro, F., Panza, F., Puxeddu, I., Rovero, P. & Migliorini, P. 2014. Antibodies from patients with rheumatoid arthritis target citrullinated histone 4 contained in neutrophils extracellular traps. *Annals of the Rheumatic Diseases*, 73 (7): 1414–22.

Ratzka, A., Kalus, I., Moser, M., Dierks, T., Mundlos, S. & Vortkamp, A. 2008. Redundant function of the heparan sulfate 6-O-endosulfatases Sulf1 and Sulf2 during skeletal development. *Developmental Dynamics*, 237 (2): 339–53.

Raza, K., Scheel-Toellner, D., Lee, C.-Y., Pilling, D., Curnow, S. J., Falciani, F., Trevino, V., Kumar, K., Assi, L. K., Lord, J. M., Gordon, C., Buckley, C. D. & Salmon, M. 2006. Synovial fluid leukocyte apoptosis is inhibited in patients with very early rheumatoid arthritis. *Arthritis Research & Therapy*, 8 (4): R120.

Reijmers, R. M., Groen, R. W. J., Kuil, A., Weijer, K., Kimberley, F. C., Medema, J. P., Kuppevelt, T. H. van, Li, J.-P., Spaargaren, M. & Pals, S. T. 2011. Disruption of heparan sulfate proteoglycan conformation perturbs B-cell maturation and APRIL-mediated plasma cell survival. *Blood*, 117 (23): 6162–71.

Reynolds-Peterson, C. E., Zhao, N., Xu, J., Serman, T. M., Xu, J. & Selleck, S. B. 2017. Heparan sulfate proteoglycans regulate autophagy in *Drosophila*. *Autophagy*, 13 (8): 1262–79.

Richter, F., Natura, G., Ebbinghaus, M., Banchet, G. S. Von, Hensellek, S., König, C., Bräuer, R. & Schaible, H. G. 2012. Interleukin-17 sensitizes joint nociceptors to mechanical stimuli and contributes to arthritic pain through neuronal interleukin-17 receptors in rodents. *Arthritis and Rheumatism*, 64 (12): 4125–34.

Roberts, A. W., Lee, B. L., Deguine, J., John, S., Shlomchik, M. J. & Barton, G. M. 2017. Tissue-resident macrophages are locally programmed for silent clearance of apoptotic cells. *Immunity*, 47 (5): 913-927.e6.

Rops, A., Loeven, M. A., Gemst, J. J. van, Eversen, I., Wijk, X. M. Van, Dijkman, H. B., Kuppevelt, T. H. van, Berden, J. H. M., Rabelink, T. J., Esko, J. D. & Vlag, J. van der. 2014. Modulation of heparan sulfate in the glomerular endothelial glycocalyx decreases leukocyte influx during experimental glomerulonephritis. *Kidney International*, 86 (5): 932–42.

Rosales, C. 2018. Neutrophil: A cell with many roles in inflammation or several cell types? *Frontiers in Physiology*, 9: 113.

Rosen, S. D. & Lemjabbar-Alaoui, H. 2010. Sulf-2: An extracellular modulator of cell signaling and a cancer target candidate. *Expert Opinion on Therapeutic Targets*, 14 (9): 935–49.

Roth, G. A., Abate, D., Abate, K. H., Abay, S. M., Abbafati, C., Abbasi, N., Abbastabar, H., Abd-Allah, F., Abdela, J., Abdelalim, A., Abdollahpour, I., Abdulkader, R. S., Abebe, H. T., Abebe, M., Abebe, Z., Abejie, A. N., Abera, S. F., Abil, O. Z., Abraha, H. N., et al. 2018. Global, regional, and national age-sex-specific mortality for 282 causes of death in 195 countries and territories, 1980–2017: a systematic analysis for the Global Burden of Disease Study 2017. *The Lancet*, 392 (10159): 1736–88.

Roth, S., Agthe, M., Eickhoff, S., Möller, S., Karsten, C. M., Borregaard, N., Solbach,

W. & Laskay, T. 2015. Secondary necrotic neutrophils release interleukin-16C and macrophage migration inhibitory factor from stores in the cytosol. *Cell Death Discovery*, 1 (1): 15056.

Rothlin, C. V., Ghosh, S., Zuniga, E. I., Oldstone, M. B. A. & Lemke, G. 2007. TAM Receptors Are Pleiotropic Inhibitors of the Innate Immune Response. *Cell*, 131 (6): 1124–36.

Sadir, R., Forest, E. & Lortat-Jacob, H. 1998. The heparan sulfate binding sequence of interferon-gamma increased the on rate of the interferon-gamma-interferon-gamma receptor complex formation. *Journal of Biological Chemistry*, 273 (18): 10919–25.

Sakaguchi, N., Takahashi, T., Hata, H., Nomura, T., Tagami, T., Yamazaki, S., Sakihama, T., Matsutani, T., Negishi, I., Nakatsuru, S. & Sakaguchi, S. 2003. Altered thymic T-cell selection due to a mutation of the ZAP-70 gene causes autoimmune arthritis in mice. *Nature*, 426 (6965): 454–60.

Sandoval, D. R., Toledo, A. G., Painter, C. D., Tota, E. M., Sheikh, M. O., West, A. M. V., Frank, M. M., Wells, L., Xu, D., Bicknell, R., Corbett, K. D. & Esko, J. D. 2020. Proteomics-based screening of the endothelial heparan sulfate interactome reveals that C-type lectin 14a (CLEC14A) is a heparin-binding protein. *Journal of Biological Chemistry*, 295 (9): 2804–21.

Sarrazin, S., Lamanna, W. C. & Esko, J. D. 2011. Heparan sulfate proteoglycans. *Cold Spring Harbor Perspectives in Biology*, 3 (7): 1–33.

Sato, K., Suematsu, A., Okamoto, K., Yamaguchi, A., Morishita, Y., Kadono, Y., Tanaka, S., Kodama, T., Akira, S., Iwakura, Y., Cua, D. J. & Takayanagi, H. 2006. Th17 functions as an osteoclastogenic helper T cell subset that links T cell activation and bone destruction. *The Journal of Experimental Medicine*, 203 (12):

2673–82.

Satpathy, A. T., Wu, X., Albring, J. C. & Murphy, K. M. 2012. Re(de)fining the dendritic cell lineage. *Nature Immunology*, 13 (12): 1145–54.

Schairer, D. O., Chouake, J. S., Nosanchuk, J. D. & Friedman, A. J. 2012. The potential of nitric oxide releasing therapies as antimicrobial agents. *Virulence*, 3 (3): 271–79.

Schaller, E., Macfarlane, A. J., Rupec, R. A., Gordon, S., McKnight, A. J. & Pfeffer, K. 2002. Inactivation of the F4/80 glycoprotein in the mouse germ line. *Molecular and Cellular Biology*, 22 (22): 8035–43.

Schett, G., Elewaut, D., McInnes, I. B., Dayer, J. M. & Neurath, M. F. 2013. Toward a cytokine-based disease taxonomy. *Nature Medicine*, 19 (7): 822–24.

Schett, G. & Gravallese, E. 2012. Bone erosion in rheumatoid arthritis: mechanisms, diagnosis and treatment. *Nature Reviews Rheumatology*, 8 (11): 656–64.

Schett, G. & Neurath, M. F. 2018. Resolution of chronic inflammatory disease: universal and tissue-specific concepts. *Nature Communications*, 9 (1): 3261.

Schmidt, A., Zhang, X. M., Joshi, R. N., Iqbal, S., Wahlund, C., Gabrielsson, S., Harris, R. A. & Tegnér, J. 2016. Human macrophages induce CD4+ Foxp3+ regulatory T cells via binding and re-release of TGF-β. *Immunology and Cell Biology*, 94 (8): 747–62.

Schneider, C., Nobs, S. P., Kurrer, M., Rehrauer, H., Thiele, C. & Kopf, M. 2014. Induction of the nuclear receptor PPAR-γ 3 by the cytokine GM-CSF is critical for the differentiation of fetal monocytes into alveolar macrophages. *Nature Immunology*, 15 (11): 1026–37.

Schuksz, M., Fuster, M. M., Brown, J. R., Crawford, B. E., Ditto, D. P., Lawrence, R., Glass, C. A., Wang, L., Tor, Y. & Esko, J. D. 2008. Surfen, a small molecule

antagonist of heparan sulfate. *Proceedings of the National Academy of Sciences of the United States of America*, 105 (35): 13075–80.

Schurgers, E., Billiau, A. & Matthys, P. 2011. Collagen-induced arthritis as an animal model for rheumatoid arthritis: Focus on interferon-γ. *Journal of Interferon & Cytokine Research*, 31 (12): 917–26.

Scott, C. L., T'Jonck, W., Martens, L., Todorov, H., Sichien, D., Soen, B., Bonnardel, J., Prijck, S. De, Vandamme, N., Cannoodt, R., Saelens, W., Vanneste, B., Toussaint, W., Bleser, P. De, Takahashi, N., Vandenabeele, P., Henri, S., Pridans, C., Hume, D. A., et al. 2018. The transcription factor ZEB2 is required to maintain the tissue-specific identities of macrophages. *Immunity*, 49 (2): 312-325.e5.

Scott, D. L., Wolfe, F. & Huizinga, T. W. 2010. Rheumatoid arthritis. *The Lancet*, 376 (9746): 1094–1108.

Seffouh, A., Masri, R. El, Makshakova, O., Gout, E., Hassoun, Z. E. O., Andrieu, J.-P., Lortat-Jacob, H. & Vivès, R. R. 2019. Expression and purification of recombinant extracellular sulfatase HSulf-2 allows deciphering of enzyme sub-domain coordinated role for the binding and 6-O-desulfation of heparan sulfate. *Cellular and Molecular Life Sciences*, 76 (1): 1807–19.

Seffouh, A., Milz, F., Przybylski, C., Laguri, C., Oosterhof, A., Bourcier, S., Sadir, R., Dutkowski, E., Daniel, R., Kuppevelt, T. H. van, Dierks, T., Lortat-Jacob, H. & Vivès, R. R. 2013. HSulf sulfatases catalyze processive and oriented 6-O-desulfation of heparan sulfate that differentially regulates fibroblast growth factor activity. *The FASEB Journal*, 27 (6): 2431–39.

Seffouh, I., Przybylski, C., Seffouh, A., Masri, R. El, Vivès, R. R., Gonnet, F. & Daniel, R. 2019. Mass spectrometry analysis of the human endosulfatase Hsulf-2.

Biochemistry and Biophysics Reports, 18: 100617.

Seitz, H. M., Camenisch, T. D., Lemke, G., Earp, H. S. & Matsushima, G. K. 2007. Macrophages and dendritic cells use different Axl/Mertk/Tyro3 receptors in clearance of apoptotic cells. *The Journal of Immunology*, 178 (9): 5635–42.

Shi, J., Hua, L., Harmer, D., Li, P. & Ren, G. 2018. Cre driver mice targeting macrophages. In *Methods in Molecular Biology*, 1784:263–75. Humana Press Inc.

Simon Davis, D. A. & Parish, C. R. 2013. Heparan sulfate: a ubiquitous glycosaminoglycan with multiple roles in immunity. *Frontiers in Immunology*, 4: 470.

Singh, J. A., Arayssi, T., Duray, P. & Schumacher, H. R. 2004. Immunohistochemistry of normal human knee synovium: a quantitative study. *Annals of the Rheumatic Diseases*, 63 (7): 785–90.

Smiljanovic, B., Radzikowska, A., Kuca-Warnawin, E., Kurowska, W., Grün, J. R., Stuhlmüller, B., Bonin, M., Schulte-Wrede, U., Sörensen, T., Kyogoku, C., Bruns, A., Hermann, S., Ohrndorf, S., Aupperle, K., Backhaus, M., Burmester, G. R., Radbruch, A., Grützkau, A., Maslinski, W., et al. 2018. Monocyte alterations in rheumatoid arthritis are dominated by preterm release from bone marrow and prominent triggering in the joint. *Annals of the Rheumatic Diseases*, 77 (2): 300–308.

Smolen, J. S., Aletaha, D., Barton, A., Burmester, G. R., Emery, P., Firestein, G. S., Kavanaugh, A., McInnes, I. B., Solomon, D. H., Strand, V. & Yamamoto, K. 2018. Rheumatoid arthritis. *Nature Reviews Disease Primers*, 4: 18001.

Stanford, K. I., Wang, L., Castagnola, J., Song, D., Bishop, J. R., Brown, J. R., Lawrence, R., Bai, X., Habuchi, H., Tanaka, M., Cardoso, W. V., Kimata, K. &

Esko, J. D. 2010. Heparan sulfate 2-O-sulfotransferase is required for triglyceride-rich lipoprotein clearance. *Journal of Biological Chemistry*, 285 (1): 286–94.

Staples, G. O., Shi, X. & Zaia, J. 2011. Glycomics analysis of mammalian heparan sulfates modified by the human extracellular sulfatase HSulf2. *PLoS ONE*, 6 (2): e16689.

Stuart, T., Butler, A., Hoffman, P., Hafemeister, C., Papalexi, E., Mauck, W. M., Hao, Y., Stoeckius, M., Smibert, P. & Satija, R. 2019. Comprehensive integration of single-cell data. *Cell*, 177 (7): 1888-1902.e21.

Sugahara, K. & Kitagawa, H. 2002. Heparin and heparan sulfate biosynthesis. *IUBMB Life*, 54 (4): 163–75.

Sun, W., Wei, F. Q., Li, W. J., Wei, J. W., Zhong, H., Wen, Y. H., Lei, W. Bin, Chen, L., Li, H., Lin, H. Q., Iqbal, M. & Wen, W. P. 2017. A positive-feedback loop between tumour infiltrating activated Treg cells and type 2-skewed macrophages is essential for progression of laryngeal squamous cell carcinoma. *British Journal of Cancer*, 117 (11): 1631–43.

Suzuki, M., Konya, C., Goronzy, J. J. & Weyand, C. M. 2008. Inhibitory CD8+ T cells in autoimmune disease. *Human Immunology*, 69 (11): 781–89.

Svensson, L., Jirholt, J., Holmdahl, R. & Jansson, L. 1998. B cell-deficient mice do not develop type II collagen-induced arthritis (CIA). *Clinical and Experimental Immunology*, 111 (3): 521–26.

Swanson, K. V., Deng, M. & Ting, J. P.-Y. 2019. The NLRP3 inflammasome: molecular activation and regulation to therapeutics. *Nature Reviews Immunology*, 19 (8): 477–89.

Swart, M. & Troeberg, L. 2019. Effect of polarization and chronic inflammation on macrophage expression of heparan sulfate proteoglycans and biosynthesis

enzymes. *Journal of Histochemistry & Cytochemistry*, 67 (1): 9–27.

Talsma, D. T., Katta, K., Ettema, M. A. B., Kel, B., Kusche-Gullberg, M., Daha, M. R., Stegeman, C. A., Born, J. van den & Wang, L. 2018. Endothelial heparan sulfate deficiency reduces inflammation and fibrosis in murine diabetic nephropathy. *Laboratory Investigation*, 98 (4): 427–38.

Tang, R. & Rosen, S. D. 2009. Functional consequences of the subdomain organization of the Sulfs. *Journal of Biological Chemistry*, 284 (32): 21505–14.

Tessema, M., Yingling, C. M., Thomas, C. L., Klinge, D. M., Bernauer, A. M., Liu, Y., Dacic, S., Siegfried, J. M., Dahlberg, S. E., Schiller, J. H. & Belinsky, S. A. 2012. SULF2 methylation is prognostic for lung cancer survival and increases sensitivity to topoisomerase-I inhibitors via induction of ISG15. *Oncogene*, 31 (37): 4107–16.

Torchinsky, M. B., Garaude, J., Martin, A. P. & Blander, J. M. 2009. Innate immune recognition of infected apoptotic cells directs TH17 cell differentiation. *Nature*, 458 (7234): 78–82.

Tu, J., Hong, W., Guo, Y., Zhang, P., Fang, Y., Wang, X., Chen, X., Lu, S. & Wei, W. 2019. Ontogeny of synovial macrophages and the roles of synovial macrophages from different origins in arthritis. *Frontiers in Immunology*, 10: 1146.

Uchimura, K., Morimoto-Tomita, M., Bistrup, A., Li, J., Lyon, M., Gallagher, J., Werb, Z. & Rosen, S. 2006. HSulf-2, an extracellular endoglucosamine-6-sulfatase, selectively mobilizes heparin-bound growth factors and chemokines: effects on VEGF, FGF-1, and SDF-1. *BMC Biochemistry*, 7 (1): 2.

Udalova, I. A., Mantovani, A. & Feldmann, M. 2016. Macrophage heterogeneity in the context of rheumatoid arthritis. *Nature Reviews Rheumatology*, 12 (8): 472–85.

Valencia, X., Stephens, G., Goldbach-Mansky, R., Wilson, M., Shevach, E. M. &

Lipsky, P. E. 2006. TNF downmodulates the function of human CD4+CD25hi T-regulatory cells. *Blood*, 108 (1): 253–61.

Vermeire, K., Heremans, H., Vandeputte, M., Huang, S., Billiau, A. & Matthys, P. 1997. Accelerated collagen-induced arthritis in IFN-gamma receptor-deficient mice. *The Journal of Immunology*, 158 (11): 5507–13.

Vivès, R. R., Seffouh, A. & Lortat-Jacob, H. 2014. Post-synthetic regulation of HS structure: The yin and yang of the sulfs in cancer. *Frontiers in Oncology*, 3: 331.

Walsh, D. A. & McWilliams, D. F. 2014. Mechanisms, impact and management of pain in rheumatoid arthritis. *Nature Reviews Rheumatology*, 10 (10): 581–92.

Wan, M. X., Zhang, X. W., Törkvist, L. & Thorlacius, H. 2001. Low molecular weight heparin inhibits tumor necrosis factor α-induced leukocyte rolling. *Inflammation Research*, 50 (12): 581–84.

Wang, L., Fuster, M., Sriramarao, P. & Esko, J. D. 2005. Endothelial heparan sulfate deficiency impairs L-selectin- and chemokine-mediated neutrophil trafficking during inflammatory responses. *Nature Immunology*, 6 (9): 902–10.

Waterborg, C. E. J., Beermann, S., Broeren, M. G. A., Bennink, M. B., Koenders, M. I., Lent, P. L. E. M. van, Berg, W. B. van den, Kraan, P. M. van der & Loo, F. A. J. van de. 2018. Protective Role of the MER Tyrosine Kinase via Efferocytosis in Rheumatoid Arthritis Models. *Frontiers in Immunology*, 9 (April): 742.

Weiss, M., Byrne, A. J., Blazek, K., Saliba, D. G., Pease, J. E., Perocheau, D., Feldmann, M. & Udalova, I. A. 2015. IRF5 controls both acute and chronic inflammation. *Proceedings of the National Academy of Sciences of the United States of America*, 112 (35): 11001–6.

Westhovens, R., Robles, M., Ximenes, A. C., Nayiager, S., Wollenhaupt, J., Durez, P., Gomez-Reino, J., Grassi, W., Haraoui, B., Shergy, W., Park, S.-H., Genant,

H., Peterfy, C., Becker, J.-C., Covucci, A., Helfrick, R. & Bathon, J. 2009. Clinical efficacy and safety of abatacept in methotrexate-naive patients with early rheumatoid arthritis and poor prognostic factors. *Annals of the Rheumatic Diseases*, 68 (12): 1870–77.

Williams, R. O. 2007. Collagen-induced arthritis in mice. *Methods in Molecular Medicine*, 136: 191–99.

Wong, P. K. K., Quinn, J. M. W., Sims, N. A., Nieuwenhuijze, A. Van, Campbell, I. K. & Wicks, I. P. 2006. Interleukin-6 modulates production of T lymphocyte-derived cytokines in antigen-induced arthritis and drives inflammation-induced osteoclastogenesis. *Arthritis and Rheumatism*, 54 (1): 158–68.

Woolf, C. J., Allchorne, A., Safieh-Garabedian, B. & Poole, S. 1997. Cytokines, nerve growth factor and inflammatory hyperalgesia: The contribution of tumour necrosis factor α. *British Journal of Pharmacology*, 121 (3): 417–24.

Wright, H. L., Moots, R. J. & Edwards, S. W. 2014. The multifactorial role of neutrophils in rheumatoid arthritis. *Nature Reviews Rheumatology*, 10 (10): 593–601.

Wu, G., Ma, Z., Hu, W., Wang, D., Gong, B., Fan, C., Jiang, S., Li, T., Gao, J. & Yang, Y. 2017. Molecular insights of Gas6/TAM in cancer development and therapy. *Cell Death and Disease*, 8 (3): e2700.

Wynn, T. A., Chawla, A. & Pollard, J. W. 2013. Macrophage biology in development, homeostasis and disease. *Nature*, 496 (7446): 445–55.

Xiong, H., Zhu, C., Li, F., Hegazi, R., He, K., Babyatsky, M., Bauer, A. J. & Plevy, S. E. 2004. Inhibition of interleukin-12 p40 transcription and NF-κB activation by nitric oxide in murine macrophages and dendritic Cells. *Journal of Biological Chemistry*, 279 (11): 10776–83.

Xu, D., Olson, J., Cole, J. N., Wijk, X. M. van, Brinkmann, V., Zychlinsky, A., Nizet, V.,

Esko, J. D. & Chang, Y.-C. 2015. Heparan sulfate modulates neutrophil and endothelial function in antibacterial innate immunity. *Infection and Immunity*, 83 (9): 3648–56.

Xu, J., Park, P. W., Kheradmand, F. & Corry, D. B. 2005. Endogenous attenuation of allergic lung inflammation by syndecan-1. *The Journal of Immunology*, 174 (9): 5758–65.

Xue, Q., Yan, Y., Zhang, R. & Xiong, H. 2018. Regulation of iNOS on immune cells and its role in diseases. *International Journal of Molecular Sciences*, 19 (12): 3805.

Yamada, T., Kerever, A., Yoshimura, Y., Suzuki, Y., Nonaka, R., Higashi, K., Toida, T., Mercier, F. & Arikawa-Hirasawa, E. 2017. Heparan sulfate alterations in extracellular matrix structures and fibroblast growth factor-2 signaling impairment in the aged neurogenic niche. *Journal of Neurochemistry*, 142 (4): 534–44.

Yang, X. O., Nurieva, R., Martinez, G. J., Kang, H. S., Chung, Y., Pappu, B. P., Shah, B., Chang, S. H., Schluns, K. S., Watowich, S. S., Feng, X. H., Jetten, A. M. & Dong, C. 2008. Molecular antagonism and plasticity of regulatory and inflammatory T cell programs. *Immunity*, 29 (1): 44–56.

Yeo, L., Adlard, N., Biehl, M., Juarez, M., Smallie, T., Snow, M., Buckley, C. D., Raza, K., Filer, A. & Scheel-Toellner, D. 2016. Expression of chemokines CXCL4 and CXCL7 by synovial macrophages defines an early stage of rheumatoid arthritis. *Annals of the Rheumatic Diseases*, 75 (4): 763–71.

Yin, X., Johns, S. C., Kim, D., Mikulski, Z., Salanga, C. L., Handel, T. M., Macal, M., Zuniga, E. I., Fuster, M. M., Zúñiga, E. I. & Fuster, M. M. 2014. Lymphatic specific disruption in the fine structure of heparan sulfate inhibits dendritic cell traffic and functional T cell responses in the lymph node. *The Journal of Immunology*, 192

(5): 2133–42.

Yin, X., Truty, J., Lawrence, R., Johns, S. C., Srinivasan, R. S., Handel, T. M. & Fuster, M. M. 2010. A critical role for lymphatic endothelial heparan sulfate in lymph node metastasis. *Molecular Cancer*, 9 (1): 316.

Yıldırım-Buharalıoğlu, G., Bond, M., Sala-Newb, G. & Hindmarch, C. 2017. Regulation of epigenetic modifiers, including KDM6B, by interferon-γ and interleukin-4 in human macrophages. *Frontiers in Immunology*, 8: 92.

Yoon, B. R., Yoo, S.-J., Choi, Y. ho, Chung, Y.-H., Kim, J., Yoo, I. S., Kang, S. W. & Lee, W.-W. 2014. Functional phenotype of synovial monocytes modulating inflammatory T-cell responses in rheumatoid arthritis. *PLoS ONE*, 9 (10): e109775.

Yoshino, S. & Cleland, L. G. 1992. Depletion of alpha/beta T cells by a monoclonal antibody against the alpha/beta T cell receptor suppresses established adjuvant arthritis, but not established collagen-induced arthritis in rats. *Journal of Experimental Medicine*, 175 (4): 907–15.

Yu, M. B. & Langridge, W. H. R. 2017. The function of myeloid dendritic cells in rheumatoid arthritis. *Rheumatology International*, 37 (7): 1043–51.

Yue, X. 2017. Epithelial deletion of Sulf2 exacerbates bleomycin-induced lung injury, inflammation, and mortality. *American Journal of Respiratory Cell and Molecular Biology*, 57 (5): 560–69.

Yue, X., Lu, J., Auduong, L., Sides, M. D. & Lasky, J. A. 2013. Overexpression of Sulf2 in idiopathic pulmonary fibrosis. *Glycobiology*, 23 (6): 709–19.

Zagórska, A., Través, P. G., Lew, E. D., Dransfield, I. & Lemke, G. 2014. Diversification of TAM receptor tyrosine kinase function. *Nature Immunology*, 15 (10): 920–28.

Zhang, F., Wei, K., Slowikowski, K., Fonseka, C. Y., Rao, D. A., Kelly, S., Goodman, S. M., Tabechian, D., Hughes, L. B., Salomon-Escoto, K., Watts, G. F. M. M., Jonsson, A. H., Rangel-Moreno, J., Meednu, N., Rozo, C., Apruzzese, W., Eisenhaure, T. M., Lieb, D. J., Boyle, D. L., et al. 2019. Defining inflammatory cell states in rheumatoid arthritis joint synovial tissues by integrating single-cell transcriptomics and mass cytometry. *Nature Immunology*, 20 (7): 928.

Zhu, J. & Paul, W. E. 2008. CD4 T cells: fates, functions, and faults. *Blood*, 112 (5): 1557–69.

Ziegler-Heitbrock, L., Ancuta, P., Crowe, S., Dalod, M., Grau, V., Hart, D. N., Leenen, P. J. M., Liu, Y.-J., MacPherson, G., Randolph, G. J., Scherberich, J., Schmitz, J., Shortman, K., Sozzani, S., Strobl, H., Zembala, M., Austyn, J. M. & Lutz, M. B. 2010. Nomenclature of monocytes and dendritic cells in blood. *Blood*, 116 (16): e74-80.

Zuberi, R. I., Ge, X. N., Jiang, S., Bahaie, N. S., Kang, B. N., Hosseinkhani, R. M., Frenzel, E. M., Fuster, M. M., Esko, J. D., Rao, S. P. & Sriramarao, P. 2009. Deficiency of endothelial heparan sulfates attenuates allergic airway inflammation. *The Journal of Immunology*, 183 (6): 3971–79.

Zwerina, J., Hayer, S., Tohidast-Akrad, M., Bergmeister, H., Redlich, K., Feige, U., Dunstan, C., Kollias, G., Steiner, G., Smolen, J. & Schett, G. 2004. Single and combined inhibition of tumor necrosis factor, interleukin-1, and RANKL pathways in tumor necrosis factor-induced arthritis: Effects on synovial inflammation, bone erosion, and cartilage destruction. *Arthritis & Rheumatism*, 50 (1): 277–90.

Acknowledgements

My DPhil has been an inspiring and challenging 4 years, with a closure of the University during the last 6 months, which made me drop all my labwork to limit the spread of COVID-19. I would like to thank my supervisor Dr Linda Troeberg for sparking my interest in proteoglycans, which fuelled this project. I particularly want to thank her for her open-door policy, and, after she sadly moved to Northwich after 2 years, for her instantaneous response to emails and all her advice over Skype as well.

I also wish to express my gratitude to Prof Claudia Monaco for fully adopting me into her group after Linda moved. I always really enjoyed our discussions and her exciting ideas for future experiments. I am also very grateful to Dr Richard Williams for his insight and support with the *in vivo* arthritis experiments. However, my project would not have been possible if I had not met Dr. Andia Redpath and Dr. Nicola Smart at a Queen's College dinner. They enabled me to investigate the role of *Sulf2 in vivo* by kindly allowing me to use the knockout mice that they created and allowed me to work in their lab to do the PrimeFlow experiments. I also want to thank Andia for encouraging me to start learning how to analyse scRNA sequencing data. Moreover, I am particularly grateful to Michael Goddard, Louise Topping and Joy Ogbechi for their patience teaching me *in vivo* procedures and their help with many experiments. Thank you to Bryony Stott, Ida Parisi and Marcia Curtinha in the histology team for their help sectioning mouse knees.

I would like to thank everyone in the Troeberg and Monaco group for their company and support during my DPhil: Laura Collins, Inhye Park, Natacha Zanin, Alice Robinson, Yasemin-Xiomara Zurke, Lea Dib, Warren Baker, David Ahern, Jennifer Cole, Rachel Edwards and Anasthasios Chanalaris. I want to particularly thank Henk Schipper, Ewoud Compeer and Suzanne Engelen for organising coffee

breaks and for their support during my DPhil. I am also very grateful for the support of Versus Arthritis, which made it possible for me to start my DPhil at the Kennedy Institute by awarding me a scholarship.

Finally, I would like to thank my partner Caroline Sarfaty, my parents Anne-Marie and Cor Swart; my sister Marianne Swart; friends in Oxford (Sofia Athanasopoulou, Eri Ichijo, James Isbister, Anna Jungbluth, Vangelis Oikonomou, Kc Park and Sam Wheeler) for their encouragements throughout.